

**Phosponites as new
Chemoselective Modification Tools
in Staudinger Reactions**

Dissertation zur Erlangung des akademischen Grades des
Doktors der Naturwissenschaften (Dr. rer. nat.)

Eingereicht im Fachbereich Biologie, Chemie, Pharmazie
der Freien Universität Berlin

Vorgelegt von

Moritz Robert Johannes Vallée

aus Hamburg

2013

Die Arbeit wurde zwischen dem 02.06.2009 und 06.10.2013 unter der Leitung von Prof. Dr. Christian P. R. Hackenberger im Institut für Chemie und Biochemie der Freien Universität Berlin sowie am Leibniz-Institut für Molekulare Pharmakologie (FMP) angefertigt.

1. Gutachter: Prof. Dr. Christian P. R. Hackenberger

2. Gutachter: Prof. Dr. Rainer Haag

Disputation am 31.10.2013

Declaration

I herewith confirm that I have prepared this dissertation without the help of any impermissible resources. All citations are marked as such. The present thesis has neither been accepted in any previous doctorate degree procedure nor has it been evaluated as insufficient.

Berlin, 06th October 2013

M. Robert J. Vallée

The work on this dissertation resulted so far in the following publications:

1. M. R. J. Vallée, Lukas M. Artner, Jens Dervedde and Christian P. R. Hackenberger, *Angew. Chem. Int. Ed.* **2013**, *52*, 9504–9508. / *Angew. Chem.* **2013**, *125*, 9682–9686.

Alkyne phosphonites for sequential azide-azide couplings

DOI: 10.1002/anie201302462

2. V. Böhrsch, T. Mathew, M. Zieringer, M. R. J. Vallée, L. M. Artner, J. Dervedde, R. Haag, C. P. R. Hackenberger, *Org. Biomol. Chem.* **2012**, *10*, 6211-6216.

Chemoselective Staudinger-phosphite reaction of symmetrical glycosyl-phosphites with azido-peptides and polyglycerols

DOI: 10.1039/c2ob25207d

3. M. R. J. Vallée, P. Majkut, I. Wilkening, C. Weise, G. Muller, C. P. R. Hackenberger, *Org. Lett.* **2011**, *13*, 5440-5443.

Staudinger-Phosphonite Reactions for the Chemoselective Transformation of Azido-Containing Peptides and Proteins

DOI: 10.1021/ol2020175

Acknowledgments

I would like to say *a big thank you* to all of the people who were involved in my project and without them I would have never been able to finish this work:

To my supervisor Prof. Christian Hackenberger, for giving me the opportunity to work in his group on this very fascinating topic; for leaving me all the freedom to develop my ideas and allowing me to conduct experiments on my own without interference. I would like to thank him for all his support during the years, that made life in the group so comfortable, as well as his ambitions to show us the world of chemistry outside the lab.

Prof. Dr. Rainer Haag for being my second referee and for the support given by him and his group, especially Cathleen Schlesener and Maximilian Zieringer.

My second supervisor Prof. Christopf Schalley for helpful discussions and supporting my work.

All current and former members of the Hackenberger group for positive and encouraging debates and also for the good working atmosphere, which have turned the last years into great time.

Special thanks go to Paul Majkut, který se stal mým dobrým kamarádem a se kterým jsme strávili mnoho hodin u jezera, vytvářejíce mosty mezi chemií a biochemií,

My friend and lab colleagues Lukas Artner, Verena Börsch and Michaela Mühlberg for creating such a nice working environment in the lab that makes work fun, as well as the great times outside the lab.

Katrin Wittig for taking away all bureaucratic affairs from me and always having a positive outlook.

Volker Rohde, Gregor Müller, Sebastian Wieczorek, Aryaline Kamalakumar and Jan-Hinnerk Saathoff who have worked with me on this project during their Bachelor theses or internships.

Dr. Christoph Weise and Dr. Jens Dervedde who both spent many days and nights rescuing the sinking ship with a lot of patience and faith.

Dr. Andreas Schäfer, Dr. Peter Schmieder and Brigitte Schlegel from the NMR-facilities of the Freie Universität and the FMP, for their helpful discussions and support with all the NMR desires.

Dr. Andreas Springer and Fabian Klautzsch for all the advice and knowledge towards ESI-TOF use and for solving many unexpected problems.

RiNA GmbH for supporting me with material and knowledge concerning unnatural proteins and biochemical experiments – performed by Paul Majkut.

Dagmar Krause for all the HPLC purifications and LCMS analysis she did for me.

Dr. Siegfried Wilkening for taking his time to proofread this thesis.

I would like to express my greatest gratitude to Dr. Ina Wilkening, my friend, the most honest, altruistic and helpful person I have ever met, who supported me very much in every step throughout this work.

Ina

Abbreviation

| | | |
|-----------|--|--|
| Ac | acetyl | b]pyridinium 3-oxid hexafluorophosphate |
| AU | adsorbance units | |
| BCN | bicyclo[6.1.0]nonyne | HBTU 2-(1H-benzotriazole-1-yl)-1,1,3,3- tetramethyluronium hexafluorophosphate |
| Bn | benzyl | |
| calcd. | calculated | HOBt 1-hydroxybenzotriazole |
| CuAAC | copper-catalyzed alkyne-azide coupling | HOMO highest occupied molecular orbital |
| d | day | HPLC high performance liquid chromatography |
| Da | Dalton | |
| dba | dibenzylideneacetone | HRMS high resolution mass spectrometry |
| DBU | 1,8-diazabicyclo[5.4.0]undec-7- ene | ICP-MS inductively coupled plasma mass spectrometry |
| DCM | dichloromethane | LCMS liquid chromatography–mass spectrometry |
| Dde | <i>N</i> -(1-(4,4-dimethyl-2,6- dioxocyclohexylidene)ethyl) | LRMS low resolution mass spectrometry |
| Dec | decyl | LUMO lowest unoccupied molecular orbital |
| DIBO | dibenzocyclooctyne | Me methyl |
| DIFO | difluorocyclooctyne | MeCN acetonitrile |
| DIPEA | <i>N,N</i> -diisopropylethylamine | min minutes |
| DMF | dimethylformamide | mOEG oligoethylene glycol monomethyl ether |
| DMSO | dimethyl sulfoxide | MP melting point |
| DNA | 2'-desoxyribonucleic acid | MS mass spectrometry |
| <i>ee</i> | enantiomeric excess | n. d. not detected |
| e. g. | exempli gratia | NBD 4-amino-7-nitrobenzo-2-oxa-1,3- diazole |
| ER | endoplasmic reticulum | NCL native chemical ligation |
| ESI | electrospray ionization | NMP <i>N</i> -methyl-2-pyrrolidone |
| Et | ethyl | NMR nuclear magnetic resonance |
| Fmoc | fluorenylmethyloxycarbonyl | s singulett |
| GFP | green fluorescent protein | d doublet |
| h | hours | t triplett |
| HATU | 1-[bis(dimethylamino)- methylene]-1H-1,2,3-triazolo[4,5- | |

| | |
|-------------|--|
| q | quartet |
| quint | quintet |
| m | multiplett |
| <i>J</i> | scalar coupling constant |
| Pap | <i>p</i> -azidophenylalanine |
| PEG | polyethylene glycol |
| PG | protecting group / poly glycerol |
| Ph | phenyl |
| pin | pinacol |
| pKa | acid dissociation constant |
| <i>i</i> Pr | isopropyl |
| PTM | posttranslational modification |
| R | residue |
| RCM | ring closure metathesis |
| RNA | ribonucleic acid |
| s | second |
| SPAAC | strain-promoted alkyne-azide cycloaddition |
| TEA | triethylamine |
| Tf | triflate |
| TFA | trifluoroacetic acid |
| THF | tetrahydrofuran |
| THPTA | tris(3-hydroxypropyl- triazolylmethyl)amine |
| TIC | total ion count |
| TIS | triisopropylsilane |
| TLC | thin layer chromatography |
| TMA | trimethylamine |
| TOF | time of flight |
| Ts | tosyl |
| UV | ultraviolet |

Table of contents

| | | |
|------------|---|-----------|
| 1 | Introduction | 1 |
| 1.1 | From phosphorus to phosphites and phosphonites..... | 1 |
| 1.1.1 | Synthesis of phosphites and phosphonites..... | 2 |
| 1.1.2 | Reactions of phosphites and phosphonites | 5 |
| 1.2 | The Staudinger reaction | 10 |
| 1.2.1 | Reaction mechanism | 12 |
| 1.2.2 | Staudinger ligation | 16 |
| 1.2.3 | Staudinger reaction as chemoselective modification tool for biomolecules | 19 |
| 1.3 | Functionalization of biomolecules and polymers..... | 24 |
| 1.3.1 | Modifications of proteins through natural occurring functional groups | 25 |
| 1.3.2 | Modifications of biomolecules through unnatural functional groups | 27 |
| 1.3.2.1 | Introduction of an unnatural functional group into proteins | 28 |
| 1.3.2.2 | Chemoselective functionalization reactions for biomolecules..... | 30 |
| 1.3.3 | Functionalization of polymers | 34 |
| 2 | Objective | 39 |
| 3 | Discussion..... | 43 |
| 3.1 | Retrosynthetic evaluation of functionalised phosphonite synthesis | 45 |
| 3.2 | Aryl phosphonites for the functionalization of peptides and proteins | 51 |
| 3.3 | Alkyne phosphonites for sequential azide-azide couplings in organic solvents | 57 |
| 3.4 | Alkyne phosphonites as modification tool for peptides and proteins | 65 |
| 3.4.1 | Syntheses of triazole phosphonites for applications in aqueous systems | 66 |
| 3.4.2 | Hydrolysis of triazole phosphonites | 72 |
| 3.4.3 | Staudinger reactions of triazole phosphonites in aqueous systems | 73 |
| 3.4.3.1 | Quantification of the Staudinger-phosphonite reaction by fluorophore-tagged azido peptides..... | 75 |
| 3.4.3.2 | Quantification of the Staudinger-phosphonite reaction by mass spectrometry | 84 |
| 3.4.4 | Biotinylation of Rasa1-N <i>via</i> Staudinger-phosphonite reaction..... | 95 |
| 3.5 | Synthesis of coumarin phosphites | 97 |

| | | |
|----------|---|------------|
| 3.5.1 | Syntheses of 7-substituted 4-hydroxymethylenecoumarin derivatives | 97 |
| 3.5.2 | Synthesis of coumarin phosphites..... | 99 |
| 3.6 | Glycosylation of peptides via Staudinger-phosphite reaction | 103 |
| 4 | Summary | 107 |
| 5 | Zusammenfassung | 111 |
| 6 | Outlook | 117 |
| 7 | Experimental part | 119 |
| 7.1 | General informations | 119 |
| 7.2 | Alkyne phosphonites for sequential azide-azide couplings in organic solvents (Chapter 3.3) - additional information..... | 121 |
| 7.2.1 | Deprotection of phosphonite-boranes with polystyrene-bound bases | 121 |
| 7.2.2 | <i>P</i> -Ethyneyl- <i>N</i> -(3-phenylpropyl)phosphonamidate (213) | 121 |
| 7.3 | Alkyne phosphonites as modification tool for peptides and proteins (Chapter 3.4)..... | 122 |
| 7.3.1 | <i>N</i> -(Chloro(diethylamino)phosphanyl)- <i>N</i> -ethyl-ethanamine (218)..... | 122 |
| 7.3.2 | 5-(Hydroxymethyl)-2-nitrophenol (225)..... | 122 |
| 7.3.3 | 2,5,8,11,14,17-Hexaoxonadecan-19-yl 4-methylbenzenesulfonate (226) | 123 |
| 7.3.4 | (3-(2,5,8,11,14,17-Hexaoxonadecan-19-yloxy)-4-nitrophenyl)methanol (227)..... | 124 |
| 7.3.5 | 19-Azido-2,5,8,11,14,17-hexaoxonadecane (229)..... | 124 |
| 7.3.6 | <i>N</i> -(20-Azido-3,6,9,12,15,18-hexaoxaicosyl)-5-((3 <i>a</i> S,4 <i>S</i> ,6 <i>a</i> R)-2-oxohexahydro- 1 <i>H</i> -thieno[3,4- <i>d</i>]imidazol-4-yl)pentanamide (235) | 125 |
| 7.3.7 | <i>N</i> - α -fluorenylmethyloxycarbonyl-(ϵ - <i>N</i> -((7-methoxy-2-oxo-2 <i>H</i> -chromen-4- yl)methyl)-lysine (252) | 126 |
| 7.3.8 | <i>N</i> - α -Fluorenylmethyloxycarbonyl-(ϵ - <i>N</i> -(7-Nitrobenz-2-oxa-1,3-diazol-4- ylamino)-lysine (254) | 127 |
| 7.3.9 | <i>tert</i> -Butyl 4-(7-nitrobenzo[<i>c</i>][1,2,5]oxadiazol-4-yl)piperazine-1-carboxylate (265)..... | 128 |
| 7.3.10 | 4-Nitro-7-(piperazin-1-yl)benzo[<i>c</i>][1,2,5]oxadiazole (266)..... | 128 |
| 7.3.11 | 5-(4-(7-Nitrobenzo[<i>c</i>][1,2,5]oxadiazol-4-yl)piperazin-1-yl)-5-oxopentanoic acid (267)..... | 129 |

| | | |
|----------|--|-----|
| 7.3.12 | General protocol for the synthesis of alkyne phosphonite-boranes..... | 129 |
| 7.3.12.1 | Diethyl ethynylphosphonite-borane (200) | 130 |
| 7.3.12.2 | Bis(2-(2-methoxyethoxy)ethyl) ethynylphosphonite-borane (215)..... | 130 |
| 7.3.12.3 | Bis(4-(2,5,8,11,14,17-hexaoxonadecan-19-yloxy)-3-nitrobenzyl) ethynyl- phosphonite-borane (216)..... | 131 |
| 7.3.13 | General protocol for the CuAAC of alkyne phosphonite-boranes..... | 131 |
| 7.3.13.1 | Diethyl 1-(2,5,8,11,14,17-hexaoxonadecan-19-yl)-1H-1,2,3-triazol-4- ylphosphonite-borane (196)..... | 132 |
| 7.3.13.2 | Bis(2-(2-methoxyethoxy)ethyl) (1-(2,5,8,11,14,17-hexaoxonadecan-19-yl)- 1H-1,2,3-triazol-4-yl)phosphonite-borane (230) | 132 |
| 7.3.13.3 | Bis(4-(2,5,8,11,14,17-hexaoxonadecan-19-yloxy)-3-nitrobenzyl) (1- (2,5,8,11,14,17-hexaoxonadecan-19-yl)-1H-1,2,3-triazol-4- yl)phosphonite-borane (231)..... | 133 |
| 7.3.13.4 | Bis(4-(2,5,8,11,14,17-hexaoxonadecan-19-yloxy)-3-nitrobenzyl) (1-(22- oxo-26-((3aS,4S,6aR)-2-oxohexahydro-1H-thieno[3,4-d]imidazol-4-yl)- 3,6,9,12,15,18-hexaoxa-21-azahexacosyl)-1H-1,2,3-triazol-4-yl)phosphonite- borane (235) | 134 |
| 7.3.14 | General protocol for the synthesis of azido peptides | 135 |
| 7.3.14.1 | Coumarin-tagged azido peptide 256 | 135 |
| 7.3.14.2 | NBD-tagged azido peptide 257 | 137 |
| 7.3.14.3 | Piperazine-linked NDB-tagged azido peptide 269 | 138 |
| 7.3.14.4 | Azido peptide H ₃ -243..... | 140 |
| 7.3.14.5 | Azido peptide D ₃ -243..... | 141 |
| 7.3.14.6 | Azido peptide H ₆ -271..... | 142 |
| 7.3.14.7 | Azido peptide D ₆ -271..... | 143 |
| 7.3.15 | General protocol for the deprotection of borane-protected phosphonites | 144 |
| 7.3.16 | General protocol for the synthesis of phosphoramidate peptides..... | 144 |
| 7.3.16.1 | Phosphoramidate peptide H ₃ -244 | 145 |
| 7.3.16.2 | Phosphoramidate peptide D ₆ -273 | 146 |
| 7.3.16.3 | Phosphoramidate peptide H ₃ -274 | 147 |
| 7.3.16.4 | Phosphoramidate peptide H ₃ -275 | 148 |
| 7.3.17 | General protocol for Staudinger-phosphonite reaction in aqueous systems | 149 |
| 7.3.18 | Fluorescence and mass spectra for conversion studies of azido peptides with phosphonites | 150 |
| 7.3.18.1 | Fluorescence spectra for Table 3.1 | 150 |

| | | |
|------------|---|------------|
| 7.3.18.2 | Mass spectra for Table 3.2 | 152 |
| 7.3.18.3 | Mass spectra for Table 3.3 | 155 |
| 7.3.18.4 | Mass spectra for Table 3.4 | 161 |
| 7.3.18.5 | Mass spectra for Table 3.5 | 165 |
| 7.4 | Synthesis of coumarin phosphites (Chapter 3.5) | 168 |
| 7.4.1 | 2-(2-(2-Methoxyethoxy)ethoxy)ethyl-4-methylbenzenesulfonate..... | 168 |
| 7.4.2 | 7-(2-(2-(2-Methoxyethoxy)ethoxy)ethoxy)-4-methylcoumarin (284) | 168 |
| 7.4.3 | 4-(Hydroxymethylene)-7-(2-(2-(2-methoxyethoxy)ethoxy)ethoxy)-coumarin (286)..... | 169 |
| 7.4.4 | 4-Hydroxymethylene-7-(2-(2-(2-methoxyethoxy)ethoxy)ethoxy)-coumarin (286) from 7-Hydroxy-4-hydroxymethylene-coumarin (286) | 171 |
| 7.4.5 | 7-Diethylamino-4-hydroxymethylene-coumarin (287)..... | 171 |
| 7.4.6 | 4-Chloromethylene-7-hydroxy-coumarin (289)..... | 172 |
| 7.4.7 | 7-Hydroxy-4-hydroxymethylene-coumarin (290) | 172 |
| 7.4.8 | General procedure for 7-substituted-4-methylene-coumarin phosphites..... | 173 |
| 8 | References | 175 |
| 9 | Curriculum Vitae Fehler! Textmarke nicht definiert. | |
| 10 | Appendix | 187 |

1 Introduction

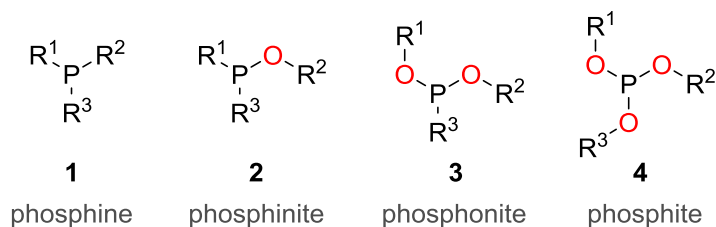
1.1 From phosphorus to phosphites and phosphonites

The name phosphorus originates from the Greek mythology and means "light-bearer" referring to the glowing of white phosphorus when it reacts with oxygen. Elemental white phosphorus was first produced in 1669.^[1]

Phosphorus has the atomic number 15 and is located in the fifth main group in the periodic table of the elements. It is characterized as non-metal. It mainly occurs in the oxidation states +III and +V whereby the latter one is more stable and the only oxidation state in phosphorus minerals. Free elemental phosphorus exists in different allotropic forms. The most common ones are white and red phosphorus. Since all allotropic forms are extremely sensitive towards air, elemental phosphorus does not occur in the native state in the crust of earth. In nature phosphorus occurs exclusively with the nucleon number of 31. ^{31}P has a spin quantum number of $\frac{1}{2}$ and is therefore NMR active.^[2]

Phosphorus plays an important role in life. In the form of phosphate it is commonly known to be part of the DNA and RNA backbone. As di- and triphosphates (ADP / ATP) it is the currency of energy in human life, but also, for example, as post-translational modification of proteins it is widely present in all living organisms in particular in signal transduction.^[3]

In organic chemistry phosphorus is involved in very famous reactions like the Staudinger or the Wittig reaction.^[4] Moreover, organic phosphorus compounds like phosphines are also one of the most popular ligands in metal-organic chemistry^[5] and find for instance application in cross-coupling reactions or olefin metathesis.^[4] Phosphines **1** are widely spread in all fields of organic chemistry, but particularly the alkoxy analogues of phosphines like phosphinites **2**, phosphonites **3** and phosphites **4** (Scheme 1.1) play an increasing role.^[6]

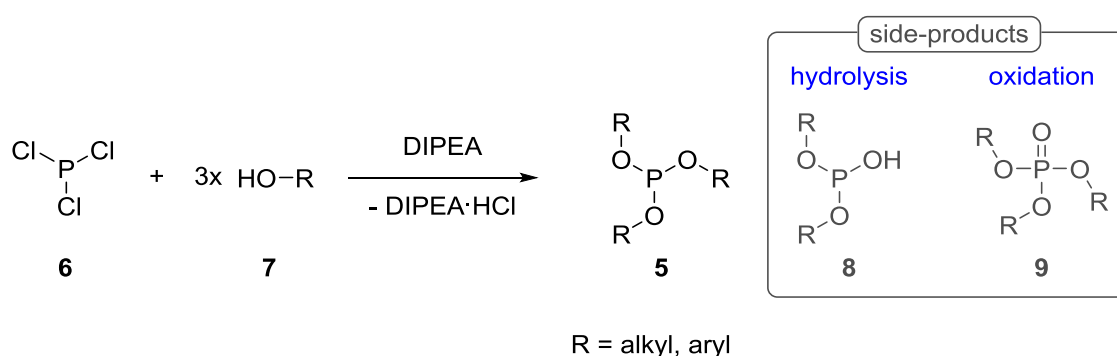


$\text{R}^1, \text{R}^2, \text{R}^3 = \text{alkyl, aryl, alkenyl, alkynyl}$

Scheme 1.1: From phosphine to phosphite.

1.1.1 Synthesis of phosphites and phosphonites

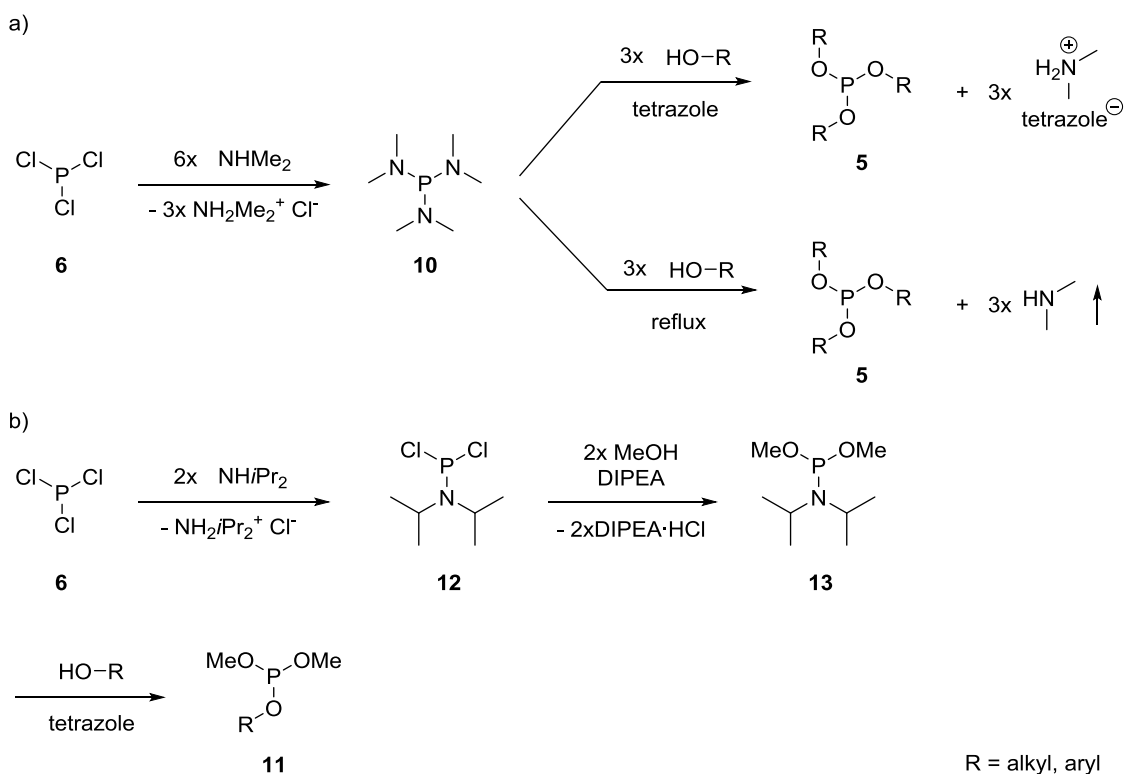
The synthesis of symmetrical phosphites **5** generally starts from a phosphorus trihalide, mostly from inexpensive phosphorus trichloride. In the presence of a non-nucleophilic base phosphorus trichloride (**6**) and three equivalents of the corresponding alcohol **7** are mixed to yield the phosphite **5** quantitatively (Scheme 1.2).^[7] Phosphorus trihalides are very reactive compounds reacting explosively with water. Dry solvents and reagents as well as a nitrogen or argon atmosphere are strictly required to avoid hydrolysis or oxidation side-products **8** and **9** during the phosphite preparation.



Scheme 1.2: Synthesis of symmetrical phosphites **5** from phosphorus trichloride (**6**).

If milder reaction conditions are required, phosphorus trichloride (**6**) can be treated with dialkylamines in a first step to give the corresponding hexaalkylphosphanetriamine **10**, which is sometimes even commercially available. In a second reaction step, the dialkylamine groups are then replaced by the alcohol, either in the presence of triazole or by heating. In the case of hexamethylphosphanetriamine (**10**) the dimethylamine by-product generated is volatile, and no purification of the phosphite product **5** is required for the thermal approach (Scheme 1.3 a).^[7b]

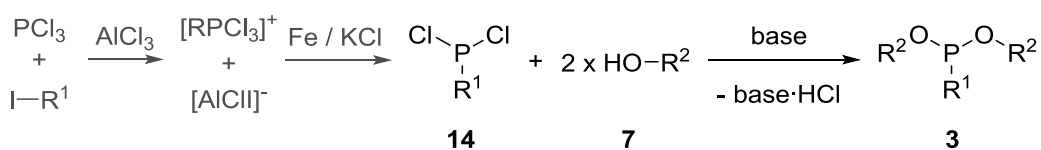
Unsymmetrical phosphites **11** are prepared by a combination of both techniques. Phosphorus trichloride (**6**) reacts with two or four equivalents of dialkylamine to the corresponding dichloro dialkylphosphanamine **12** or tetraalkylammonium chlorophosphite **17**. These unsymmetrical phosphorus compounds **12** can react selectively with an alcohol by exchange of the chloro substituents, before, in a second step, the dialkylamine groups can be replaced with a second alcohol to yield the unsymmetrical phosphite **11** as described before (Scheme 1.3 b).^[8] This methodology can even give higher purity for symmetrical phosphites **5** than the preparation from phosphorus trichloride (**6**) or hexaalkylphosphanetriamine (**10**).^[7a]



Scheme 1.3: Synthesis of symmetrical and unsymmetrical phosphites **5** and **11** in a two-step procedure from phosphorus trichloride (**6**).^[7]

The synthesis of phosphonites **3** is often very similar to the one of unsymmetrical phosphites **11**, only that a carbon nucleophile is used once. The two most common ways to prepare phosphonites **3** are shown in Scheme 1.4 and Scheme 1.5.

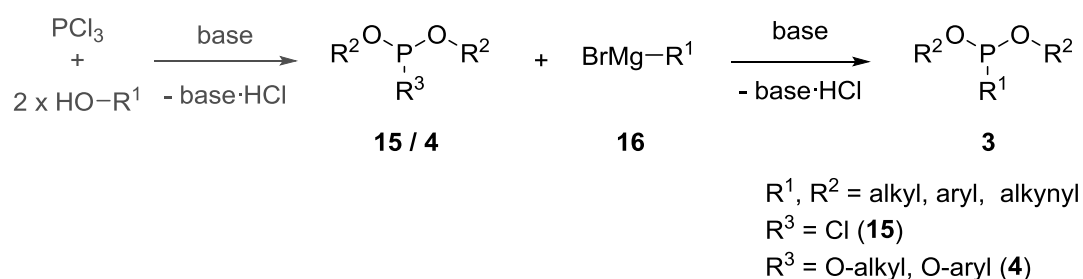
The first strategy comprises the substitution of the two chloro groups of a dichloro phosphine **14** with the desired alcohol **7** in the presence of a non-nucleophilic base (Scheme 1.4). The synthesis of dichloro phosphines **14** either requires very harsh reaction conditions such as $600\text{ }^\circ\text{C}$, gaseous hydrochloric acid^[9], or gives only low yields if synthesised from the corresponding alkylhalide and phosphorus trichloride (**6**) with the attendance of aluminium trichloride.^[10] Consequently, this reaction pathway to phosphonites **3** is only preferred if the desired dichloro phosphine **14** is commercially available.



$\text{R}^1, \text{R}^2 = \text{alkyl, aryl, alkenyl, alkynyl}$

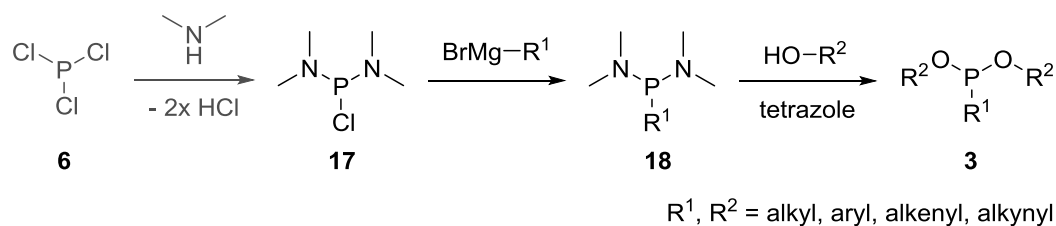
Scheme 1.4: Phosphonite **3** synthesis by alcoholysis, starting from dichloro phosphines **14**.^[10a]

The second strategy employs the substitution of the chloride group of dialkyl chlorophosphite **15** with a strong carbon nucleophile, e. g a Grignard **16** or organolithium reagent (Scheme 1.5). The required Grignard **16** or organolithium reagents are easily accessible from the corresponding halide compounds. Dialkyl chlorophosphites **15**, which are often commercially available, are either accessible from phosphorus trichloride (**6**) and the corresponding alcohol^[11] or from the corresponding dialkyl phosphonate^[12]. As an alternative to dialkyl chlorophosphites **15**, phosphites **4** can be substituted by Grignard reagents **16** to the corresponding phosphonites **3**, respectively.^[13]



Scheme 1.5: The synthesis of phosphonites **3** through a nucleophilic substitution reaction with a carbon nucleophile.

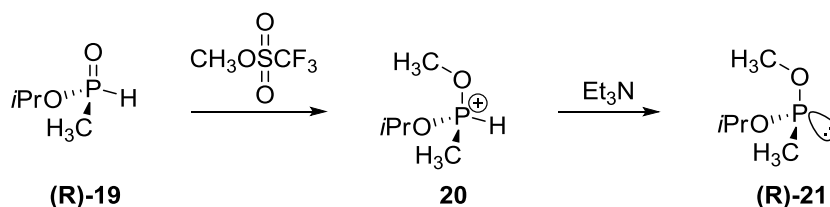
As already described for the synthesis of phosphites **5** and **7** (Scheme 1.3) the reactivity of phosphorus trichloride (**6**) can be lowered by exchanging the chloro substituents by dialkyl amine groups. This methodology is also suitable for the synthesis of phosphonites **3**. However, the first step of the reaction sequence is still the formation of the carbon-phosphorus bond by substitution of the chloro substituent of the tetraalkylamino chlorophosphite **17**. In the second step, the dialkyl amino groups are substituted by the alcohol groups **7** either by heating and / or by addition of tetrazole as weak Brønsted acid (Scheme 1.6).^[14] This methodology has the advantage of a selective single alkylation at the phosphorus starting material in the first reaction step. Due to its higher reactivity phosphorus trichloride (**6**) the dichloro analogue of tetraalkylamino chlorophosphite **17** tends to undergo more side reactions and, for instance a double alkylation reaction if a small excess of the alkylation reagents **16** is present. Another advantage of lowering the reactivity of the alkylated phosphorus reagent **18** is the much easier purification compared to the reaction that starts from dichloro phosphines **14**.



Scheme 1.6: Phosponite synthesis from less reactive diamino chlorophosphite **17**.

The free electron pair of all phosphorus(III) species renders the moiety tetrahedral and therefore chiral when three different substituents are attached. Other than in the homologues amines the energy barrier for the (R) \leftrightarrow (S) flipping is high enough that chiral phosponites can be handled and even stored for a short period of time.^[15]

The first stereospecific phosponite synthesis was performed by H. S. Aaron *et. al.* in 1982. They started from (R)-isopropyl methylphosphinate (**R**)-**19** and methylated the double-bonded oxygen with methyl triflate. The resulting phosphonium salt (**R**)-**20** could be deprotonated to the corresponding (R)-isopropyl methyl methylphosphonite (**R**)-**21** (Scheme 1.7). With regard to a conversion rate of 69% and 27% to the isolated product of only 88% purity, this method is hardly feasible for the synthesis of non-chiral phosponites.



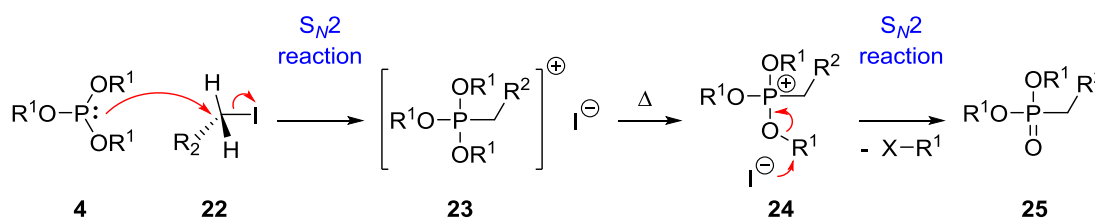
Scheme 1.7: The first enantioselective phosponite synthesis.^[15]

1.1.2 Reactions of phosphites and phosponites

The Michaelis-Arbuzov reaction (Scheme 1.8) is one of the best-known reactions of phosphites **4** in organic chemistry beside the Staudinger reaction (chapter 1.2). The phosphonate product **25** is an important reagent e. g. for the Horner–Wadsworth–Emmons reaction, used for agriculture or pesticides.^[16]

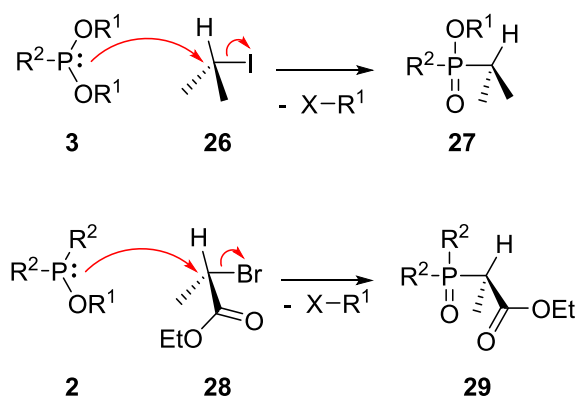
The Michaelis-Arbuzov phosphonate synthesis

In 1898 R. Kaehne and A. Michaelis reported the first formation of dialkyl phosphonates **25** from the reaction of primary alkyl iodides **22** with trialkyl phosphites **4**.^[17] In 1906 A. E. Arbuzov published a detailed investigation of the reaction where he described its scope and limitations.^[18] The first step of the reaction is an S_N2 reaction. The electron lone pair of the phosphite **4** attacks at the carbon-atom of the alkyl iodide along with a simultaneous separation of the iodide. The iodide anion attacks a carbon atom of one of the alkoxy substituents of the phosphonium ion **23** in a second S_N2 reaction. The driving force in this reaction is the formation of the very stable phosphorus-oxygen double bond of the dialkyl phosphonate product **25**.



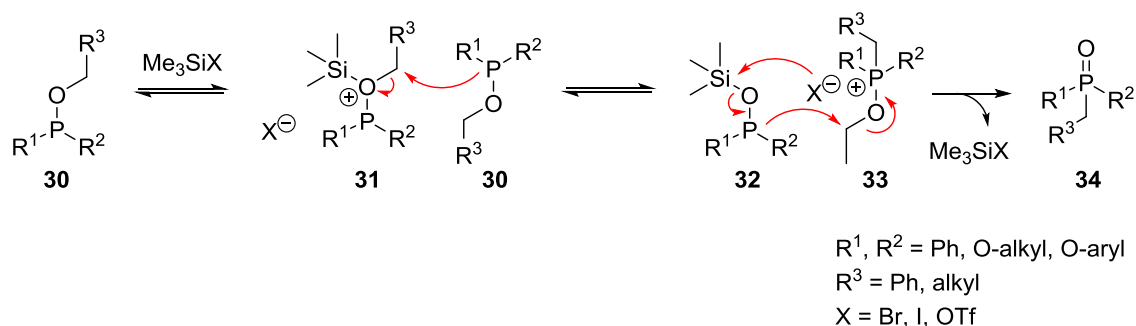
Scheme 1.8: Reaction mechanism of the Michaelis-Arbuzov reaction.^[18]

The Michaelis-Arbuzov reaction is not limited to phosphites **4**. It proceeds in the same manner with phosphonites **3** and phosphinites **2** to the corresponding phosphinic acid ester and phosphine oxide (Scheme 1.9). The reaction usually proceeds with primary alkyl halides but is not limited to it. Isopropyl iodide (**26**) or ethyl α -bromopropionate (**28**) do react as well to the corresponding phosphorus(V) products **27** or **29**. Most of the other secondary and all the tertiary alkyl, aryl, and alkenyl halides do not undergo S_N2 reactions.^[16, 18a]



Scheme 1.9: Michaelis-Arbuzov reaction with secondary alkyl halides.^[18a, 19]

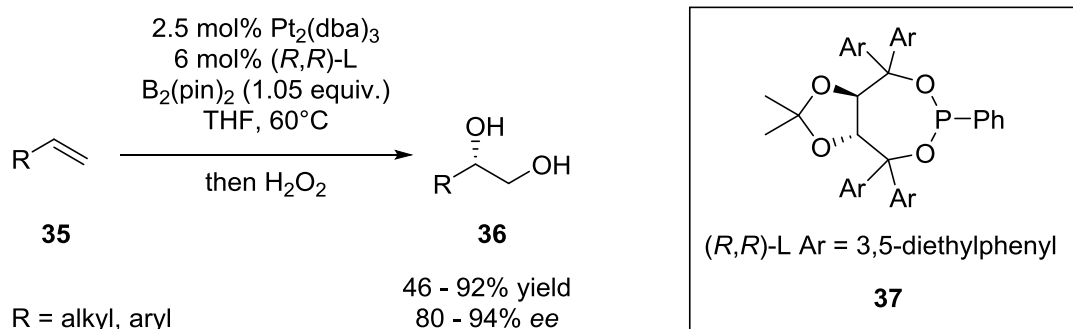
Furthermore, not only alkyl halides can initiate the Michaelis-Arbuzov reaction, but also the addition of a Lewis acid like trimethylsilyl-triflate or halide leads to the so-called Michaelis-Arbuzov rearrangement. This is a Lewis acid-catalysed intermolecular alkyl transfer reaction between two phosphinites **2**, phosphonites **3** or phosphites **4** yielding the corresponding structural isomeric phosphorus(V) compounds **34**. The Lewis acid binds to an oxygen next to the phosphorus and enables thus a nucleophilic attack of another phosphorus(III) derivative **30** on the α -carbon atom next to the oxonium ion **31**. The next step in the reaction sequence is again a nucleophilic attack, in this case from the phosphorus(III) compound **32** on the α -carbon atom of the newly formed phosphonium ion **33**. The release of the Lewis acid results in the formation of two phosphonates **34** (Scheme 1.10).^[10b, 20]



Scheme 1.10: Reaction mechanism of the Michaelis-Arbuzov rearrangement.^[10b, 20]

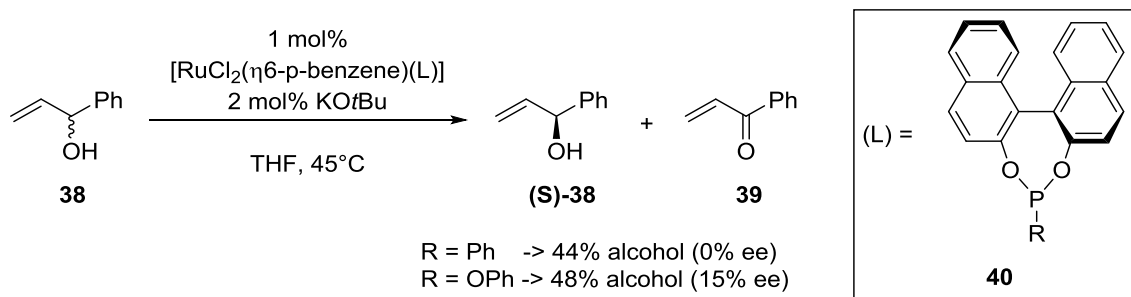
Phosphites and phosphonites as ligands in metal-organic chemistry

In modern metal-organic chemistry phosphonites **3** and phosphites **4** are widely used ligands. The good accessibility of phosphonites **3** and phosphites **4** from phosphorus chlorides and the desired alcohol enables the synthesis of a huge variety of derivatives. Especially chiral diols, such as (S)-1,1'-bi-2-naphthol opens up an fast pathway to chiral ligands for enantioselective catalysis. J. P. Morken *et. al.* used chiral phosphonite ligands in an enantioselective palladium-catalyzed diboration reaction of terminal alkenes. They could demonstrate that in the presence of the chiral phosphonite ligand **37**, terminal alkenes **35** could be converted to the corresponding dioles **36** with an enantiomeric excess (*ee*) from 80 to 94% (Scheme 1.11).^[6a]



Scheme 1.11: Enantioselective dihydroxylation of terminal alkenes **35**.^[6a]

A very fascinating example of the application of chiral phosphite or phosphonite ligands for the kinetic resolution of allylic alcohols was shown by J. Gimeno *et. al.* The racemic allylic alcohol **38** is oxidized to the corresponding ketone **39** in the presence of a rhodium-catalyst. By addition of the chiral phosphite or phosphonite ligand **40** only one enantiomer in the racemic mixture **38** is oxidized and the remaining enantiomeric enriched alcohol (**S**)-**38** can be separated from the reaction mixture (Scheme 1.12).^[6b]

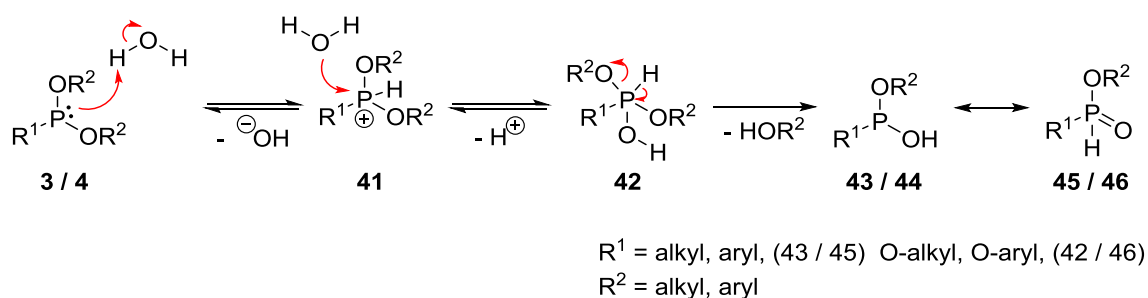


Scheme 1.12: Chiral phosphites and phosphonites **40** in the kinetic resolution of allylic alcohol **38**.^[6b]

Oxidation and hydrolysis of phosphites and phosphonites

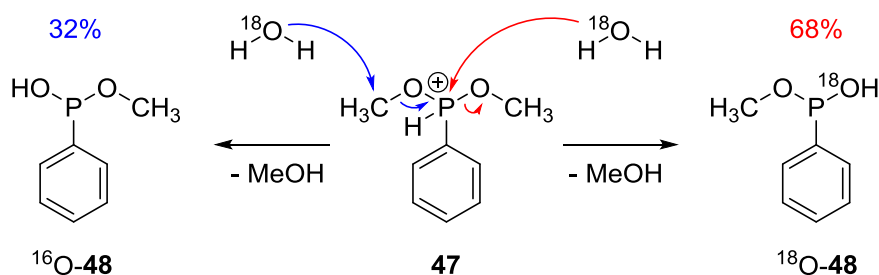
Phosphites **4** and phosphonites **3** tend to oxidize if exposed to oxygen due to their electron lone pair.^[21] Phosphites and aryl phosphonites are kinetically stable but alkyl phosphonites have to be handled under a nitrogen atmosphere to avoid oxidation. The phosphorus(III) atom is sp^3 hybridized and the electron lone pair undergoes only minor interactions with π -orbitals from neighbouring atoms. Therefore, substituents on the phosphorus with stronger negative inductive effects like oxygen or sp^2 configured carbon atoms kinetically stabilise the phosphorus(III) compound against oxidation. In chemical laboratories oxidation of phosphites and phosphonites to their corresponding oxides is achieved with standard oxidation reagents, such as hydrogen peroxide.

The electronic nature of the phosphonite **3** and phosphite **4** electron lone pair is also responsible for its tendency to hydrolyse in water. In the first step an electrophilic phosphonium ion **41** is formed by protonation either from water or Brønsted acids. The phosphonium ion **41** is then attacked by a water molecule and an alkoxy substituent is cleaved off. The resulting hydrogen phosphonite **43** or hydrogen phosphite **44** is in equilibrium with the corresponding structural isomeric phosphinate **45** or phosphonate **46**. The missing electron lone pair of phosphinate **45** or phosphonate **46** makes them more stable and catalytic amounts of acid are optimal for further hydrolysis (Scheme 1.13).



Scheme 1.13: Hydrolysis of phosphonites **3** and phosphites **4**.

An alternative hydrolysis mechanism that is of particular interest for the methoxy substituents of phosphorus(III) compounds is described in Scheme 1.14. It had been shown by labelling experiments that water can also attack the carbon atom in the methoxy substituent in dimethyl phenylphosphonium ion **47** instead of the phosphorus (Scheme 1.14).^[22] It is assumed that this mechanism does not play a significant role for higher substituted alkoxy groups.



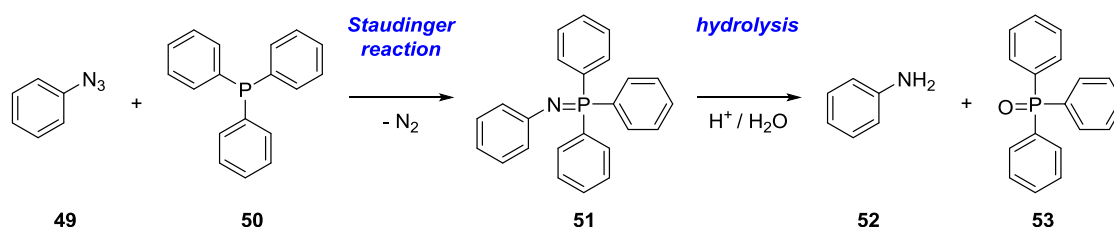
Scheme 1.14: The two competing hydrolysis mechanisms of dimethyl phenylphosphonite.

One of the most versatile and interesting reaction of phosphonites **3** and phosphites **4**, as well as of all the other phosphorus(III) reagents, is the Staudinger reaction. It was first discovered almost 100 years ago^[23], and still new variations and applications of the Staudinger reaction in various areas of chemistry are discovered.^[7a, 8, 24]

1.2 The Staudinger reaction

In 1919 Jules Meyer and Hermann Staudinger reported the *explosive* reaction of phenylazide (**49**) with triphenylphosphine (**50**) and identified the product as triphenylphosphine-phenylimine (**51**).^[23] This reaction is not limited to phosphines **1**, since all kind of trivalent phosphorus species including phosphinites **2**, phosphonites **3** and phosphites **4** react with azides in the same way to their corresponding phosphorus-nitrogen double bond products. Moreover, it seems that there is no limitation with regard to the azide.^[24a] Triphenylphosphine (**50**) is known to react with diethyl phosphorazidate, methanesulfonyl azide,^[25] benzoyl azide,^[26] azidotrimethylsilane^[27] or dimethylphosphinothioyl azide^[28] to its corresponding aza-ylides. Today all these types of reaction are called *Staudinger reaction*.

Although phosphorimines like **51**, which are always in equilibrium with their aza-ylide form, are interesting compounds themselves, the overwhelming success of the Staudinger reaction can be concluded from follow-up reactions. In their original publication in 1919 Jules Meyer and Hermann Staudinger already reported the acid catalysed hydrolysis of triphenylphosphine-phenylimine (**51**) to aniline (**52**) and triphenylphosphine oxide (**53**)^[23] – the so-called *Staudinger reduction* (Scheme 1.15).



Scheme 1.15: The first reaction of an azide with a trivalent phosphorus compound reported by Jules Meyer and Hermann Staudinger in 1919.^[23]

The Staudinger reaction grants access to seemingly endless interesting structures that are accessible from phosphorimines depending on the used phosphorus(III) compound and further reagents that are added to the reaction mixture (Figure 1.1). For example the aza-ylide can undergo dimerization to diazadiphosphetidine structures (Figure 1.1 a).^[29] Depending on the phosphorus substituents also rearrangements can take place, e. g. alkyl substituents undergo a 1,2-shift^[30] and alkoxy substituents undergo 1,3-shifts either Lewis acid-catalysed^[31] or uncatalysed^[32] (Figure 1.1 b). The reaction of an aza-ylide with an electron poor alkyne leads to an insertion reaction resulting in a (2-phosphanylidene)ethan-1-imine (Figure 1.1 c).^[33]

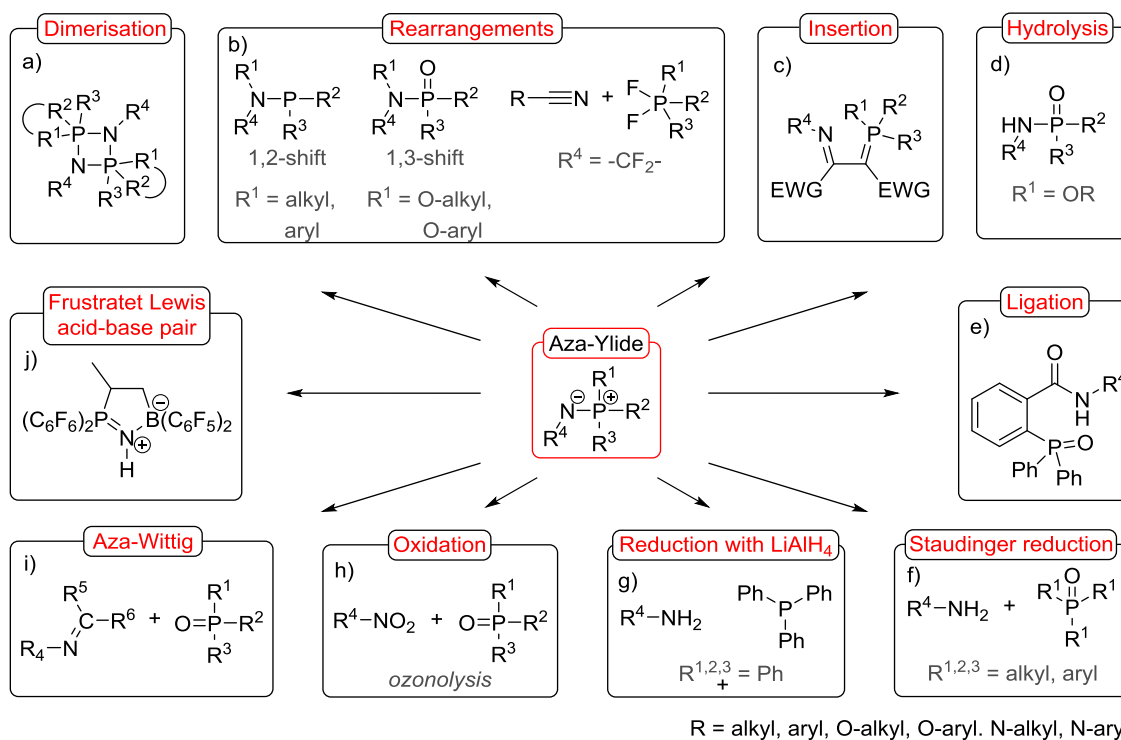


Figure 1.1: Reaction scope of aza-ylides.

Besides phosphines **2**, phosphonites **4** and phosphites **5** can also undergo hydrolyses reactions but they do not lead to the formation of an amine. Instead, one of the alkoxy substituents is cleaved off after the initial attack of water and stable phosphoramidates or phosphonamidates respectively are formed (Figure 1.1 d; a detailed discussion of this very important reaction is given in chapter 1.2.3).^[7-8, 34]

In 2000 Bertozzi *et. al.* found that the nucleophilic nitrogen from the aza-ylide can be trapped by installation of an electrophilic ester in close proximity. This reaction is known as Staudinger ligation (Figure 1.1 e; a detailed discussion is given in chapter 1.2.2).^[24b-d, 35]

The classical Staudinger reduction (Figure 1.1 f) is not the only redox reaction of aza-ylides. Reduction to the corresponding amine can also be achieved by reducing agents like lithium aluminium hydride generating an amine and a phosphane (Figure 1.1 g). These protocols allow the protection of some phosphorus(III) species as their corresponding phosphorus(V) compounds. This protection strategy is a versatile method to avoid side reactions or degradation of some phosphorus(III) compounds during further reaction steps.^[36] Aza-ylides can also react with oxidation reagents. In an ozonolysis-type oxidation reaction the corresponding nitro-derivative and phosphinoyl are formed (Figure 1.1 h).^[37]

Another well-known reaction of aza-ylides is the aza-Wittig reaction that converts an aldehyde or ketone to the corresponding imine. Because of its similarity of this reaction to the famous Wittig reaction this reaction is referred to aza-Wittig reaction in literature,^[38] even

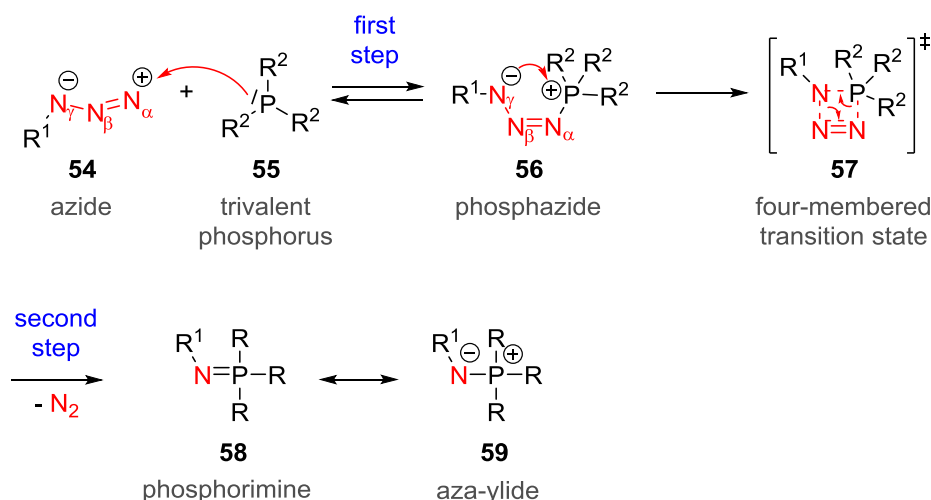
though Georg Wittig himself claimed the reaction as ‘variation of the Staudinger theme’^[36a] (Figure 1.1 i).

Only recently it was reported that an intramolecular vicinal frustrated phosphine-borane Lewis acid-base pair can react with an azide to form an internally borane stabilized P=NH phosphinimine (Figure 1.1 j).^[39] Furthermore isocyanates,^[40] isothiocyanates,^[38a, 40] carbodiimides (not shown) and many others interesting structures are accessible from azaylides. Figure 1.1 gives a brief overview about the variety of compounds available through the Staudinger reaction, a much more detailed overview is given by Y. G. Gololobov.^[24a, 36a]

In context of this work, the most important reactions of phosphorimines are the Staudinger ligation and the hydrolysis of phosphon- and phosphorimidates, which will be discussed in more detail in chapter 1.2.2 and chapter 1.2.3.

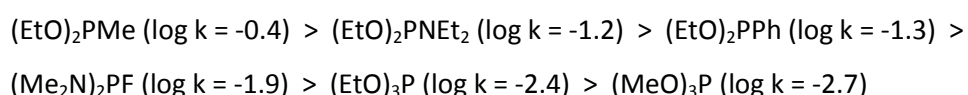
1.2.1 Reaction mechanism

The most important aspect of every organic reaction is a detailed investigation of its reaction mechanism. Only if the right transition states, the intermediates formed as well as their stabilities and kinetics are known, rational optimisation or modification of the reaction can be made. The Staudinger reaction is no exception to this rule and over the last century many important experiments and calculations have been performed that deliver an ensured reaction mechanism. The kinetics of the Staudinger reaction can either be of first or second order, which depends whether the bimolecular formation of the phosphazide (**56**) or the unimolecular decomposition is the rate determining step (Scheme 1.16).

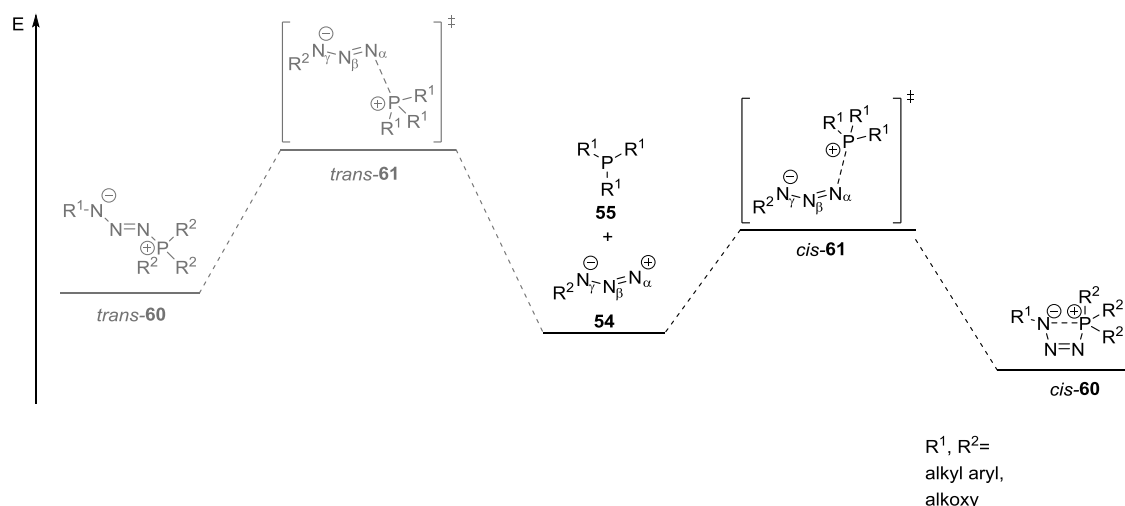


Scheme 1.16: General reaction mechanism of the Staudinger reaction.^[24a]

The first step of the Staudinger reaction is the nucleophilic attack of the trivalent phosphorus(III) compound **55** on the terminal nitrogen of the azide **54** that results in the formation of a phosphazide **56**. The existence of phosphazides **56** as intermediates was first observed by H. Staudinger by cooling a reaction to $-80\text{ }^{\circ}\text{C}$.^[24a, 41] The phosphorus and azide substituents have a huge influence on the reaction outcome. On the one hand, they can change the first step of the reaction from equilibrium to an irreversible reaction. Whereas the phosphazide formed from triphenylphosphine can dissociate into the starting materials,^[42] the reaction of a phosphine with strong donor substituents like hexamethylphosphanetriamine reacts irreversible with azido compounds to the phosphazides.^[43] On the other hand, the inductive effects of the substituents have a strong influence on the rate of the first reaction step. Taking a look at the rate constants (k) from Staudinger reactions of some phosphonites **3** and phosphites **4** with phenyl azide in tetrahydrofurane at $20\text{ }^{\circ}\text{C}$, the effect is clearly visible and shows e.g. that phosphonites **3** react ten to one hundred times faster with azides than phosphites **4**.^[24a]

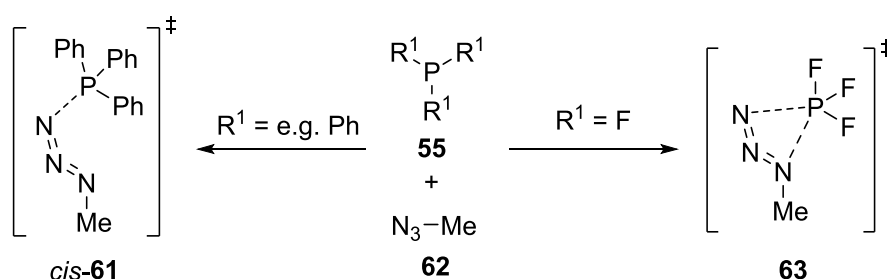


It has been well established, both experimentally and theoretically, that the $\text{N}_\alpha\text{N}_\beta\text{N}_\gamma$ backbone of an azide **54** is not linear, but with an angle of about 170° .^[44] Taking this into account, the attack of the phosphorus electron lone pair on the N_α of the azide **54** can either lead to a *cis*-**61** or a *trans*-**61** transition state (Scheme 1.17). In the *trans* transition state *trans*-**61** the phosphorus and the residue of the azide are on the same side. This has been calculated to be 12-26 kcal/mol higher than the *cis* transition state where the phosphorus is in closer proximity to the N_γ of azide. From a steric point of view the lower energy of the *cis* transition state *cis*-**61** and its corresponding intermediate *cis*-**60** seems to be paradox at first glance, but the high gain in energy results from the interaction of the positively charged phosphorus and the negatively charged N_γ of the azido compound.



Scheme 1.17: *Cis* and *trans* attack of phosphorus on an azide.^[44]

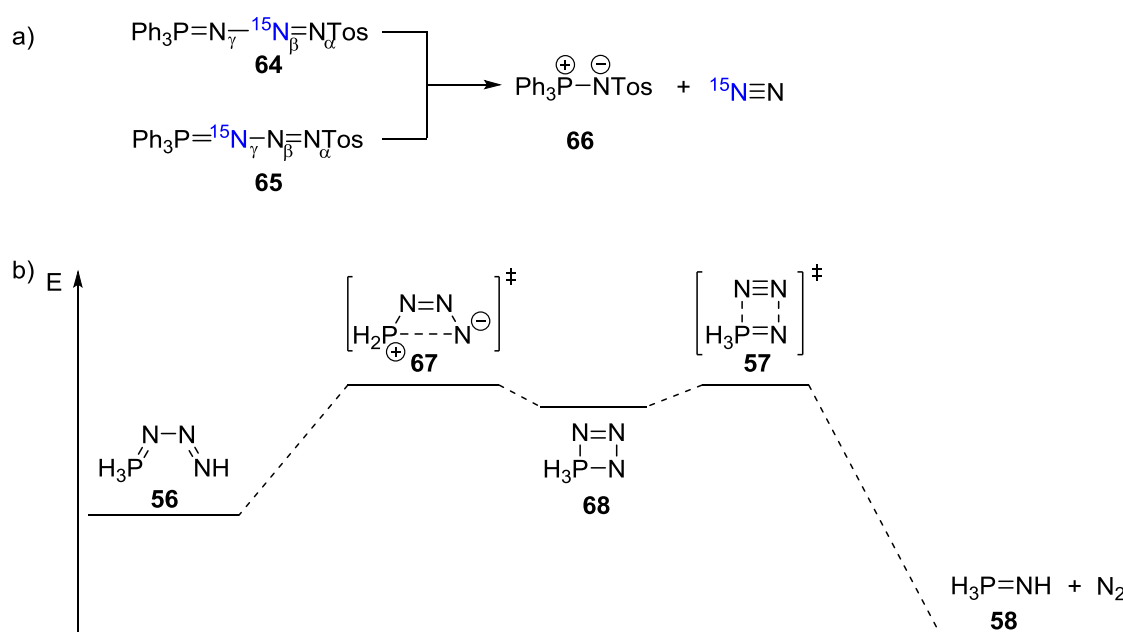
Another possibility would be a simultaneous attack of the phosphorus of **55** at the N_α and N_γ, which has only been found for the very electron-poor phosphorus trifluoride (Scheme 1.18). With respect to other phosphorus(III) compounds this dihapto transition state **63** has a higher energy compared to the monohapto transition state *cis-61* and is therefore unlikely to occur.^[45]



Scheme 1.18: The electronic propensities of the phosphorus determine the attack on an azido compound.^[45]

The second step of the Staudinger reaction is the release of molecular nitrogen (Scheme 1.16). In this step inductive and mesomeric effects have a great influence on the reaction rate. In general, donor substituents stabilize the phosphazide **56** and therefore lower the reaction rate of the second step. If the donor capability is high enough, the reaction order can change from bimolecular to monomolecular. Whereas the reaction of diethyl cyclohexylphosphite follows a bimolecular reaction order, the reaction of cyclohexyl tetramethylphosphane-diamine with azido compounds is unimolecular.^[46] Differently from the first step of the Staudinger reaction the second step is dependent on the size of all the substituents on the phosphazide such as a single adamantly group on the phosphorus can influence the reaction rate by up to two powers of ten.^[47]

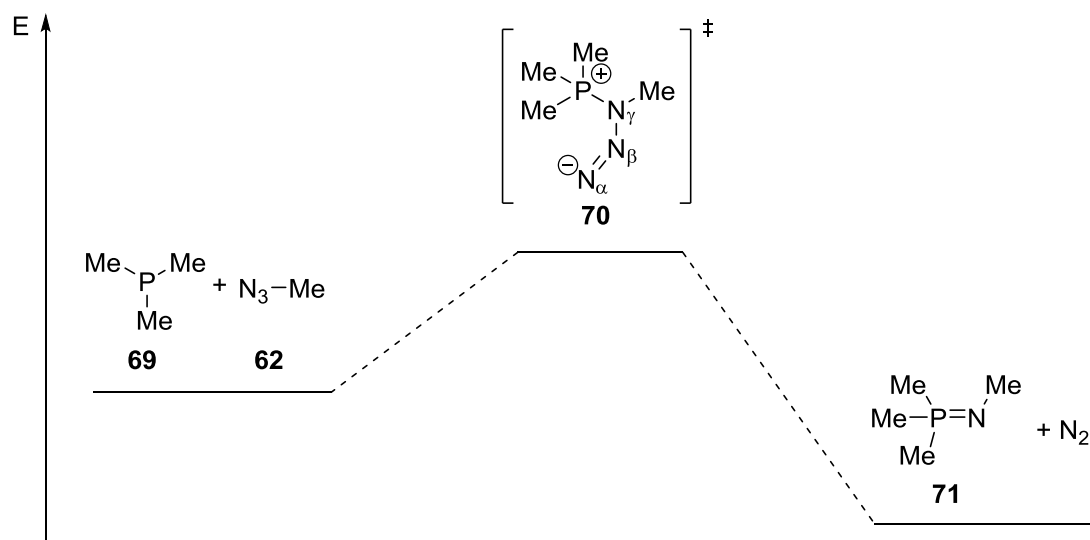
Today it is ensured that the phosphazides **56** releases molecular nitrogen through a four-membered transition state **57**. The first experimental proof that N_α and N_β are released were done by ^{15}N -labelling experiments (Scheme 1.19 a). The exclusive formation of unlabelled azaylide product **66** revealed that N_γ stays in the product.^[48] This suggested the existence of the four-membered heterocyclic intermediate **68** (Scheme 1.19 b). However, DFT calculations of the relative energies of the intermediate and the involved transition states **67** and **57** are so low that it is predicted that the *cis*-phosphazide transition state **66** can release nitrogen without the intermediary formation of the four-membered heterocyclic transition state **57**.^[45]



Scheme 1.19: a) Isotopic labelling experiments verified the proposed reaction mechanism.^[48a]

b) Calculated transition states and intermediates for the release of nitrogen from a phosphazide **56**.^[45]

A one-step mechanism where a direct attack of trimethyl phosphine **69** at the N_α of methyl azide (**62**) occurred was also calculated (Scheme 1.20). The energy of this transition state **70** is higher than in the N_γ *cis* pathway and is therefore insignificant. This is due to the fact that there are no stabilizing effects in the one-step transition state **70**.^[44]

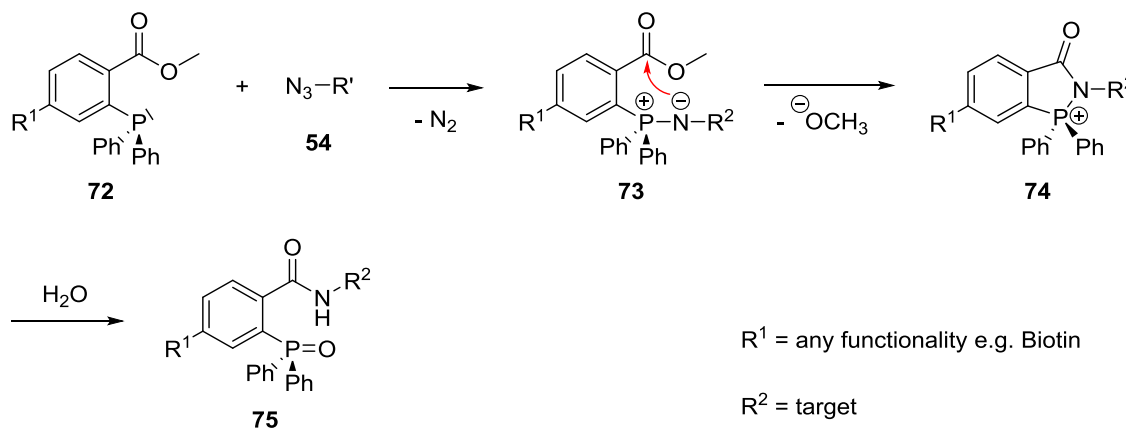


Scheme 1.20: One-step mechanism of the Staudinger reaction.^[44]

1.2.2 Staudinger ligation

After the investigation of several applications of the Staudinger reaction (see Chapter 1.2, Figure 1.1) with different phosphorus(III) species with azides as well as further reactions of the aza-ylides, in the year 2000 a second revolutionary Staudinger-type reaction was described by Eliana Saxon and Carolyn R. Bertozzi: the Staudinger ligation (Figure 1.1 d, Scheme 1.21).^[24d] The aza-ylide product **73** from the reaction of triphenylphosphine **72** and an azide **54** is rather stable in aqueous solution at around neutral pH. Bertozzi *et. al.* came up with the idea to install an electrophilic trap in form of a methyl ester in close proximity to the aza-ylide. By this means, the nucleophilic nitrogen of the aza-ylide **73** can attack the carbonyl group and form a stable amide bond. The resulting phosphonium ion **74** hydrolyses very rapidly to the final phosphine oxide product **75** (Scheme 1.21). To demonstrate the applicability of this new type of Staudinger reaction as bioorthogonal labelling tool, Bertozzi *et. al.* used a biotin-functionalised phosphine **72** in a cell surface labelling assay. In this assay they fed Jurkat cells with *N*-azidoacetylmannosamine which they assumed to be well tolerated by the sialic acid biosynthetic machinery and be presented on the cell surface. Incubation of the azido-containing cells with biotin phosphine **72** and subsequent addition of fluorescein isothiocyanate (FITC)–avidin confirmed the labelling of the cells by the Staudinger ligation. Control experiments with *N*-acetylmannosamine revealed that without the azide function no unspecific reaction of the phosphine **72** occurred.^[24d] There was the concern that the phosphine is not only reacting as electrophile in the Staudinger reaction but in addition acts as reducing agent and destroys disulfide bonds of present proteins. Fortunately, Bertozzi *et. al.*

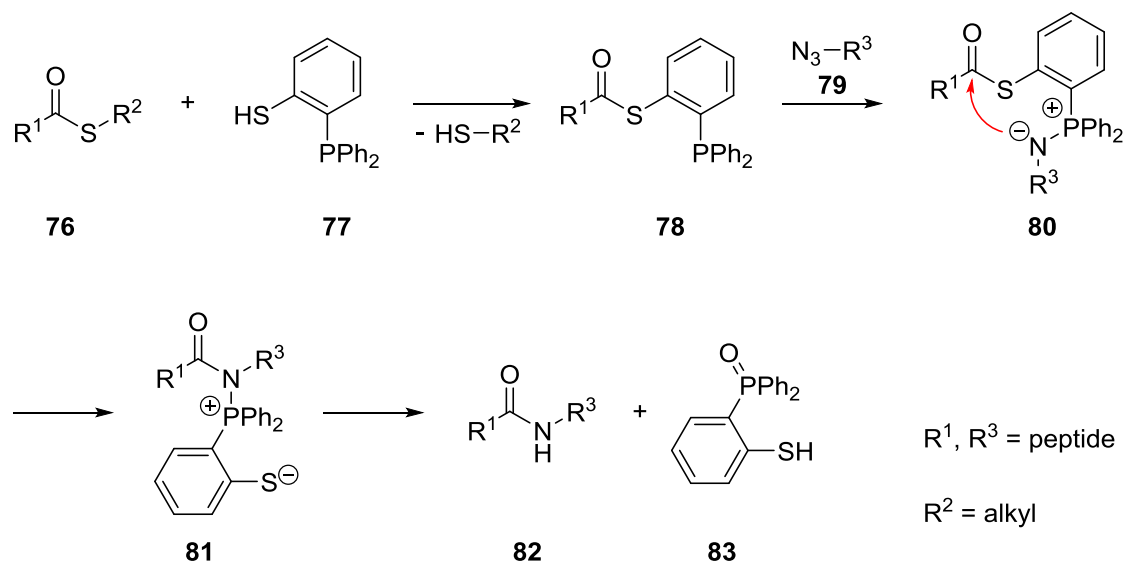
were able to demonstrate that this does not take place by incubating Jurkat cells with triarylphosphine followed by tagging the free thiol groups with iodoacetylbiotin and quantified them by FITC-avidin.^[24d]



Scheme 1.21: Staudinger ligation, as first described by E. Saxon and C. R. Bertozzi.^[24d]

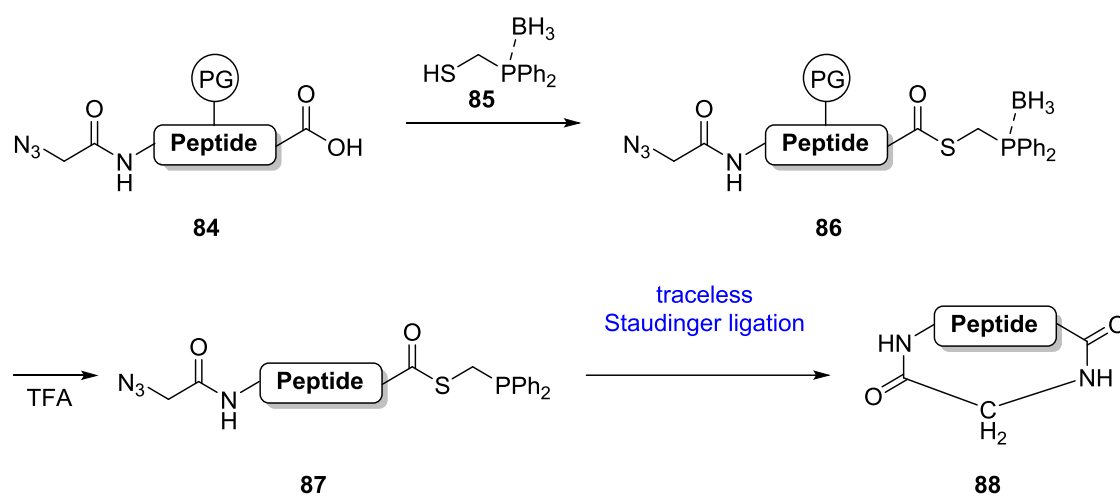
With the formation of an amide bond as product of the Staudinger ligation, the obvious question was whether this reaction can be used as a new peptide ligation reaction. To form a natural peptide bond, it was crucial to remove occurring phosphine oxide after the reaction. This goal was achieved shortly after the first Staudinger ligation was published independently by Bertozzi^[24c] and Raines.^[24b] In the original Staudinger ligation methanolate is kicked out during the amide bond formation (Scheme 1.21: **73** -> **74**). As a result, a potential mechanism for the removal of the phosphine unit already existed in the original reaction: The triarylphosphine **72** must only be attached to this leaving group to make the whole amid bond formation ‘traceless’. Raines *et. al.* used therefore 2-(diphenylphosphanyl)benzenethiol (**77**) and attached the phosphine *via* transesterification onto the C-terminus of a thioester-peptide **76**. In the second step an azido peptide **79** was added to form an aza-ylide **80**. The nitrogen of the aza-ylide **80** attacked the carbonyl group of the thioester to form an amide bond in the same manner as in the original Staudinger ligation. After the final hydrolysis of the phosphonium ion **81** a natural peptide bond **82** is left (Scheme 1.22).^[24b] Bertozzi *et. al.* came up with the same idea for the cleavable phosphine but in addition they also probed similar molecules with ester- or amide-bound leaving groups as well as alkyl and hetero-aromatic linker systems between the phosphine and the leaving group.^[24c] An in-depth investigation of the reaction mechanism and of its kinetics was done a few years later by the group of R. Raines as well.^[49]

Since the Staudinger reaction is known to be a chemoselective reaction, peptides do not necessarily have to be protected during the reaction.^[50] Apart from the well-established *native chemical ligation* (NCL) where a N-terminal cysteine is required at the ligation side, the traceless Staudinger ligation has no restrictions regarding the coupled amino acids (α -azido amino acids at the N-terminus are required but are independent from the nature of their side chain).



Scheme 1.22: Traceless Staudinger ligation as described by Raines *et. al.* in 2000.^[24b]

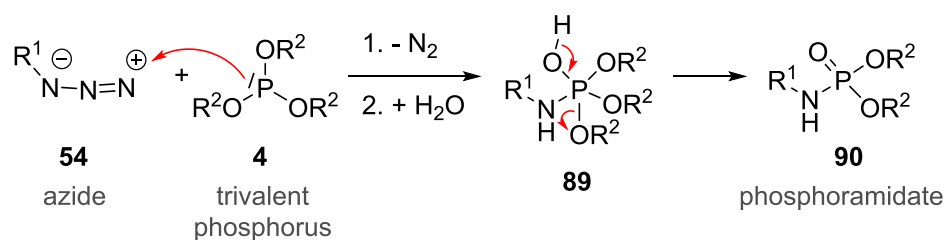
An important step towards the synthesis of proteins by the Staudinger ligation was achieved by Raines *et. al.* in 2007 with the transfer of the reaction into aqueous systems.^[51] Hence, the synthesis of a fully functional protein in a *round bottom flask* has not been achieved through traceless Staudinger ligation yet. Nevertheless, many other fascinating applications have been shown, such as site-specific immobilization of peptides on surfaces^[52] or the ligation of protected (glyco-)peptide fragments^[53]. The Staudinger ligation is also not restricted to intermolecular reactions. Recently, it could be shown that also intramolecular reactions are possible leading to cyclic peptides. To prevent the Staudinger reduction as a side reaction, the phosphine **85** was protected as borane adduct during its installation on the C-terminus of an azido peptide **84**. After global deprotection of all side chain protecting groups as well as the borane group with trifluoroacetic acid, the intramolecular traceless Staudinger reaction could take place to yield the desired cyclic peptide **88** (Scheme 1.23).^[50a] Since cyclic peptides show remarkable stability^[54] as well as very interesting biological functions, such as antibacterial activity or of high cell penetrating properties,^[55] strategies for their synthesis are of prime interest, especially if they are accessible from peptides with unprotected side chains.



Scheme 1.23: The traceless Staudinger ligation as a key step for peptide cyclisation.^[50a]

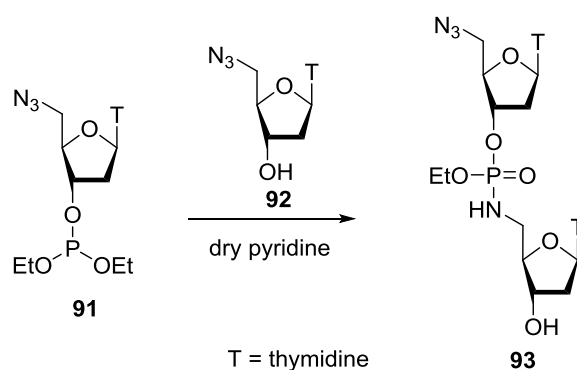
1.2.3 Staudinger reaction as chemoselective modification tool for biomolecules

In modern bioscience, there is a constant demand for potent labelling reagents and reactions. Several research groups and start-up companies exist that focus on this topic, and successful approaches that meet the high requirements are very rewarding in terms of publications, patents and applications.^[56] A long-known variant of the Staudinger reaction is a very promising candidate to fulfil this task. Other than the in the Staudinger reduction (Scheme 1.15) where a phosphine reacts with the azide and subsequent acid-catalysed hydrolysis splits both reaction partners apart again, a substituent with high leaving group propensities is attached onto the phosphorus, thereby changing the reaction outcome. In that case, after the addition of water to the phosphorimidates the amine is no longer the best leaving group. If a phosphite **4** is used instead of a phosphine, an alkoxy substituent acts as the leaving group to form the phosphorimidate and a stable phosphoramidate **90** (Scheme 1.24). An alternating hydrolysis pathway, analogue to phosphonite hydrolysis (Scheme 1.14), in which water attack the proximal carbon atom of the alkoxy substituent instead of the phosphorus of the phosphorus-nitrogen double should be possible as well. This reaction is known for over 50 years and was first described by Kabachnik *et. al.*^[34b]



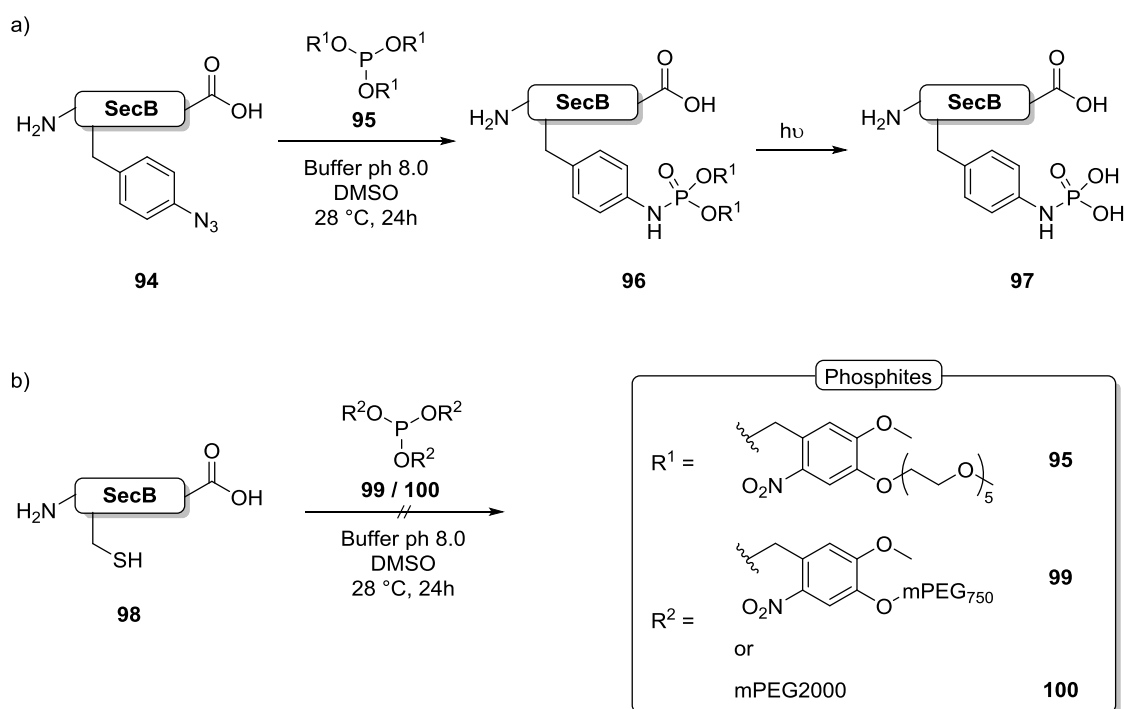
Scheme 1.24: Stable phosphoramidate formation *via* Staudinger-phosphonite reaction.

In 1919 Phoebus Levene identified that DNA is build-up of bases, carbohydrates and phosphates. He proposed that the nucleosides are linked *via* phosphates. After the elucidation of the DNA structure by Watson and Crick^[57] it was straight forward that one of the first biochemical related applications of the Staudinger-phosphite reaction was the coupling of nucleosides **92** (Scheme 1.25),^[34c] since the phosphoramidate **93** moiety is a mimic of the original phosphordiester in the DNA structure.



Scheme 1.25: Nucleoside coupling by Staudinger-phosphite reaction in an organic solvent.^[34c]

When it comes to labelling or modification reactions in biological chemistry, aqueous systems are the essential reaction medium since most biological relevant molecules are not soluble or stable in organic solvents. This was first shown in 2009 by the Hackenberger group, for the reaction of phenyl azide and trimethyl- and triethyl phosphite in pure water with 78 and 80% yield.^[7a] This reaction could afterwards be successfully transferred to unprotected azido peptides. Based on these results the applicability of the Staudinger reaction on a biological substrate, a protein e.g., was pursued. The first Staudinger-phosphonite reaction on the protein level was also achieved in 2009 by the Hackenberger group. In this study a photo-cleavable nitrobenzyl phosphordiester **96** was installed in SecB **94**, which was expressed with *p*-azidophenylalanine incorporated by nonnatural protein translation using the amber-suppression based orthogonal system^[58] at position 156. The light-induced deprotection of the *o*-nitrobenzyl groups yielded a phosphoramidate **97** which is an phosphotyrosine analogue (Scheme 1.26 a).^[7a]

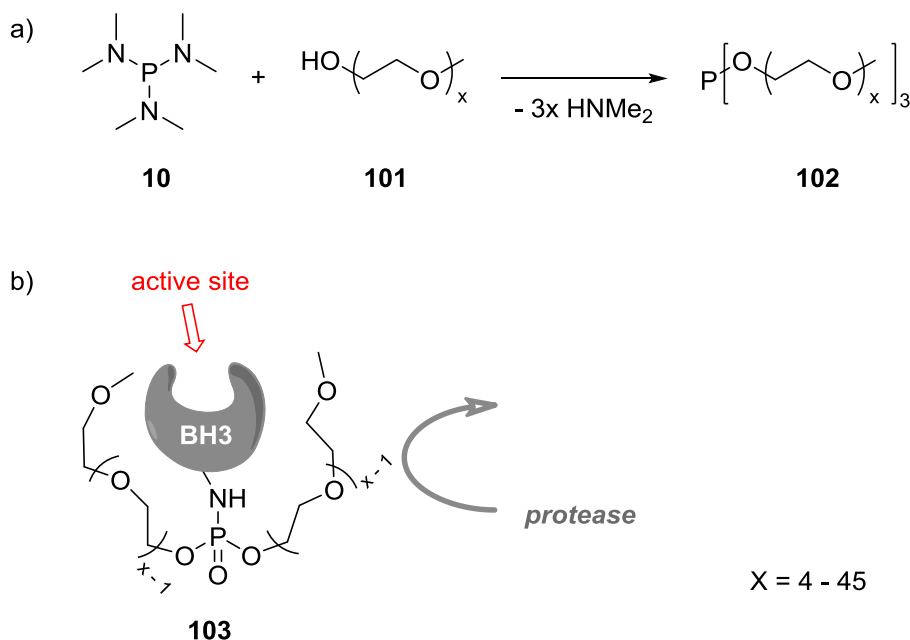


Scheme 1.26: a) The first Staudinger-phosphite reaction as chemical biological labelling reagent. b) Prove of chemoselectivity on the model azido protein SecB.^[7a]

The second very important requirement for bioorganic labelling reaction is its chemoselectivity (see chapter 1.2 for more details).^[35d, 56a] This was first demonstrated on the protein SecB where the *p*-azidophenylalanine containing mutant showed a clear shift on the SDS-PAGE that correlates to the size of the desired phosphoramidate **96** (the product was also confirmed by mass spectrometry). In the control experiment with SecB containing a cysteine **98** instead of *p*-azidophenylalanine no reaction with the phosphite **99** occurred (Scheme 1.26 b).^[7b] These experiments confirmed that the Staudinger-phosphite reaction is applicable as a bioorthogonal labelling tool.

Symmetrical phosphites contain three functional groups of the same kind. For this reason the Staudinger-phosphite reaction with symmetrical phosphites always leads to double functionalization (compare Scheme 1.24). This can be used as an advantage over other methods where only one functional module is introduced (e.g. CuAAC). For example, branched polyethylene glycols can be used to achieve the same bi-functionalization as with phosphites bearing two linear polyethylene glycol substituents. Phosphites **102** with linear mPEG substituents can be synthesised by a very simple one-step procedure from hexaalkylphosphanetriamine (**10**) and mPEG alcohol **101**, which do not even need a purification step (Scheme 1.27 a).^[59] This procedure is superior to the highly synthetic effort required for the synthesis of branched polyethylene glycol reagents. The later reagents have recently been used to *shield* a proapoptotic peptide BH3 **103** to enhance its proteolytic stability without

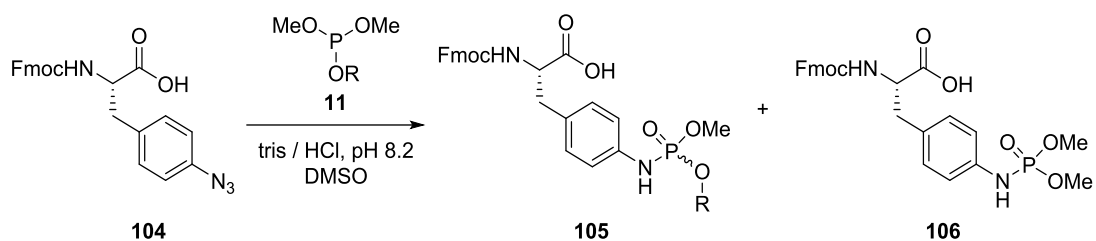
abolishment of its biological functional module (Scheme 1.27 b).^[59] These experiments demonstrated a very nice application of the Staudinger-phosphite reaction as a potent modification tool in chemical biology.



Scheme 1.27: a) Synthesis of symmetrical mPEG phosphites. b) Dipegylation of the peptide BH3 to enhance its proteolytic stability.

If double functionalization is an issue, unsymmetrical phosphites can be used to circumvent this problem. The key point is that phosphites contain three possible leaving groups (compare Scheme 1.24) and the one that carries the actual functional module has to stay at the phosphorus after hydrolysis of the phosphorimidate. Therefore, different substituents on an unsymmetrical phosphite **11** were probed by V. Böhrsch and R. Serwa against methoxy groups in a model system with Fmoc-*p*-azidophenylalanine **104** (Table 1.1)^[8] Careful design of the substituents on the phosphorus could now lead to an increased monofunctionalization (**105**) of an azido substrate. That was used to verify the presence of an azido protein in an *E. coli* lysate by chemoselective monobiotinylation in a western blot assay.^[8] Other than in the case of symmetrical phosphites **5**, does the reaction of unsymmetrical phosphites **11** with an azide lead to the formation of two diastereomers.

Table 1.1: Comparison of different leaving groups of unsymmetrical phosphonites in the Staudinger-phosphite reaction.



| Entry | R | 105 [%] | 106 [%] |
|-------|-------------|---------|---------|
| 1 | Dec | 85 | 15 |
| 2 | <i>i</i> Pr | 79 | 21 |
| 3 | Et | 71 | 29 |
| 4 | Ph | 50 | 50 |
| 5 | Bn | 28 | 72 |

Another interesting approach is the installation of the phosphite moiety on the substrate in order to allow a reaction with an unprotected azido carbohydrate in a Staudinger-phosphite reaction. Phosphites are synthesised by nucleophilic attack at the phosphorus (see chapter 1.1.1) and for this reason, nucleophilic groups at the substituents, such as free hydroxyl groups of carbohydrates, are not tolerated during the synthesis. Therefore, till now the synthesis of unprotected carbohydrate phosphites has not been realised. Protected carbohydrate phosphonites can be synthesised but the deprotection on the phosphite level was so far not successful and has to be done at the phosphoramidate level. Azides, however, tolerate most other functional groups and many reaction conditions.^[60] Therefore, introduction of an azide group to most functional modules is possible and unprotected carbohydrate azides are easily accessible. The Hackenberger group has addressed this issue and installed a phosphite moiety on the serine side chain of a protected peptide to functionalize it with an azido-carbohydrate.^[61]

1.3 Functionalization of biomolecules and polymers

An important field of research in modern life sciences is the study of biomolecules to reveal their structure and function. Many biomolecules in living organisms are enzymatically modified after their biosynthesis to control their desired folding and function, such as activation or inactivation. However, the isolation of fully intact biomolecules, such as proteins, with their complex modifications is often rather difficult if not impossible at all.^[62] For this reason, chemical and biochemical techniques to gain natural or modified active biomolecules are highly desirable and are a prerequisite for their detailed investigation.

Most of the unmodified proteins are accessible by overexpression in a cell-based (*in vivo*) or a cell-free (*in vitro*) system, but only very limited possibilities are given for the installation of natural occurring enzymatic modifications. Exceptions are disulfide bridges, because they are posttranslational modification that occur protein unspecific after the expression of the protein in the oxidative environment of the endoplasmic reticulum.

One of the most frequently occurring posttranslational modification is the phosphorylation of enzymes. Thereby a phosphate group is attached enzymatically onto an amino acid side chain. The most frequent residue for phosphorylation is the hydroxyl group of serine but also threonine, tyrosine, histidine arginine and lysine are phosphorylated in nature.^[63] This modification can turn a hydrophobic area of a protein into a very hydrophilic one which results in a conformational change of the protein. Nature is often using this technique as an activation mechanism.^[64] Therefore, a selective phosphorylation of the expressed enzyme is crucial to study its function and mode of action. Other important natural occurring posttranslational modifications are, for example, acylation, lipidation, glycosidation and methylation.^[65]

Besides natural occurring posttranslational modifications also unnatural modifications of biomolecules are of high interest in modern life science. They allow, on the one hand, the adjustment of their properties, such as their resistance against proteolytic degradation and, on the other hand, the attachment of special tags that enable there purification or tracking of the target protein in a living organism.^[66]

In 1962 the fundamental work for a revolutionary protein visualisation method was discovered by Shimomura by the isolation of the green fluorescent protein (GFP) from *Aequorea Jellyfish*.^[67] 30 years later, in 1992 Douglas Prasher could isolate the DNA of wtGFP. After successful cloning of the DNA, he was able to report its nucleotide sequence.^[68] Two years later, Martin Chalfie was the first who achieved the expression of GFP from *E. coli* cells, which now enables the cloning of the GFP gene into the gene sequence of interest.^[69] By using

this fusion protein a fluorescence marker is directly expressed together with the targeted protein. This revolutionary concept was so successful that it was honoured with the Nobel Prize in 2008.^[70] Nevertheless, due to its size of about 200 amino acids^[71] the fusion of GFP onto a target protein can hinder its function^[72] which may influence the experiment and lead to deceptive results. Therefore, the need of small biocompatible sensors is still an important field of research.

For the chemical modification of proteins two general strategies exist. The first one uses the natural occurring functional groups of a protein,^[73] whereas the second one makes use of functional groups that do not occur in nature and are capable to undergo chemoselective reactions without interference of any natural occurring functional group.

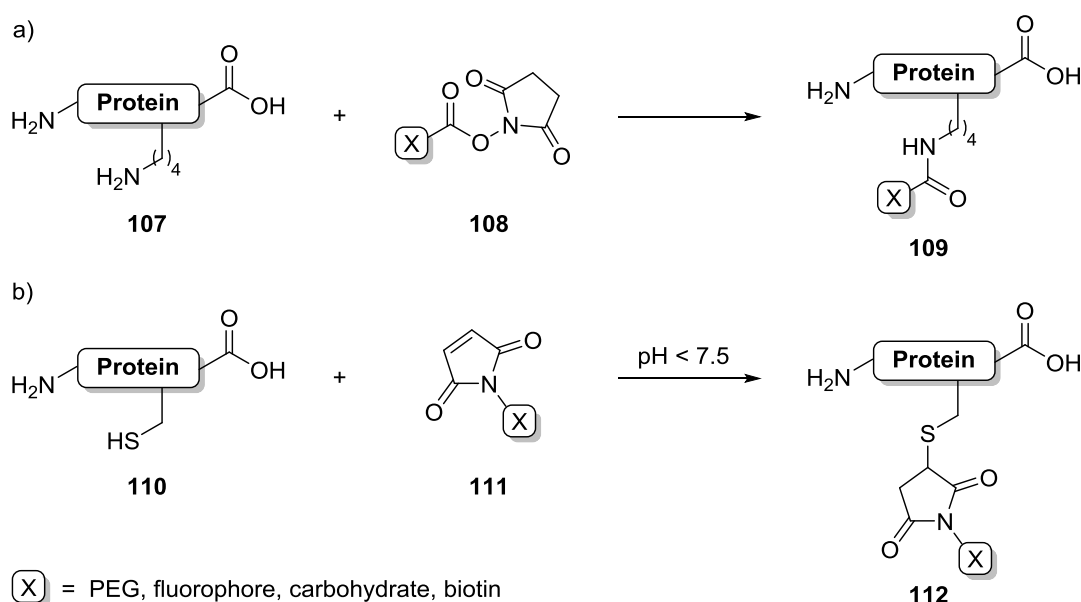
Chemoselective reactions have allowed the access to modified biomolecules to which access is very difficult to be reached by means of classical genetics. One of the most powerful tools to visualize biological processes *in vitro* as well as *in vivo* is the selective labelling of the target molecule by the attachment of a fluorophore in a chemoselective reaction. By means of this technique Bertozzi *et. al.* were able to illuminate the sialome^[74] of zebrafish embryos during their development by fluorogenic labelling of *N*-azidoacetylmannosamine *via* copper-free alkyne-azide cycloaddition.^[75] Another very important modification in life science is the attachment of polyethylene glycol chains (PEGylation) onto a protein or a targeted drug.^[59] Polyethylene glycol chains can wrap around the target and protect it from an immune response from proteases which is known as "*umbrella effect*".^[76] An additional benefit of PEGylation of pharmaceutical drugs is the increase in molecular weight that reduces its renal clearance drastically. Graf *et. al.* found that 66% poly(lactic-co-glycolic acid) microspheres were removed from the bloodstream through renal clearance. After attachment of a 20 kDa PEG group two hours later only 30% of the PEGylated drug was removed from the bloodstream.^[77] For that reason the selective modification of biomolecules has become an important tool in bioorganic research.

1.3.1 Modifications of proteins through natural occurring functional groups

Proteins already bring a lot of different functional groups that can undergo chemical reactions after translation. All functional groups available in a protein have different pK_a values and therefore their reactivity can be controlled by the pH. This fact allows a selective reaction on one kind of amino acid residue as mostly applied for modification strategies of the amine group of lysines, the thiol group of cysteines and the N-terminus of the protein. Nevertheless,

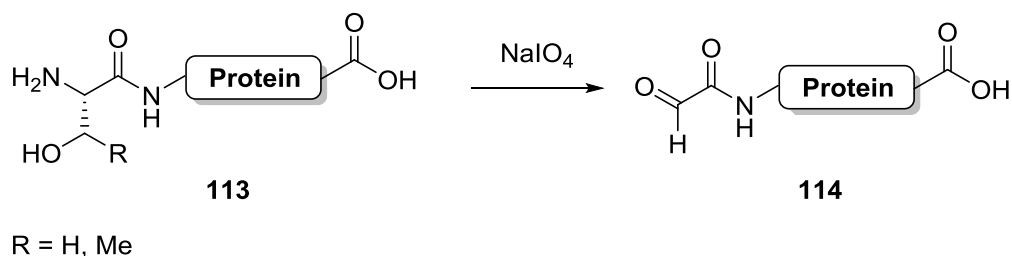
the pK_a value is dependent on the individual local environment of the functional group and some functional groups are not accessible at all due to protein folding.^[56a, 78]

Lysine is a common target for modification reactions because a lot of reactions are available for the selective modification of primary amines. Activated esters like *N*-hydroxysuccinimides of functional modules **108** form stable amid bonds **109** with primary amines **107** (Scheme 1.28 a) but also other electrophilic reagents like sulfonyl chlorides, isocyanates or isothiocyanates react selectively on the amino-residue of lysine.^[56a, 73, 78] Cysteine peptide **110** can either form disulfide bridges with a thio group bearing a functional module or act as a nucleophile. The latter reacts very selectively with maleimides **111** at pH values below 7.5 in a thiol-Michael reaction to the addition product **112** (Scheme 1.28 b). At higher pH's the maleimide **111** favours the primary amine group of lysine.^[79]



Scheme 1.28: Selective modifications of a) lysins^[73, 78] and b) cysteins in proteins.^[79]

The N-terminus ($pK_a \sim 8$) of a protein is slightly more acidic than the primary amine group of lysine ($pK_a \sim 10.5$) due to the electron withdrawing carbonyl group in β -position.^[80] Therefore, the N-terminus offers the possibility of a single-site modification of a protein.^[81] The whole N-terminal amino acid of a protein also allows specific reactions that additionally depend on the amino acid side chain. N-terminal serine or threonine **113** can be oxidised by periodate to form glyoxylamide proteins **114** (Scheme 1.29).^[82] This modification is interesting because it introduces an aldehyde as chemical reporter into the protein. At a later stage this aldehyde moiety of the glyoxylamide can undergo oxime or hydrazone formation with aminoxy or hydrazine reagents (see 1.3.2.2). All the preceding reactions only allow the modification of solvent accessible side chains but not those inside the folded protein.



Scheme 1.29: Glycol cleavage of N-terminal serine or threonine proteins **113**.^[82]

1.3.2 Modifications of biomolecules through unnatural functional groups

The incorporation of unnatural amino acids in peptides is routinely achieved by solid-phase peptide synthesis.^[83] Because this technique is independent from any biological enzymatic process, all kinds of protected, unnatural amino acids can be introduced as long as they are compatible with the applied coupling and deprotection conditions. In addition, due to the large variety of available protecting groups, chemical modifications of peptides are routine protocols in any laboratory.^[84]

On the protein level, global protecting group strategies are not available. Therefore, direct chemical modifications at a desired position are mostly not possible. Moreover, the biological organism is only able to incorporate molecules which are similar to the original ones with respect to structure and charge.^[58b, 58d, 58f] The fact that the biological machinery is capable to introduce similar unnatural amino acids opens the opportunity to a two-step reaction sequence for chemical modification of peptides. Based on this strategy the introduction of a functional group that is not naturally occurring in biological systems, a so-called chemical reporter, is possible. The combination of a chemoselective reaction that exclusively reacts with the introduced chemical reporter enables the selective modification or the attachment of a functional module at a specific position.^[56a] In 2003 Bertozzi *at. al.* introduced the term *bioorthogonal* for chemoselective reactions of chemical reporters that are capable to proceed *in vivo*, are stable towards the biological environment and giving only harmless by-products.^[85]

Amongst these chemical reporters, azides, alkynes and alkenes have been used most frequently,^[56a] since these functional groups do not occur in biological systems. Consequently, they are so-called bioorthogonal reporters. In addition, these functional groups could be introduced into a variety of proteins by *in vivo* expression methods.^[86]

1.3.2.1 Introduction of an unnatural functional group into proteins

The first introduction of an unnatural amino acid to a protein was achieved by the use of an *Escherichia coli* strain that is auxotrophic for a certain amino acid. The strain has to ingest the missing amino acid from the growth medium. By growing in minimal medium, this amino acid can be replaced by a structurally similar non-natural analogue that is instead incorporated into the protein instead.^[58d, 87] Methionine is the most frequently used amino acid replaced by so-called *auxotrophic expression*^[88] because it is one of the least abundant amino acids with only 1.7% in the average amino acid composition of proteins.^[3] Therefore, a single or 'only' double incorporation into a protein is often achieved. Other amino acids that can be replaced by this technique are leucine^[89], isoleucine^[90], phenylalanine^[91], tryptophan^[92] and proline^[93].

One of the drawbacks of auxotrophic expression is the often poor recognition of the unnatural amino acid by the *tRNA*. The *tRNA* can genetically be modified to loosen its specificity leading to an increased incorporation rate. Additionally, overexpression of the *tRNA* can enhance the yield of the unnatural protein. Another disadvantage of the auxotrophic expression method is that the position cannot be randomly chosen and, as already mentioned, that it is in most cases not possible to exchange a single amino acid.

The site-specific incorporation of an unnatural amino acid into a protein requires a separate codon that exclusively encodes the unnatural amino acid. To avoid any interference with existent triplet codons for natural occurring amino acids, the three nonsense codons (TAG, TAA and TGA)^[58a, 58e, 86b, 94] or frameshift (quadruplet) codons^[95] are capable to fulfil this task.

The side-specific incorporation of an unnatural amino acid into a protein *via* modified *tRNA* was achieved by P. G. Schultz *et. al.* in 1989.^[94b] This methodology makes use of an orthogonal *tRNA* in which the original anticodon is exchanged to CUA e. g. to bind to the amber stop codon UAG. This suppressor *tRNA* is chemically acylated with the unnatural amino acid. Then the acylated suppressor *tRNA* is added to an *in vitro* or *in vivo* expression system. The acylated *tRNA* can be transferred into the cell either by microinjection or electroporation. The applied suppressor *tRNA* must fulfil two major requirements. First, it must neither be acylated nor deacylated by any endogenous aminoacyl-*tRNA* synthetase present in the expression system. This is achieved by utilising a *tRNA* from a different organism than the host. Secondly, the unnatural amino acid must be efficiently inserted in response to the UAG message to yield sufficient quantities of protein which can be accomplished by knocking out the release factor one (RF1).^[58a, 86b] Because the suppressor *tRNA* is acylated chemically and is therefore independent of any aminoacyl-*tRNA* synthetase, a wide structural variety of the amino acid is tolerated. Over 80 different unnatural amino acids have been incorporated into proteins by this

technique.^[96] The drawbacks of this methodology are the poor yield of protein and the bad molecular economy as every chemically acetylated tRNA can only be used once.^[86b]

In 2001 Schultz *et. al.* were able to overcome the drawback of the chemical aminoacylation of the suppressor tRNA. They introduced an orthogonal tRNA^{Tyr}_{CUA} / tyrosyl-tRNA synthetase pair derived from *Methanococcus jannaschii* into an *E. coli* strain that encodes *O*-methyl-tyrosine by the amber stop codon (UAG).^[94d] The orthogonal synthetase was mutated to only accept the non-natural amino acid. This is essential to avoid cross interactions with the endogenous synthetases. Additionally, the orthogonal tRNA / tRNA synthetase pair must not be depredated by endogenous metabolic enzymes.^[58a, 58b] With respect to the unnatural amino acid the limitations are given, on the one hand, by the synthetase which only accepts unnatural amino acids that are similar in size and charge to the original one and, on the other hand, by the membrane permeability of the amino acid which is necessary for sufficient uptake by the host organism.^[86b] The spectrum of viable amino acids was broadened by the introduction of new orthogonal tRNA / tRNA synthetase pairs such as for *p*-azidophenylalanine^[97] or the 22nd proteinogenic amino acid pyrrolysine.^[98] Pyrrolysine (Pyl) was found in the *Methanosarcina barkeri*, where it is encoded by an UAG codon being the amber stop codon in most organisms. Therefore, the tRNA must not be genetically modified to bind at the nonsense codon in an expression system like *E. coli*.^[94e] The orthogonal tRNA^{Pyl} / Pyl-tRNA synthetase pair allows for example the incorporation of azide and alkyne containing lysine derivatives into proteins where they function as chemical reporters for chemoselective modification reactions.^[99]

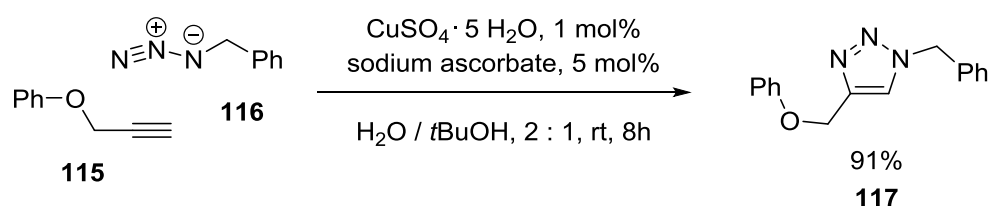
Unnatural functional groups can also be introduced enzymatically into a protein. Biotinylation of a protein can be achieved by the biotin protein ligase BirA. BirA binds biotin and converts it with the help of ATP to its active form biotinoyl-5'-AMP (bioAMP). In a second step, the bioAMP containing BirA binds to a specific biotin acceptor tag (BAT), which is fused to the protein of interest. The bioAMP-containing BirA can now biotinylate a lysine residue within the BAT sequence.^[100] Another example for the enzyme-mediated introduction of an unnatural functional group into proteins is the oxidation of a cysteine within a recognition sequence to C_α-formylglycine by the formylglycine-generating enzyme (FGE).^[101]

1.3.2.2 Chemoselective functionalization reactions for biomolecules

One important chemoselective modification reaction for biomolecules is the Staudinger ligation. The development of the Staudinger ligation was already described in chapter 1.2.2. Over the last years many other potent reactions had been evolved as chemoselective and / or bioorthogonal modification reactions such as the copper-catalysed alkyne-azide cycloaddition (CuAAC), the strain-promoted alkyne-azide cycloaddition (SPAAC), the Diels-Alder based tetrazine ligation or the oxime and hydrazone ligation.

The copper-catalysed alkyne-azide cycloaddition (CuAAC)

The [3+2] cycloaddition between an azide and an alkyne was first described by A. Michael in 1893^[102] and was later examined in detail by R. Huisgen.^[103] In 2002 K. B. Sharpless^[104] and M. Meldal^[105] discovered independently that copper(I) catalyses the [3+2] cycloaddition between an azide and an alkyne. The copper(I)-catalysed cyclisation between alkynes **115** and azides **116** forms a regio-selective 1,2,3-triazoles **117** at room temperature in aqueous systems (Scheme 1.30) and since both, the alkyne **115** and the azide **116**, are bioorthogonal reporters, it seems like the ideal functionalization reaction for biomolecules. The only disadvantage is the high toxicity of copper that limits its application in living systems. A lot of investigations are in progress in order to achieve the complexation of the free copper(I) to accelerate the reaction, to lower its toxicity as well as its tendency to oxidise to the catalytically inactive copper(II).^[106]

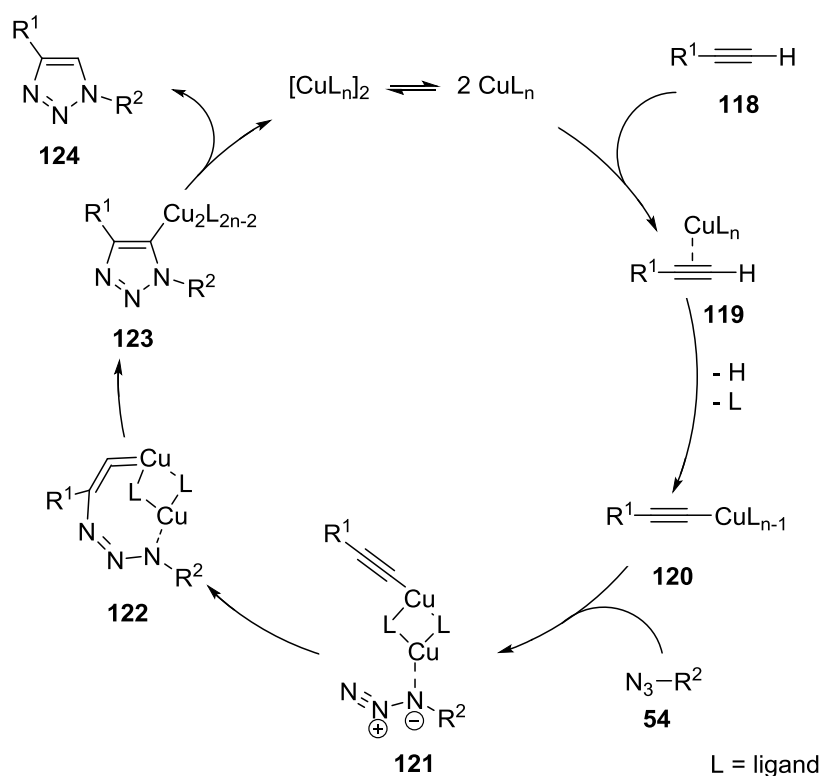


Scheme 1.30. The first copper-catalysed alkyne-azide cycloaddition as described by Sharpless.^[104]

It is very important that the CuAAC cannot be classified as [3+2] cycloaddition anymore as the uncatalysed variant. The reaction mechanism of the CuAAC (Scheme 1.18) starts with the coordination of the copper to the π -electrons of the alkyne **118** under formation of complex **119** which drastically lowers the pK_a value of the terminal alkyne **118**. Basic removal of the terminal proton of the copper-alkyne π -complex **119** leads to the formation of the copper-acetylide intermediate **120**. The copper-acetylide intermediate **120** coordinates another

copper ion that is now able to coordinate the azide **54** through the nitrogen proximal to the carbon. After the distal nitrogen of the complex **122** attacks the C-2 carbon of the acetylide, the triazole **123** is formed. In the last step, the triazole **123** is protonated and the copper catalyst is cleaved off to yield the 1,2,3-triazole product **124**.^[107]

Although the copper-catalysed alkyne-azide cycloaddition is commonly not denoted as bioorthogonal because of the required toxic copper catalyst,^[108] it is frequently used for the modification of peptides and proteins.^[109]

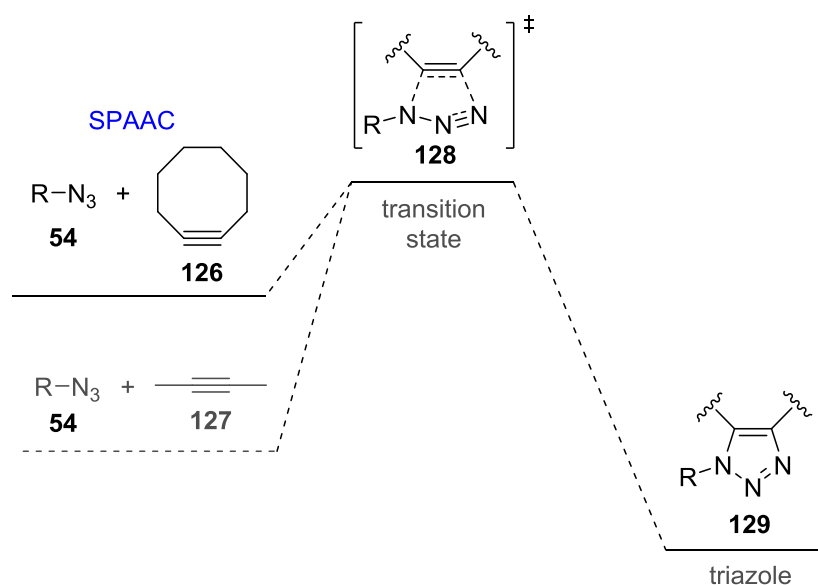


Scheme 1.31: Reaction mechanism of the copper-catalysed alkyne-azide cycloaddition.^[107a]

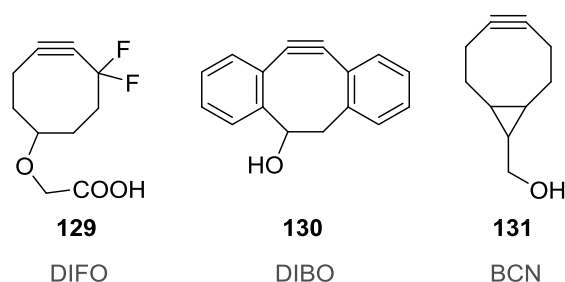
Strain-promoted alkyne-azide cycloaddition (SPAAC)

The major drawback of the CuAAC is the required cytotoxic copper catalyst. For this reason, Bertozzi *et. al.* introduced cyclooctynes as bioorthogonal reagents.^[110] The *explosive* reaction between azides and cyclooctynes was already described by Wittig and Krebs in 1961^[111] but it had not been applied in the field of bioorganic chemistry before. *Cis*-cyclooctynes are considered to be the smallest stable cycloalkynes. Their bond-angle is curved to 163°^[112] and because of this fact they exert a ring strain of about 18-19.9 kcal/mol.^[113] This results in an about 8.2 kcal/mol lower activation energy due to the lower energy gap between the transition

state **127** and the cyclooctynes **125** compared to linear alkynes **126** (Scheme 1.32). The lower activation energy of the [3+2] cycloaddition leads to an increased reaction rate of ten to the power of six.^[114] The reaction rate of cyclooctynes with azides ($k = 10^{-3} \text{ M}^{-1} \text{ s}^{-1}$) is slower than the one of the Staudinger reaction.^[110] The reaction rate can be enhanced by either lowering the LUMO of the cycloalkyne by the attachment of two electron withdrawing groups next to the alkyne moiety as in difluorocyclooctyne **129** for example^[115] or by further enhancement of the ring strain as in dibenzocyclooctyne **130** or bicycle[6.1.0]nonyne **131** shown by Boons *et. al.* and van Delft *et. al.* (Scheme 1.33).^[116] Differently from the CuAAC, the SPAAC is not regio-selective and leads to a mixture of isomers depending on the cyclooctyne.



Scheme 1.32: The strain-promoted [3+2] azide-alkyne cycloaddition and in comparison to the 2-butyne.^[113a, 117]



Scheme 1.33: The second and third generation of cyclooctyne reagents.^[56a]

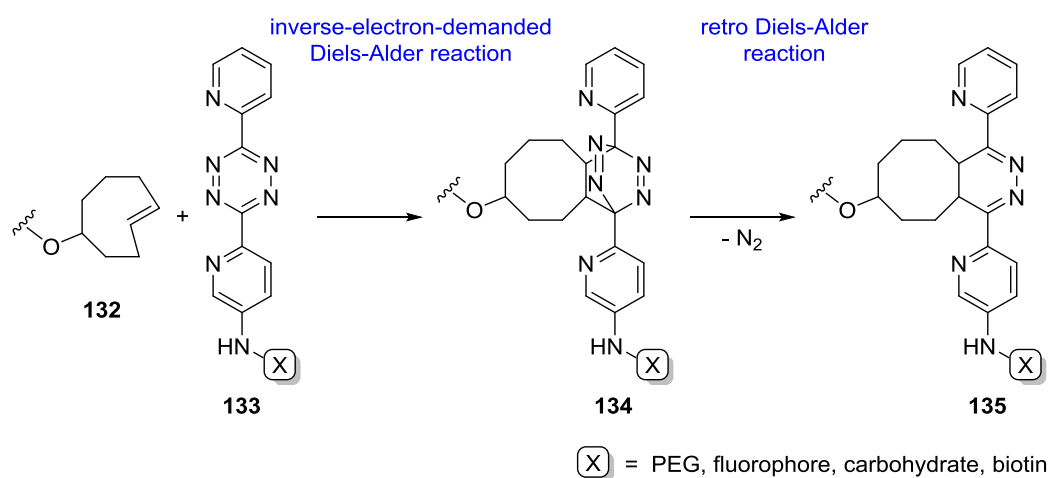
The enhancement in reactivity of the cyclooctyne reagents goes simultaneously with the decrease of its stability. Harsh reaction conditions must be avoided during the attachment of a functional module onto e. g. 9-hydroxymethylene bicycle[6.1.0]nonyne (**131**) because the cyclooctyne moiety gets degraded. The chemoselectivity of modified cyclooctynes is still not clarified. Both C. R. Bertozzi^[110] and H. S. Overkleeft^[118] reported high background fluorescents if

cyclooctyne based markers were used for the labelling of Jurkat cells incubated with *N*-azidoacetylmannosamine or azide-modified proteasome in an HEK293T cell lysate. The background fluorescents occur 'perhaps because of nonspecific hydrophobic interactions or as yet uncharacterized reactions with protein functionalities' (C. R. Bertozzi^[56a]).

Nevertheless, cyclooctynes are very potent reagents for the modification of cell surfaces^[75], proteins^[118-119], or *in vivo* labelling of life cells^[115, 120] and Zebrafish embryos^[121] at low concentrations. With commercially available bicycle[6.1.0]nonyne **131** as building block or fluorescent labelling an biotinylation reagents ready to use, the number of SPAAC based applications in biological chemistry will further increase.

Diels-Alder based tetrazine-ligation

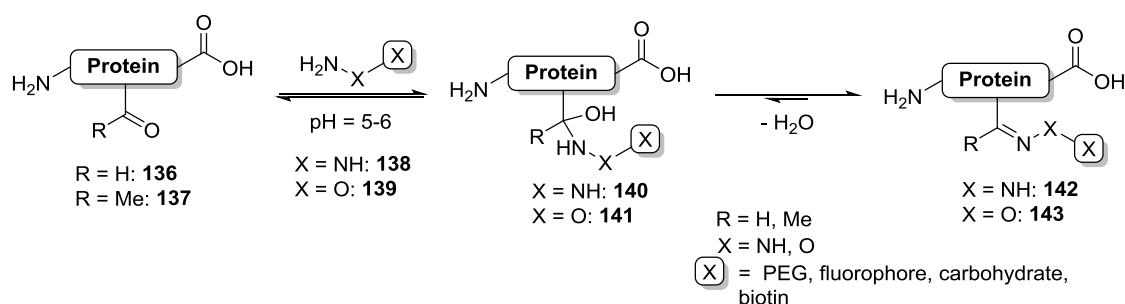
The Diels-Alder reaction is a classic organic reaction with numerous applications in organic synthesis.^[122] The Diels-Alder reaction was also applied for bioconjugations but the required dienophiles, which are also Michael acceptors, can undergo Michael additions with other nucleophilic residues (see Scheme 1.28 b).^[123] In 2008 Fox and co-workers applied the tetrazine **133** reverse-electron-demanded Diels-Alder leading to **134** - retro Diels-Alder leading to **135** sequence^[124] for the first time as a bioconjugation method.^[125] Fox used a strained *trans*-cyclooctene **132** to achieve an incredibly fast, second rate order reaction ($k = 2 \times 10^3 \text{ M}^{-1} \text{ s}^{-1}$) (Scheme 1.34). Combined with a high tolerance of other functional groups and molecular nitrogen as the only by-product, these chemical reporters are very potent for *in vivo* protein modifications at low concentrations.



Scheme 1.34: Diels-Alder-based tetrazine-ligation with *trans*-cyclooctene.^[125]

Oxime and hydrazone ligation

Aldehydes **136** and ketons **137** undergo condensation reactions with amines to form oximes. Oximes derived from primary amines hydrolyse in the presence of water very fast and no oxime formation with lysine or the N-terminus of proteins is observed. Hydrazides **138** and alkoxyamines **139** were however found to form water-stable hydrazones **142** or oximes **143** due to the α -effect.^[126] The reaction proceeds best at a pH between five and six because nucleophilic attack of the nitrogen is favoured if the carbonyl group is protonated.



Scheme 1.35: Formation of water-stable oximes or hydrazones from hydrazides or alkoxyamines.^[126]

Due to the requirement of low pH, extracellular applications are highly favoured. Nevertheless, Schultz *at. al.* were able to demonstrate the intracellular labelling of a ketone-functionalized protein.^[127] In 2006 Dawson and co-workers introduced aniline as catalyst for the oxime-^[128] and hydrazine-ligation.^[129] The presence of 1000 mol% of aniline accelerated the relatively slow hydrazone formation ($0.03 \text{ M}^{-1} \text{ s}^{-1}$) to $170 \text{ M}^{-1} \text{ s}^{-1}$. The reaction rate of the oxime-ligation could only be accelerated to $8.2 \text{ M}^{-1} \text{ s}^{-1}$ under the same conditions.

1.3.3 Functionalization of polymers

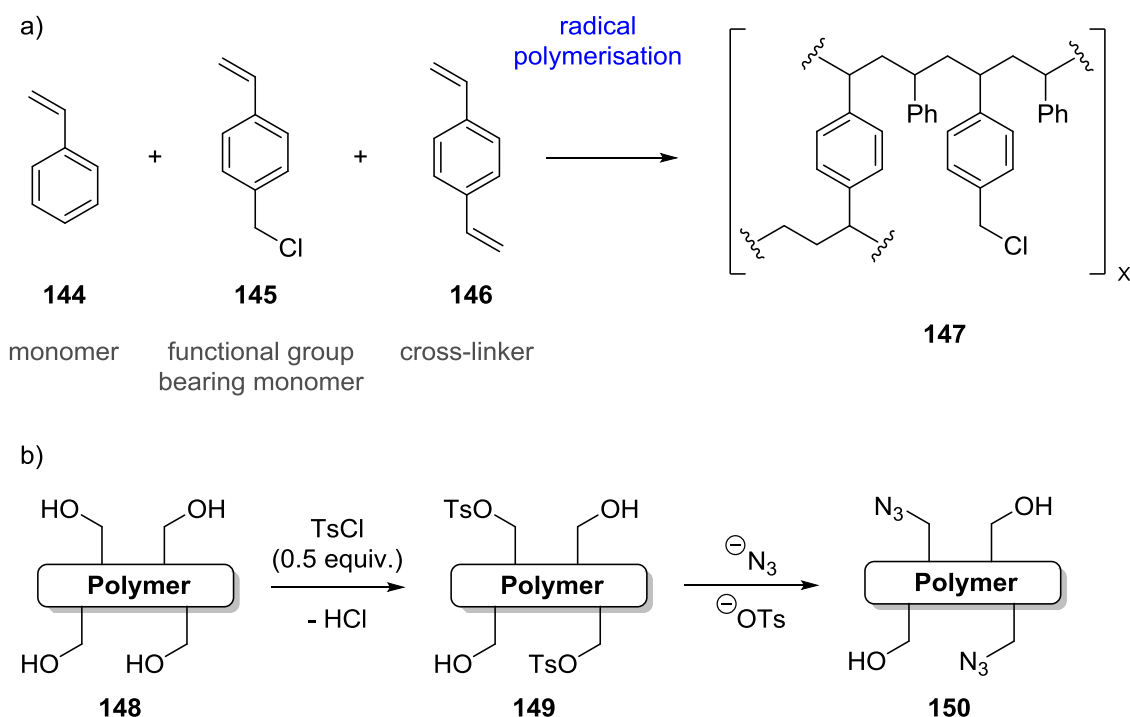
In addition to proteins and other biopolymers, polymers represent also an important class of target molecules when it comes to the application of functionalization methods due to their very interesting properties. Polymers are chemically very inert, potentially soluble in water and most organic solvents, non-toxic, and can easily be purified by dialysis or filtration. All these exceptional properties make polymers very attractive for a high number of applications. Furthermore, most polymers are accessible from very cheap starting materials in standard straightforward procedures.

One well-known application of polymer functionalization in the field of chemistry is the solid-phase synthesis. This technique is mainly applied for the synthesis of peptides in automated processes using a polystyrene core, invented by Robert Bruce Merrifield in 1963.^[83] In the so-called solid-phase peptide synthesis (SPPS), the peptide chain is bound to the solid support during all coupling steps, which allows easy separation of excessive reagents by simple filtration. This advantage results in a great benefit in time and effort, especially when combined with modern microwave technique. The ground-breaking technique of SPPS was honoured with the Nobel Prize in 1984.^[130] However, peptides are not the only molecules that are normally synthesised by polymer-based solid-phase synthesis, also DNA and RNA sequences are commonly synthesised on solid support. For example large-scale custom synthesis of DNA primers is only possible because of solid-phase synthesis. Moreover, the only recently by P. H. Seeberger developed automated carbohydrate synthesis on solid-support opens up a fast entrance to high amounts of glycans that can act as potential inoculants for many diseases.^[131]

In the field of solid-support synthesis, the most common polymers are polystyrenes but also other polymeric materials, especially polyethylene glycol and polyglycerol play an important role in chemical research. The functionalization of polystyrene is permitted by the addition of functional group-containing monomers e. g. 4-(chloromethyl)-styrene (**145**) to the polymerisation process to functionalized polystyrene **147** (Scheme 1.36 a). The degree of functionalization is thereby controlled by the amount of the functional group-bearing additive **145**. However, different applications also require differently functionalized polymers and interconversion of the given functional group is a standard protocol in polymer chemistry. For the functional group interconversion on the polymer (not only polystyrene but also polyglycerol) special requirements with regard to the applied chemical reactions must be fulfilled. As a single polymer molecule carries many units of a functional group, separation of unreacted starting material or undesired by-products from the product is impossible. With many reactions like tosylation or S_N2 reactions available most functional groups can be introduced onto polymers. During the functional group interconversion (**148** -> **149** -> **150**) the quantity of reagents can be used to generate bi-functional polymers (**149**, **150**). Polyglycerols, in which only 40% of the natural hydroxyl groups are exchanged to another functional group for further modifications, show a high solubility in polar solvents like water due to the remaining hydroxyl groups (Scheme 1.36 b).^[132]

A significant difference between polystyrene and polyglycerol is there solubility. Whereas polystyrene is not soluble at all, polyglycerol is a liquid and soluble in many organic solvents and even in water depending on its functional groups attached. Therefore, reactions of polystyrene are biphasic reactions and particular caution must be taken during the reactions in

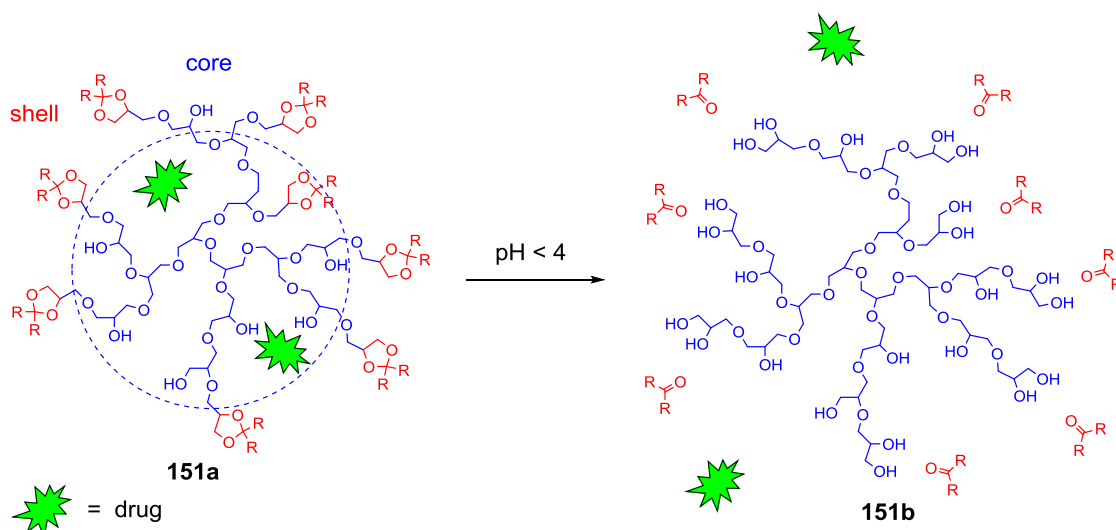
order not to mechanically destroy the polystyrene by magnetic stirrers. Polystyrene has got the advantage of easy purification by filtration. Polyglycerols on the other hand are in solution during its reactions and can be handled as 'normal' chemicals. This variance results in different fields of applications for both types of polymers.



Polymer = e. g. polystyrene, polyethylene glycole

Scheme 1.36: a) Radical polymerisation of styrene with functional group-bearing monomer and cross-linker. b) A general functional group interchanging sequence for polymers.

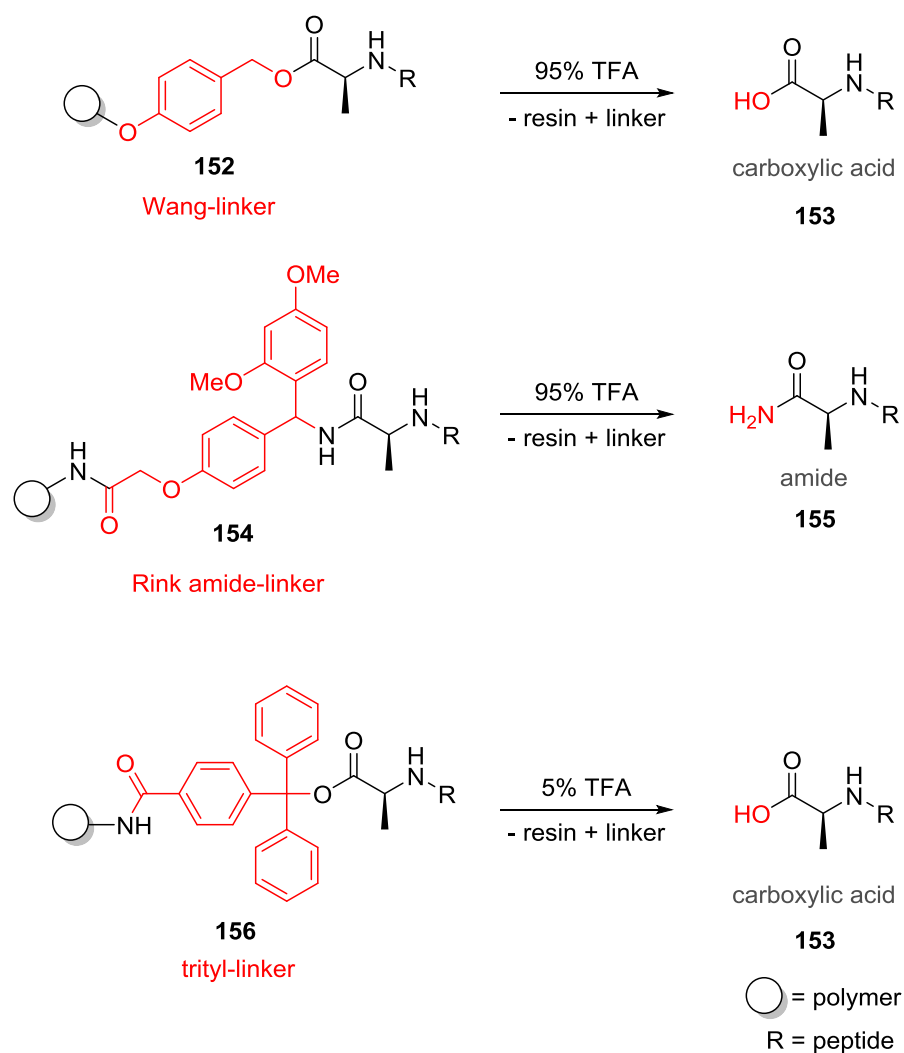
A smart functionalization interconversion strategy of polyglycerol offers the possibility for pH-dependent, selective drug delivery systems. In this case, the hydroxyl groups of the polyglycerol core were functionalized with an acid-labile acetal shell **151a**.^[133] The drug was non-covalently bound in the polyglycerol core. Under acidic conditions (pH < 4), as in some tumour cells, the acetal shell is cleaved and the drug is released into the cell (Scheme 1.37).^[134]



Scheme 1.37: A core-shell-functionalized polyglycerol for pH-dependent drug delivery.^[134]

The functionalization strategies of polymers for the solid-phase synthesis must fulfil additional criteria. Firstly, the connection to the solid-support must be compatible with all further applied reaction conditions and secondly must allow cleavage of the final product from the polymer. This can be achieved by the introduction of special linkers.^[135] The linker is attached to a polymer core as described in Scheme 1.36 and afterwards further functionalised with the starting molecule for the solid-phase synthesis. The linker is bound to the resin *via* a very strong covalent bond, an amide or an ether bond for example, that is stable under the cleavage conditions. The binding of the starting molecule for the synthesis must be individually chosen in dependence on its stability and the applied reaction conditions. For the solid-phase peptide synthesis three examples of different linkers are given in Scheme 1.38. The first amino acid is always attached by coupling of its corresponding active ester. All three connection systems shown are stable against basic conditions but the cleavage conditions differ in the examples. The Wang-linker **152**^[136] and the Rink amide-linker **154**^[137] release the peptide with 95% TFA, whereas the trityl-linker **156**^[138] is cleaved already if only 5% TFA is applied. The Wang-linker **152** and the trityl-linker **154** deliver the free carboxylic acid **153** as cleavage product, whereas the Rink amide-linker **154** gives the corresponding amide product **154** (Scheme 1.38). A countless number of different linker systems for solid-phase synthesis are available on the market for all kind of reaction conditions and cleavage conditions.^[139]

Block copolymers like TentaGel® resins can combine different properties. The polystyrene core gets first functionalized with a polyethylene glycol chain to which the linker for the solid-phase synthesis is attached.^[140] That allows an easy purification after every reaction step due to the polymer core and at the same time the block copolymer is in a suspension state that allows NMR measurements.^[141]



Scheme 1.38: Three examples of linker systems for solid-phase peptide synthesis.^[136a, 137-138]

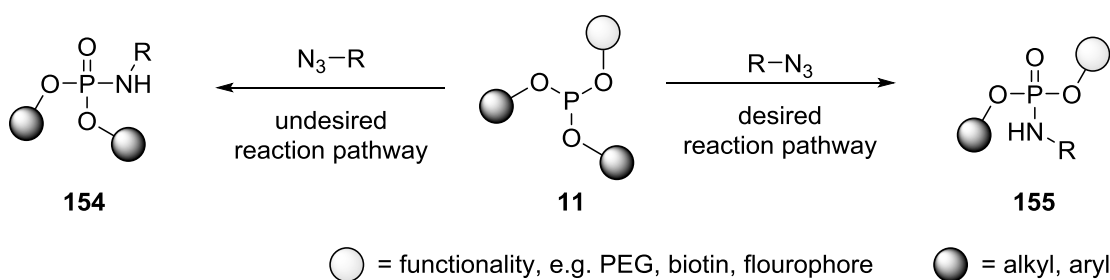
Dendritic polymers are another very interesting class of polymers that require additional functionalization techniques. Dendritic polymers with their ball-like shape and functional groups presented at the surface are excellent model substrates for cell surface receptor-binding studies. The carbohydrate moieties responsible for the recognition of the cell-surface receptors are synthesised in solution and must then be efficiently bound to the dendritic polymer.^[132, 142] The copper-catalysed alkyne azide cycloaddition is often used to reach this target, even so the copper catalyst is difficult to be removed from the chelating hydroxyl groups of polyglycerols. Therefore, efficient coupling reactions under mild reaction conditions are of high interest.

2 Objective

Inspired by the huge success of the Staudinger ligation^[24b-d, 35b, 35c, 143], the Hackenberger group started to further expand the Staudinger reaction into a modification tool for biomolecules^[7-8]. In contrast to in the Staudinger ligation, where an amide group is cleaved from the phosphonium ion, in Staudinger-phosphite reactions an alkoxy group acts as the leaving group and a stable phosphorus-nitrogen bond is formed. The Staudinger-phosphite reaction was successfully applied for the synthesis of PEGylated peptides and proteins, glycosylation and for the synthesis of a phosphotyrosine analogue at the peptide and protein level.

It is advantageous to introduce the functional module *via* the phosphite, which is synthetically much easier to achieve in terms of purification than the incorporation of the phosphite into the target peptide followed by the introduction of the functional module through the corresponding azido compound. On the peptide level orthogonal protecting groups are required for the selective incorporation of a phosphite group. During the final cleavage of the other protecting groups from the peptide some of the phosphite is taken off again as well.^[61]

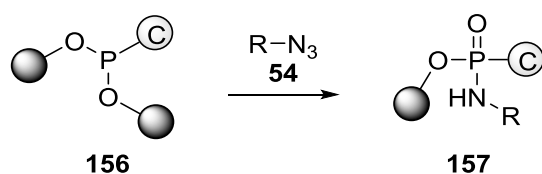
Nevertheless, two obvious problems are given by the nature of phosphites. Firstly, in the case of symmetrical phosphites **5**, double-functionalization occurred, which is only desirable at some occasions^[7b, 59]. Second, if mono-functionalised phosphoramidates **155** are required, unsymmetrical phosphites **11** can solve the problem but selectivity of the leaving group propensities is problematic and can lead to undesired side products **154** (Scheme 2.1).^[8]



Scheme 2.1: Staudinger reaction of an azido compound with an unsymmetrical phosphite **11**.

These two deficiencies can be overcome by functionalised phosphonites **156**. Compared to the phosphorus-oxygen bond the phosphorus-carbon bond in phosphonites **156** is much more stable. This ensures that carbon bond functionalities stay in the newly formed phosphoramidate product **157** (Scheme 2.2). Another advantage of phosphonites **156** compared to phosphites **11** is their higher reaction rate in both consecutive steps of the

Staudinger reaction because they only hold two electron-withdrawing substituents.^[24a] Since aryl phosphonites are less prone to oxidation as compared to alkyl phosphonites due to the slightly higher electron negativity of the sp^2 hybridised carbon atom, this work focuses on aryl phosphonites. All the given properties make the Staudinger-phosphonite reaction a very promising reaction with high potential as labelling reaction in bioorganic chemistry.



Ⓒ = carbon bound functionality, e.g. PEG, biotin, fluorophore ● = alkyl, aryl

Scheme 2.2: Staudinger reaction of an azido substrate and a phosphonite.

First project: Development of the Staudinger-phosphonite reaction as modification

tool

➤ Synthesis of functionalised phosphonites

The first aim of the project was to establish a synthetic route for functionalised phosphonites **156** (Figure 2.1). The synthesis should be as versatile as possible to enable the incorporation of different functionalities with as little optimisation of the protocol required as possible. Since these phosphonites **156** should be used for protein and peptide modification, for which the reaction media is mostly a buffer, water-solubility would be worthwhile.



Ⓒ = functional module, e.g. PEG, biotin, fluorophore

● = aryl, alkyl, alkynyl

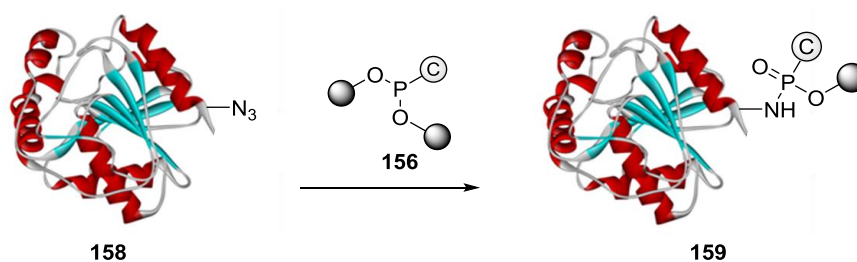
Figure 2.1: The first goal was to establish a versatile synthesis route to functionalised phosphonites **156**.

➤ Investigating the Staudinger-phosphonite reaction

In the second part of this project the synthesised phosphonites **156** should be applied in Staudinger reactions with different azido-containing molecules. Since the reaction of a phosphonite with an azide in water was never achieved before, it would be necessary to analyse the whole reaction process. This includes probing the chemoselectivity, side product formation and stability of the phosphonite reagents **156** as well as the phosphoramidate products **157** under biorelevant conditions.

A core part in this project is the quantification of the phosphoramidate **157** in the Staudinger reaction under different reaction conditions. Since peptide and especially protein reactions are normally performed at very low concentrations, optimal conditions had to be found with regard to the azide and phosphonite concentration leading to high conversions of the azide to the phosphoramidate product **157**.

As a final goal of this project an application of the Staudinger-phosphonite reaction on the protein level is desired in order to demonstrate its applicability as modification method (Scheme 2.3).



Scheme 2.3: Protein functionalization by Staudinger-phosphonite reaction.

Second project: Synthesis of coumarin phosphites

It has already been shown that phosphites **4** are very efficient for the functionalization of azido peptides and proteins by the Staudinger reaction.^[7-8] The applicability of such a functionalization method is highly dependent on the variety of compounds which are synthetically available. The aim of this project was now to synthesise coumarin phosphites **160**, to be used in Staudinger-phosphite reactions.

Coumarins offer some very interesting properties which can be particularly useful in Staudinger reactions. First of all, coumarin is fluorescent and can be used to visualise the substrate molecule.^[144] Secondly, coumarins can easily be further functionalised at position 7,

Objective

which allows the attachment of additional functionalities to enhance, for example, water-solubility. Finally, coumarins can be cleaved off by light irradiation if they are bound through a 4-methoxymethyl group (Figure 2.2) and thereby serve as fluorescent photolabile protecting group that can be chemoselectively installed. Light cleavable coumarin phosphoramidates have the additional advantage that only non-toxic cleavage-products are generated.^[145]

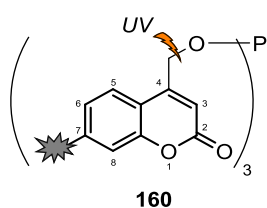


Figure 2.2: Functionalised and light-cleavable coumarin phosphite **160**.

3 Discussion

The Staudinger-phosphonite reaction offers a huge potential for the side-selective and chemoselective labelling of biomolecules or molecules with similar requirements such as polymers. The Staudinger reaction has the advantage to be a metal-free reaction. The absence of any toxic metals is an important aspect for *in vivo* applications. Furthermore, the Staudinger reaction does not require any catalyst or co-reagents that could limit its applicability when it comes to the transfer from test tubes to actual applications such as labelling of proteins in cell lysates where the accessibility of these could be hindered. Especially the absence of any toxic metals is important which is the major drawback of the copper-catalysed alkyne-azide cycloaddition (CuAAC) and limits its applicability for *in vivo* experiments.

A crucial requirement for labelling reagents is their chemoselectivity, because unspecific reactions will adulterate the results. The chemoselectivity of the Staudinger phosphite reaction has already been demonstrated for peptides and proteins, which assumes the same reactivity for phosphonites. Most importantly, as compared to the Staudinger-phosphite reaction, phosphonites assure a mono-functionalization because the functional module is attached through the phosphorus-carbon bond which is not cleaved during aza-ylide hydrolysis. Phosphonites further benefit from the two alkoxy and the carbon bound substituents at the phosphorus centre, which can be independently designed with respect to their electronic and steric nature. This offers numerous options for the accurate optimisation of the phosphonite with respect to the azide substituent and its environment.

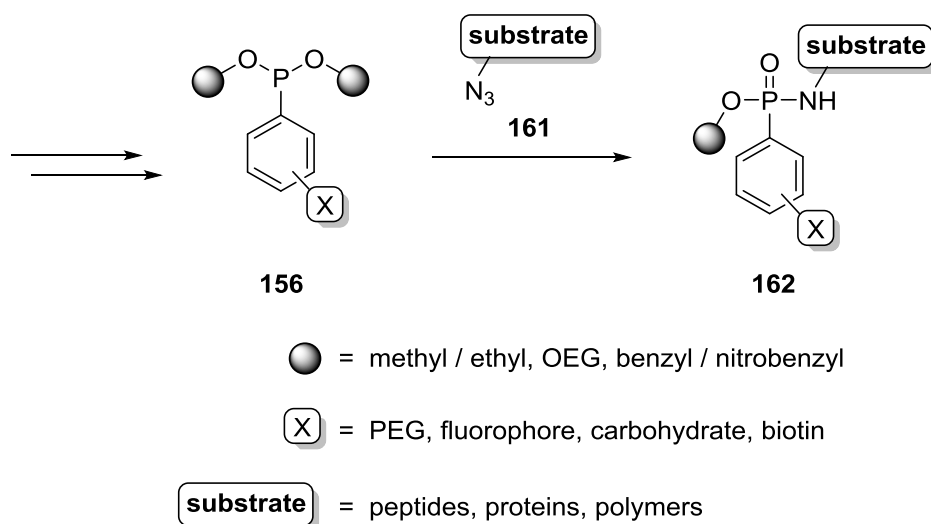
The first step to evolve the Staudinger-phosphonite reaction to a labelling method for bio-relevant substrates was the development of a synthetic pathway to functionalised phosphonites **156**. Small alkyl groups like methyl or ethyl served as good starting points for the alkoxy substituents at the phosphorus. Later small oligoethylene glycol chains were envisioned to improve water-solubility, especially when hydrophobic functionalities are attached. Benzyl substituents, which exhibit the best leaving group abilities in case of phosphites (see Table 1.1), or photocleavable *o*-nitrobenzyl groups can further enhance the hydrolysis and applicability of the phosphonite reagent. For the functional modules that are attached to the phosphonite moiety all kinds of bio-relevant tags are of interest, including polyethylene glycols as chemically very inert functionalities for stabilisation or transporter reagents for drug delivery,^[77b, 146] fluorophores for visualisation, carbohydrates for specific binding assays and biotin as purification tag or as further binding domains (Scheme 3.1).

In the second step the behaviour of the new functionalised phosphonites **156** was probed in the Staudinger reactions under various reaction conditions and with different azido

substrates **161**. Particular attention was paid to the reaction of phosphonites **156** with azido peptides. Peptides and proteins are two of the most interesting substrates for modification reactions in modern life science. Polymers represent another very interesting category of targets since they offer a lot of advantages as carrier for enhanced drug delivery.

1. developing a synthesis of functionalized phosphonites

2. screening reaction conditions and targets



Scheme 3.1: Evolving the Staudinger-phosphonite reaction to a bio-compatible labelling reaction.

3.1 Retrosynthetic evaluation of functionalised phosphonite synthesis

Functionalised aryl phosphonites **156** contain four elements that had to be connected, the phosphorus, the aromatic system, the alkoxy substituents and the functional module on the aromatic system. Since hundreds or more substituted benzene derivatives are commercially available, there is no need to synthesise the aromatic system. Four different retrosynthetic pathways are available for which the first key-retrosynthetic step is shown in Figure 3.1. Even though charges on the synthons are already given, because they are chemically most reasonable (see chapter 1.1.1 for a general overview of phosphonite synthesis), interchanging of the charges is in principle possible. The first three pathways are phosphorus(III)-related and differ in the order by which the substituents are introduced to the aromatic ring. The fourth retrosynthetic pathway includes a phosphorus(V) compound which is reduction to the corresponding phosphorus(III) derivative.

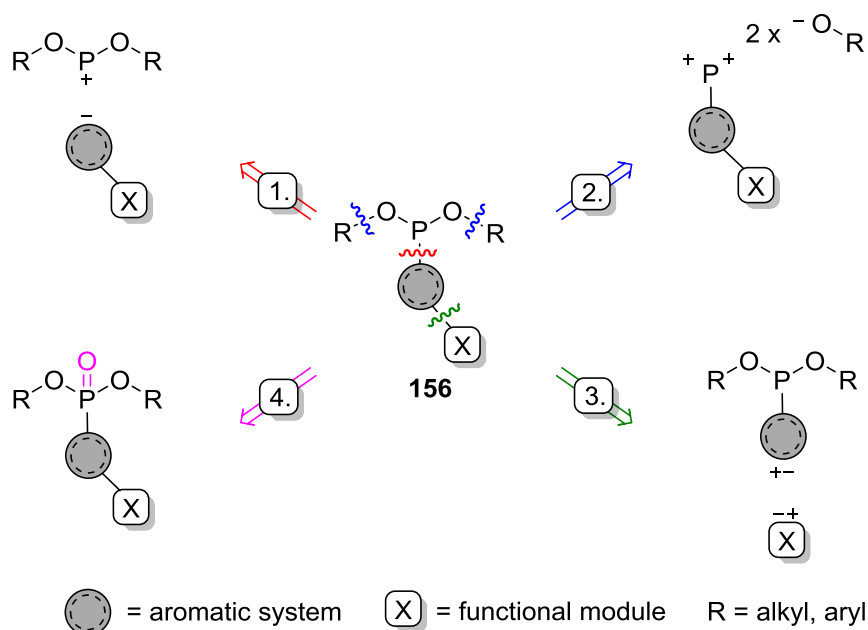
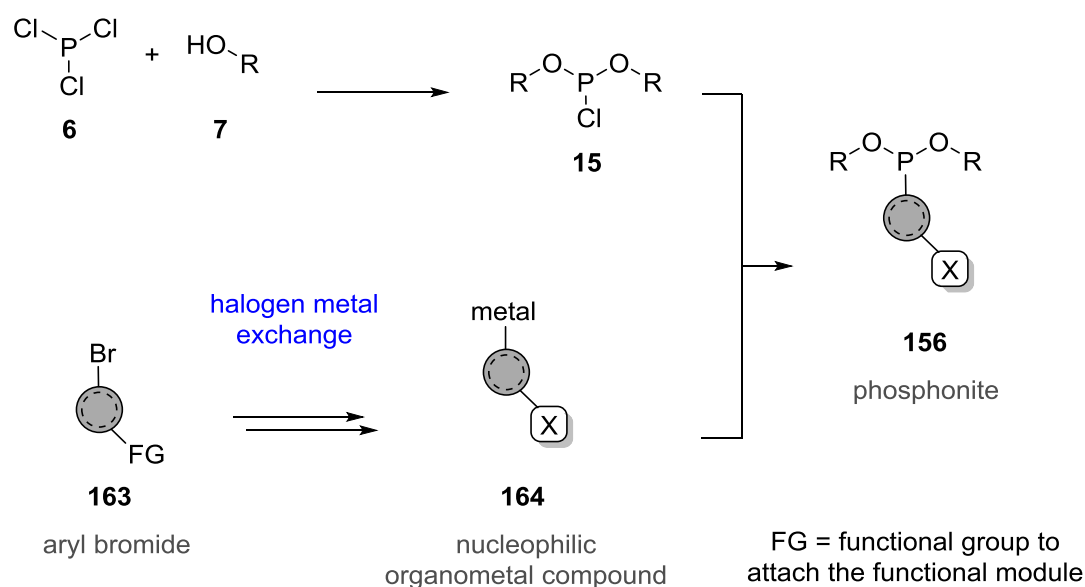


Figure 3.1: First step of four retrosynthetic routes to functionalised phosphonites **156**.

The first route starts with the breaking of the phosphorus-carbon bond, leading to a functionalised aromatic system and a phosphorus with two alkoxy groups already attached. In contrast to Arbuzov-type reactions, in which the electron lone pair of the phosphorus(III) reacts as a nucleophile to form a phosphorus(V) product, the phosphorus(III) reacts in this case as an electrophile with a +III oxidation state at the phosphorus. The first synthon is a nucleophilic aromatic ring with the attached functional module that can be represented by a Grignard reagent **164**. The second synthon is an electrophilic dialkyl or aryl phosphorus(III) reagent such

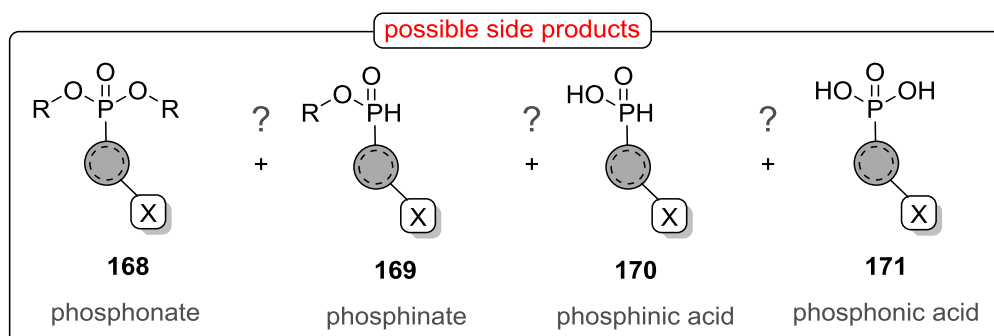
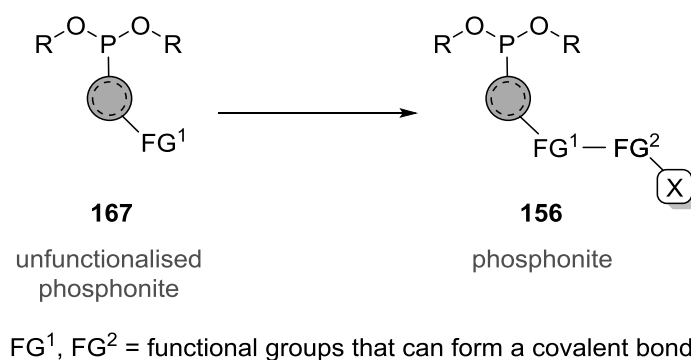
as a chlorophosphite **15** or phosphonites **3**. By the use of many commercially available chlorophosphites this pathway has the advantage that only one reaction step involving a phosphorus(III) species is necessary. Every reaction step in which phosphorus(III) is involved a high risk of oxidation or hydrolysis is faced, and therefore limits the applicable reagents and reaction conditions. If more complex oxy-bound groups are desired, the phosphite **15** can be synthesised by literature-known protocols from commercially available phosphorus trichloride (**6**). Especially in case of more complex oxy-bound substituents this convergent synthesis is superior to a linear approach (as described in the second route) because less valuable functional modules, such as expensive fluorophores, are involved in lesser synthetic steps (Scheme 3.2).



Scheme 3.2: Phosphonite synthesis according to the first retrosynthetic pathway.

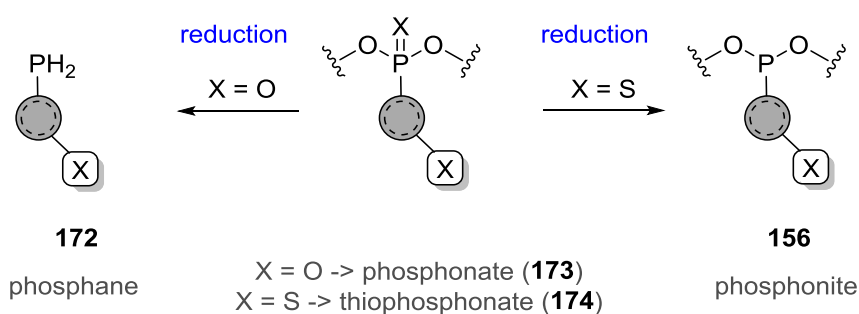
In the second route the phosphorus-oxygen bonds are installed in the last step of the synthesis. This allows more flexibility in choosing the phosphorus reagent that is used for the phosphorus-carbon bond formation. The drawback is here that an additional reaction step has to be performed after the introduction of the phosphorus onto the aromatic system which has to be compatible with the functional module. An additional reaction step in which phosphorus(III) is involved represents also the risk of a possible hydrolysis or oxidation of the phosphorus.

The introduction of the alkoxy substituents at the phosphorus is done by a nucleophilic substitution. The leaving groups present at the phosphorus are chloro groups which can be substituted by an alcohol in the presence of a non-nucleophilic base. The dichloro phosphanes **165** can be synthesised from phosphorus trichloride (**6**) and a nucleophilic



Scheme 3.4: Phosponite synthesis according to the third retrosynthetic pathway and possible side products.

The last route differs from all the previous ones because every part is already connected and merely the oxidation state of the phosphorus must be reduced from +V to +III. A closer look at the literature reveals that there are no suitable protocols available for the reduction of phosphonates **173**. Because of the very stable phosphorus oxygen bond strong reducing reagents, mostly lithium aluminium hydride, are required and the reduction does not stop at the phosponite **156** level but reduces the phosphorus further to the phosphane **172**.^[147] That turns us back to retrosynthetic route 2 where a double positive phosphorus synthon is required. The only protocol known for the reduction of a phosphonate **173** to the corresponding phosponite **156** starts with the exchange of the double bound oxygen to sulfur with Lawesson's reagent in moderate yields.^[148] The thiophosphonate **174** could then be further reduced to the corresponding phosponite by treatment with Raney-Ni.^[148a, 149]



Scheme 3.5: Phosponite synthesis according to the fourth retrosynthetic pathway.

3.2 Aryl phosphonites for the functionalization of peptides and proteins

This chapter was published in the following journal:

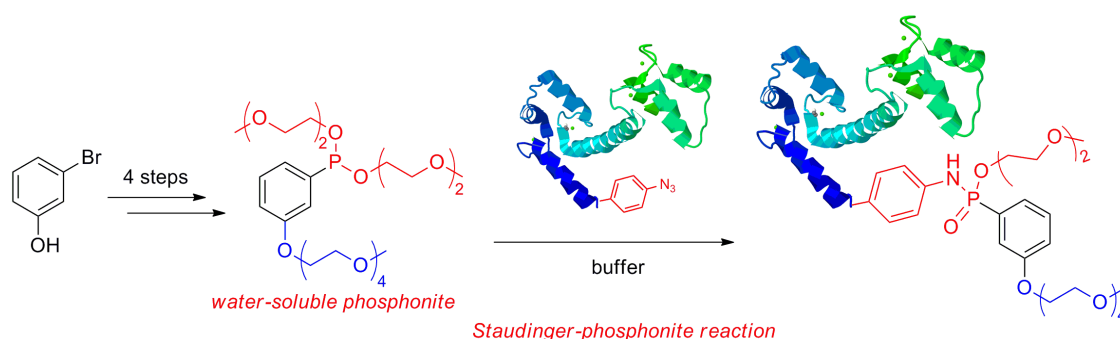
M. Robert J. Vallée, Paul Majkut, Ina Wilkening, Christoph Weise, Gregor Müller, and
Christian P. R. Hackenberger

“Staudinger-Phosponite Reactions for the Chemoselective Transformation of Azido-
Containing Peptides and Proteins“

Organic Letters **2011**, *13*, 5440–5443.

Publication Date (Web): 29 September 2011

The original article is available at: <http://dx.doi.org/10.1021/ol2020175>



Scheme 3.7: Synthesis of a water-soluble phosphonite and its application as modification reagent of azido-calmodulin.

Abstract

Site-specific functionalization of proteins by bioorthogonal modification offers a convenient pathway to create, modify, and study biologically active biopolymers. In this paper the Staudinger reaction of aryl phosphonites for the chemoselective functionalization of azido-peptides and proteins was probed. Different water-soluble phosphonites with oligoethylene-substituents were synthesised and reacted with unprotected azido-containing peptides in aqueous systems at room temperature in high conversions. Finally, the Staudinger-phosponite reaction was successfully applied to the site-specific modification of the protein calmodulin.

Responsibility assignment (others than the author)

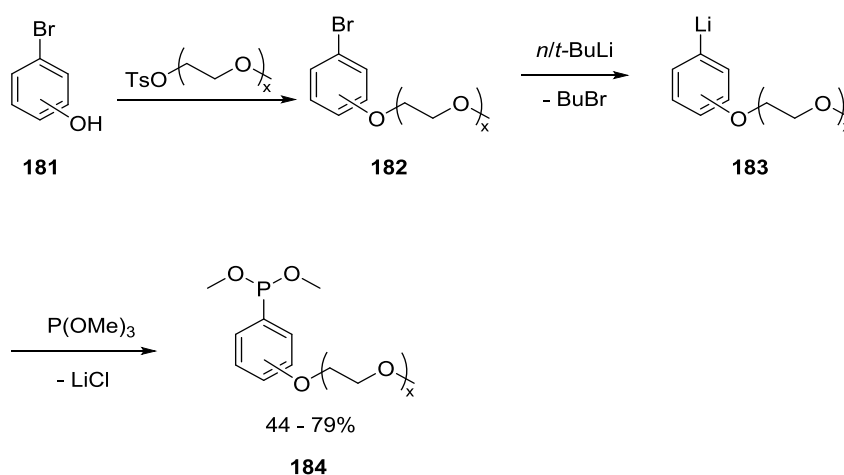
The concept of research for the Staudinger-phosponite reaction was provided by Professor C. P. R. Hackenberger. Paul Majkut was responsible for the expression of calmodulin and SDS-page analysis. Ina Wilkening performed preliminary studies on Staudinger reactions with phosphonites in organic solvents. Christoph Weise was responsible for digestion experiments

of the calmoduline and MALDI measurements. Gregor Müller did a twelve week internship, in which he was involved in the synthesis of the phosphonites.

Compendium of content and additional information

Following the first route of the retrosynthetic analysis for the functionalised phosphonites **167** (chapter 3.1) substituted benzene was used as core building block. At first the functional module should be attached and in the second part the phosphonite should be build up. As a model functional module short oligoethylene glycols were chosen because, on the one hand, they are chemically very inert and should enhance the water-solubility of the aryl phosphonites and, on the other hand, they are small and easier to handle variants of larger polyethylene glycols. Moreover, polyethylene glycols are very interesting functionalities for shielding the protein surface from proteases and from inducing an adaptive immune response^[76, 150] or clearance in the kidney^[151].

The synthesis of the first functionalised phosphonite **184** was started, according to the retrosynthetical route 1 (chapter 3.1), from commercially available bromophenol **181** by, attachment of the oligoethylene glycol by nucleophilic substitution. Subsequently, the bromo substituent was exchanged to lithium to yield **183**, with either *t*BuLi or with the less pyrophoric *n*BuLi, to create a strong nucleophile. In the second step of this one-pot reaction sequence, commercially available trimethyl phosphite was added to the organolithium compound **183** to react *via* nucleophilic substitution to the functionalised phosphonite **184** (Scheme 3.8).



Scheme 3.8: First synthesis of functionalised phosphonites **184**.

The crude ³¹P NMR of this reaction showed a big peak at 141 ppm that corresponds to the phosphonite product and only minor by-products (see Figure 3.2 as an example). Attempts to

further purify the phosphonite **184** by filtration over Celite® or column chromatography led to high amounts of degraded phosphonite even in the presence of triethylamine (1%), which was a successful optimisation for purification of phosphites^[7a]. Although the achieved purity of this phosphonite **184** (Scheme 3.8) was high enough, for more complicated phosphonites higher amounts of impurities were expected. For this reason a reliable purification method was strongly requested.

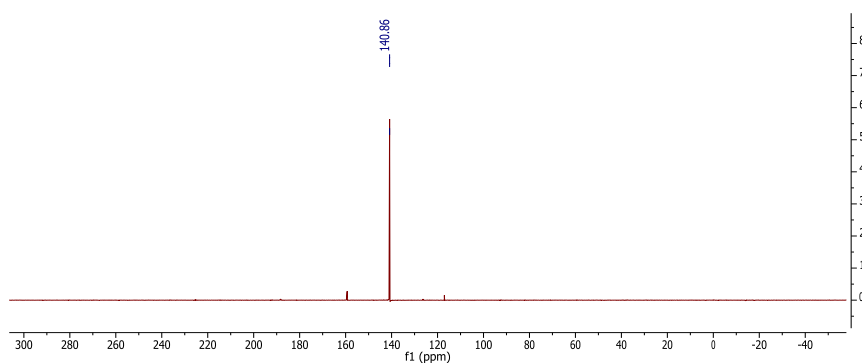
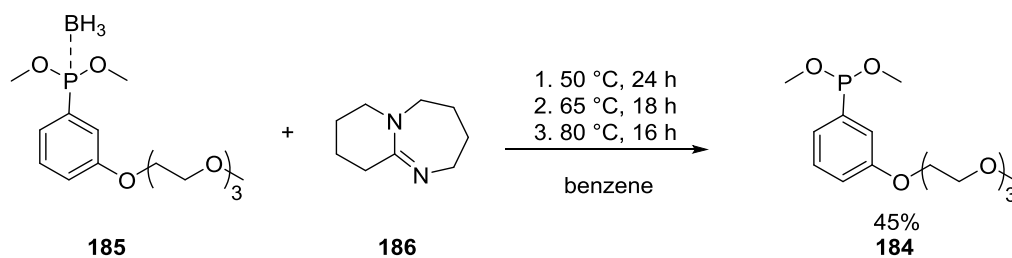


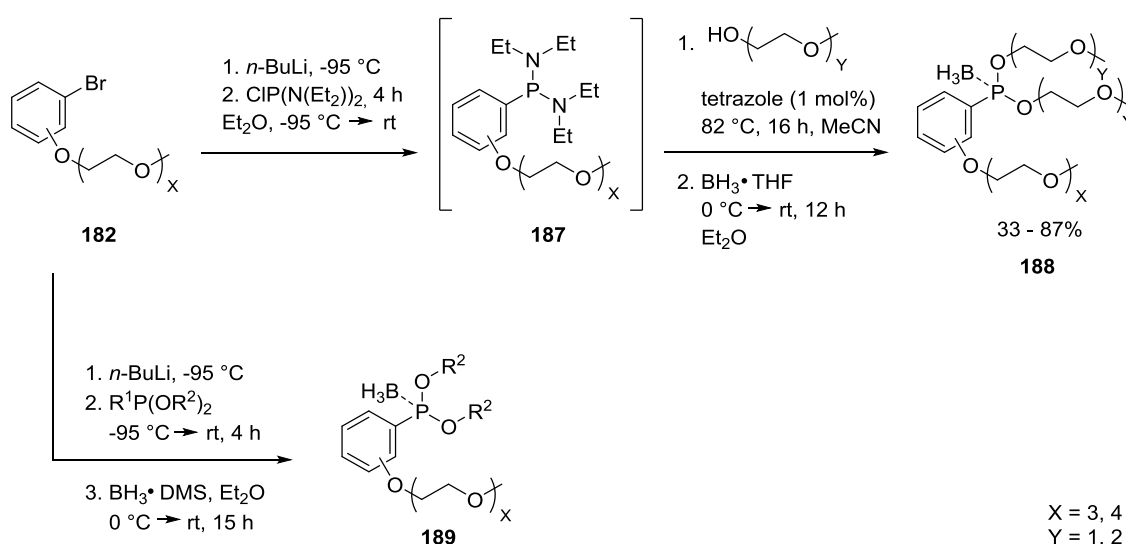
Figure 3.2: Sample ³¹P NMR spectrum of crude phosphonite **184** synthesis.

To solve the purification issue, a borane was introduced to the crude phosphonite as protecting group. The protection of a phosphorus(III) compound through a stable frustrated Lewis acid Lewis base pair is achieved by the unique electronic properties. The electron lone pair of the Lewis basic phosphorus(III) is still located around the phosphorus but it is not available for other reagents. This means that the phosphorus cannot get protonated to form an electrophilic phosphonium ion, which is the first step of its hydrolysis. This allows the purification of the resulting phosphonite-borane **185** by column chromatography, preparative HPLC or even dialysis in water for over four days without decomposition. The borane protecting group could be removed afterwards with DABCO® at 50 °C. The unprotected phosphonite was then used without further purification in Staudinger reactions, since the only by-products were the DABCO® and the DABCO®-borane complex. Both are biocompatible and do not interfere with the Staudinger reaction. Attempts were made to use triethylamine or DBU (**186**) as alternative non nucleophilic bases for the deprotection of the phosphonite-borane **185** but these did not lead to the free phosphonite **184** under the same reaction conditions as applicable for deprotection with DABCO (50 °C, 24 h). When using DBU (**186**), elongating the reaction time to 58 hours and heating the reaction mixture stepwise to 80 °C, free phosphonite **184** was only obtained in 45% (Scheme 3.9). Therefore, the search for other deprotection conditions was not further pursued.



Scheme 3.9: Alternative approach for the deprotection of phosphonite-boranes using DBU as non-nucleophilic base.

With this synthesis in hand, different phosphonites **188** with oligoethylene-substituents at the aryl system were synthesised (Scheme 3.10). These phosphonites were synthesised *via* the second retrosynthetic route (chapter 3.1) by an optimised procedure of the classical tetrazole-assisted substitution of amino groups with alkoxy groups at the phosphorus.



Scheme 3.10: Synthesis of borane protected aryl phosphonites.

The hydrolysis rate of the synthesised phosphonites was determined by integration of the ^{31}P NMR signals over one hour. ^{31}P NMR spectra were recorded every seven minutes. Complete hydrolysis of dimethyl phosphonites **184** was already observed after nine minutes. In contrast, the mOEG phosphonites **188** displayed a considerable higher stability, and complete hydrolysis of the mOEG phosphonites **188** was reached after 17 and 25 minutes. By using these phosphonites the first Staudinger-phosphonite reaction with unprotected *p*-azidophenylalanine-containing peptides in aqueous systems was performed. Although the chemoselectivity was even proven by control experiments, the unexpected formation of the corresponding *p*-aminophenylalanine-containing peptide was observed. Stability studies of the phosphonamidate product indicated that amine formation took place during phosphonamidate

formation and cannot be attributed to product degradation. A detailed explanation based on underpinning experimental proofs is described in chapter 3.3 for a related phosphonite system. Finally, the Staudinger-phosphonite reaction was successfully applied for the site-specific modification of the protein azido-calmodulin. The unnatural amino acid *p*-azidophenylalanine was incorporated at position two into the protein by *in vitro* translation in RF1-deficient *E. coli* lysates by using the Amber suppression methodology. The Staudinger-phosphonite reaction was performed in tris/HCl buffer at pH = 8.2 and gave the desired phosphoramidate with 70% conversion. A control experiment with Calmodulin that has a serine at position two instead of the *p*-azidophenylalanine was performed to prove the chemoselectivity of the Staudinger-phosphonite reaction in this system.

3.3 Alkyne phosphonites for sequential azide-azide couplings in organic solvents

This chapter was published in the following journal

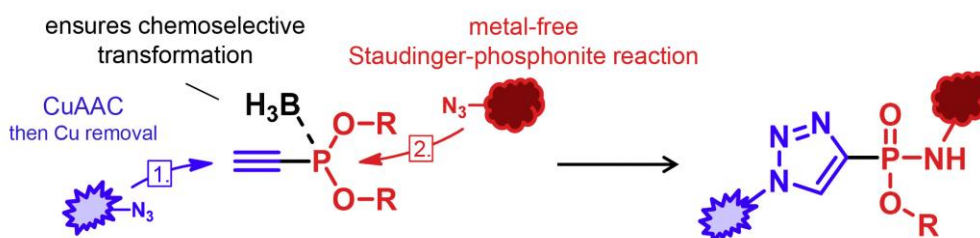
M. Robert J. Vallée, Lukas M. Artner, Jens Dervedde and Christian P. R. Hackenberger

“Alkyne phosphonites for sequential azide-azide couplings”

Angew. Chem. Int. Ed. **2013**, 52, 9504–9508. / *Angew. Chem.* **2013**, 125, 9682–9686.

Publication Date (Web): 16 July 2013

The original article is available at: <http://dx.doi.org/10.1002/anie.201302462>



Scheme 3.11: Borane-protected alkyne phosphonites for the sequential coupling of two different azides.

Abstract

When Staudinger meets Huisgen! A combination of the Cu-catalyzed azide alkyne cycloaddition and the Staudinger reaction, the two most successful chemoselective reactions for the transformation of azides, led to a very versatile chemical tool that allows the sequential coupling of two different azido building blocks in high yields. This modular protocol allows a final metal-free conjugation of functional building blocks to azides.

Responsibility assignment (others than the author)

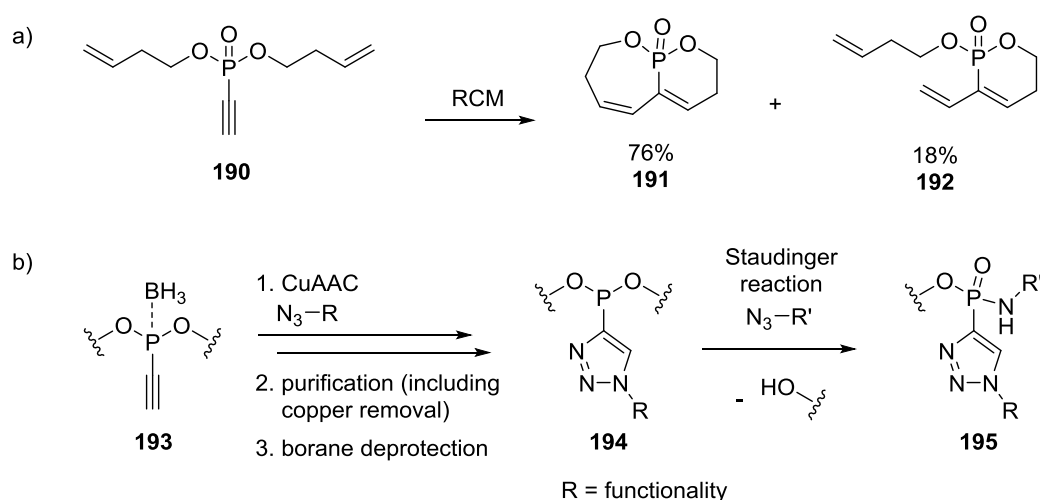
The concept of research for the Staudinger-phosphonite reaction was provided by Professor C. P. R. Hackenberger. Lukas M. Artner was responsible for the synthesis of azido carbohydrates. Surface plasmon resonance measurements were done by Lukas M. Artner and Jens Dervedde.

Compendium of content and additional information

After the successful synthesis of water-soluble phosphonites and their application as chemoselective modification tool for the protein calmodulin, the next goal was an improved functionalization pathway. Building up the phosphonite moiety in the presence of the functional module can lead to side-reactions if e.g. the attached fluorophore or biotin is not compatible with the harsh reaction conditions required so far for the synthesis of phosphonites, such as *n*BuLi. An ideal building block would already contain the phosphonite moiety, which can then be equipped with a functional module under mild reaction conditions.

An alkyne-phosphonite **190** was described in the literature (Scheme 3.12a),^[152] which gave the decisive hint for a very elegantly solution to the synthetical issue. In their borane-protected form, alkyne-phosphonites **193** would allow the chemoselective attachment of an azido-bearing functional module *via* copper-catalysed alkyne azide cycloaddition, which at the same time converts the alkyne-phosphonite into a triazole phosphonite **194**. After purification and borane deprotection the free phosphonite would be available for the metal-free Staudinger-phosphonite reaction (Scheme 3.12b). This synthesis route is in accordance with the third retrosynthetic pathway described in chapter 3.1 (Scheme 3.1 and Scheme 3.4). Because the functional module is attached to a protected phosphonite, which is deprotected under mild conditions, the synthesis of nucleophilic group bearing phosphonites like carbohydrate-phosphonites, are accessible for the first time.

The objective of this project was the synthesis of borane-protected alkyne phosphonites **193** and the investigation of all three reaction steps involved (CuAAC, borane-deprotection, Staudinger reaction).



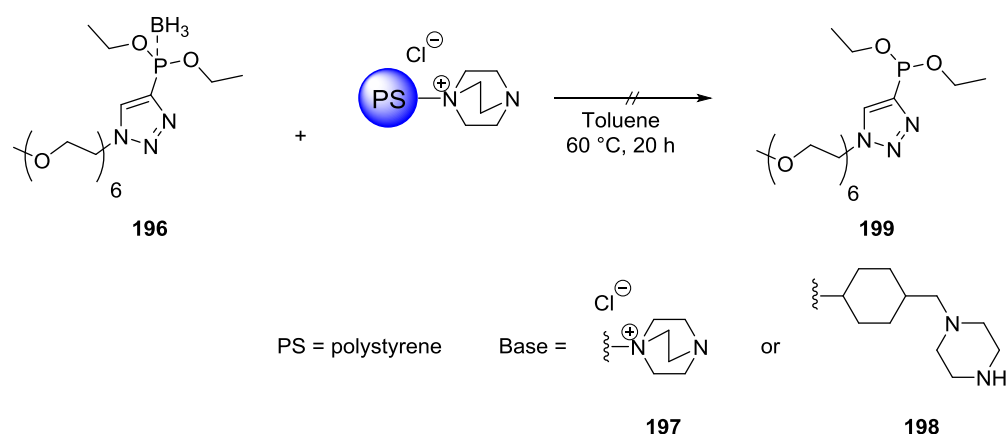
Scheme 3.12: a) The inspiring phosphonite was originally used for ring closure methathesis.

b) Full functionalization sequence of second generation phosphonites.

The synthesis of the alkyne phosphonite **193** was started from commercially available diethyl chlorophosphite and alkynyl Grignard reagent followed by *in situ* borane protection. This simple two-step one-pot reaction gave diethyl alkyne phosphonite-borane **200** in very good yield of 92%. The same synthesis route was also published by Stéphanie Ortil and Jean-Luc Montchamp who used alkyne phosphonites for the selective formation of Z-alkenyl phosphorus compounds.^[153] It is notable that phosphonite formation was not observed if lithium acetylide was used instead of the organomagnesium analogue.

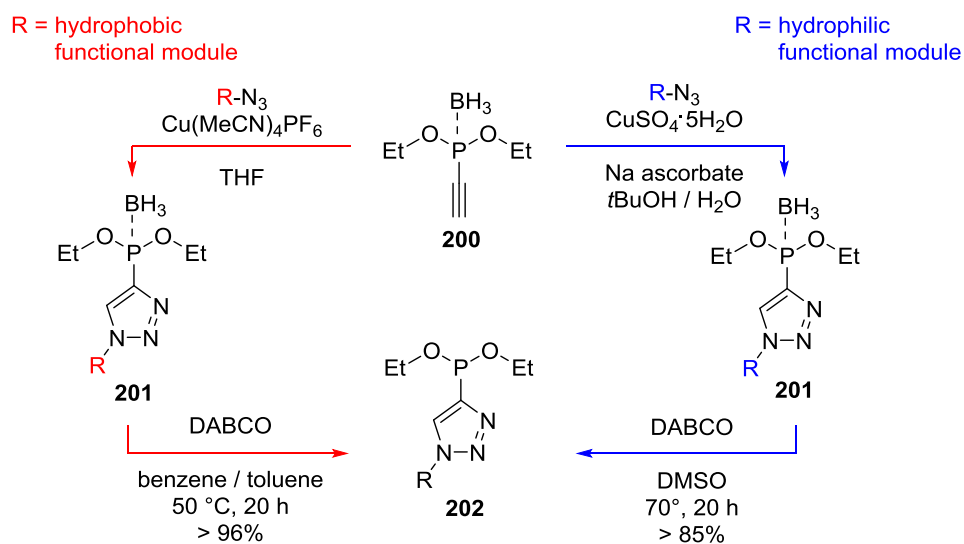
The first azide coupling was the copper-catalysed azide alkyne cycloaddition. The borane-protected phosphonite moiety ensured a chemoselective reaction of the alkyne with the azide without any side reaction on the phosphorus. Independent of the properties of the azido functional module, quantitative conversion was observed either in the classical tert-butyl alcohol water mixture with copper(II) sulfate and sodium ascorbate for hydrophilic azides or in tetrahydrofuran with tetrakis(acetonitrile)copper(I) hexafluorophosphate in the case for more hydrophobic azido functionalities.

In order to activate the phosphonite-borane **196** for the second azide coupling the borane group was removed. Therefore, the reaction conditions used previously for the deprotection of aryl phosphonite-boranes were adapted to the triazole-phosphonites-borane **196**. It was found that three equivalents instead of one and a half equivalents of DABCO[®] were required for the quantitative removal of the borane group from the phosphonite in less than 24 hours. The separation of the DABCO[®]-borane complex as well as excess of DABCO[®] from the free phosphonite turned out to be impossible without partial oxidation or hydrolysis of the phosphonite. We also envisioned polymer bound bases to remove the base and its borane complex. Polymer bound DABCO (**197**) and piperazine (**198**), were probed under similar deprotection conditions successfully used with DABCO[®], but unfortunately neither polymer bound base were able to initiate deprotection of the phosphonite-borane **196** (Scheme 3.13). Together with the previous results for the deprecation of phosphonite-boranes with alternative bases (Scheme 3.9) left DABCO[®] as only adequate base for borane removal.



Scheme 3.13: Attempts to deprotect phosphonite-borane **196** with polystyrene bound bases.

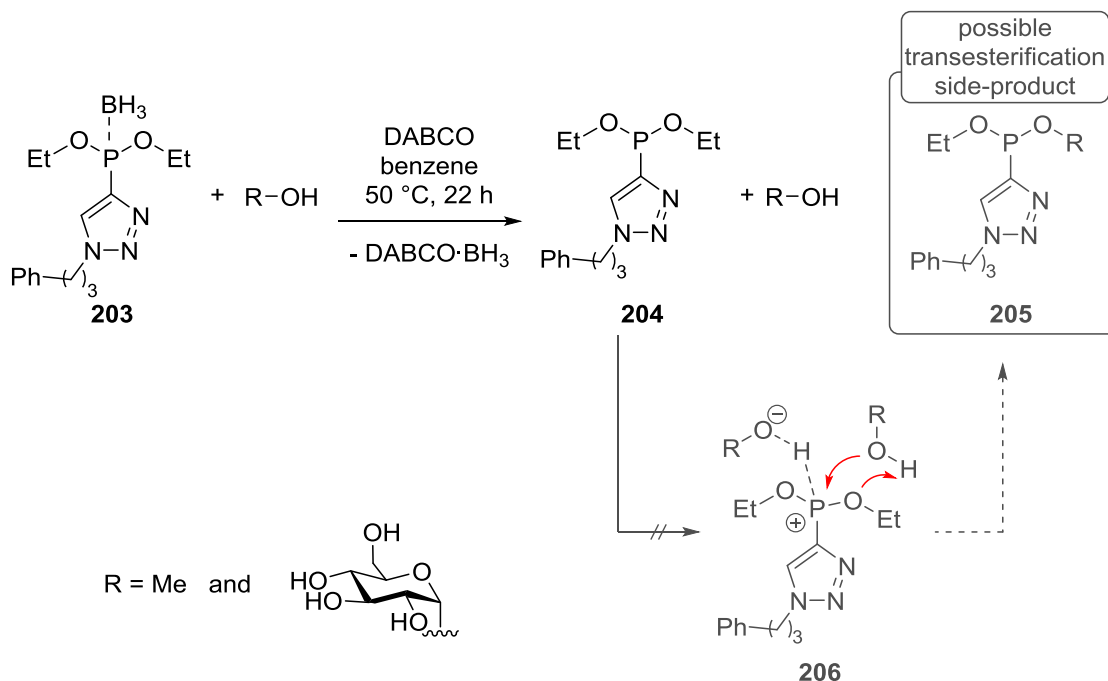
Since benzene or toluene were used in this deprotection step, the reaction was limited to unpolar compounds. This limitation was overcome by changing the solvent to dimethyl sulfoxide requiring a slight increase in the reaction temperature. Considering the flexibility of the copper-catalysed azide alkyne cycloaddition, an extreme versatile synthesis route for functionalised diethyl triazole phosphonites **202** was established (Scheme 3.14). With the free phosphonites **202** in hand the next objective was an in-depth investigation of their behaviour in Staudinger reactions.



Scheme 3.14: Synthesis route for hydrophobic and hydrophilic functionalised phosphonites **202**.

The deprotection of phosphonite-boranes generates free phosphonites in solvent at 50 °C and therefore, water and oxygen must be avoided. In addition, the attached functional module must be compatible to this reaction conditions and must not react with the free phosphonite **202**. Especially hydroxyl groups, from carbohydrates for example, are common

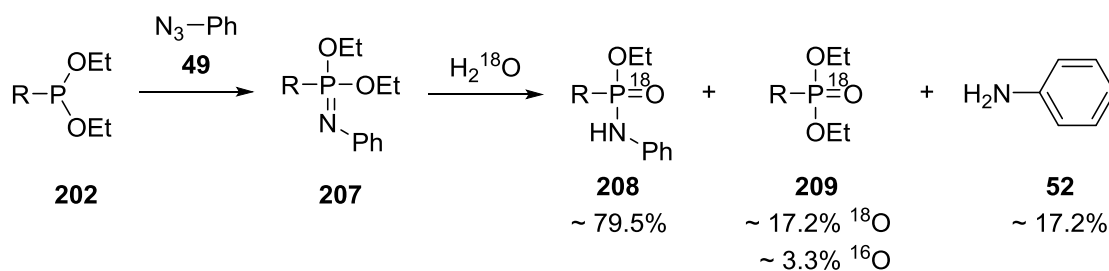
functional groups that can potentially react with the phosphonite **204**.^[154] To address these issues two equivalents of methanol and glucose were added to the deprotection reaction of a model phosphonite-borane **203**. Analysis of the crude reaction mixture by mass spectrometry and ³¹P NMR did not reveal any transesterification side-products **205**. This was supposed to be due to the basic reaction conditions (three equivalents of DABCO®) since the formation of a phosphonium ion **206** must precede a nucleophilic attack of water at the phosphorus (Scheme 3.15).



Scheme 3.15: Transesterification side-products with hydroxyl groups during phosphonite-borane deprotection were not observed.

The Staudinger-phosphonite reaction itself proceeded very smoothly with a large variety of azides, even though the reaction rate decreased in the order phenyl > benzyl > primary > secondary azide drastically. In general the yields for phosphonamidates **208** were between 94–80%. Only in the case of Staudinger-phosphonite reaction with phenyl azide ~20% phosphonate by-product **209** formation was observed. The origin of the phosphonate **209** could be proven by a labelling experiment with ¹⁸O labelled water. This mechanistical investigation revealed that the phosphonate ¹⁸O-**209** emanates mainly from unselective phosphonimidate **207** hydrolyses and not from the oxidation of the phosphonite **202** (Scheme 3.16). During the hydrolysis of the phosphonimidate **207** an alcohol group should act as leaving group. Comparing the pK_a values of alkyloxonium ions (pK_a = -2.4), anilinium ions (pK_a = 4.4) and alkylammonium ions (pK_a = 10.6) reveals a significantly higher chance for aniline **52** then for an alkylamine to act as leaving group in Staudinger-phosphonite

reactions. This result also explained the formation of 4-aminophenylalanine peptide observed during the Staudinger reaction of aryl phosphonites (see chapter 3.2).



R = functionalised triazole

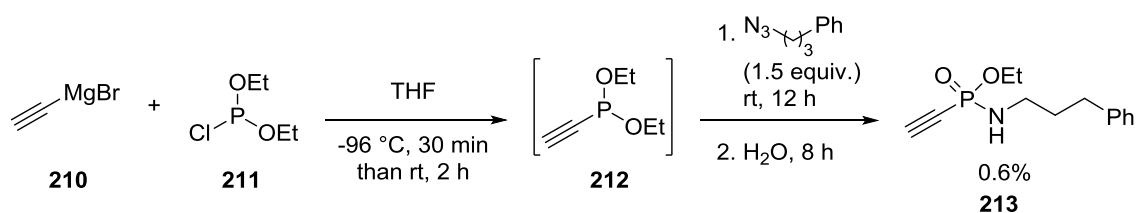
Scheme 3.16: Phosphonate **208** and aniline **52** formation during the Staudinger-phosponite reaction with phenyl azide **49**.

For many applications e.g. functionalization of polymers, the copper-catalysed alkyne azide cycloaddition is very wide spread. Even so, due to the many Lewis basic residues in polyglycerol, copper ions tend to adhere to the polyglycerol, which makes purification often very difficult and a metal-free functionalization method highly desirable. This new sequential azide-azide coupling should fulfill this requirement as versatile metal-free functionalization method for polyglycerols. Therefore, an azido polyglycerol was functionalised with lactose-triazole phosphonite. The glycosylated polyglycerol was obtained in 78% yield and good purity (>94% determined by $^1\text{H-NMR}$). Surface plasmon resonance (SPR) measurements of the polyglycerol functionalised with lactose by Staudinger-phosponite reaction showed high binding affinity of the conjugate to immobilized peanut agglutinin (PNA) and therefore the power of this new sequential azide-azide coupling.

Staudinger reaction of alkyne phosphonites

The coupling sequence of alkyne phosphonites, including the CuAAC and the Staudinger-phosponite reaction can also be turned around by starting with the Staudinger-phosponite reaction to generate alkyne phosphonamidates **213** after the first azide coupling (Scheme 3.17). In this way an electron-withdrawing phosphonamidate **213** moiety is generated next to the alkyne group, which presumably lowers the relative energy of its lowest unoccupied molecular orbital (LUMO) significantly. In general, electron-deficient alkynes show a higher reactivity compared to electron-rich alkynes and undergo [3+2]-cycloadditions under milder reaction conditions due to the lower activation energy.^[155]

The required alkyne phosphonite **212** was synthesised from an alkyne-Grignard reagent **210** and diethyl chlorophosphite **211** in tetrahydrofuran. The obtained alkyne phosphonite **212** was subsequently used *in situ* in the Staudinger reaction with 3-phenyl propylazide (Scheme 3.17). The crude ^{31}P NMR of the reaction showed two defined peaks at 9.13 and -2.80 ppm and a huge very broad peak between 30 and 20 ppm indicating an undefined polymerisation product. Nevertheless, the desired alkyne phosphonamidate product **213** was only isolated in a yield of 0.6% (Figure 3.3).



Scheme 3.17: First approach to synthesise alkyne phosphonamidate **213**.

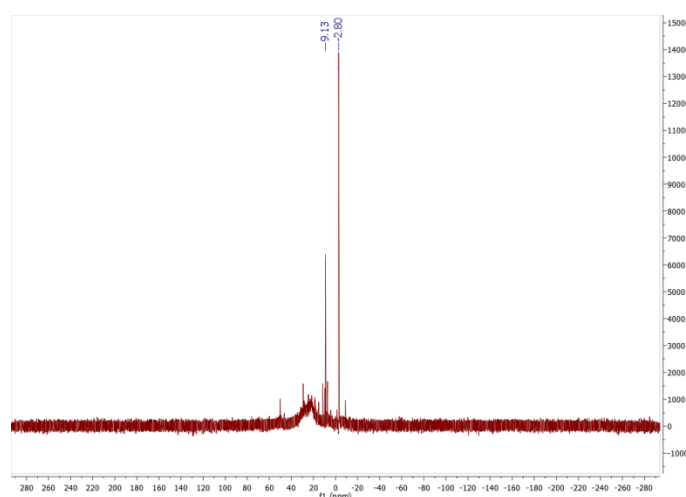


Figure 3.3: Crude ^{31}P NMR of the first approach to synthesise alkyne phosphonamidate **213**.

To avoid undefined polymerisation reactions after the addition of the azide, the *in situ* generated alkyne phosphonite **212** was diluted from 0.5 M to 0.05 M with either acetonitrile or toluene before azide addition. The crude ^{31}P NMR of both approaches showed a peak at -2.7 ppm as major product which corresponds to the alkyne phosphonamidate **213** (Figure 3.4).

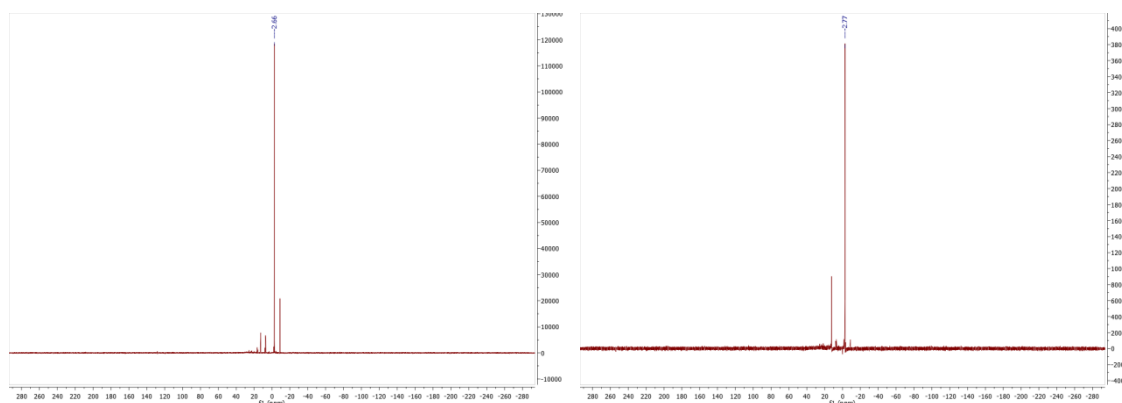
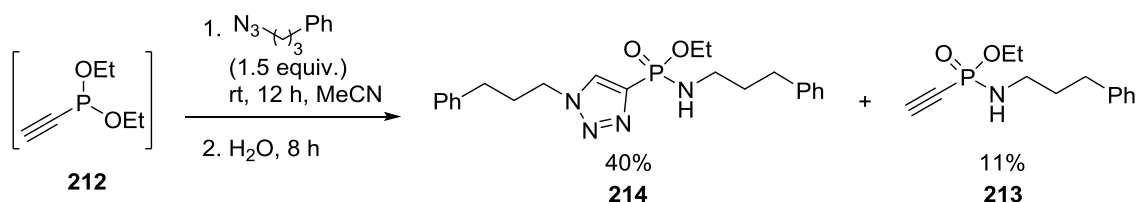


Figure 3.4: Crude ^{31}P NMRs of the Staudinger reactions from the alkyne phosphonite **212** with the (3-phenyl)-propyl azide diluted with acetonitrile (left) or toluene (right) to alkyne phosphonamidate **213**.

After this proof of principle, the crude products were stored at $-20\text{ }^{\circ}\text{C}$. The crude product (the acetonitrile diluted approach Figure 3.4 right) was purified by column chromatography with a surprising result. Since the major peak of the crude ^{31}P NMRs was at -2.66 ppm (Figure 3.4) corresponding to the alkyne phosphonamidate **213**, it was assumed that the phosphonamidate **213** should be the main product after the purification. Instead the triazole phosphonamidate **214** was isolated in 40% yield as single regioisomer (by ^1H NMR) and only 11% of the expected alkyne phosphonamidate **213** was obtained (Scheme 3.18).



Scheme 3.18: Isolated triazole phosphonamidate **214** and alkyne phosphonamidates **213**.

These first promising results indicated that the alkyne phosphonamidates can at least be generated *in situ* as major products. Moreover, the outcome of the reaction proves that the resulting electron deficient alkyne is capable to further undergo [3+2]-cycloadditions under very mild conditions. This project was handed over to Tom Sauer, a master student in the Hackenberger group, who is currently performing in-depth investigations of the reactivity and possibilities that arise from these preliminary studies.

3.4 Alkyne phosphonites as modification tool for peptides and proteins

Chemoselective transformations, especially of azido-biopolymers, have emerged as powerful tools in modern life science, since they allow the study of biological and functional aspects of protein modifications. It has already been demonstrated that the Staudinger-phosphonite reaction allows the chemoselective conversion of azido-peptides and proteins under mild conditions in high yields and is suitable for their site-specific functionalization. In chapter 3.3 borane-protected diethyl alkyne phosphonites were presented as new versatile and modular chemical tool for the metal-free conjugation of functional azido building blocks. The borane-protected alkyne phosphonites were employed for the conjugation of two different azido-containing molecules by means of two well-known and successful reactions, namely the copper-catalysed alkyne-azide cycloaddition (CuAAC) and the metal-free Staudinger reaction. Various azido compounds could be reacted in the CuAAC to yield the borane-protected triazole phosphonites, which could after borane-deprotection undergo the Staudinger reaction again with different azido derivatives to the desired phosphonamidates in organic solvents in excellent yields. After this successful introduction of diethyl alkyne-phosphonites and their promising results in organic solvents, the reaction of triazole phosphonites should be transferred to aqueous systems to further exploit its applicability for biopolymers. Especially for the functionalization of proteins, which are very sensitive towards many metal ions, metal free functionalization reactions are highly desirable. In order to achieve a successful conversion of azido biopolymers in aqueous system, not only the reaction conditions had to be optimised, but also the alkyne phosphonites themselves had to be further adapted with respect to their stability in water and their solubility.

For this reason, the first goal was to optimise the alkyne phosphonite synthesis route to enable the attachment of more complex oxy-bound substituents at the phosphorus. After the reaction of the alkyne phosphonite **200** and these new alkyne phosphonites to the corresponding triazole derivatives, hydrolysis and reaction studies on the peptide level were performed. The resulting data should then give evidence, whether conditions suited for proteins applications can be found.

Two alkyne phosphonite derivatives were chosen to improve the *sequential azide-azide coupling* concept for its feasibility in aqueous systems. From the aryl phosphonite studies (see chapter 3.2), ethylenglycole chain substituents at the phosphorus were known to enhance the water-solubility of the phosphonites and additionally improve the conversion rates. In consequence, the first phosphonite derivative **215** was synthesised with two diethylenglycole chain substituents at the phosphorus. The second phosphonite derivative **216** was designed

analogously to the photocleavable phosphite **95** developed in the Hackenberger group,^[7a] which showed good stability in water and high leaving group propensities (see Table 1.1). To avoid any photocleavage during the first studies, the nitro group from the original photocleavable phosphite substituent was moved from the *ortho*- to the *meta*-position (Figure 3.5).

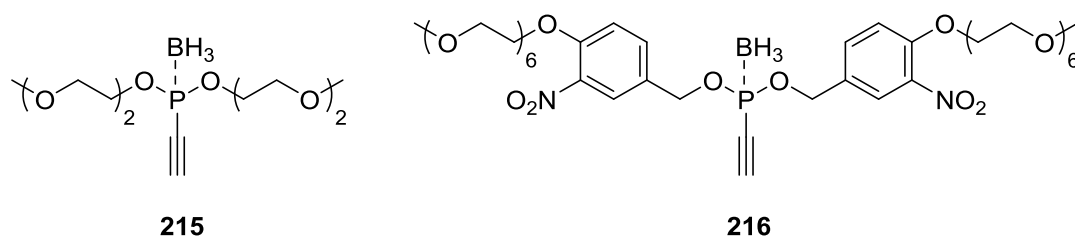
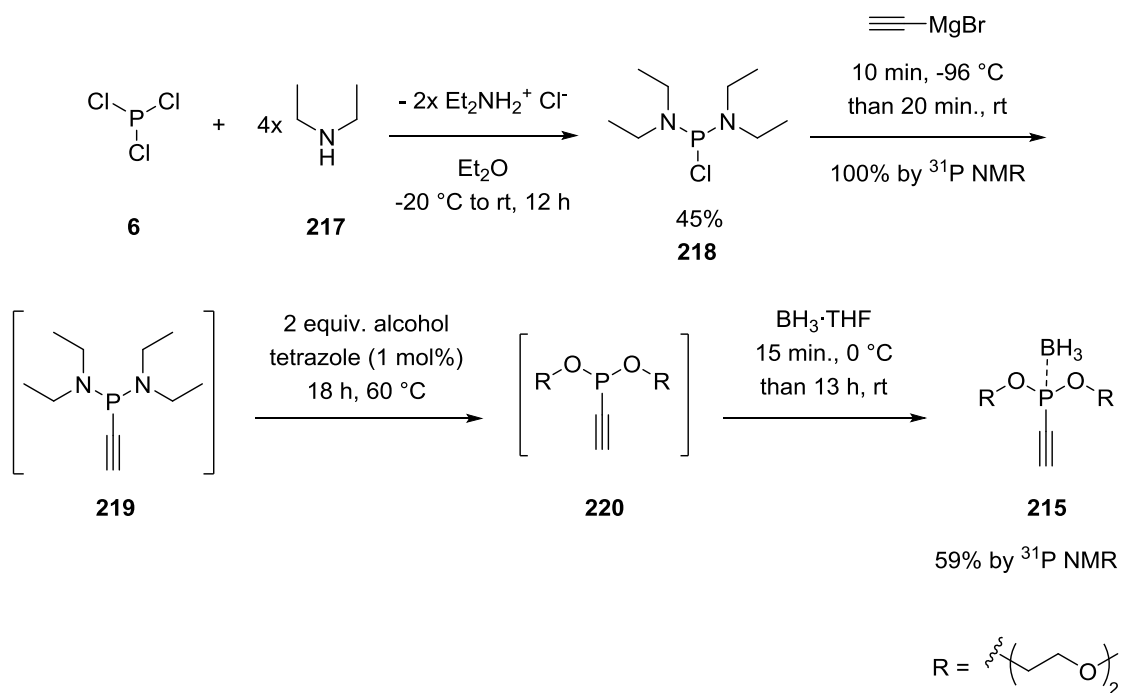


Figure 3.5: Improved alkyne phosphonites **215** and **216** for applications in aqueous systems.

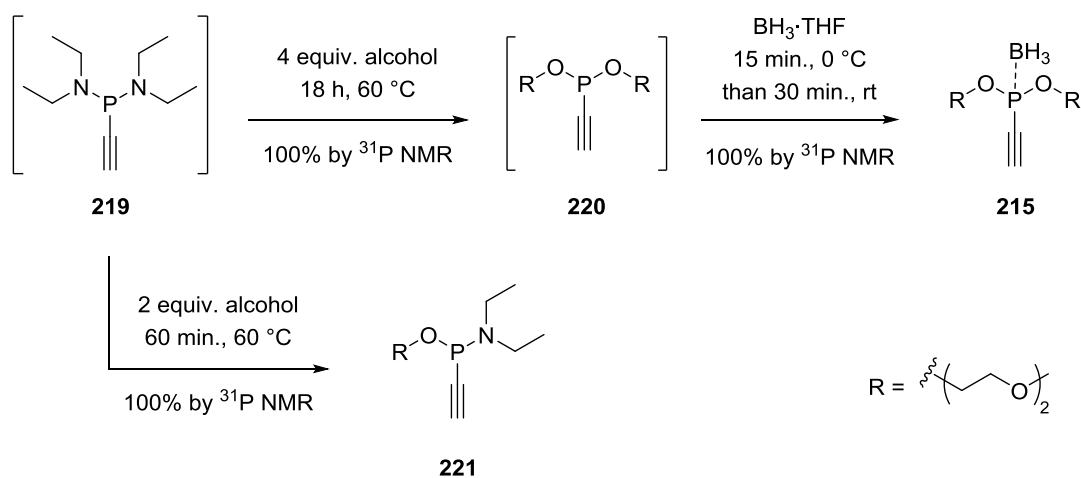
3.4.1 Syntheses of triazole phosphonites for applications in aqueous systems

The synthesis of the more complex oxy-substituents bearing alkyne phosphonites **215** and **216** was performed analogously to the successful synthesis of aryl phosphonites **188** (see Scheme 3.10), based on the second retrosynthetic route (see chapter 3.1). Starting from phosphorus trichloride (**6**), two chloro groups were substituted with diethylamine (**217**) to yield 1-chloro-*N,N,N',N'*-tetraethylphosphanediamine (**218**) followed by substitution of the remaining chloro group with the alkyne-Grignard reagent **210** to. The tetrazole-assisted substitution of the diethylamine groups from *N,N,N',N'*-tetraethyl-1-ethynylphosphane-diamine (**219**) with diethylene glycole monomethyl ether followed by *in situ* borane protection gave 59% product (**215**) formation as determined by ³¹P NMR (Scheme 3.19).



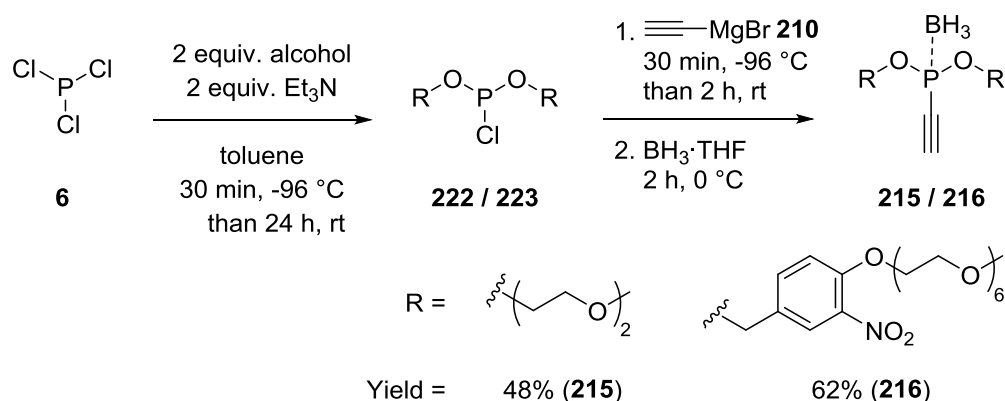
Scheme 3.19: The tetrazole-assisted synthesis of di-mOEG₂ alkyne phosphonite-borane **215**.

The first attempt to optimise the synthesis of the alkyne phosphonite **215** was performed by changing the triazole-assisted substitution of the diethylamine groups to a thermal approach. Unfortunately, two equivalents of diethylene glycol monomethyl ether were required to substitute one diethylamine group leading to compound **221**. Regarding the expensive nitrobenzyl derivative, the excess of two equivalents of alcohol as necessary for this reaction route was not desirable, although the conversion determined by ^{31}P NMR was quantitative (Scheme 3.20).



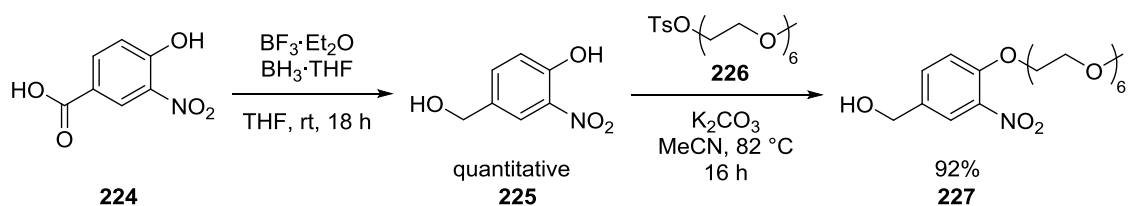
Scheme 3.20: The thermal synthesis of mOEG₂-substituted phosphonite **215**.

In the second attempt to improve the synthesis of alkyne phosphonites **215**, the introduction order of the alcohol groups and the alkyne by nucleophilic substitution at the phosphorus was exchanged. The synthesis started with the direct substitution of two chloro groups of phosphorus trichloride (**6**) with the desired alcohol (**217** or **218**) in the presence of triethylamine to trap the generated hydrochloric acid. The substitution of the third chloro group with the alkyne-Grignard reagent and the subsequent borane protection were both performed *in situ*. The desired alkyne phosphonite-boranes **212** and **213** were obtained in 48% and 62% yields after HPLC purification (Scheme 3.21).



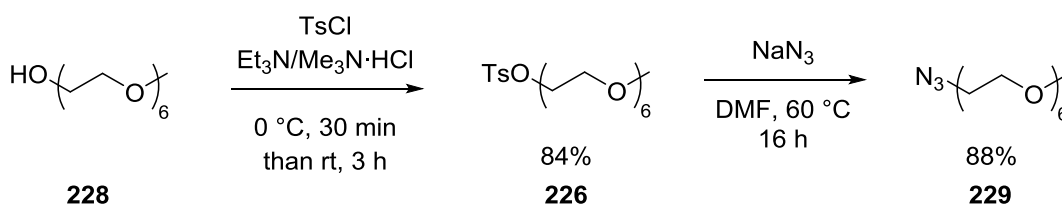
Scheme 3.21: Final synthesis route for alkyne phosphonites bearing complex oxy-bound substituents.

For the synthesis of the second phosphonite **216**, *p*-hexaethylene glycol monomethyl ether *p*-mOEG₆-*m*-nitro-benzyl alcohol **227** was required as starting material. The synthetic route of *p*-mOEG₆-*m*-nitro-benzyl alcohol **227** is described in Scheme 3.22. In the first step, the acid moiety of commercially available 3-hydroxy-4-nitrobenzoic acid **224** is quantitatively reduced to the corresponding alcohol **225** with a mixture of borane / borane trifluoride. In the second step, the tosylated mOEG₆ (**226**, see Scheme 3.23 for synthesis) was attached by a S_N2 reaction at the phenylic position of **225** (Scheme 3.22).



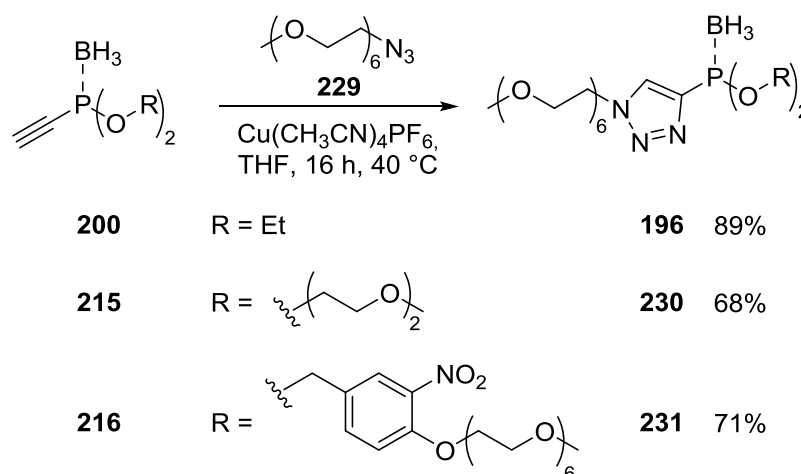
Scheme 3.22: Synthesis of *p*-nitro-*m*-mOEG₆-benzyl alcohol **227** as substituent for alkyne phosphonites **216**.

Having to different borane-protected alkyne phosphonites **215** and **216** in hand, the CuAAC was performed with different azido compounds. For the hydrolysis and the reactivity study azido hexaethylene glycol monomethyl ether (mOEG₆) was chosen as functional module to be attached to the alkyne phosphonites. On the one hand, the mOEG₆-chain should ensure water-solubility and, on the other hand, it is chemical very inert. The synthesis of the required mOEG₆-azide **229** starts from the corresponding commercially available alcohol **228**, which is first transformed into its tosylate **226** and in a second step converted to the mOEG₆-azide **229** via an S_N2 reaction with sodium azide (Scheme 3.23).



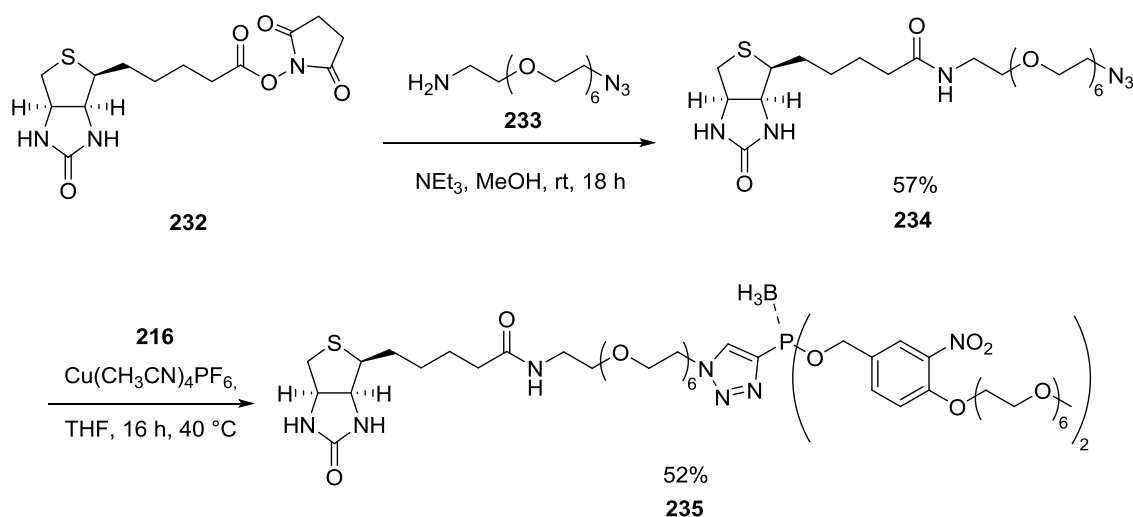
Scheme 3.23: Synthesis of mOEG₆-derivatives **226** and **229** for the synthesis of the OEG-substituents at the phosphorus as functional module for the CuAAC.

The attachment of the mOEG₆-azide **229** to the alkyne phosphonites **200**, **215** and **216** was realised by copper-catalysed alkyne-azide cycloaddition in tetrahydrofuran and tetrakis(acetonitrile)copper(I) hexafluorophosphate as copper(I) source (Scheme 3.24). Quantitative formation of triazole phosphonites **196**, **230** and **231** was confirmed by ³¹P NMR in all cases. The crude reaction mixtures were purified by column chromatography for **196** or preparative high-performance liquid chromatography for **230** and **231** to yield the desired triazole phosphonite-boranes **196**, **230** and **231** in good yields (Scheme 3.24).



Scheme 3.24: CuAAC of different alkyne phosphonites with mOEG₆ as functional module to ensure water-solubility.

Additionally to the ethyleneglycole-containing triazole phosphonites **196**, **230** and **231**, a functional module with a biotin attached through an azido-OEG₇-chain was synthesised and coupled to alkyne phosphonite **216** (Scheme 3.25). The synthesis of biotin-OEG₇-azide **234** started with an amide coupling between biotin *N*-hydroxysuccinimide ester **232** and commercially available azido-OEG₇-amine **233**. The copper-catalysed alkyne-azide cycloaddition of the biotin-OEG₇-azide **234** with the alkyne phosphonite **216** was performed under the same conditions as shown in Scheme 3.24 with tetrakis(acetonitrile)copper(I) hexafluorophosphate as copper(I) source to give borane phosphonite **235** (Scheme 3.25). The high affinity of biotin to avidin and streptavidin should be applied for the immobilisation of a protein functionalised with the biotin-triazole phosphonite.



Scheme 3.25: Synthesis of triazole-phosphonite **235** with an attached biotin immobilisation tag.

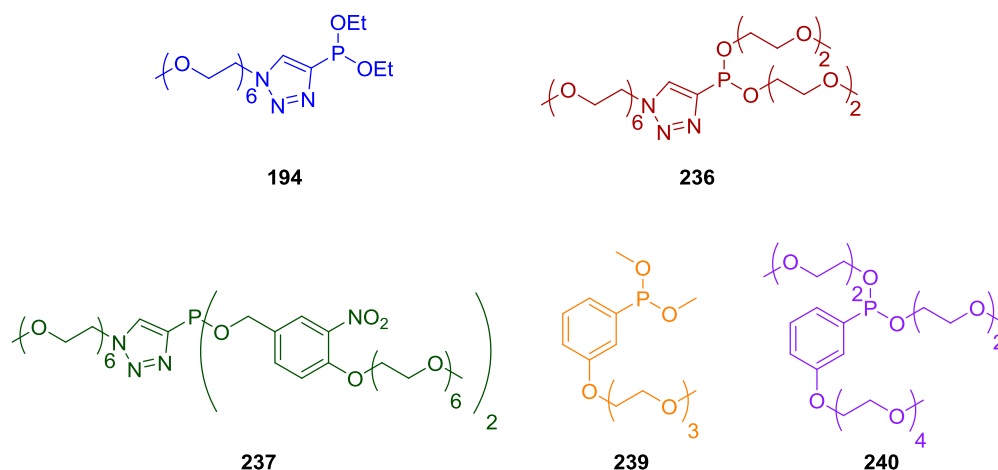
After purification the copper-content of the phosphonite was determined by ICP-MS. Although oligoethylene glycol chains are potential chelators of copper ions, we were pleased to find complete copper removal from triazole phosphonites **231** and **335** after HPLC purification could be proven.

As an alternative to the chromatographic purification of triazole phosphonite-boranes, dialysis in *n*-propanol / water 3:1 with a molecular weight cut off (MWCO) of 500 Da for three days gave similar pure products as determined by ¹H NMR (Figure 3.6). Although, dialysis was capable to remove all organic impurities, the copper removal was not acceptable with still 51% of the added copper left.

3.4.2 Hydrolysis of triazole phosphonites

Due to the hydrolysis of phosphonites in aqueous systems the time frame, in which the Staudinger-phosphonite reaction must proceed, is limited. The hydrolysis study of aryl phosphonites already revealed an enormous impact of the different oxy-bound substituents at the phosphorus to the hydrolysis rate. The hydrolysis rate of three triazole phosphonites with an attached mOEG₆ chain at the triazole (**199**, **236** and **337**) to ensure water-solubility was determined by ³¹P NMR over six hours (Figure 3.7). The hydrolysis rate was measured in tris / HCl buffer at a pH of 8.2 containing 10% dimethyl sulfoxide. The half-life time of the ethoxy substituted phosphonite **199** under these conditions was 26 minutes. The *p*-mPEG₆-*m*-nitro-benzyl substituents already duplicated the stability of the phosphonite **237**, which shows a half-life time of 47 minutes. The most stable phosphonite was the mOEG₂ substituted one **236** with 50% phosphonite left after 57 minutes.

Additionally, Figure 3.7 shows two aryl phosphonites (**239** and **240**) as comparison. The triazole phosphonites revealed all a significant increase in stability against hydrolysis compared to the aryl phosphonites **239** and **240**, which hydrolysed to over 90% within minutes (Figure 3.7). These results indicated that higher conversions of azido-peptides and proteins with triazole phosphonites can be expected compared to aryl phosphonites. For this reason, the triazole phosphonites can be considered as even more promising candidates for the functionalization of biomolecules.



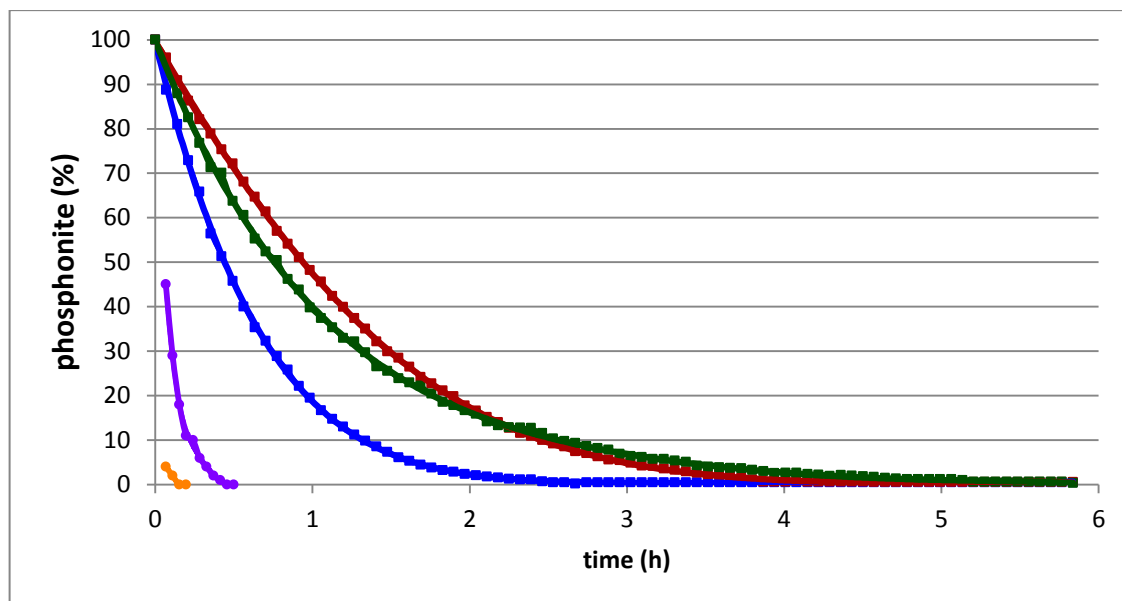
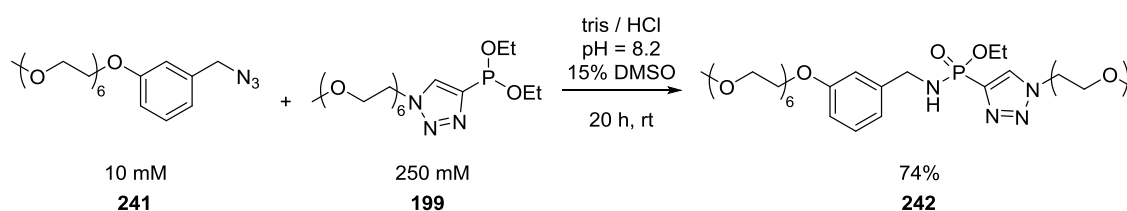


Figure 3.7: Hydrolysis rate of triazole phosphonites **199**, **236** and **237** in comparison to aryl phosphonites **239** and **240**.

3.4.3 Staudinger reactions of triazole phosphonites in aqueous systems

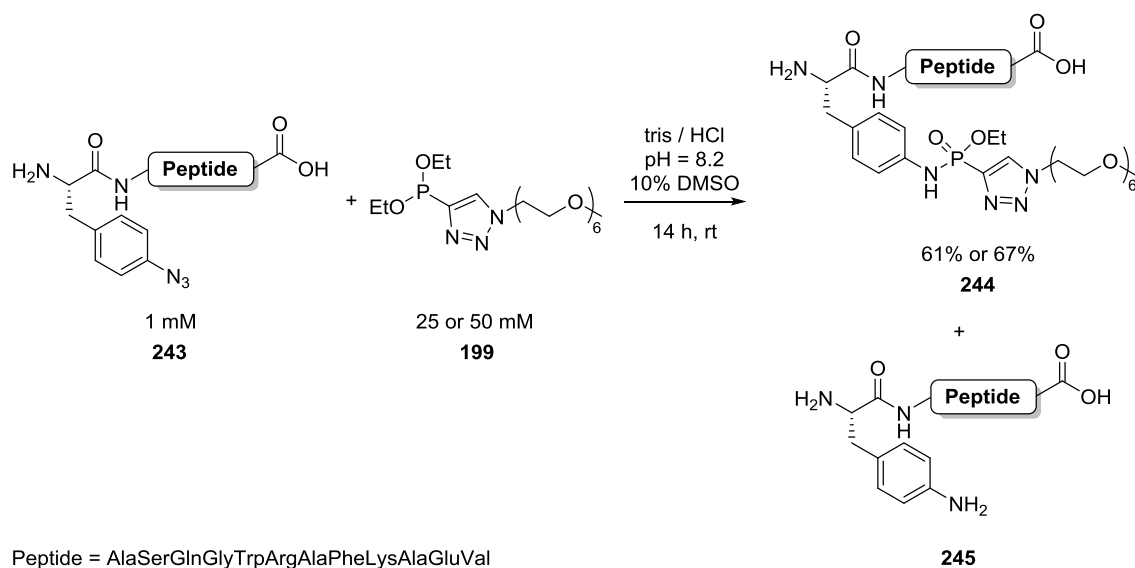
The first Staudinger reaction of a triazole phosphonite in water was already done during the initial studies of *alkyne phosphonites for sequential azide-azide couplings in organic solvents* (Chapter 3.3). Within these studies, a water-soluble benzyl azide **241**, (10 mM) was reacted with 25 equivalents of diethyl mOEG₆-triazole phosphonite **199** in water (+15% DMSO). HPLC-UV analysis revealed complete conversion of the benzyl azide **241** to the corresponding phosphonamidate **242**. The phosphonamidate product **242** was isolated in a yield of 74% (Scheme 3.27).



Scheme 3.27: First Staudinger reaction of a triazole phosphonite **199** in water.

The Staudinger reaction of diethyl mOEG₆-triazole phosphonite **199** could also be transferred to the peptide level. A model peptide **243** with a *p*-azidophenylalanine (Pap) at the N-terminus was synthesised by standard Fmoc-solid-phase peptide synthesis. The Staudinger-phosphonite reaction of peptide **243** (1 mM) was performed with 25 and 50 equivalents of diethyl mOEG₆-triazole phosphonite **199** (Scheme 3.28) in tris / HCl buffer at pH = 8.2 (+10% DMSO). HPLC-UV

analysis revealed full conversion of the azido peptide under these reaction conditions for both phosphonite equivalents. Besides the desired phosphoramidate peptide product **244** small amounts of the expected amine by-product **245** were found in both reactions but could not be isolated in pure form. Nevertheless, under both reaction conditions the phosphoramidate peptide product **244** was isolated in good yields of 61% (25 equivalents) and 67% (50 equivalents), respectively, after HPLC purification (Scheme 3.28).



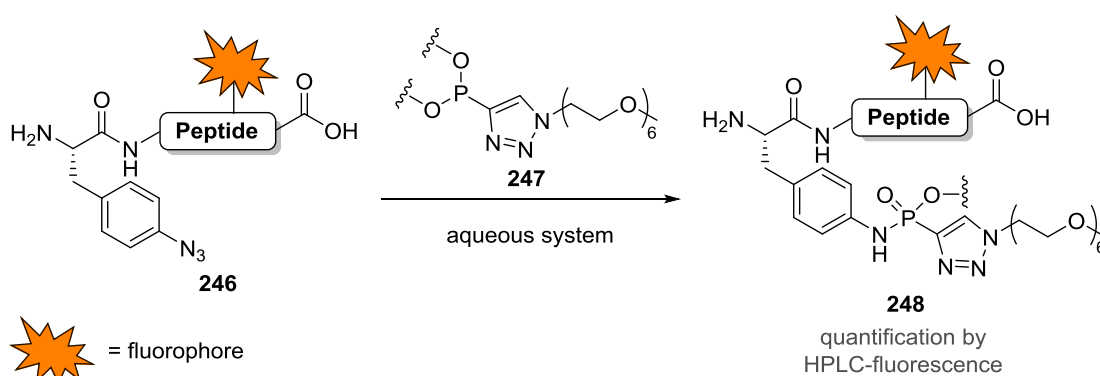
Scheme 3.28: First Staudinger reaction of triazole phosphonite **199** with an azido peptide **243** in buffer.

These results already demonstrated the feasibility of the Staudinger reaction with triazole phosphonites in aqueous systems and its potential for the functionalization of biomolecules, such as proteins. The *p*-nitrobenzyl substituted phosphonites **237** are the most promising ones because on the one hand, they should have the best leaving group abilities and on the other hand, they are structural isomers of the photocleavable *o*-nitro benzyl group which presumably will show the same reactivity as oxy bound phosphonite substituents in Staudinger reactions. The *o*-nitro benzyl substituents could later expand the scope of the *sequential azide-azide coupling* concept by light-induced cleavage of the phosphoramidate bond. However, protein concentrations of 1 mM (as in the example above) are in most cases not reachable due to their insolubility at such high concentrations, especially when applied in cell lysates where numerous other molecules are present. For this reason, it was crucial to find a balance between azide concentration and conversion rates. In order to identify the optimal ratio, model azido peptides were used. The quantification of the peptide reaction by isolation or HPLC-UV was not suitable for very low peptide and high phosphonite concentration so that an

alternative quantification method had to be established. Especially, in case of the above mentioned *p*-nitro benzyl substituted phosphonites, UV signals of the peptide were not detectable anymore due to the high background signals of the *p*-nitro benzyl hydrolysis by-products (compare Scheme 3.4 for hydrolysis by-products).

3.4.3.1 Quantification of the Staudinger-phosphonite reaction by fluorophore-tagged azido peptides

One of the most common methods to analyse peptide reactions with respect to their conversion and their product ratios, is the installation of a fluorescence tag onto the peptide of interest **246**. The very high sensitivity of fluorescent spectrometry enables accurate detection of even low amounts of the fluorophore-tagged molecule. Therefore, this methodology was considered as the ideal method to study the product and by-product formation of the Staudinger reaction in aqueous systems. This method should allow the detection and separation of the formed compounds by HPLC-fluorescence without being influenced and interfered by the non-fluorescence phosphonite **247** derivatives and their hydrolysis by-products (Scheme 3.29).

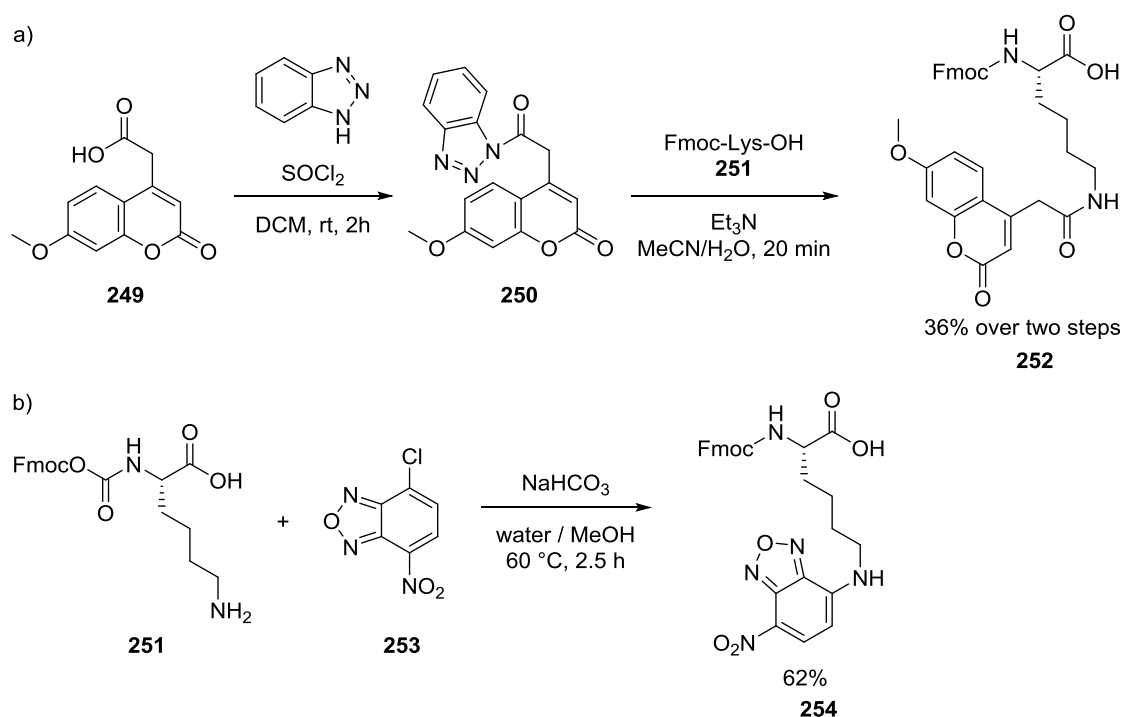


Scheme 3.29: General strategy for the quantification of the Staudinger-phosphonite reaction via fluorescence-tagged azido peptides.

Two frequently applied fluorophores for the labelling of peptides or biomolecules are coumarin^[85, 156] and 4-amino-7-nitrobenzo-2-oxa-1,3-diazole (NBD). The two fluorophores differ in their extinction and emission wavelength. Whereas coumarin shows an emission at 410 nm, NBD is detected at 550 nm. An advantageous aspect of both fluorophores is their possibility to be incorporated into a peptide chain by SPPS as their lysine-bound building blocks. Moreover, NBD has a high quantum yield and Fmoc-Lys(ϵ -NBD)-OH (**254**) was already be used successfully

by Waldmann *et al.* to track the membrane binding of the protein chimeras, which consists of a cholesterol molecule bound *via* a heptapeptide to N-RasG12V.^[157]

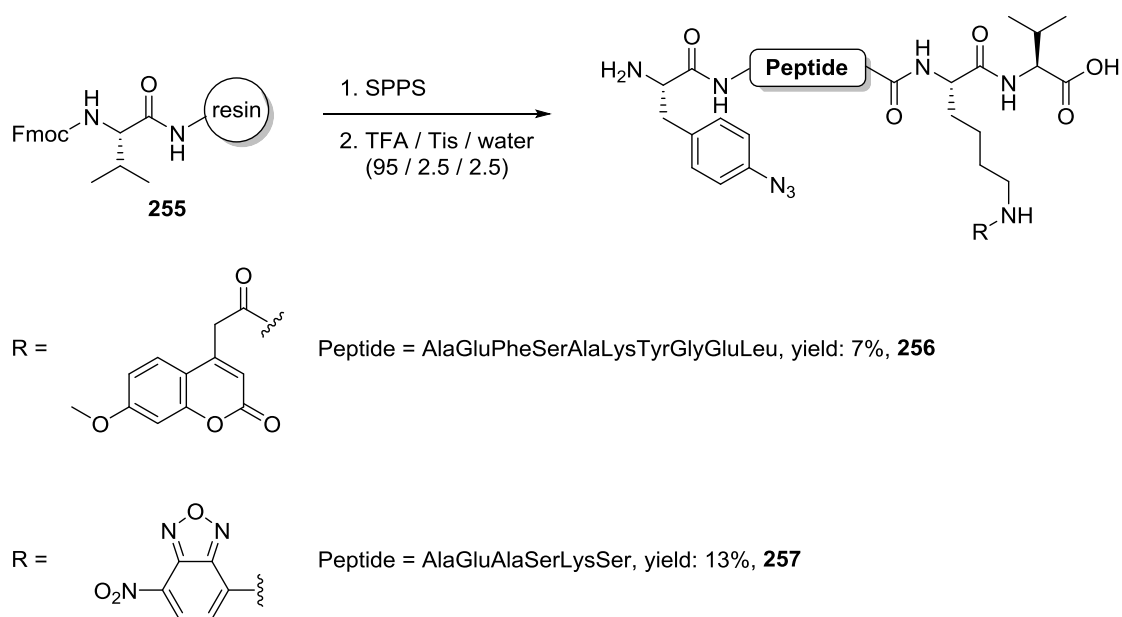
The attachment of the fluorophores can in both cases easily be achieved starting from commercially available fluorophore derivatives. The commercially available 7-methoxycoumarin-4-acetic acid **249** bears an acetic acid at the position four, which enables coupling to a lysine **251** side chain under standard coupling conditions, which leads to the formation of a stable amide bond in a yield of 36% (Scheme 3.30 a). Fmoc-Lys(ϵ NBD)-OH **254** was synthesized in yield of 62% starting from Fmoc-Lys-OH **251** and 4-chloro-7-nitrobenzofurazan **253** in water/MeOH under basic conditions. In this case, the connection was not realised by an amide bond but *via* a secondary amine bond at the aromatic system of the NBD by nucleophilic aromatic substitution (Scheme 3.30 b).



Scheme 3.30: Synthesis of a) Fmoc-Lys(ϵ -coumarin)-OH **252** and b) Fmoc-Lys(ϵ -NBD)-OH **254** building blocks for SPPS.

Both fluorophore-tagged Fmoc-Lys-OH **252** and **254** were afterwards introduced into a model azido peptide by SPPS (Scheme 3.31). The fluorophore-tagged amino acid **252** and **254** were incorporated into the peptide chain at position two, whereas the *p*-azidophenylalanine for the Staudinger reaction was attached as N-terminal amino acid. The fluorophore peptides **256** and **257** were obtained in 7% and 13% yield after HPLC purification. Unfortunately, even after several HPLC purifications no completely pure coumarin-tagged azido peptide **256** was gained

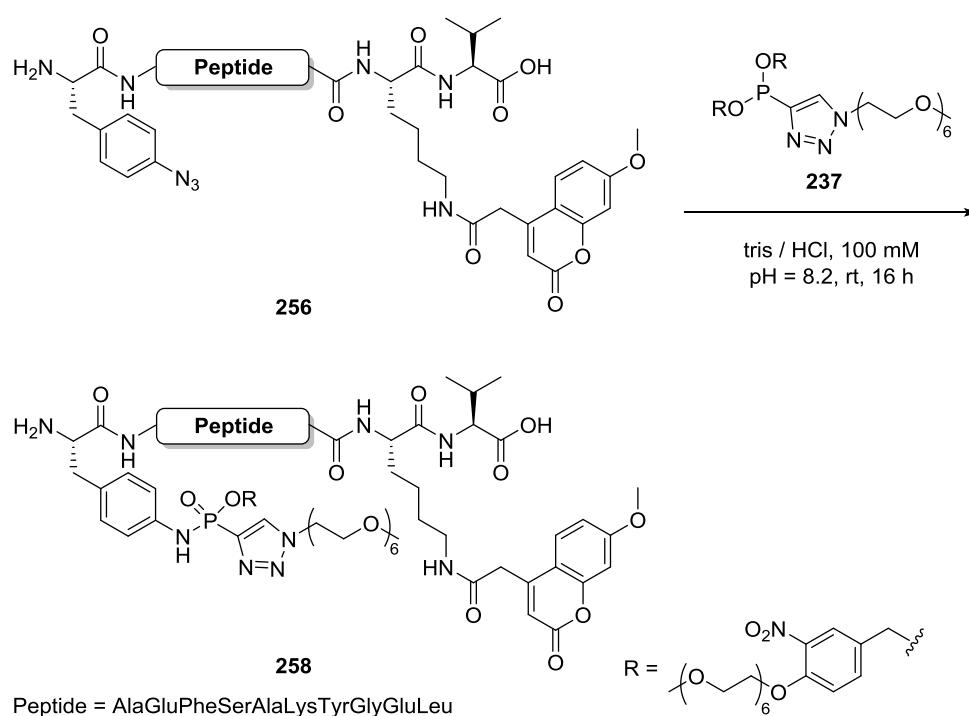
(Figure 3.8 a). Nevertheless, both azido peptides **256** and **257** were applied in the Staudinger-phosponite reaction with di-*p*-mOEG₆-*m*-nitrobenzyl triazole phosphonite **237**.



Scheme 3.31: Solid-phase peptide synthesis of coumarin-tagged azido peptide **256** and NBD-tagged azido peptide **257**.

Afterwards, the Staudinger reaction was performed with coumarin-tagged azido peptide **256** (25 mM) (Scheme 3.32) as well as with NBD-tagged azido peptide **257** and phosphonite **237** (500 equiv.) in tris / HCl (100 mM, pH = 8.2, 10% DMSO) at room temperature for 16 hours (Scheme 3.32). The Staudinger reaction of the NBD-tagged azido peptide **257** with phosphonite **237** was additionally probed with a lower azido peptide concentration of 25 mM with 500 and 250 equivalents of phosphonite **237** (Table 3.1). After the Staudinger reaction a HPLC-fluorescence as well as a HPLC-MS spectrum was measured. The conversion was determined by integration of the corresponding azido, amino and phosphoramidate peptide **258** signals in the fluorescence trace. In the case of the coumarin-tagged azido peptide after 16 h only a very small peak of residual azido peptide **256** could be observed. A very large peak with a two minutes higher retention time appeared in the HPLC-fluorescence spectrum, which could be attributed to the desired phosphoramidate peptide **258** as proven by mass spectrometry. Besides the expected signal for the phosphoramidate **258** and the azido peptide **256**, a phosphonate **259** coming from the hydrolysis and oxidation of the phosphonite as well as some small undefinable peaks probably originating from the applied peptide, could be detected by analysis of the HPLC spectra (Figure 3.8 b). Unfortunately, the applied phosphonites and decomposition product **259** showed some fluorescence activity in the same wavelength region as the fluorescence-tag. For this reason, it is likely that the peak intensity of

the peptides is influenced and does not give the accurate ratio after integration. Moreover, this peptide seems to be degraded after some time, which makes complete purification leading to a single peak for the starting material impossible. The degradation products of the peptide **256** were observed at a similar retention time as the starting material so that precise integration of the peaks was likewise not possible due to their overlap. Nevertheless, the fact that the phosphoramidate **258** gave the major peak in the spectrum is a first very promising result which shows that high amounts of phosphoramidate product can be obtained *via* Staudinger-phosphonite reaction in aqueous systems.



Scheme 3.32: Staudinger-phosphonite reaction with a coumarin-tagged azido peptide **256**.

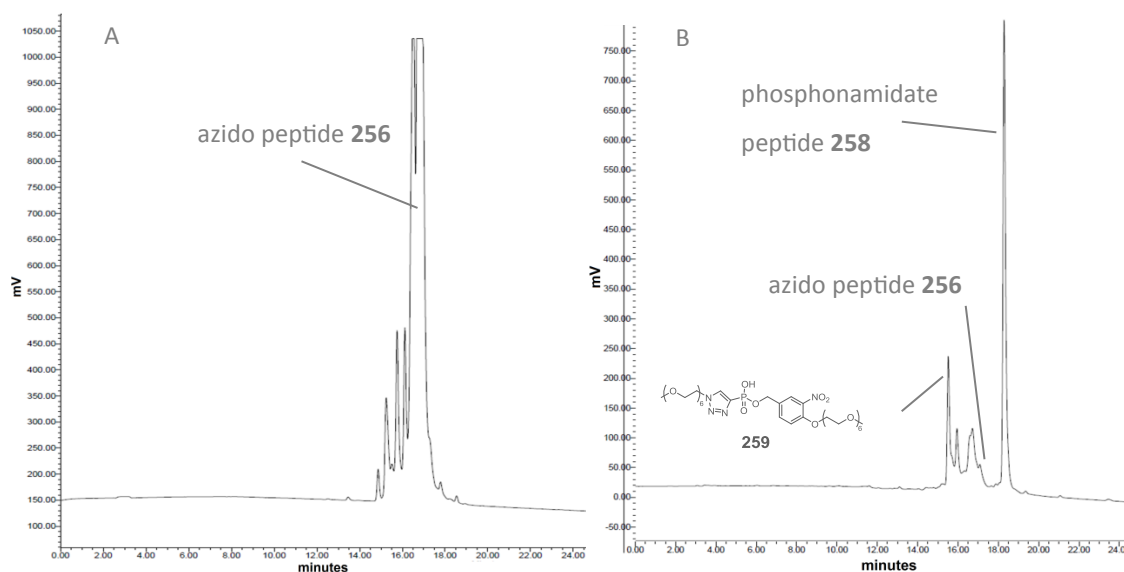
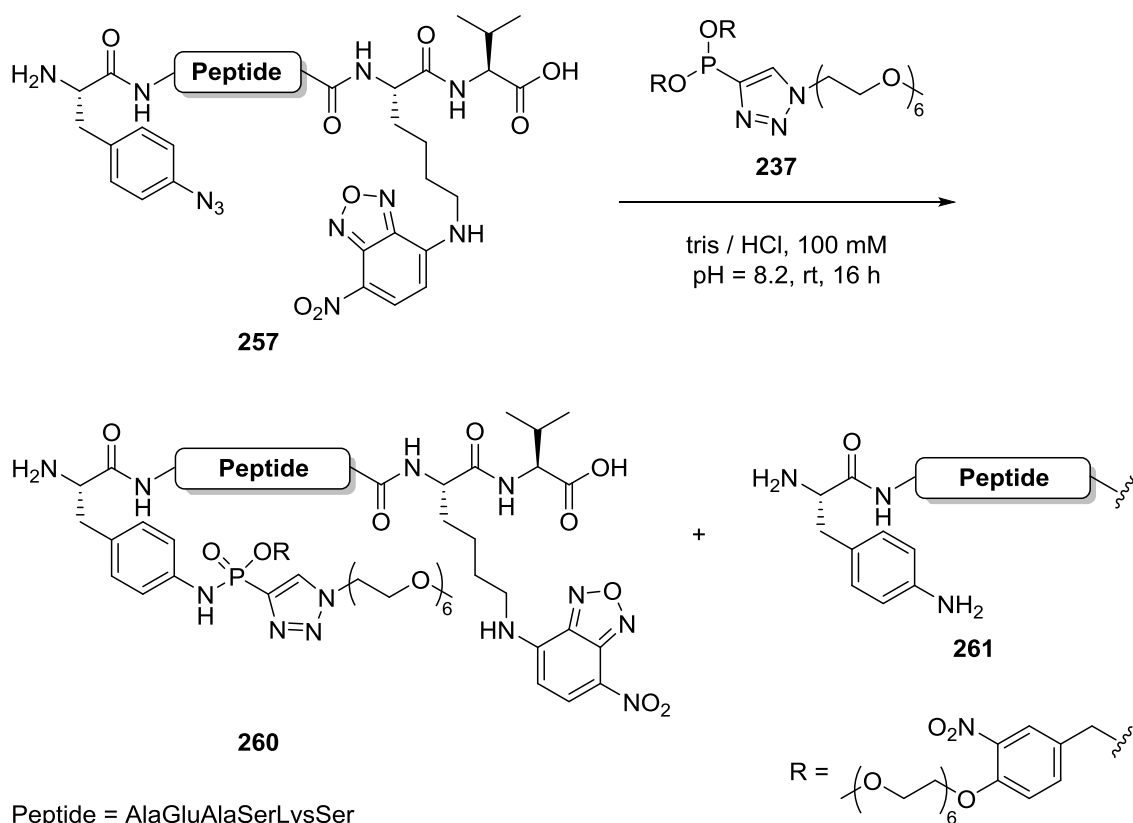


Figure 3.8: A) Fluorescence spectrum of coumarin tagged azido peptide **256** after HPLC purification. B) Fluorescence spectrum of Staudinger reaction of azido peptide **256** with phosphonite **237**. (Ex [nm]: 360, Em [nm]: 410)

The result of the Staudinger reaction of the NBD-tagged azido peptide **257** with phosphonite **237** showed the desired phosphonamidate product **260**, which could be detected in the fluorescence spectra and was confirmed by mass spectrometry. Under all three reaction conditions, the phosphonamidate **260** was formed as major product and minor amounts of the azido peptide **257** and the amino peptide **261** (Scheme 3.33), coming from the Staudinger reaction, could be observed. Furthermore, no other major side reaction could be perceived. With a 25 mM concentration of azido peptide **257** and 250 equivalents of phosphonite **237**, 69% of phosphonamidate product **260** formation was determined by integration of the fluorescence spectrum (Table 3.1). If the concentration of the azido peptide **257** was increased to 50 mM, the phosphonamidate **260** was formed with a conversion of 86% (see Figure 3.9 for an exemplary spectrum). The same result could be achieved with the lower azide concentration of 25 mM but 500 equivalents of phosphonite **237** (Table 3.1). This leads to the assumption that high concentrations of starting materials are needed to ensure high amounts of the functionalised molecule.



Scheme 3.33: Staudinger-phosphonite reaction with a NBD-tagged azido peptide **257**.

Table 3.1: Conversion of the NBD-tagged azido peptide **257** (Scheme 3.33) determined by fluorescence HPLC.

| entry | NBD-tagged azido peptide 257 [μM] / equivalents of phosphonite 237 | formed phosphoramidate 260 [%] |
|-------|---|---------------------------------------|
| 1 | 50 / 250 | 86 |
| 2 | 25 / 500 | 86 |
| 3 | 25 / 250 | 69 |

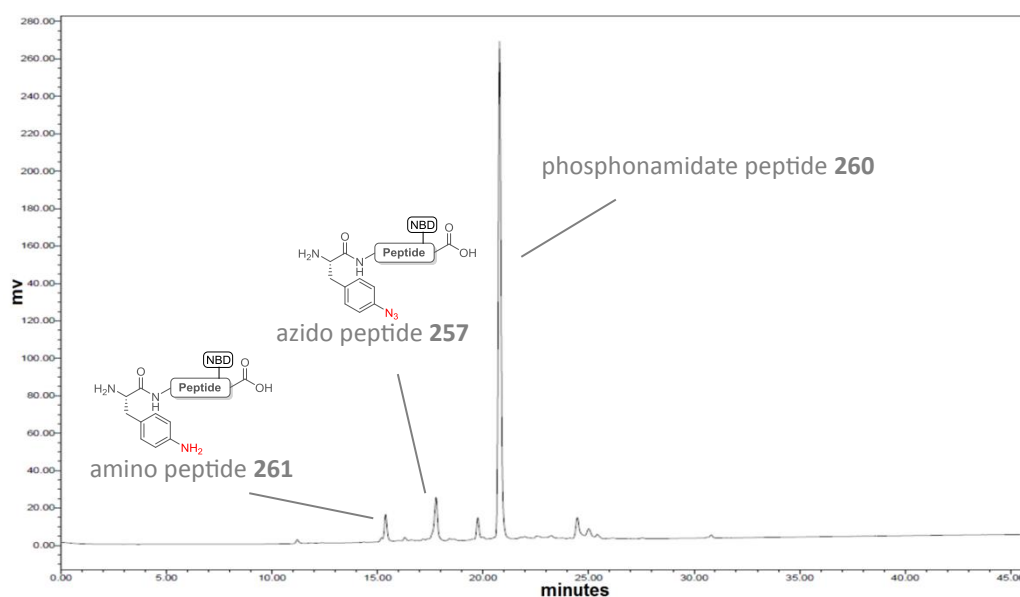
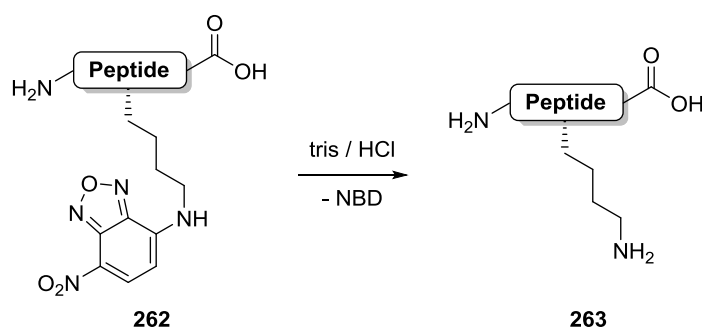


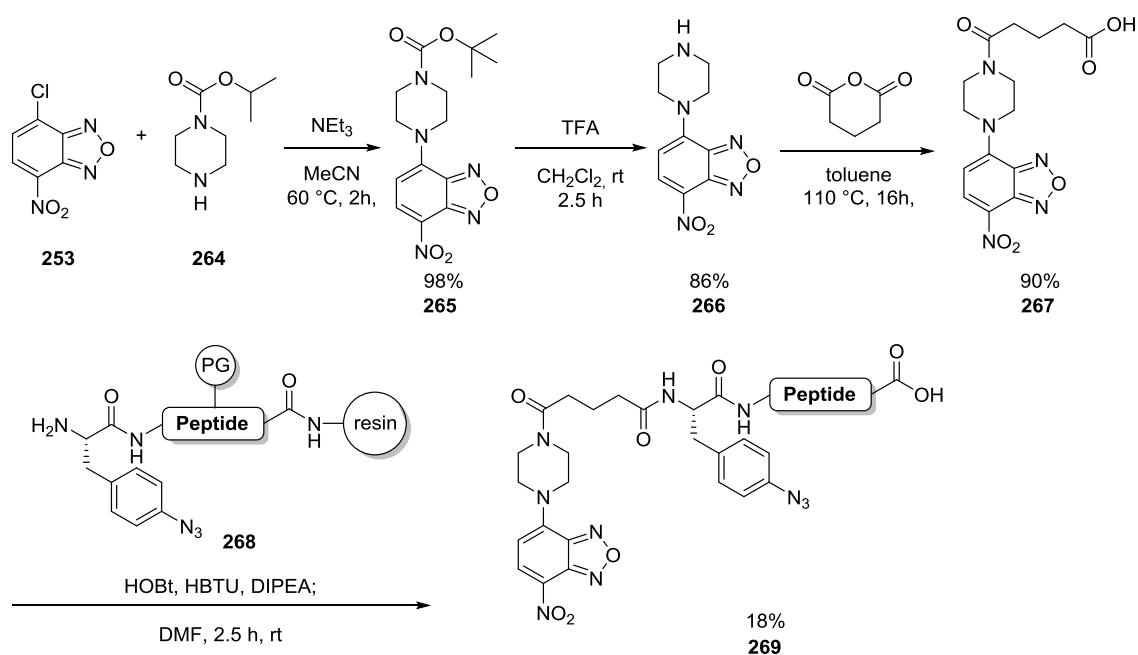
Figure 3.9: Exemplary fluorescence spectrum of Staudinger-phosphonite reaction with NBD-tagged peptide **256**. (Ex [nm]: 470, Em [nm]: 550)

Although the results obtained by these preliminary investigations suggest that the Staudinger-phosphonite reaction proceeds in aqueous systems, more investigations are needed to confirm the obtained data. The fluorescence trace of the NBD-tagged azido peptide **257** displayed an intensity of about 700 mV. In contrast, its phosphonamidate peptide, which is the major peak in the fluorescence trace after the reaction, only had an intensity of about 270 mV though the same concentration and amount was injected to the HPLC-fluorescence. This leads to the supposition that also this fluorophore degrades, is cleaved off during the reaction, or that the fluorescence is diminished due to quenching with the applied phosphonite or formed phosphonamidate. It could be proven by Jordi Bertran-Vicente, a PhD student in the Hackenberger group, that NBD-peptides **262** decompose in tris / HCl buffer over time to the corresponding un-tagged peptides **263** (Scheme 3.34).



Scheme 3.34: General decomposition of NBD-tagged peptides **262**.

It was assumed that the stability of the NBD group can be increased if it is attached *via* tertiary amine as opposed to the secondary amine in Lys(ϵ -NBD) as in peptide **257** or **262**. For this reason, NBD was coupled to the N-terminus of the peptide *via* a tertiary amine / glutaric acid linker (see Scheme 3.35). The stability of this new NBD-peptide **269** was tested as well in tris / HCl buffer over 48 hours. It could be observed that the NBD-group was cleaved of in tris / HCl buffer. Over the first six hours the stability of the new peptide was sufficient with only small amounts of NBD-amine being formed. After 24 hours already 15% were cleaved of and finally after 48 hours 31% of the NBD-tagged peptide **269** were decomposed to the un-tagged peptide **270** (Figure 3.10). Although quenching of the fluorophore cannot be excluded, the observed instability of the NBD linkage already prohibits the applicability of NBD as reliable quantification tag in buffer systems.



Peptide = AlaGluPheAlaSerIleLysVal

(PG) = protecting groups

Scheme 3.35: Synthesis of the second NBD-tagged azido peptide **269**.

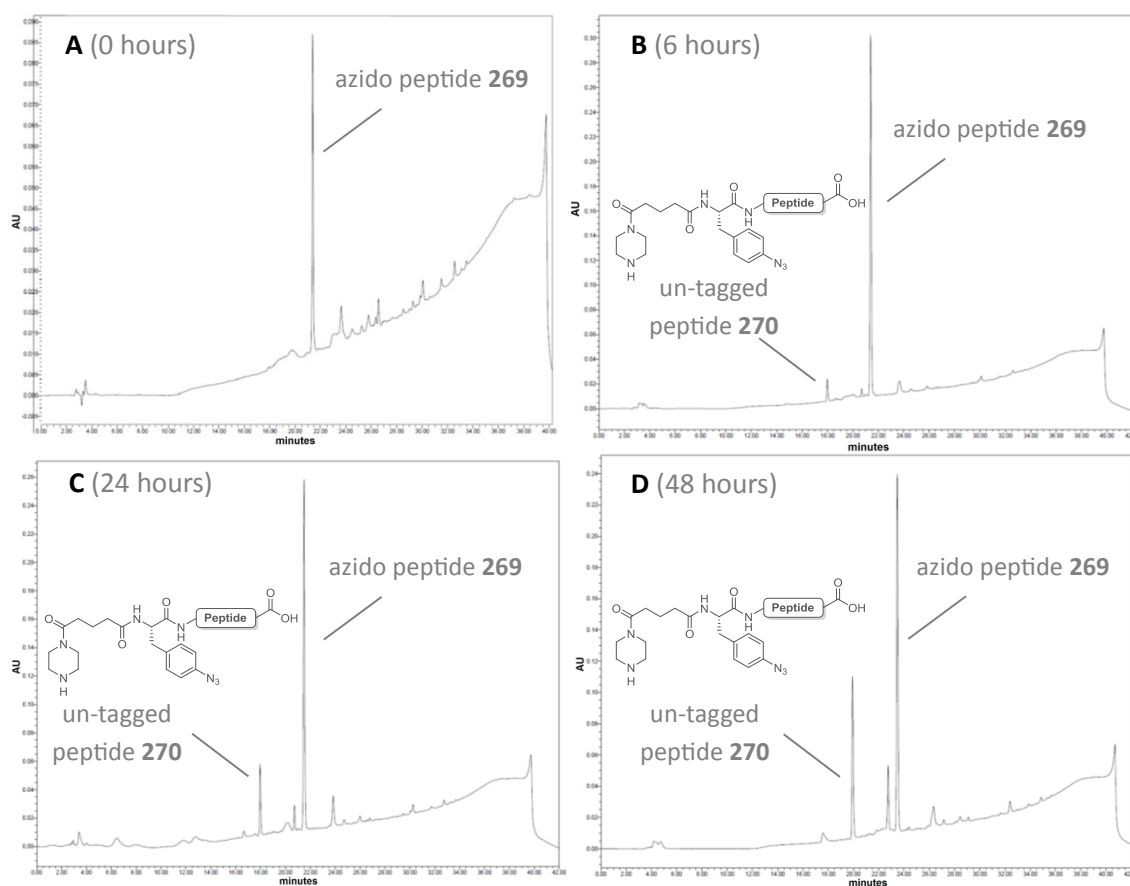


Figure 3.10: HPLC-UV (280 nm) investigation of the stability of the new NBD-tagged azido-peptide **269** in tris / HCl buffer at pH = 8.2 over 48 hour. A) 0 hours, B) 6 hours, C) 24 hours, D) 48 hours.

Nevertheless, the results of the quantification by fluorophore-tagged azido peptide should still give a relatively realistic picture of the Staudinger-phosphonite and the formed product ratios. As cleavage of the NBD group as well as quenching of the NBD-signals by the phosphonite or its hydrolysed derivatives would affect all detected peptide compounds in the reaction mixture in the similar manner, the ratios obtained by integration of the fluorescence trace should still give a realistic picture of the reaction outcome. Moreover, if quenching is caused by the formation of the phosphoramidate moiety formed the amount of phosphoramidate determined so far is even lower than the real one.

In conclusion, the Staudinger-phosphonite reaction with fluorophore-tagged azido peptides **256** and **257** could demonstrate that the desired phosphoramidates can be obtained in high conversions with only minimal amounts of azido peptide or amino peptide in the reaction mixture under different reaction conditions. Nevertheless, a more precise method, such as quantitative mass spectrometry, was needed to receive more reliable and more accurate results.

3.4.3.2 Quantification of the Staudinger-phosphonite reaction by mass spectrometry

Another very sensitive analysis method, which requires only very small amounts of compound, is mass spectrometry. Mass spectrometry normally provides only qualitative information about a sample because the peak intensity is highly dependent on the ionisation of every molecule, the applied voltage for the ionisation as well of the concentration of molecules and salts present during the ionisation.

In order to turn mass spectrometry into a quantitative analysis method, every parameter except the molecular weight of the molecule of interest and a known standard must be identical to make their signals comparable. Molecules that meet these requirements are isotopic isomers of the molecule of interest. With the same HPLC retention time, the outer influence is for both the same at the moment they are ionised. Moreover, they are chemically identical and their ionisation behaviour is alike. The isotopic isomer can be added in a known quantity so that from the relative peak integrals the unknown amount of the desired molecule can be calculated.^[158] With this methodology, HPLC-MS can be used to quantify small amounts of a given sample and therefore, meets all the required criteria given for the quantification of the Staudinger-phosphonite reaction of peptides in aqueous media. The obvious drawback of this method is the high synthetic effort because for every molecule that needs to be quantified the isotopic isomer must first be synthesised and isolated.

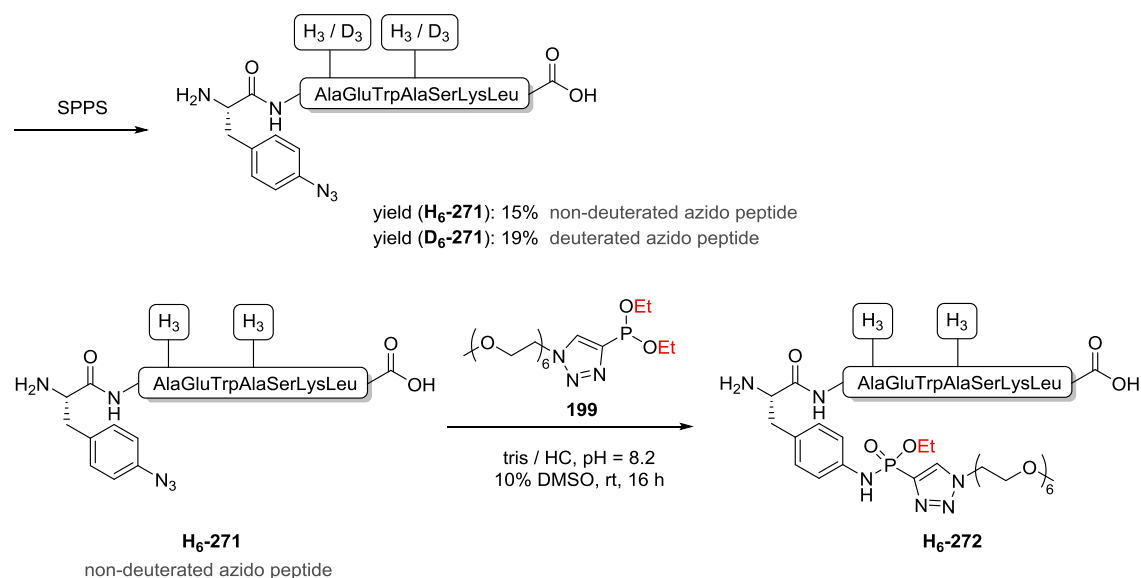
The crucial part of the isotopic-based mass spectrometry quantification is the ionisation. Salts and other organic molecules, which are present during the ionisation, can lead to an unsuccessful ionisation of the molecule of interest. This can result either in complete disappearance of the desired peaks or an unnatural isotopic pattern in the mass spectrum.^[158b] For this reason, the isotopic pattern of the azido peptide and the phosphoramidate products was determined from purified peptides.

Four stable heavy isotopes come into consideration for isotopic labelling of peptides, namely ^2H , ^{13}C , ^{15}N and ^{18}O . With about 350 € per gram, the application of deuterated amino acids is the most cost-efficient option. In case of alanine, the three protons at the methyl group are exchanged to deuterium leading to a mass difference of three, which is sufficient for an effective differentiation of the two isotopic isomers. Nevertheless, due to the high mass difference from protons and deuterium the isotopic effect can lead to a small delay in HPLC retention time.^[159] Therefore, ^{15}N , which costs about 1000 € per gram amino acid, is mostly used in proteomics nowadays.^[158b]

Within this study, the outcome of the Staudinger-phosphonite reaction between different phosphonites and azido peptides was quantified by mass spectrometry under different reaction conditions: a) influence of the buffer concentration on the Staudinger-phosphonite reaction with diethyl triazole phosphonite **199**, b) influence of the azido peptide and di-*o*-mOEG₆-*m*-nitrobenzyl triazole phosphonite **237** concentration on the Staudinger-phosphonite reaction c) investigation of the Staudinger-phosphonite reaction with different azido peptide concentrations and three different triazole phosphonites bearing oxy-bound diethyl- **199**, di-mOEG₂- **236** or di-*p*-mOEG₆-*m*-nitrobenzyl **237** substituents and d) influence of different buffer systems and pH values on the Staudinger-phosphonite reaction in dependency of the oxy-bound substituents. For the quantification of the observed products, deuterated azido peptides were used as internal standard. The preparation of isotopically labelled peptides, triple deuterated alanines (D₃-Ala) was chosen for the incorporation into a model azido peptide **H₆-271**. The deuterated azido peptide **D₆-271**, which contained two D₃-alanines for a higher mass difference, was synthesised analogous to the corresponding non-deuterated azido peptide (**H₆-271**) by SPPS and purified by HPLC.

Influence of the buffer concentration on the Staudinger-phosphonite reaction

In order to probe the influence of different buffer concentration, the Staudinger reaction was performed with diethyl tetazole phosphonite **199** and azido peptide **H₆-271** (Scheme 3.36) in a tris / HCl buffer at pH 8.2 with different azide, phosphonite and buffer concentrations (Table 3.2). After the reaction, a known amount of deuterated azido peptide **D₆-271** was added to the reaction mixture before the solution was injected to HPLC-MS (Agilent 6210 TOF LC/MS at the FU-Berlin). In the received high resolution mass spectra, the peaks of the deuterated and non-deuterated azido peptides **D₆-271** and **H₆-271** were integrated to calculate the amount of remaining starting azido peptide **H₆-271** from the Staudinger reaction.



Scheme 3.36: Synthesis of azido peptide **H₆-271** and **D₆-271** as internal standard for HPLC-MS quantification and Staudinger reaction of azido peptide **H₆-271** and phosphonite **H₆-272**.

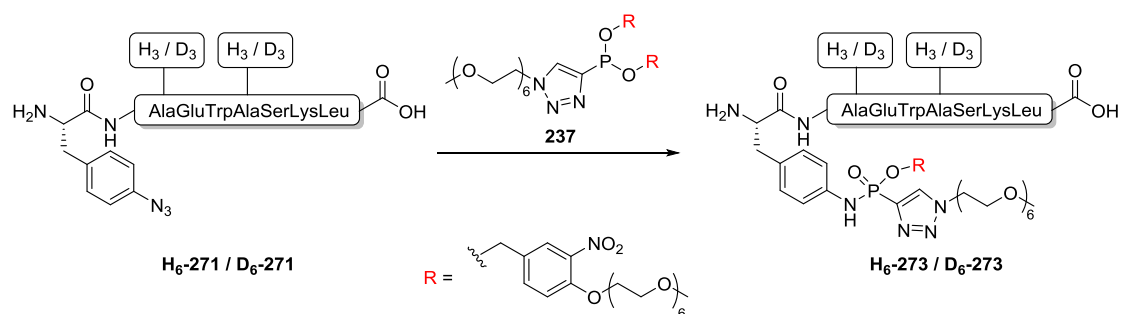
Table 3.2: Influence of buffer concentration on the Staudinger-phosphonite reaction of azido peptide **H₆-272** quantified by mass spectrometry.

| buffer concentration | conversion of azido peptide H₆-271 | | | |
|----------------------|--|--|--|--|
| | azido peptide H₆-271 [100 μM] | | azido peptide H₆-271 [50 μM] | |
| | diethyl triazole phosphonite 199 [500 equiv.] | diethyl triazole phosphonite 199 [250 equiv.] | diethyl triazole phosphonite 199 [500 equiv.] | diethyl triazole phosphonite 199 [250 equiv.] |
| 1 M | 90 | 40 | 68 | 28 |
| 0.1 M | 100 | 53 | 95 | 33 |

The calculated amounts of unreacted azido peptide **H₆-271** demonstrated that the conversions in a lower concentrated tris / HCl of 0.1 M are significantly higher (5-27%) than in the 1 M tris / HCl buffer. Moreover, if 500 equivalents of diethyl triazole phosphonite **199** were added to the reaction mixture, in almost all cases a nearly quantitative conversion of the azido peptide **H₆-271** could be observed. Only when the buffer concentration was 1 M and the azido peptide **H₆-271** concentration was only 50 μM the conversion dropped to 68%. In contrast, if the phosphonite concentration was decreased to 250 equivalents, the conversion of the azido peptide **H₆-271** had a much higher influence on the conversion rate. The conversion differed by about 20% depending on the azido peptide **H₆-271** concentration. In conclusion, this experiment revealed a higher conversion in lower buffer concentration (0.1 M) and higher concentration of azido peptide **H₆-271** and diethyl triazole phosphonite **199**.

Influence of the azido peptide and di-*o*-mOEG₆-*m*-nitrobenzyl triazole phosphonite concentration on the Staudinger-phosponite reaction

The next step was the application of di-*o*-mOEG₆-*m*-nitrobenzyl triazole phosphonite **237** in Staudinger reactions with the same azido H₆-peptide **H₆-271** under the optimal buffer concentration of 0.1 mM (Scheme 3.37, Table 3.3). Also here different concentrations of di-*o*-mOEG₆-*m*-nitrobenzyl triazole phosphonite **237** and azido peptide **H₆-271** were probed, however based on the previous results only the 0.1 M tris / HCl buffer was used. To get a better idea of the reaction outcome and to determine the amount of by-product formation, for the deuterated analogue of the formed phosphoramidate peptide **D₆-273** was synthesised as additional internal standard. Consequently, the deuterated azido peptide **D₆-271** was converted with di-*o*-mOEG₆-*m*-nitrobenzyl triazole phosphonite **237** in dry acetonitrile (Scheme 3.37). The deuterated phosphoramidate product **D₆-273** was purified by HPLC. Subsequently, the Staudinger reaction was performed with azido peptide **H₆-271** and di-*o*-mOEG₆-*m*-nitrobenzyl triazole phosphonite **237** under different reaction conditions but this time both, the azido peptide **D₆-271** and the phosphoramidate peptide **D₆-273** were added for quantification in a known amounts as internal standards before the HPLC-HRMS measurement.



reaction conditions

H₆-271: tris / HCl, pH = 8.2, 0.1 M, 10% DMSO, rt, 16 h.

D₆-271: 1. MeCN, 14 h, rt, 2. + H₂O, 6 h, rt, 55%.

Scheme 3.37: Staudinger reaction of azido peptide **H₆-271** with di-*o*-mOEG₆-*m*-nitrobenzyl triazole phosphonite **237** in acetonitrile or tris / HCl buffer.

Table 3.3: Quantification of the Staudinger reaction of azido peptide **H₆-271** and di-*o*-mOEG₆-*m*-nitrobenzyl triazole phosphonite **237** under different reaction conditions by high resolution mass spectrometry.

| azido peptide H₆-271 [μM] | phosphonite 237 [equiv.] | DMSO [%] | conversion of azido peptide H₆-271 [%] | formed phosphonamidate H₆-273 [%] |
|--|------------------------------------|-------------|---|---|
| 50 | 500 | 10 | 100 | 100 |
| 50 | 250 | 10 | 100 | 100 |
| 50 | 250 | 5 | 100 | 100 |
| 50 | 100 | 10 | 84 | 86 |
| 25 | 500 | 5 | 94 | 85 |
| 25 | 250 | 10 | 81 | 81 |
| 25 | 250 | 5 | 75 | 77 |
| 25 | 100 | 5 | 37 | 54 |

The integrals of the obtained HRMS-spectra showed that with a 50 μM concentration and at least 250 equivalents of di-*o*-mOEG₆-*m*-nitrobenzyl triazole phosphonite **237** full conversion to the phosphonamidate **H₆-271** could be detected without any side-products observed. Nevertheless, it is unlikely that no reduction of the *p*-azidophenylalanine to the corresponding *p*-aminophenylalanine occurred as observed before. If the phosphonite concentration was decreased to 100 equivalents the conversion dropped to 86%. Lowering the amount of azido peptide **H₆-271** to 25 μM was accompanied by a decrease in phosphonamidate **H₆-273** formation (34-81%). Thus, high concentrations of di-*o*-mOEG₆-*m*-nitrobenzyl triazole phosphonite **237** (500 equivalents) were necessary to reach a conversion of 85%. With a 25 μM azido peptide **H₆-271** concentration and only 100 equivalents of di-*o*-mOEG₆-*m*-nitrobenzyl triazole phosphonite **237** the yield of phosphonamidate **H₆-273** was significantly diminished to around 50%. In general, it has to be noted that the obtained ratios display a considerable high mistake of up to 17% and so do not always sum up to 100%. As mentioned above, the ionisation of the sample in the mass spectrometer plays a crucial role for the correct detection of the desired molecule ions. Especially, if high amounts of other organic compounds or salts are present the ionisation of the desired molecule can be reduced drastically or even totally disappear. Pre-purification or voltage tuning at the MS instrument can lead to enhanced signal intensity. Another factor that can influence the results is the overall pollution of the instrument. Therefore, regular maintenance of the used mass spectrometer is highly recommended for accurate quantifications.

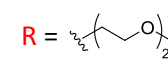
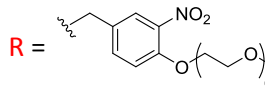
Investigation of the Staudinger-phosphonite reaction with different azido peptide concentrations and three different triazole phosphonies

In order to verify the above displayed results the reaction was repeated with the diethyl triazole phosphonite **199** and the di-*p*-mOEG6-*m*-nitrobenzyl triazole phosphonite **237** with another peptide. Additionally, another phosphonite **236** bearing two mOEG₂ substituents at the phosphorus was applied in the Staudinger reaction. The Staudinger reaction was again performed under various reaction conditions (buffer or water) and the conversion was determined by addition of the corresponding deuterated azido and phosphoramidate peptides as internal standards. In order to reduce the costs of this experiment, the non-deuterated azido peptide **H₃-243** and the non-deuterated phosphoramidate peptides **H₃-274**, **H₃-275** and **H₃-244** were synthesised in acetonitrile and purified by HPLC to serve as internal standard whereas the deuterated azido peptide **D₃-243** was used for the Staudinger-phosphonite reaction in aqueous systems (Scheme 3.38).

The reactions were measured on a Waters Acquity Ultra Performance LC[®] equity with a Waters Micromass LCT Premier (ESI-ToF) at the FMP. Unfortunately, the quantification of all phosphoramidate products as well as the azido peptides **D₃-243** in the reaction of phosphonite **236** bearing mPEG₂ substituents turned out to be impossible in these measurements. This is probably caused by insufficient ionization leading, on the one hand, to an incorrect isotopic pattern (the main mass signal for M+2H²⁺ is 784.39 m/z and not 785.31 m/z) and, on the other hand, to a low signal-to-noise ratio in the obtained spectra which makes integration of the peaks due to their deformation and thereby calculation of the phosphoramidate formation very inaccurate (Figure 3.11). For this reason, only the conversion of the azido peptide **D₃-243** could be determined with an adequate accuracy and the results are given in Table 3.4.

Evaluation of the results showed that with a 100 μM concentration of azido peptide **D₃-243** and 250 equivalents of diethyl triazole phosphonite **199** or di-*o*-mOEG₆-*m*-nitrobenzyl triazole phosphonite **237** as well as with a 50 μM concentration of azido peptide **D₃-243** and 500 equivalents of phosphonite **199**, **236** or **237** a quantitative conversion of the azido peptide **D₃-243** could be achieved in all cases. With a high azido peptide concentration of 100 μM and only 100 equivalents of diethyl triazole phosphonite **199** or di-*o*-mOEG₆-*m*-nitrobenzyl triazole phosphonite **237**, still a conversion of around 60% was acquired. At lower concentrations of both, azido peptide **D₃-243** and phosphonite, the di-*o*-mOEG₆-*m*-nitrobenzyl triazole phosphonite **237** revealed significantly higher conversions of the azido peptide **D₃-239** than diethyl triazole phosphonite **199**. The reason for the higher efficiency of di-*o*-mOEG₆-*m*-

Table 3.4: Conversion of azido peptide **D₃-243** with different substituted triazole phosphonites in Staudinger reactions quantified by mass spectrometry.

| azido peptide D₃-243 [μM] / equivalents of phosphonite | DMSO [%] | conversion of azido peptide D₃-243 [%] with phosphonite | | |
|---|-------------|--|--|---|
| | | 199 | 236 | 237 |
| | | R = Et | R =  | R =  |
| | | tris / HCl buffer, pH = 8.2, 100 mM, rt, 16 h | | water, pH = 6.1, rt, 16 h |
| 100 / 250 | 10 | 99 | quantitative* | |
| 100 / 100 | 5 | 60 | | 59 |
| 50 / 500 | 10 | 99 | quantitative* | |
| 50 / 250 | 5 | 71 | | 93 |
| 50 / 100 | 5 | 12 | | 44 |
| 25 / 1000 | 10 | | | 92 |
| 25 / 500 | 5 | | | 63 |

*conversion of azido peptide **D₃-243** was determined by HPLC-UV analysis

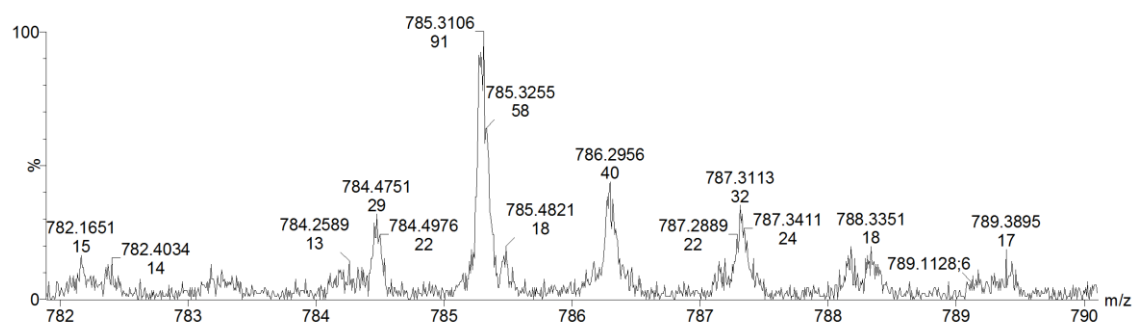


Figure 3.11: Exemplary mass spectrum which shows a *wrong* isotopic pattern as well as a too low signal to noise ratio. Therefore the peaks are too noisy for an accurate quantification.

Influence of different buffer systems and pH values on the Staudinger-phosphonite reaction in dependency of the oxy-bound substituents

The conversions at different azido peptide **D₃-243** and phosphonite concentrations in Table 3.4 already demonstrated the predominance of di-*o*-mOEG₆-*m*-nitrobenzyl triazole phosphonite **237** over diethyl triazole phosphonite **199**. A direct comparison of both phosphonites **199** and **237** with azido peptide **D₃-243** additionally revealed the influence of the

pH and different buffer systems on the conversion of an azido peptide **D₃-243** (Table 3.5). The pH influence on diethyl triazole phosphonite **199** was the most striking result in this study. The conversion of the azide peptide **D₃-243** dropped from 71% at pH = 8.2 to only 8% at pH = 7.4 in 100 mM tris / HCl buffer. In general, a faster hydrolysis of phosphonites, which should be accompanied by lower conversions of the azide, can be expected at lower pH values due to protonation of the phosphonite to the corresponding phosphonium ion, which represents the first step of their hydrolysis (see chapter 1.1.2, Scheme 1.13). In case of the di-*o*-mOEG₆-*m*-nitrobenzyl triazole phosphonite **237**, this dependency cannot be observed as in both cases a full conversion of the azido peptide **D₃-243** was achieved. An explanation for this result could be that diethyl triazole phosphonites **199** are more prone to hydrolyse *via* attack of a water molecule at the proximal carbon atom of the ethoxy substituent instead of at the phosphorus (see chapter 1.1.2, Scheme 1.14) than phosphonite **237** bearing two *p*-mOEG₆-*m*-nitrobenzyl substituents with a stronger negative inductive effect than the ethyl groups of phosphonite **199**. Exchanging the buffer from tris / HCl to phosphate buffer at the same concentration and pH (8.2) resulted in a lower conversion rate of the azido peptide **D₃-243** in Staudinger reactions with both phosphonites **199** and **237**. This interesting outcome demonstrates that the di-*o*-mOEG₆-*m*-nitrobenzyl triazole phosphonite **237** is more dependent on the applied buffer than the pH, whereas the diethyl triazole phosphonite **199** is highly dependent on both, the buffer system and, even more, reliant on the pH due to its more distinct hydrolysis pathway. In conclusion, this study revealed that a 100 mM tris / HCl buffer at a pH of 8.2 is the best reaction media for Staudinger reactions of di-*o*-mOEG₆-*m*-nitrobenzyl triazole phosphonites **237** with azido peptides **D₃-243** (50 μM) and 250-500 equivalents of di-*o*-mOEG₆-*m*-nitrobenzyl triazole phosphonite **237**.

Table 3.5: Influence of the applied buffer system and pH on the Staudinger-phosphonite reaction with azido peptides **D₃-243**, quantified by mass spectrometry.

| buffer | conversion of azido peptide D₃-243 [%] | |
|--------------------------------|--|--------------|
| | R = Et | R = |
| 50 μM / 250 equivalents | | |
| tris / HCl pH = 8.2, 100 mM | 71 | quantitative |
| tris / HCl pH = 7.4, 100 mM | 8 | quantitative |
| phosphate pH = 8.2, 100 mM | 32 | 90 |
| water | | 93 |

Summary of Staudinger-phosponite reactions with azido peptides in aqueous systems

In conclusion, the quantification of the Staudinger-phosponite reaction by fluorescence and high resolution mass spectrometry showed a clear tendency with respect to the reaction conditions. Moreover, the results obtained by both techniques are fairly consistent. All results of this chapter are summarized in Table 3.6. Generally, the best results are gained in 100 mM tris / HCl buffer at a pH of 8.2. In this buffer system mostly quantitative conversions of the azido peptide (**D₃-243** and **H₆-271**) were achieved if either high concentration of azido peptide (100 μ M) and at least 250 equivalents of phosponite or peptide concentrations of 50 μ M but 500 equivalents of phosponite were used in the Staudinger-phosponite reaction. With less equivalents of phosponite (<250), *p*-mOEG₆-*m*-nitrobenzyl substituents at the phosponite **237** are required to obtain over 90% conversion of an azido peptide. At even lower azido peptide concentrations (25 μ M) a huge excess of phosponite (1000 equivalents) is needed for a high conversion. Otherwise, if the ratio of phosponite to azido peptide is further decreased the conversion rates starts to drop drastically. In general higher conversions of azido peptides and therefore more phosphoramidate were achieved with di-*o*-mOEG₆-*m*-nitrobenzyl triazole phosponite **237** than with diethyl triazole phosponite **199**.

In these studies several problems occurred during the measurements in regard to stability of the fluorophore-tagged azido peptides and the accuracy of the high resolution mass spectrometry quantification results, so that further experimental investigations are needed to completely describe the ratio between azido and phosphoramidate peptide as well as the amount of expected amino peptide. Nevertheless, with some reaction conditions in hand that led to full conversion of the tested azido peptides, the Staudinger reaction of triazole phosponites was ready for the transformation to the protein level.

Table 3.6: Compendium of azido peptide conversions and phosphoramidate formation via Staudinger reaction of triazole phosphonites.

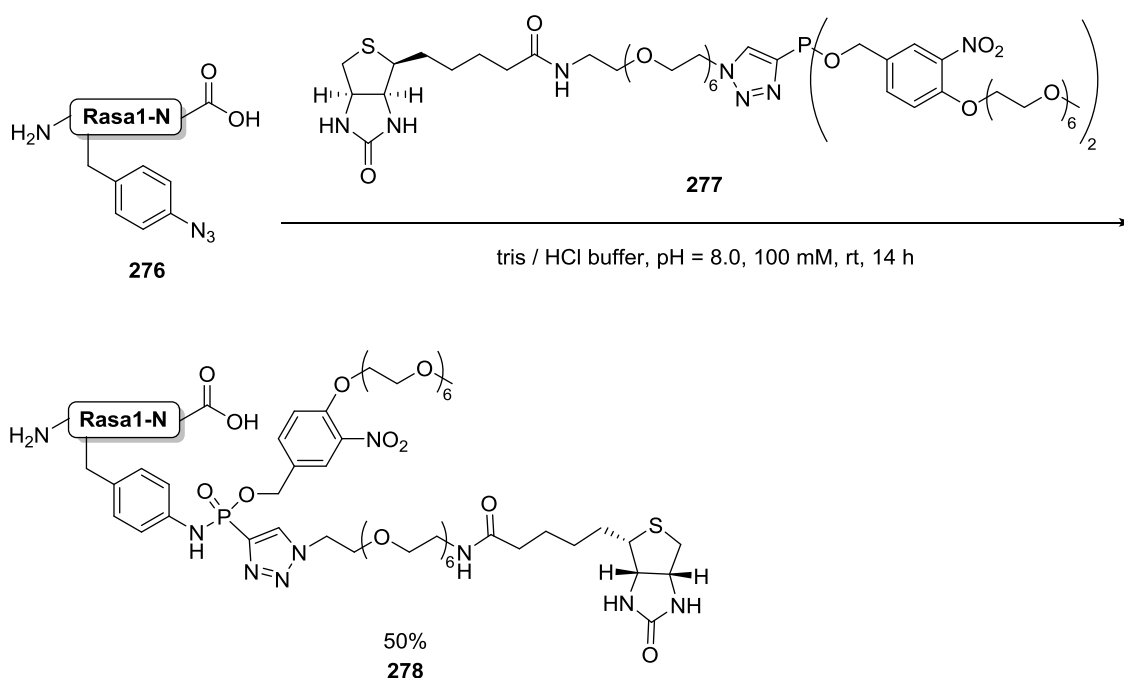
| azido peptide [μM] | | | phosphonite [equivalents] (substituents shown) | reaction media | | | conversion of azido peptide [%] | | formed phosphon- amidate [%] | |
|------------------------------------|---|---|--|----------------|------------|-------------------|---------------------------------------|----|---------------------------------------|------|
| NBD-peptide 257 | H ₆ -peptide H ₆ -271 | D ₃ -peptide D ₃ -243 | | buffer system | pH | DMSO (%) | MS | MS | fluorescence | |
| | | | | | | | | | | |
| | | | 199 | 236 | 237 | | | | | |
| 100 | | | 500 | | | tris / HCl, 0.1 M | 8.2 | 10 | 100 | |
| | 100 | | 250 | | | tris / HCl, 0.1 M | 8.2 | 10 | 100* | |
| | 50 | | 500 | | | tris / HCl, 0.1 M | 8.2 | 10 | 100* | |
| 50 | | | | 500 | | tris / HCl, 0.1 M | 8.2 | 10 | 100 | 100 |
| 50 | | | | 250 | | tris / HCl, 0.1 M | 8.2 | 10 | 100 | 100 |
| 50 | | | | 250 | | tris / HCl, 0.1 M | 8.2 | 5 | 100 | 100 |
| | 50 | | | 250 | | tris / HCl, 0.1 M | 8.2 | 5 | 100 | |
| | 100 | | 250 | | | tris / HCl, 0.1 M | 8.2 | 10 | 99 | |
| | 50 | | 500 | | | tris / HCl, 0.1 M | 8.2 | 10 | 99 | |
| | 50 | | 500 | | | tris / HCl, 0.1 M | 8.2 | 10 | 94 | |
| | 25 | | | 500 | | tris / HCl, 0.1 M | 8.2 | 5 | 94 | 85 |
| 50 | | | | 250 | | tris / HCl, 0.1 M | 8.2 | 10 | | 86 |
| 25 | | | | 500 | | tris / HCl, 0.1 M | 8.2 | 10 | | 86 |
| | 50 | | | 100 | | tris / HCl, 0.1 M | 8.2 | 10 | 84 | 86 |
| | 25 | | | 250 | | tris / HCl, 0.1 M | 8.2 | 10 | 81 | 81 |
| | 25 | | | 250 | | tris / HCl, 0.1 M | 8.2 | 5 | 75 | 77 |
| | 50 | | 250 | | | tris / HCl, 0.1 M | 8.2 | 5 | 71 | |
| 25 | | | | 250 | | tris / HCl, 0.1 M | 8.2 | 10 | | 69 |
| | 1000 | | 50 | | | tris / HCl, 0.1 M | 8.2 | 10 | | 67** |
| | 1000 | | 25 | | | tris / HCl, 0.1 M | 8.2 | 10 | | 61** |
| | 100 | | 100 | | | tris / HCl, 0.1 M | 8.2 | 5 | 60 | |
| 100 | | | 250 | | | tris / HCl, 0.1 M | 8.2 | 10 | 53 | |
| 25 | | | | 100 | | tris / HCl, 0.1 M | 8.2 | 5 | 37 | 54 |
| 50 | | | 250 | | | tris / HCl, 0.1 M | 8.2 | 10 | 33 | |
| | 50 | | 100 | | | tris / HCl, 0.1 M | 8.2 | | 12 | |
| | 50 | | | 250 | | tris / HCl, 0.1 M | 7.4 | 5 | 100 | |
| | 50 | | 250 | | | tris / HCl, 0.1 M | 7.4 | 5 | 8 | |
| 100 | | | 500 | | | tris / HCl, 1 M | 8.2 | 10 | 90 | |
| 50 | | | 500 | | | tris / HCl, 1 M | 8.2 | 10 | 68 | |
| 100 | | | 250 | | | tris / HCl, 1 M | 8.2 | 10 | 40 | |
| 50 | | | 250 | | | tris / HCl, 1 M | 8.2 | 10 | 28 | |
| | 50 | | | 250 | | phosphate, 0.1 M | 8.2 | 5 | 90 | |
| | 50 | | 250 | | | phosphate, 0.1 M | 8.2 | 5 | 32 | |
| | 50 | | | 500 | | water | 6.1 | 10 | 100 | |
| | 50 | | | 250 | | water | 6.1 | 5 | 93 | |
| | 25 | | | 1000 | | water | 6.1 | | 92 | |
| | 25 | | | 500 | | water | 6.1 | | 63 | |
| | 100 | | | 100 | | water | 6.1 | 5 | 59 | |
| | 50 | | | 100 | | water | 6.1 | | 44 | |

*conversion of azido peptide **D₃-243** was determined by HPLC-UV analysis; **isolated yield

3.4.4 Biotinylation of Rasa1-N *via* Staudinger-phosphonite reaction

After the successful conversion of azido peptides with triazole phosphonites, the next step was to investigate their conversion on the protein level. The most important questions that had to be addressed were whether the conversion of the protein is successful and whether the function of the protein is maintained. To answer these questions the protein Rasa1-N **276** was chosen, which contains a *p*-azidophenylalanine at position 2. This protein was expressed by Paul Majkut at the RiNA GmbH, where it is used to study its binding to phosphorylated ADAP-P.

The purified azido protein (50 μ M) was reacted with 600 equivalents of biotin phosphonite **277** in tris /HCl buffer (100 mM) at room temperature for 14 hours (Scheme 3.39). Afterwards Paul Majkut was able to demonstrate that 50% of the Rasa1-N **276** was converted to the Rasa1-N biotin phosphonamidate **278**. Furthermore, ADAP-P binding studies revealed that Rasa1-N biotin phosphonamidate **278** was fully active after the Staudinger-phosphonite reaction. These experiments demonstrated the first successful Staudinger reaction of triazole phosphonites on the protein level in aqueous buffer.



Scheme 3.39: Staudinger-phosphonite reaction of azido Rasa1-N **276** with biotin phosphonite **277** to the corresponding biotin-tagged protein Rasa1-N **278**.

3.5 Synthesis of coumarin phosphites

The Hackenberger group has successfully demonstrated the applicability of phosphites **95** bearing light-cleavable substituents to generate a phosphotyrosine analogue on a protein (see chapter 1.2.3, Scheme 1.26).^[7a] 4-methylenecoumarin substituted phosphites **160** can potentially further improve this application. Like the nitrobenzyl ester, the coumarin protecting group can be cleaved off after the Staudinger reaction by UV irradiation. Moreover, coumarin phosphites bring in the the additional advantage of delivering non-toxic cleavage products after irradiation and of being fluorescent (Figure 3.12). This enables the possibility to track the functionalised protein in its protected state in living organisms by fluorescent readout. The disappearance of the fluorescent signal of the phosphoramidate protecting group can be used to visually track its light-induced cleavage and thereby the formation of the phosphotyrosine analogue.

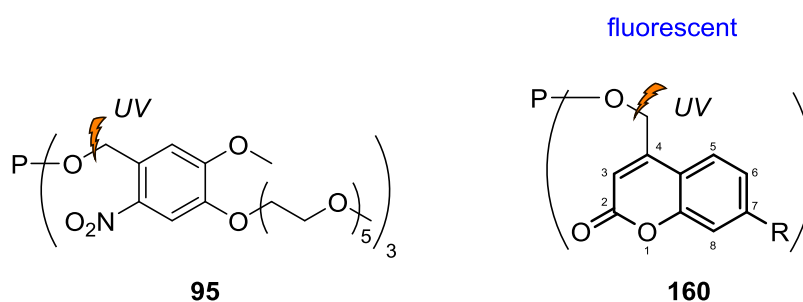
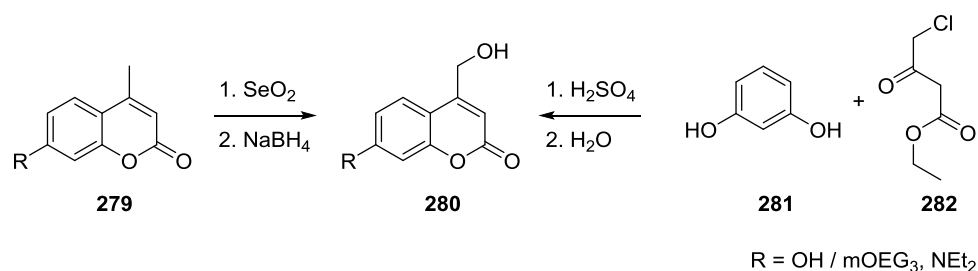


Figure 3.12: Photocleavable phosphites for the chemoselective installation of phospho-amino acid analogues.

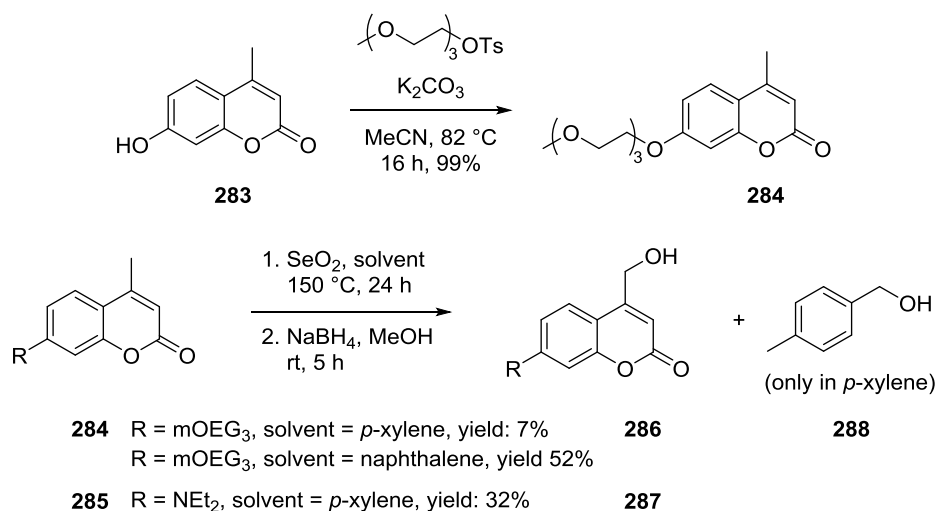
3.5.1 Syntheses of 7-substituted 4-hydroxymethylenecoumarin derivatives

The key step in the synthesis of 7-substituted 4-hydroxymethylenecoumarin derivatives is the installation of the hydroxyl group at the benzylic position, which is accessible through two different synthetic pathways. The first one starts from commercially available 4-methylcoumarin derivatives **279** which can be oxidised to the corresponding carboxylic acid. Subsequent reduction of the acid leads to the desired 4-hydroxymethylenecoumarin **280**. The second synthetic pathway starts from resorcinol (**281**) and ethyl 4-chloro-3-oxobutanoate (**282**), which forms in a one-pot two-step reaction 4-chloromethylene-7-hydroxycoumarin. After nucleophilic substitution of the chloro group, 4-hydroxymethylene-coumarin derivative **280** can be obtained (Scheme 3.40).



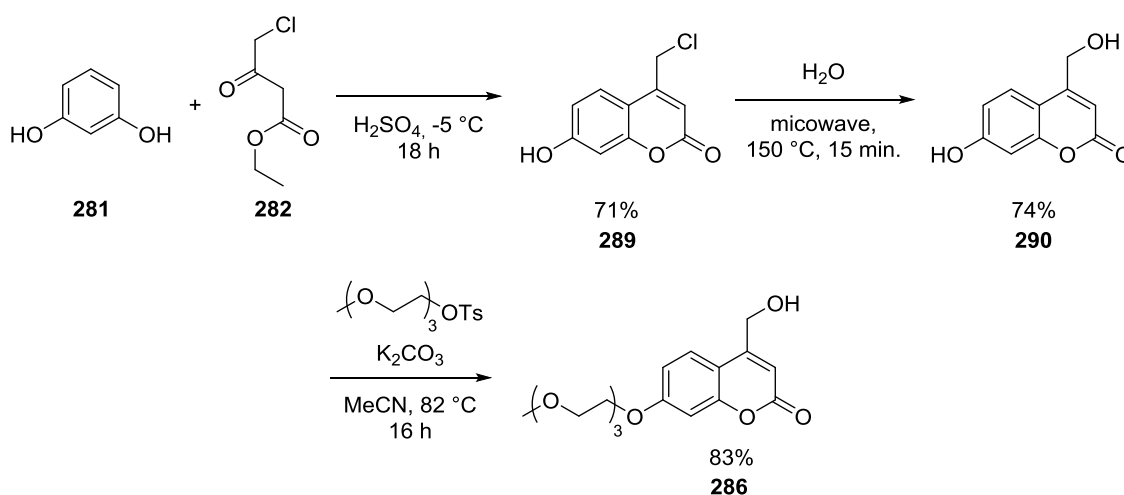
Scheme 3.40: Synthetic pathways to 7-substituted 4-hydroxymethylenecoumarin derivatives **280**.

Following the first reaction pathway, commercially available 7-hydroxy-4-methylcoumarin (**283**), which was functionalised with oligoethylene glycol monomethyl ether at position 7 to give **284** in a previous step, or 7-diethylamino-4-methylcoumarin (**285**) were used as starting materials for the oxidation of the 4-methyl group. Both were oxidised at the 4-methylene group to the corresponding carboxylic acid derivatives with selenium dioxide in *p*-xylene to achieve the required reaction temperature. The crude products were directly reduced with sodium borohydride to the desired 4-hydroxymethylenecoumarin derivatives **286** or **287**, which were isolated after chromatographic purification in moderate yields of 7 or 32%, respectively. It was found that this literature-known protocol oxidises not only the 4-methylcoumarins **284** or **285** but also the methyl groups of the required solvent *p*-xylene. To avoid this side-reaction of the solvent, which was supposed to be responsible for the low yields, naphthalene (melting point 80 °C) was chosen because of its similarity and high boiling point. This optimised procedure results in a significant increase in the isolated yield of coumarin derivative **286** from 7 to 52% (Scheme 3.41).



Scheme 3.41: Synthesis of 7-substituted 4-hydroxymethylenecoumarin derivatives **286** and **287**.

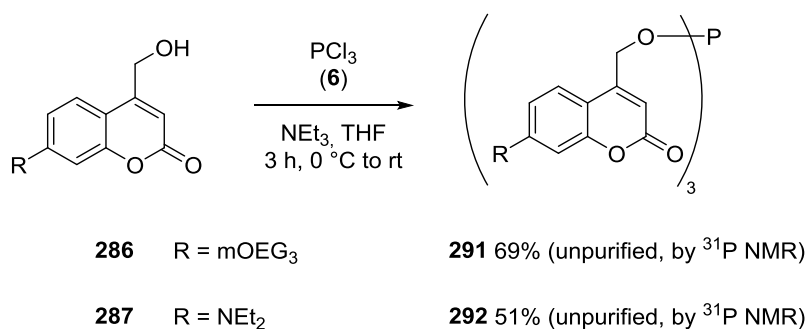
The second synthetic pathway to 7-mOEG₃-4-hydroxymethylenecoumarin (**286**), which starts with the condensation of resorcinol (**281**) and ethyl 4-chloro-3-oxobutanoate (**282**) (Scheme 3.42) is superior to the selenium dioxide protocol (Scheme 3.41) not only because of its handling and the laborious procedure effort but also because of the yield (44% compared to 6.9%, over three steps).



Scheme 3.42: Preferred synthesis of 7-mOEG₃-4-hydroxymethylenecoumarin (**286**).

3.5.2 Synthesis of coumarin phosphites

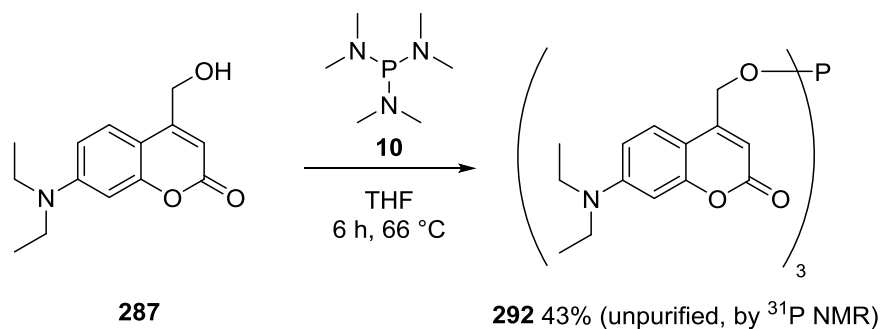
The most straightforward synthesis for symmetrical phosphites starts from phosphorus trichloride (**6**) and the desired alcohol. Therefore, this strategy was used in the first approach to synthesise coumarin phosphites **291** and **292** from the previously synthesised 4-hydroxymethylene-coumarin derivatives **286** and **287** (Scheme 3.43).



Scheme 3.43: Synthesis of coumarin phosphites **291** and **292** from phosphorus trichloride (**6**).

The crude ^{31}P NMRs of both reactions showed a very characteristic peak at 141 ppm corresponding to desired phosphites **291** or **292**. Beside the desired peak at 141 ppm, the ^{31}P NMRs revealed 31% and 49% (for **291** and **292**) phosphorus(V) by-products. Unfortunately, purification of the phosphites **291** and **292** by column chromatography only yielded phosphorus(V) products. Even the addition of 1% triethylamine to the elution solvent, which was successfully for the isolation of sensitive carbohydrate phosphonites, did not yield any phosphite.^[160] All further attempts to purify the phosphites either by precipitation from different solvents or crystallisation only led to complete decomposition of the coumarin phosphites **291** and **292**.

Since the purification of coumarin phosphites **291** and **292** by standard organic chemistry procedures was not successful another synthesis route to coumarin phosphites was designed. The thermal conversion of hexamethylphosphanetriamine (**10**) should not lead to any salts as by-product as in the case of the phosphorus trichloride (**6**) related synthesis of phosphites. Heating 7-diethylamino-4-hydroxymethylene-coumarin (**287**) in the presence of hexamethylphosphanetriamine (**10**) successfully led to the desired coumarin phosphite **292** (Scheme 3.44). Nevertheless, again a lot of phosphorus(V) by-products were visible in the ^{31}P NMR of the crude product (Figure 3.13) and the amount of phosphite **292** was even lower than in the phosphorus trichloride related synthesis.



Scheme 3.44: Synthesis of coumarin phosphite **292** from hexamethylphosphanetriamine (**10**).

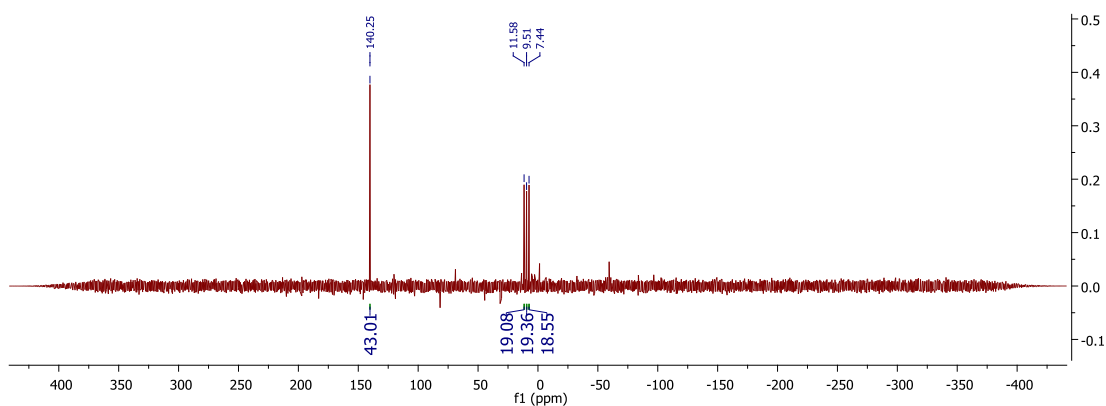


Figure 3.13: Crude ^{31}P NMR of the thermal synthesis of coumarin phosphite **292** (Scheme **3.44**).

These results strongly indicate the instability of coumarin phosphites **291** and **292**, not only under aqueous conditions but also in general. Since they should be used as modification reagents for azido peptides and azido proteins in buffer media, which is not accomplishable under these circumstances, the project was stopped at this point. Nevertheless, the ^{31}P NMR of the crude proves that coumarin phosphites **291** and **292** are obtainable in 69% and 51% (by ^{31}P NMR), respectively, and can potentially be used without purification for Staudinger reactions or other applications in organic solvents.

3.6 Glycosylation of peptides via Staudinger-phosphite reaction

This chapter was published in the following journal:

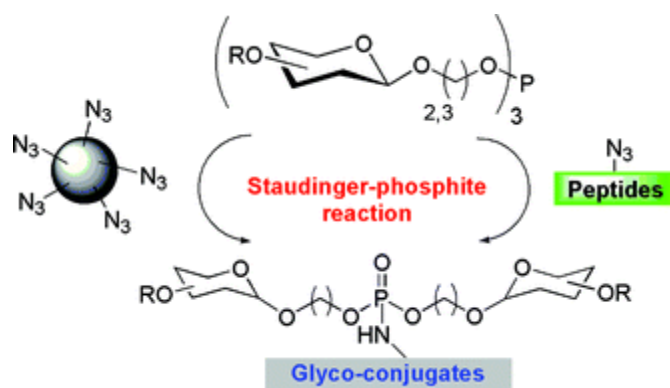
Verena Böhrsch, Thresen Mathew, Maximilian Zieringer, M. Robert J. Vallée, Lukas M. Artner,
Jens Dervedde, Rainer Haag and Christian P. R. Hackenberger,

“Chemoselective Staudinger-phosphite reaction of symmetrical glycosyl-phosphites with
azido-peptides and polyglycerols“

Org. Biomol. Chem. **2012**, *10*, 6211–6216.

Publication Date (Web): 27 January 2012

The original article is available at: <http://dx.doi.org/10.1039/c2ob25207d>



Scheme 3.45: Phosphites for preparation of dibranched glycosylated peptides and polyglycerols.

Abstract

In this paper we present the synthesis of glycol phosphoramidate conjugates as easily accessible analogues of glyco-phosphorous esters via the Staudinger-phosphite reaction. This protocol takes advantage of synthetically accessible symmetrical carbohydrate phosphites in good overall yields, in which ethylene or propylene linkers can be introduced between phosphorous and galactose or lactose moieties. The phosphites were finally applied for the chemoselective reaction with azido-peptides and polyazido(poly)glycerols.

Responsibility assignment

The author is responsible for the synthesis of the azido-, deuterated azido- and azido-fluorophore-peptides, the performed Staudinger reactions of the peptides with peracetylated glycosyl-phosphites as well as their analysis by HPLC-MS and fluorescence-HPLC.

Compendium of content

Glycosylation is a very important posttranslational modification in living organism since carbohydrates are for example responsible for the regulation of molecular recognition, immune response, pathogen interaction and intracellular transport of the protein.^[161]

In this publication, the synthesis of three peracetylated galactose phosphites **293**, **294** and **295** (Figure 3.14) and one peracetylated lactose phosphite **296** starting from phosphorus trichloride is described. The reactivity of the synthesised glycosyl phosphites was first tested on small organic aryl and alkyl azides. It was found that the reaction rate was highly dependent on the electronic properties of the applied azide. Whereas the reaction of peracetylated galactose phosphite **293** with Fmoc-protected *p*-azidophenylalanine in DMSO was complete after six hours at 28 °C, the reaction of the same phosphite **293** with Fmoc-protected ϵ -azidolysine needed 28 hours at 40 °C for completion. A similar dependency of the electronic nature of azides on the Staudinger reaction was found for phosphonites (see chapter 3.3).

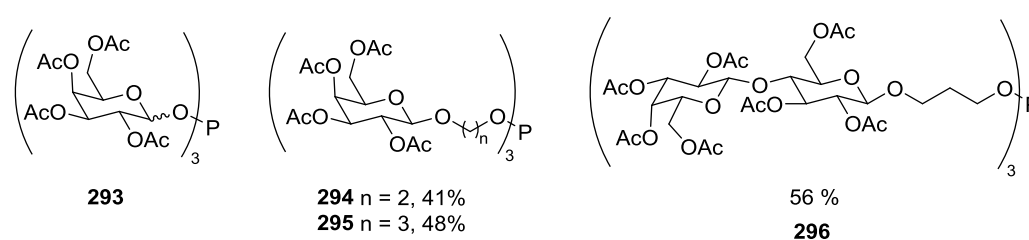
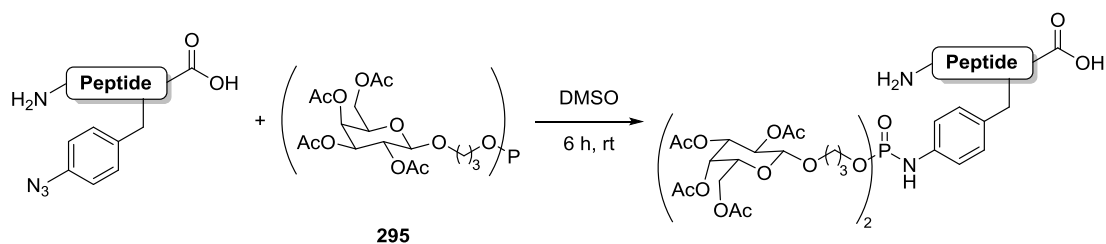


Figure 3.14: Synthesised peracetylated carbohydrate phosphites **293**, **294**, **295** and **296**.

Knowing the required reaction temperature and time for full conversion of the azide, these reaction conditions were used for the chemoselective glycosylation of azido peptides. Two different types of peptides were synthesised. The first one was a simple octapeptide with a *p*-azidophenylalanine at the N-Terminus **H₆-271**. The conversion of this peptide to the glycopeptide **297** with galactose phosphite **295** was determined by HPLC-MS with a deuterium-labelled peptide **D₆-271** analogue as internal standard. The second peptide was equipped with a fluorescent NBD-group attached to the ϵ -amino group of lysine. This NBD-tagged azido peptide **257** was also converted to its corresponding glycopeptide **298** with galactose phosphite **295** (Scheme 3.46). HPLC-fluorescence analysis revealed 98% glycopeptide **298** formation (Figure 3.15). During the reaction of NBD-tagged azido peptide **257** no cleavage of the NBD group was observed as it was during the study of Staudinger-phosphonite reactions in buffer (Scheme 3.34). The higher stability of the NBD-tagged azido peptide **257** in wet DMSO occurred from less nucleophilic hydroxyl groups present in the DMSO solution than in the basic buffer.



Peptide **271** = PapAlaGluTrpAlaSerLysLeu
 Peptide **257** = PapAlaGluAlaSerLysSerLys(NDB)Val

Glycopeptide **297**: 86% conversion
 Glycopeptide **298**: 98% product

Scheme 3.46: Chemoselective glycosylation of azido peptides **271** and **257**.

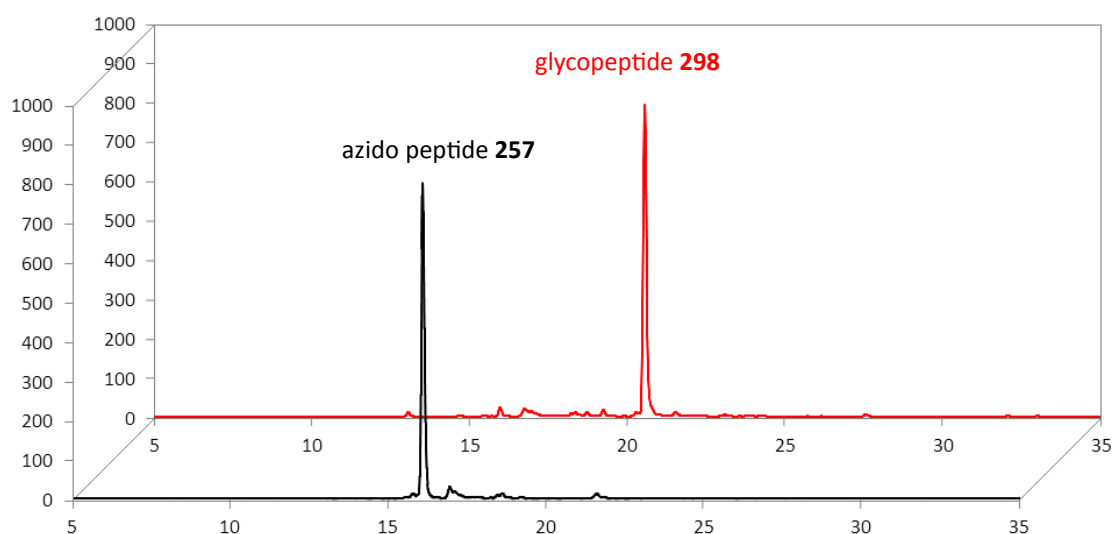


Figure 3.15: Fluorescence spectra of NDB-tagged azido peptide **257** (black) and glycopeptide **299** (red).

After the successful glycosylation of peptides by galactose phosphite **295**, azido polyglycerols were glycosylated for lectin–peanut agglutinin (PNA) binding studies. Because symmetrical phosphites attach two carbohydrate units per azido group it was assumed that the glycosylated polyglycerols would show high multivalent bindings. Two different azido polyglycerols (7.7 kDa, DF 100% and 12.6 kDa, DF 98%) were glycosylated with all four peracetylated carbohydrate phosphites (**293**, **294**, **295** and **296** see Figure 3.14) in DMSO at 40 °C with conversions of 23-91%. To enable binding of the carbohydrate moieties to Thomsen–Friedenreich (TF) antigen, the acetyl protecting groups were quantitatively removed with sodium methanolate within 30 minutes.

The inhibitory effect of both lactose functionalised polyglycerols (7.7 kDa and 12.6 kDa) on PNA binding to the immobilized TF antigen was probed *via* a competitive surface plasmon resonance (SPR) binding assay. For both lactose polyglycerol derivatives, inhibition values of about 60% were determined.

In conclusion carbohydrate phosphites are easily accessible from commercially available starting materials. They enable the straightforward chemoselective and metal-free glycosylation of polymers and biopolymers, which are highly interesting targets for glycan binding studies.

4 Summary

Part I: Phosphonites in Staudinger reactions

The chemoselective modification of peptides and proteins is a very important tool in biological research allowing the investigation or monitoring of biological processes. The Hackenberger group could already show that phosphites can be successfully used for the chemoselective and site-specific modification of biopolymers.

In this thesis, phosphonites were investigated as an alternative functionalization tool in Staudinger reactions. Phosphonites have one outstanding advantage over phosphites. They bear a stable phosphorus-carbon bond, which cannot be cleaved during hydrolysis of the phosphonimidate and simultaneously makes the introduction of a single functional module much easier. The phosphonites synthesised in this context could be effectively applied for the metal-free functionalization of peptides and proteins as well as polyglycerols.

Firstly, different aryl phosphonites bearing a model functional mOEG group at the aromatic ring were synthesised with various alkoxy substituents including alkyl and small mOEG groups. The phosphonites were synthesised starting from bromobenzene derivatives. The phosphorus(III) moiety was introduced *via* halogen-lithium exchange followed by a nucleophilic attack at a phosphorus(III)-chloride species as the key step of the synthesis protocol. All the phosphonites could be obtained in yields between 33 and 87%. To protect the phosphonites against oxidation or hydrolysis during purification and storage, a borane protection group was introduced, which can be cleaved off with DABCO prior to the Staudinger reaction. Subsequently, the mOEG-functionalized phosphonites were probed in the Staudinger reaction with fully unprotected azido peptides in buffer systems with up to 92% conversion of the azido peptide. As the most important result, the first successful functionalization of the protein calmodulin bearing a *p*-azidophenylalanine at position 2, *via* the Staudinger-phosphonite reaction was accomplished (Figure 4.1). SDS-page analysis revealed 70% conversion of azido calmodulin to the phosphonamidate protein, proving the feasibility of the Staudinger-phosphonite reaction on proteins in aqueous systems.

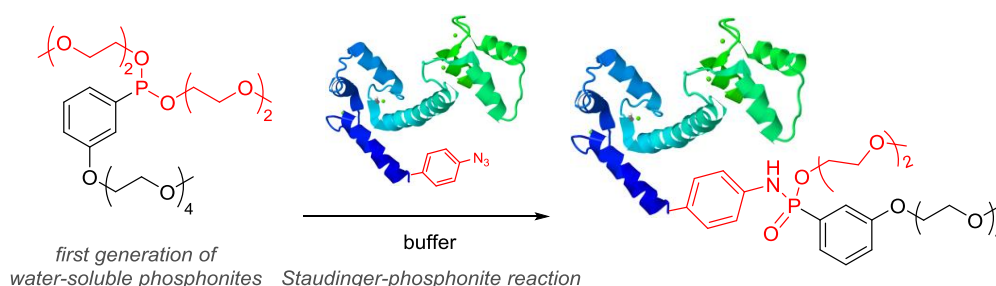


Figure 4.1: First protein modification *via* Staudinger-phosphonite reaction.

In order to develop a general synthesis pathway for functionalized phosphonites and to ease the introduction of various functional modules such as fluorophores, carbohydrates etc., a second generation of phosphonites was established. The aromatic system was replaced by an alkyne substituent, which allows the introduction of the functional module by CuAAC. The CuAAC does not interfere with any other functional groups of both, the functional module and the protected phosphonite. Moreover, the borane protected phosphonite can react without oxidation or hydrolysis during the introduction of the functional module. It is most important to acknowledge that after CuAAC reaction and purification copper-free borane-protected tetrazole phosphonites were obtained (Figure 4.2). It can be concluded that this new reaction protocol stands out for its high flexibility with regard to the introduction of the functional module and its short reaction sequence.

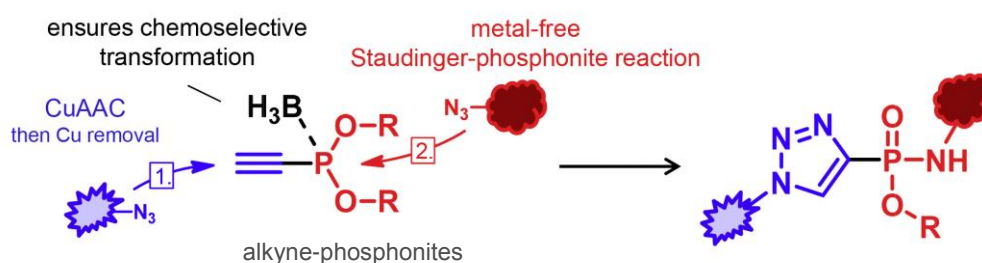


Figure 4.2: The general reaction-concept for the second generation of phosphonites for Staudinger reactions.

Afterwards, the second generation of phosphonites was investigated in-depth with respect to different functional modules and their behaviour in Staudinger reactions in organic solvents. It could be demonstrated that a wide variety of functional modules could be attached to the alkyne phosphonite, such as, biotin, mOEG groups or fluorophores. Even very challenging phosphonites such as unprotected carbohydrate phosphonites were accessible. These phosphonites were successfully utilised in Staudinger reactions with different azides, such as, primary, secondary, benzyl and phenyl azides, in good overall yields of 51 to 94%.

Finally, the synthesized carbohydrate tetrazole phosphonite was converted with azido polyglycerol to obtain a carbohydrate functionalized polymer, which showed excellent binding in a SPR-based peanut agglutinin-carbohydrate binding assay.

During the Staudinger-phosphonite reaction with aryl azides, the formation of the corresponding aryl amines was observed as a side product. In theory, their formation could be explained by unselective hydrolysis of the phosphonimidate leading to the amino peptide and a phosphonate. This hypothesis was proven by the hydrolysis of the corresponding phosphonimidate with ^{18}O -labelled water. This result provides additional insight into the

mechanism of the Staudinger reaction which might help to further improve its applicability as modification tool.

After successful application of the Staudinger-phosphonite reaction in organic solvents, the reaction was transferred to aqueous buffer systems. To achieve a good solubility in water and an increased stability against hydrolysis, phosphonites with oxy-bound mOEG₂ as well as *p*-mOEG-*m*-nitrobenzyl substituents at the oxygen were synthesized in very good overall yields of 48 to 62%. The new triazole phosphonites showed a three- to five-fold enhancement in stability against hydrolysis compared to the first generation of phosphonites. The diethyl triazole phosphonite was then applied in Staudinger reactions with an azido peptide in a buffer system at concentrations of 1 mM. The desired phosphoramidate peptide was isolated in a yield of 67%. In addition, the conversion of different azido peptides with phosphonites and its dependence on pH values as well as substrate concentrations was investigated. To study the conversion of azido peptides at low concentrations, either fluorophore-tagged peptides were used and the resulting product mixture was analysed by HPLC-fluorescence, or conversions were determined by quantitative mass spectrometry with deuterated peptide as internal standard. These studies revealed that the best conversion of azido peptides was achieved in 100 mM tris / HCl buffer at a pH of 8.2, at an azido peptide concentration of 50 μ M and with 250 to 500 equivalents of phosphonite in dependence on the oxy-bound substituents.

Finally, the previous findings on the Staudinger-phosphonite reaction with tetrazole phosphonites were applied for the biotinylation of Rasa1-N (Figure 4.3). The biotinylated protein was immobilized onto Streptavidine-coated magnetic beads and phosphorylation binding studies were performed.

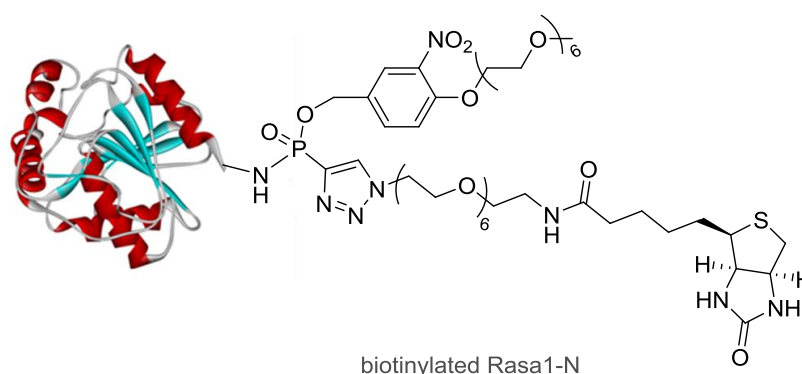


Figure 4.3: The ADAP-P binding protein Rasa1-N was biotinylated *via* Staudinger-phosphonite reaction for immobilisation.

Part II: Phosphites in Staudinger reactions

Phosphites have already proven to be very useful for the functionalization of biomolecules. It was shown that *o*-nitrobenzyl phosphites can react with azido phenylalanine-containing peptides and proteins to form the desired phosphoramidate products. Furthermore, the *o*-nitrobenzyl group could be removed by irradiation with UV light to obtain unprotected phosphoramidate peptides or proteins. The foregoing phosphoramidate-modified phenylalanine in the peptide or protein can therefore be regarded as analogue of phosphotyrosine, which is an important posttranslational modification in nature. To further advance this strategy, coumarin phosphites should be synthesized. The coumarin moiety can like the *o*-nitrobenzyl group also be cleaved off by irradiation with UV light but has additionally the advantage that the coumarin moiety is fluorescent and allows localisation of the molecule of interest.

Different coumarin alcohol derivatives were synthesized and were converted with phosphorus trichloride to the desired coumarin phosphites. Unfortunately, the synthesized coumarin phosphites proved to be extremely unstable so that no purification of the final product was possible. Nevertheless, the formation of the phosphite could be proven by ³¹P NMR which may allow future applications with the crude reaction products in organic solvents.

Moreover, phosphites cannot only be used for the preparation of phosphotyrosine analogues but also for the introduction of other functional units such as PEG chains for the PEGylation of peptides and proteins. Beside PEG chains, also other functionalities, such as, carbohydrates, which serve as biological binding moiety, would be interesting to attach to a (bio-)polymer.

For this reason and to extend the reaction scope of the Staudinger-phosphite reaction, acetylated sugar phosphites were prepared and successfully reacted with small azido molecules and azido peptides in wet DMSO. The quantitative conversion of the azido peptides was either determined by quantitative mass spectrometry or by using a fluorophore-tagged peptide. Furthermore, the protected acetylated sugar phosphites were applied for the functionalization of azido polyglycerols. After deprotection of the carbohydrate moiety, the functionalized polyglycerols were applied in lectin-peanut agglutinin (PNA) binding studies which revealed very good inhibition values of about 60%.

5 Zusammenfassung

Teil I: Phosphonite in Staudinger-Reaktionen

Die chemoselektive Modifikation von Peptiden und Proteinen ist eine wichtige Methode in der chemischen Biologie. Sie erlaubt die Einführung von Reportermolekülen, die die Untersuchung und Isolierung von Biomolekülen ermöglichen. Die Arbeitsgruppe von Professor Hackenberger konnte bereits erfolgreich die Chemoselektivität der Staudinger Reaktion zwischen Phosphiten und Aziden demonstrieren. Sie ermöglicht die Einführung von funktionellen Gruppen und die ortsspezifische Modifizierung von Biomolekülen.

Im Rahmen dieser Arbeit wurden Phosphonite als Alternative zu den bereits untersuchten Phosphiten hergestellt und auf ihre Anwendbarkeit für die Modifikation von Biomolekülen und Polymeren mittels der Staudinger Reaktion untersucht. Phosphonite besitzen einen wesentlichen Vorteil gegenüber den Phosphiten. Im Unterschied zu den Phosphiten besitzen sie eine stabile Phosphor-Kohlenstoff-Bindung, welche nicht während der Hydrolyse der zunächst gebildeten Phosphonimide gespalten werden kann und dadurch die Einführung einer einzelnen funktionalen Einheit wesentlich vereinfacht. Die hier hergestellten Phosphonite konnten erfolgreich für metallfreie Funktionalisierung von Peptiden, Proteinen und Polymeren verwendet werden.

Zunächst wurden Arylphosphonite mit unterschiedlichen Alkoxy-substituenten - ausgehend von Brombenzol-Derivaten - synthetisiert, die eine zusätzliche kurze mOEG-Einheit als funktionelle Gruppe am Aromaten besaßen. Die Phosphor-Kohlenstoffbindung wurde dabei durch einen Halogen-Lithium-Austausch unter anschließender Substitution an einer Phosphor(III)chlorid-Verbindung hergestellt. Die so synthetisierten Phosphonite wurden in Ausbeuten von 33-87% erhalten. Um eine Oxidation oder Hydrolyse der Phosphonite während der Synthese zu verhindern, wurde eine Boran-Schutzgruppe eingeführt, welche im letzten Schritt unter Verwendung von DABCO® vor der nachfolgenden Staudinger Reaktion wieder abgespalten werden konnte.

Die Anwendung der ungeschützten mOEG-funktionalisierten Phosphonite wurde nachfolgend in der Staudinger Reaktion mit ungeschützten Azido-peptiden in verschiedenen Puffersystemen getestet, wobei ein Umsatz der Azido-peptide von bis zu 92% beobachtet werden konnte. Anschließend konnte durch erfolgreiche Umsetzung des Proteins Calmodulin, in welches an Position 2 anstelle von Tyrosin *p*-Azidophenylalanin eingebaut wurde, die erste erfolgreiche Funktionalisierung eines Proteins mittels Staudinger-Phosphonite Reaktion gezeigt und somit das Potential der Reaktion als Funktionalisierungsmethode untermauert werden

(Abbildung 5.1). Die Analyse der Reaktion mittels SDS-page bewies dabei einen Umsatz zu dem gewünschten Phosphonamidat-Protein von 70%.

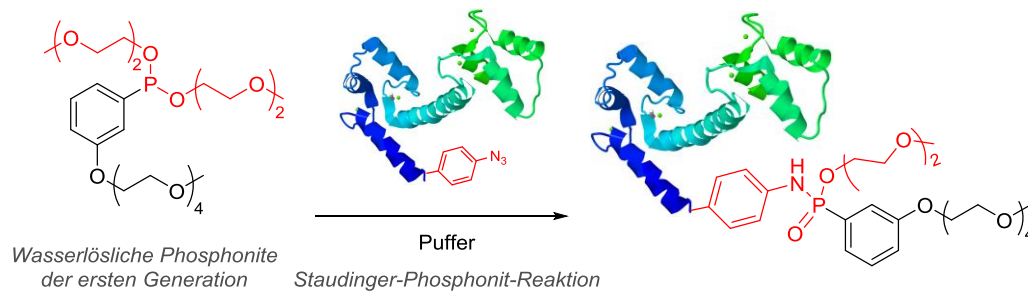


Abbildung 5.1: Die erste Modifizierung eines Proteins mittels Staudinger-Phosphonit-Reaktion.

Um einen einfacheren Zugang zu den funktionalisierten Phosphoniten zu ermöglichen, wurde eine modulare Synthese für eine zweite Generation von Phosphoniten entwickelt. Diese modulare Synthese ermöglicht es, auch komplexe funktionale Einheiten, wie Fluorophore, PEG-Gruppen und Kohlenhydrate ohne komplizierte Schutzgruppenmanipulationen einzuführen. Dazu wurde das aromatische System gegen ein Alkin ausgetauscht, welches die Einführung einer funktionalen Einheit über CuAAC ermöglicht. Die CuAAC zeichnet sich insbesondere dadurch aus, dass keine Kreuzreaktion mit anderen funktionellen Gruppen, hier der funktionalen Einheit und des Phosphonits, auftreten. Darüber hinaus kann das Alkinphosphonit in der Boran-geschützten Form verwendet werden, sodass keine Gefahr durch Oxidation oder Hydrolyse der Phosphor(III)-Verbindung während der Umsetzung droht. Ein weiterer wichtiger Aspekt ist, dass nach der CuAAC Reaktion das erhaltene Phosphonit vollständig vom Kupfer-Katalysator befreit werden kann, was auf Grund der Toxizität des Kupfers eine wesentliche Rolle spielt für die spätere Anwendung der Staudinger-Reaktion an Biomolekülen (Abbildung 5.2). Zusammenfassend wurde gezeigt, dass sich das neu entwickelte Syntheseprotokoll unter Verwendung der Alkinphosphonite durch seine hohe Flexibilität bezüglich der einzuführenden funktionalen Einheit und durch den einfachen und kurzen Syntheseweg auszeichnet.

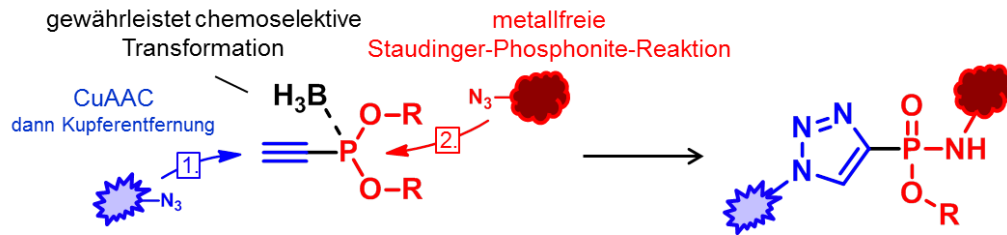


Abbildung 5.2: Generelles Reaktionskonzept der zweiten Generation von Phosphoniten für die Staudinger-Reaktion.

Diese zweite Generation von Phosphoniten wurde in grundlegenden Studien bezüglich der Zugänglichkeit von Triazol-Phosphoniten und deren Verhalten in der Staudinger-Reaktion in organischen Lösungsmitteln untersucht. Es konnte gezeigt werden, dass eine große Vielfalt an funktionalen Einheiten wie Biotin, Fluorophore oder auch OEG-Gruppen an das Phosphonit gebracht werden konnten und sogar synthetisch sehr anspruchsvolle Verbindungen wie ungeschützte Zuckerphosphonite zugänglich waren. All diese Phosphonite konnten anschließend erfolgreich in Staudinger-Reaktionen mit unterschiedlichen Aziden, u.a. primären, sekundären, benzylichen und auch phenylischen, in Ausbeuten von 51-94% umgesetzt werden.

Darüber hinaus konnte auch ein Azidopolyglycerol mit dem Laktose-Triazol-Phosphonit umgesetzt und ein glykosyliertes Polymer erhalten werden. Anschließende SPR-Messungen zeigten exzellente Bindung des Laktose-Phosphonamidat-Polyglycerol in einem Lektin-peanut agglutinin (PNA) Bindungsassay.

Allerdings wurde bei der Staudinger-Phosphonit-Reaktion mit Arylaziden die Entstehung eines Arylamins beobachtet, welches durch eine unselektive Hydrolyse des Phosphonimidates erklärt werden kann. Diese Hypothese konnte mit Hilfe von ¹⁸O-markiertem Wasser bewiesen werden. Dieses Resultat brachte neue Erkenntnisse bezüglich der Staudinger-Reaktion, und lieferte damit wichtige Informationen für die Weiterentwicklung der Phosphonite als Modifikationsmethode.

Nach der erfolgreichen Verwendung der Alkin-Phosphonite in organischen Lösungsmitteln, wurde die Reaktion auf wässrige Puffersysteme übertragen. Dafür wurden Phosphonite sowohl mit mOEG als auch mit *p*-Nitrobenzyl-Substituenten an den Sauerstoffen des Phosphonits in Ausbeuten von 48 und 62% hergestellt, um eine ausreichende Wasserlöslichkeit und Stabilität der Phosphonite zu gewährleisten. Diese neuen Phosphonite zeigten dabei eine drei- bis fünffach höhere Stabilität gegen Hydrolyse. Das Diethyl-Triazol-Phosphonit wurde in einem ersten Versuch erfolgreich in einem Puffersystem mit einem Azidopeptid bei einer Konzentration von 1 mM umgesetzt und mit einer Ausbeute von 67% isoliert. Ferner wurde die

Umsetzung dieser Phosphonite mit unterschiedlichen Azidopeptiden unter Veränderung der Azid-, Phosphonit- und Pufferkonzentration sowie der pH-Werte untersucht und die Umsetzung entweder mit HPLC-Fluoreszenz oder über quantitative Massenspektrometrie analysiert. Diese Studien zeigten, dass das beste Ergebnis der Staudinger-Phosphonit-Reaktion in einem 100 mM tris / HCl Puffer bei einem pH-Wert von 8.2, einer Peptid Konzentration von 50 μ M und 250 bis 500 Äquivalenten an Phosphonit erhalten werden konnte.

Anschließend wurde die Staudinger-Phosphonite-Reaktion mit Triazol-Phosphoniten zur biotinylierung von Rasa1-N verwendet (Abbildung 5.3). Das biotinylierte Protein wurde auf magnetischen-Beads immobilisiert um anschließend bindungsstudien mit phosphoryliertem ADAD-P durchzuführen. Diese Untersuchungen zeigten das Rasa1-N zu 50% mit dem Biotin-Triazol-Phosphonite funktionalisiert werden konnte ohne das die Aktivität der Proteins beeinflusst wurde.

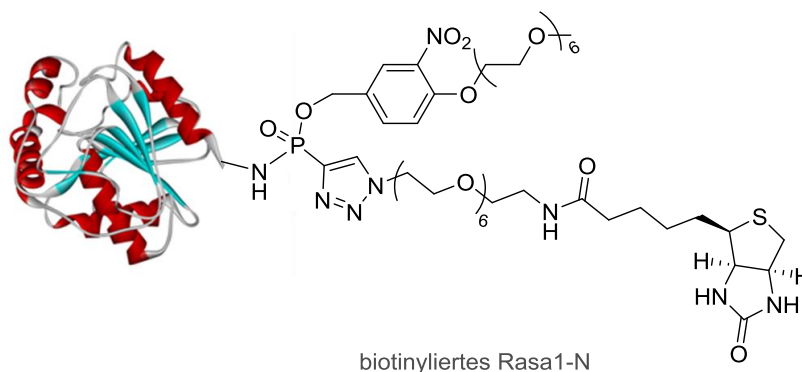


Abbildung 5.3: Das ADAP-P bindende Protein Rasa1-N konnte zur Immobilisierung mittels Staudinger-Phosphonit-Reaktion biotinyliert werden.

Teil II: Phosphite in Staudinger-Reaktionen

Wie bereits gezeigt werden konnte, sind Phosphite ausgezeichnet zur Funktionalisierung von Biomolekülen geeignet. So wurde *o*-Nitrobenzyl-Phosphit mit Peptiden und Proteinen, welche Azidophenylalanin in ihrer Sequenz besaßen, zum gewünschten Phosphoramidat-Peptid oder -Protein umgesetzt. Darüber hinaus konnte die *o*-Nitrobenzyl-Gruppe durch Bestrahlung mit UV-Licht abgespalten werden, so dass ungeschützte Phosphoramidat-Einheiten erhalten wurden, welche ein Analogon des Phosphotyrosins darstellen. Um diese Methodik weiterzuentwickeln, sollte die bereits verwendete *o*-Nitrobenzyl-Gruppe durch Coumarin ersetzt werden. Die über das Sauerstoff an den Phosphor gebundene Coumarin-Gruppe bietet

nicht nur die Möglichkeit auch hier über Bestrahlung mit Licht die ungeschützte Phosphoramidat-Einheit zu erhalten, sondern hat zusätzlich den Vorteil, dass nach der Entschützung lediglich ungiftige Produkte zurückbleiben. Des Weiteren kann Coumarin als Fluorophor zur Visualisierung des Phosphoramidat-haltigen Biomoleküls genutzt werden.

Es wurden unterschiedliche Coumarin-Derivate ausgehend von Phosphortrichlorid hergestellt. Leider konnten die so erhaltenen Coumarin-Phosphite aufgrund ihrer geringen Stabilität nicht aufgereinigt isoliert werden. Allerdings konnte ihre Entstehung in guten Ausbeuten über ^{31}P -NMR nachgewiesen werden, sodass eine Verwendung der unaufgereinigten Coumarin-Phosphite in organischen Lösungsmitteln grundsätzlich möglich wäre.

Phosphite können allerdings nicht nur zur Herstellung von Phosphotyrosin-analoga benutzt werden, sondern auch zur Einführung von anderen funktionellen Einheiten. Es konnte bereits gezeigt werden, dass auch PEG-Gruppen zur PEGylierung über die Phosphite eingeführt werden können. Neben der PEGylierung ist auch die Einführung von Zuckereinheiten in Biomoleküle als biologisches Bindungsmotiv von großem Interesse.

Aus diesem Grund, und um den Anwendungsbereich der Staudinger-Phosphit Reaktion zu erweitern, wurden verschiedene acetylierte Zuckerphosphite hergestellt und mit unterschiedlichen Aziden und Azidopeptiden in nassem DMSO umgesetzt. Die quantitative Umsetzung der Azidopeptide wurde dabei entweder über quantitative Massenspektrometrie oder durch Fluorophor-markierte Peptide mittels HPLC-Fluoreszenz bestimmt. Darüber hinaus wurden die Acetyl-geschützten Zucker-Phosphite zur Funktionalisierung von Azidopolyglycerol verwendet. Nach anschließender Entschützung der Zucker-Einheiten zeigte das Laktose-Phosphoramidat modifizierte Polyglycerol eine Inhibition von 60% in einem Lektin-peanut agglutinin (PNA) Bindungsassay.

6 Outlook

The here synthesised phosphonites represent a great potential for the site-selective and metal-free functionalization of biomolecules. Among these phosphonites, the alkyne phosphonites are the most promising ones. Therefore, further investigations should mainly focus on optimizing their application. The alkyne moiety allows the attachment of various functional azido molecules by CuAAC, like fluorophores, tags or PEG units, which could already be demonstrated within this thesis. As a result, the nearly countless number of accessible phosphonites opens up a variety of different applications and turns them into very interesting building blocks in the field of biological or medicinal chemistry. The successful conversion of polymers, peptides and proteins could already be attested and future investigations should concentrate on the biological evaluation of the synthesized functional molecules and the scope of obtainable compounds.

In this work, many fundamental properties of the phosphonites and the Staudinger-phosphonite reaction are already described, including the synthesis of different phosphonites, their hydrolysis and reactivity as well as their conversion with various azides under different reaction conditions has been. Nevertheless, several aspects still remain to be probed. Especially the applicability in aqueous systems requires a more detailed investigation and optimization with respect to the reaction conditions and the oxygen-bound substituents at the phosphorus of the phosphonite. More precisely, the conversion of azido peptides with tetrazole phosphonites bearing different substituents at the phosphorus centre, such as Et, mOEG₂ and *p*-mOEG₆-*m*-nitrobenzyl, has to be further studied in different buffer systems to follow up the results shown here. Thereby, reaction conditions with an azido peptide concentration of 1 mM and less than 25 equivalents of phosphonites are of major interest to find the threshold of the phosphonite concentration. A lower phosphonite concentration would facilitate the separation of the phosphoramidate from the hydrolysis by-products of the phosphonite and would allow easier isolation of the functionalized molecule. Moreover, isolation and quantification of the expected amino peptide by-product might reveal whether its formation can be subdued by tuning the substituents on the phosphorus.

The second very interesting question, which needs further investigation, is the hydrolysis pathway of the phosphonite in dependence on different substituents. As the stability of the phosphonites in aqueous systems is the only drawback of this functionalization method, the prevention of their hydrolysis is a major topic of future studies and optimizations. Since water can either directly attack at the adjacent phosphorus or at the proximal carbon of the oxygen bound substituent, a hydrolysis experiment with ¹⁸O labelled water with triazole phosphonites,

bearing different oxy bound substituents, at different pH values would give new valuable information. For example, the hydrolysis pathway which proceeds *via* the attack of water at the proximal carbon atom of the oxy-bound substituent could potentially be suppressed by the installation of additional methyl groups at this position (Figure 6.1).

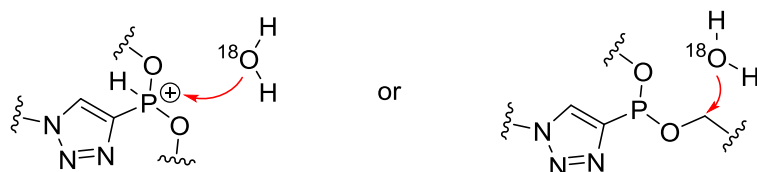


Figure 6.1: The two possible positions where water can attack a phosphonite to induce its hydrolysis.

In order to reduce hydrolysis of the phosphonite through direct attack of water at the corresponding phosphonium ion, the negative inductive effect (-I) of the carbon-phosphorus bond could be increased by modifying the C-substituent. The positioning of an electron-withdrawing group, such as a CF₂-group, between the phosphorus and the alkyne moiety (Figure 6.2) would make the phosphonite less basic. Therefore, formation of the phosphonium ion would be less likely. Unfortunately, this modification may also reduce the reaction rate of the Staudinger-phosphonite reaction due to a lower nucleophilicity of the phosphorus accompanied by a lower reactivity of the phosphonite towards the azide. For this reason, the thin line between reactivity and stability has to be adjusted.



Figure 6.2: Strong electron-withdrawing groups next to the phosphorus ought to reduce the tendency of phosphonites to be hydrolysed.

7 Experimental part

7.1 General informations

Materials: All reagents, starting materials, amino acids and solvents were purchased from commercial suppliers and used without further purification if not further mentioned. Dry solvents (acetonitrile, benzene, dichloromethane, DMSO, methanol, tetrahydrofurane, toluene) were purchased from ACROS ORGANICS or Sigma-Aldrich. Polyglycerol azides (68% and 30% degree of functionalization) were synthesised according to the literature and provided by the Haag group.^[162]

Methods and Instruments: ¹H NMR, ¹³C NMR and ³¹P NMR spectra were recorded on a Jeol ECX/400, Bruker AVANCE 500, Bruker AVANCE 600 or Bruker AVANCE 700 in [D₃]CH₃CN, [D]CHCl₃, [D₇]DMF, [D₆]DMSO [D₄]MeOH or [D₂]H₂O. The chemical shifts are reported in ppm relatively to the residual solvent peak. All phosphorus(III) related reactions (except reactions in water) were performed in dry solvents under argon atmosphere. Dialysis was performed with benzoylated cellulose tubing, MWCO 2000 Da purchased from Sigma Aldrich or with Biotech (CE), MWCO 500 Da, from Spectrum labs against water or chloroform (in case of acetylated carbohydrate derivatives) for one to four days with frequent changing of solvent. Preparative HPLC purification was performed on a Gilson® PLC 2020 Personal Purification System using a Nucleodur VP 250/32 C18 HTec 5 µm column from Macherey-Nagel at a flow rate of 30 mL/min. Analytical HPLC was applied on a Waters™ with a 717 plus autosampler, a 600S controller, 2 pumps 616 and a 2489 UV/Visible detector connected to a 3100 mass detector, using a Kromasil C18 5 µm, 250x4.6 mm RP-HPLC-column with a flow rate of 1.0 mL/min or a Shimadzu system with an SIL-20A autosampler, CBM-20A a controller, 2 LC-20AT pumps, a CTO-20A column oven and a SPD-M20A UV/visible detector using an Agilent eclipse cdb-c18, 5 µm, 250x4.6 mm column with a flow rate of 1.0 mL/min. HRMS were performed on an Agilent 6210 TOF-MS system, Agilent Technologies, Santa Clara, CA, USA. Spray voltage was set to 4 kV. Drying gas flow rate was set to 25 psi. U-HPLC-MS were performed on an Waters Acquity Ultra Performance LC® connected to an Waters Micromass LCT Premier (ESI-ToF) using an Atlantis dC-18 3 µm, 2.1x30 mm column with a flow rate of 0.2 mL/min. UV/Vis spectra were recorded on a Scinco S-3100 UV/Vis spectrometer. IR spectra were measured a Nexus FT-IR spectrometer equipped with a Nicolet Smart DuraSampleIR ATR. Melting points were determined using a Stuart Scientific melting point apparatus SMP3. Copper quantification has been done on an ELEMENT 2 ICP-MS from Thermo Fischer Scientific. Column chromatography was performed on silica gel (Acros Silica gel 60 A, 0.035-0.070 mm; for phosphonamidates Aldrich Silica gel

spherical 75-200 μm). TLC was performed on aluminium-backed silica plates (60 F254, 0.2 mm) which were developed using potassium permanganate as visualising agent. Solid-phase peptide synthesis was performed on an ABI 433A *Peptide Synthesizer* from Applied Biosystems or an Activotec Activo-P11 *Automated Peptide Synthesizer*.

7.2 Alkyne phosphonites for sequential azide-azide couplings in organic solvents (Chapter 3.3) - additional information

7.2.1 Deprotection of phosphonite-boranes with polystyrene-bound bases

The polystyrene-bound base (6 equiv.) was added to a solution of the borane-protected phosphonite (1 equiv.) in dry toluene (0.5 M). The reaction mixture was stirred for 20 hours at 60 °C and the filtrate was afterwards analysed by ^{31}P NMR. To avoid mechanical damage of the polystyrene particles by the magnetic stir bar, the reaction was performed in a round-bottom flask, which was attached to a KPG-stirrer allowing gentle agitation.

7.2.2 *P*-Ethynyl-*N*-(3-phenylpropyl)phosphoramidate (**213**)

A solution of alkyne-Grignard reagent (2.00 mL, 0.5 M in THF, 1.00 mmol, 1 equiv.) was cooled to -96 °C and diethyl chlorophosphite (0.144 mL, 0.157 g, 1.00 mmol, 1 equiv.) was added. After 1 hour the solution was warmed to 0 °C and was stirred for additional 2 hours before it was diluted with acetonitrile (8 mL). 3-Phenylpropylazide (0.242 g, 1.50 mmol, 1.5 equiv. in 1 mL acetonitrile) was added and the solution was slowly warmed to room temperature. After 12 hours, water (4 mL) was added and the solution was stirred for additional 4 hours. The crude product was stored at -18 °C for 6 month before it was purified by column chromatography. *P*-ethynyl-*N*-(3-phenylpropyl)phosphoramidate (**213**) was obtained in a yield of 11%(28 mg, 0.11 mmol, ~95% purity by ^{31}P NMR).

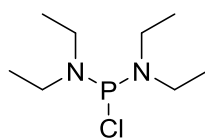
^1H NMR (400 MHz, $[\text{D}]\text{CHCl}_3$): δ = 7.29-7.18 (m, 5H, 5xCH), 4.08-3.98 (m, 2H, CH_2), 3.77 (s, 1H, NH), 3.28 (d, J = 12.2 Hz, 1H, CH), 2.90 (dq, J = 11.3, 6.9 Hz, 2H, CH_2), 2.65, (t, J = 7.8 Hz, 2H, CH_2), 1.79 (dt, J = 14.7, 7.2 Hz, 2H, CH_2), 1.31 (dt, J = 14.7, 7.2 Hz, 3H, CH_3). ^{31}P NMR (171.8 MHz, $[\text{D}_3]\text{CH}_3\text{CN}$): δ = -2.74. HRMS for $\text{C}_{13}\text{H}_{19}\text{NO}_2\text{P}^+$ $[\text{M}+\text{H}]^+$ calcd.: 252.2732, found: 252.2731.

Ethyl *N*-(3-phenylpropyl)-*P*-(1-(3-phenylpropyl)-1H-1,2,3-triazol-4-yl)-phosphoramidate (**214**)

Additionally to the desired product **213**, 40% ethyl *N*-(3-phenylpropyl)-*P*-(1-(3-phenylpropyl)-1H-1,2,3-triazol-4-yl)-phosphoramidate (**214**) (166 mg, 0.402 mmol) were isolated from the reaction mixture. Analytical data are given in the supporting information of chapter 3.3.

7.3 Alkyne phosphonites as modification tool for peptides and proteins (Chapter 3.4)

7.3.1 *N*-(Chloro(diethylamino)phosphanyl)-*N*-ethyl-ethanamine (**218**)

**218**

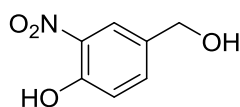
A solution of diethylamine (23.7 mL, 228.9 mmol) in diethyl ether (70 mL) was added dropwise to a solution of phosphorus trichloride (5 mL, 57.2 mmol) in diethyl ether (400 mL) at -20 °C. The solution was slowly warmed to room temperature and stirred for 12 hours. The obtained suspension was filtered through celite[®] to remove Et₂NH·HCl. The solvent was removed by distillation. The resulted yellow liquid was transferred to a small round-bottom flask and distilled under high vacuum to yield bis(diethylamino)chlorophosphine **218** (5.47 g, 26.0 mmol, 45%) as a colourless liquid.

¹H NMR (400 MHz, [D]CHCl₃): δ = 3.13 (q, *J* = 7.1 Hz, 8H, 4xCH₂), 3.66 (t, *J* = 7.1 Hz, 12H, 4xCH₃).

³¹P NMR (171.8 MHz, [D₃]CH₃CN): δ = 160.52. BP = 110 - 113 °C (15 Torr); 87 - 90 °C (2 Torr).

The obtained NMR data are in accordance with those reported in the literature.^[163]

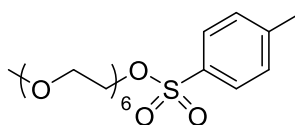
7.3.2 5-(Hydroxymethyl)-2-nitrophenol (**225**)

**225**

Boron trifluoride etherate (1.23 mL, 10.0 mmol, 1 equiv) and borane-tetrahydrofuran complex (1 M in THF, 20.0 mL, 20.0 mmol, 2 equiv.) were slowly added to a solution of 3-hydroxy-4-nitrobenzoic acid **224** (1.8312 g, 10.000 mmol, 1 equiv.) in dry THF (100 mL). After 18 hours, the reaction was carefully quenched with water (30 mL) and methanol (10 mL) before the organic solvents were removed under reduced pressure. The aqueous suspension was extracted with ethyl acetate (3x 100 mL). The organic layers were dried over magnesium sulfate, filtrated and concentrated under reduced pressure to yield 5-(hydroxymethyl)-2-nitrophenol (**225**) (1.69 g, 9.97 mmol, 100%) as yellow solid.

^1H NMR (400 MHz, $[\text{D}_6]\text{DMSO}$): δ = 7.86 (d, J = 8.5 Hz, 1H), 7.10-7.09 (m, 1H), 6.90-6.87 (m, 1H), 4.51 (s, 2H). ^{13}C NMR (100 MHz, $[\text{D}_6]\text{DMSO}$): δ = 152.7 (C), 151.5 (C), 134.9 (C), 125.3 (CH), 117.0 (CH), 116.0 (CH), 62.0 (CH_2). HRMS for $\text{C}_8\text{H}_{10}\text{NO}_4^+$ $[\text{M}+\text{H}]^+$ calcd.: 184.0604, found: 184.0617. MP = 98 - 99 °C. R_f (ethyl acetate/*c*-hexane : 2/1) = 0.3.

7.3.3 2,5,8,11,14,17-Hexaoxonadecan-19-yl 4-methylbenzenesulfonate (226)

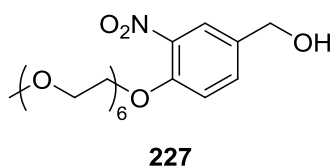


226

Trimethylamine hydrochloride (626 mg, 6.55 mmol, 1 equiv.) was slowly added to a solution of 2,5,8,11,14,17-hexaoxonadecan-19-ol (**228**) (1.94 g, 6.55 mmol, 1 equiv.), *p*-toluenesulfonyl chloride (1.62 g, 8.51 mmol, 1.3 equiv.) and triethylamine (1.33 g, 1.82 mL, 13.1 mmol, 2 equiv.) in acetonitrile (100 mL), at 0 °C. 30 minutes after addition was completed, the ice bath was removed and the mixture was stirred for three hours at room temperature. The suspension was filtered and the filtrate was condensed under reduced pressure. The residue was dissolved in toluene and washed twice with hydrochloride acid (10%). The organic layers were dried over magnesium sulfate and concentrated to yield 2,5,8,11,14,17-hexaoxonadecan-19-yl 4-methylbenzenesulfonate (**226**) in 84% yield (2.47 g, 5.48 mmol) as colourless liquid.

^1H NMR (400 MHz, $[\text{D}]\text{CHCl}_3$): δ = 7.78 (d, J = 8.1 Hz, 2H, 2xCH), 7.33 (d, J = 8.1 Hz, 2H, 2xCH), 4.14 (t, J = 4.9 Hz, 2H, CH_2), 3.68-3.52 (m, 22H, 11x CH_2), 3.36 (s, 3H, CH_3), 2.43 (s, 3H, CH_3). ^{13}C NMR (100 MHz, $[\text{D}]\text{CHCl}_3$): δ = 144.9 (C), 133.1 (C), 129.9 (2xCH), 128.1 (2xCH), 70.2 (CH_2), 70.9 (CH_2), 70.7-70.6 (8x CH_2), 69.4 (CH_2), 68.8 (CH_2), 59.1 (CH_3), 21.7 (CH_3). HRMS for $\text{C}_{20}\text{H}_{34}\text{NaN}_3\text{O}_9\text{S}^+$ $[\text{M}+\text{Na}]^+$ calcd.: 473.1816, found: 473.1804.

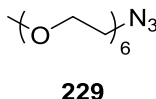
7.3.4 (3-(2,5,8,11,14,17-Hexaoxonadecan-19-yloxy)-4-nitrophenyl)methanol (**227**)



A solution of 5-(hydroxymethyl)-2-nitrophenol (**225**) (1.3229 g, 7.8218 mmol, 1 equiv.), 2,5,8,11,14,17-hexaoxonadecan-19-yl 4-methylbenzenesulfonate (**226**) (3.5213 g, 7.8218 mmol, 1 equiv.) and potassium carbonate (2.5945 g, 18.723 mmol, 2.4 equiv.) in acetonitrile (80 mL) was heated under reflux for 16 hours. The mixture was brought to room temperature and insoluble material was removed by filtration over a pad of silica. The crude product was purified by column chromatography to yield (3-(2,5,8,11,14,17-hexaoxonadecan-19-yloxy)-4-nitrophenyl)-methanol (**227**) (3.2306 g, 7.2195 mmol, 92%) as yellow liquid.

^1H NMR (400 MHz, $[\text{D}_6]\text{DMSO}$): δ = 7.44 (d, J = 8.3 Hz, 1H, CH), 6.89 (s, 1H, CH), 6.67 (d, J = 8.3 Hz, 1H, CH), 4.29 (s, 2H, CH_2), 3.94–3.90 (m, 2H, CH_2), 3.49–3.44 (m, 2H, CH_2), 3.31–3.27 (m, 2H, CH_2), 3.25–3.16 (m, 16H, CH_2), 3.13–3.09 (m, 2H, CH_2), 2.94 (s, 3H, OCH_3). ^{13}C NMR (100 MHz, $[\text{D}_6]\text{CD}_3\text{CN}$): δ = 150.7 (C), 139.5 (C), 127.0 (CH), 125.4 (CH), 119.7 (C), 114.4 (CH), 112.8 (CH), 73.4 (CH_2), 72.9 (CH_2), 72.5 (CH_2), 71.9 (CH_2), 71.5 (CH_2), 71.1 (CH_2), 70.4 (CH_2), 70.0 (CH_2), 69.7 (CH_2), 69.0 (CH_2), 68.5 (CH_2), 63.7 ($\text{CH}_2\text{-OH}$), 58.2 (CH_3). HRMS for $\text{C}_{21}\text{H}_{35}\text{NaNO}_{10}^+$ $[\text{M}+\text{Na}]^+$ calcd.: 484.2153, found: 484.2151. R_f (ethyl acetate/methanol: 9/1) = 0.22.

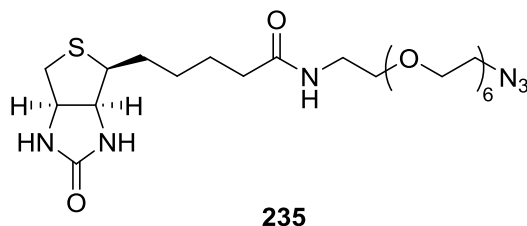
7.3.5 19-Azido-2,5,8,11,14,17-hexaoxonadecane (**229**)



To a solution of 2,5,8,11,14,17-hexaoxonadecan-19-yl 4-methylbenzenesulfonate **228** (2.40 g, 5.33 mmol, 1 equiv.) in DMF (50 mL) was added sodium azide (1.39 g, 21.4 mmol, 4 equiv.) and the reaction mixture was heated to 60 °C for 16 hours. Insoluble material was filtered off and the solvent was removed under reduced pressure. The residue was redissolved in dichloromethane and washed with water and brine. The organic layers were dried over magnesium sulfate and concentrated to yield 19-azido-2,5,8,11,14,17-hexaoxonadecane (**229**) in 88% yield (1.51 g, 4.70 mmol) as colorless liquid.

$^1\text{H-NMR}$ (400 MHz, $[\text{D}]\text{CHCl}_3$): δ = 3.62-3.57 (m, 20H, 10xCH₂), 3.50-3.48 (m, 2H, CH₂), 3.34-3.30 (m, 5H, CH₂, CH₃). $^{13}\text{C-NMR}$ (100 MHz, $[\text{D}]\text{CHCl}_3$): δ = 71.9 (CH₂), 70.6 (9xCH₂), 59.0 (CH₃), 50.6 (CH₂-N₃). HRMS for C₁₃H₂₇NaN₃O₆⁺ [M+Na]⁺ calcd: 344.1792, found: 344.1804.

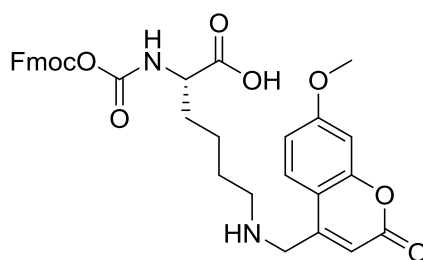
7.3.6 *N*-(20-Azido-3,6,9,12,15,18-hexaoxaicosyl)-5-((3a*S*,4*S*,6a*R*)-2-oxohexahydro-1*H*-thieno[3,4-*d*]imidazol-4-yl)pentanamide (**235**)



A suspension of D-biotin *N*-hydroxysuccinimide ester **232** (470.0 mg, 1.377 mmol 1.05 equiv.) in methanol (15 mL) was added to a solution of alpha-amino- ω -azido hepta(ethylene glycol) **233** (460.0 mg, 1.313 mmol, 1 equiv.) and triethylamine (1 equiv.) in methanol (25 mL). After 18 hours, the solvent was removed under reduced pressure and the crude product purified by column chromatography to yield *N*-(20-azido-3,6,9,12,15,18-hexaoxaicosyl)-5-((3a*S*,4*S*,6a*R*)-2-oxohexahydro-1*H*-thieno[3,4-*d*]imidazol-4-yl)pentanamide (**235**) (0.4312 g, 0.7477 mmol, 57%) as colourless sticky solid.

$^1\text{H NMR}$ (400 MHz, $[\text{D}_4]\text{CH}_3\text{OH}$): δ = 7.93 (s, 1H, NH), 4.55–4.52 (dd, 1H, J = 7.7, 4.7 Hz, CH), 4.36–4.33 (dd, 1H, J = 7.8, 4.4 Hz, CH), 3.72–3.64 (m, 22H, 11xCH₂), 3.59–3.56 (t, 2H, J = 5.4 Hz, CH₂), 3.42–3.38 (dt, 4H, J = 8.8, 5.2 Hz, 2xCH₂), 3.27–3.22 (m, 1H, CH), 2.99–2.94 (dd, 1H, J = 12.7, 4.9 Hz, CH), 2.76–2.73 (d, 1H, J = 12.6 Hz, CH), 2.28–2.24 (t, 2H J = 7.3 Hz, CH₂), 1.80-1.59 (m, 4H, 2xCH₂), 15.1–1.43 (m, 2H, CH₂). $^{13}\text{C NMR}$ (100 MHz, $[\text{D}_4]\text{CH}_3\text{OH}$): δ = 173.3 (C=O), 163.9 (C=O), 70.8, 70.8, 70.7, 70.7, 70.6, 70.6, 70.5, 70.5, 70.2, 70.2, 70.1, 70.1 (12x CH₂), 61.9 (CH), 60.3 (CH), 55.6 (CH), 50.8 (CH₂), 40.7 (CH₂), 39.3 (CH₂-N₃), 35.9 (CH₂), 28.1 (CH₂), 25.7 (CH₂), 22.7 (CH₂). HRMS for C₂₄H₄₄N₆NaO₈S⁺ [M+Na]⁺ calcd.: 599.6992, found: 599.7008. R_f (chloroform/methanol: 10/1) = 0.20.

7.3.7 *N*- α -fluorenylmethoxycarbonyl-(ϵ -*N*-((7-methoxy-2-oxo-2H-chromen-4-yl)methyl)-lysine (**252**)

**252**

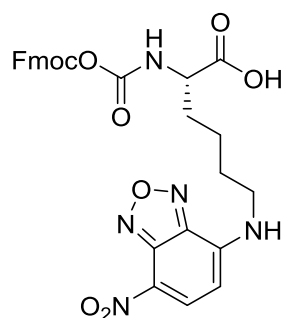
Thionyl chloride (0.7018 g, 6.016 mmol) was added to a solution of 1H-benzotriazole (2.406 g, 20.05 mmol) in dry CH_2Cl_2 (75 mL) at 20°C and the reaction mixture was stirred for 20 min. Afterwards, 7-methoxycoumarin-4-ylacetic acid (**249**) (1.174 g, 5.013 mmol) was added to the reaction mixture, and the mixture was stirred for additional 2 hours at 20 °C. The white precipitate formed during the reaction was filtered off and the filtrate was diluted with additional CH_2Cl_2 (400 mL). The solution was washed with 6 M HCl (3×250 mL), brine (50 mL), and dried over MgSO_4 . Filtration and removal of the solvent under reduced pressure yielded crude 4-(benzotriazole-1-ylacetyl)-7-methoxycoumarin (**250**), which was used in the next reaction step without further purification.

Crude 4-(benzotriazole-1-ylacetyl)-7-methoxycoumarin (**250**) (1.804 g, 5.514 mmol) was added to a solution of Na-Fmoc-L-lysine (2.857 g, 9.023 mmol) and Et_3N (3.759 mL, 27.07 mmol) in MeCN/ H_2O (125 mL/25 mL). The reaction mixture was stirred at 20 °C for 20 min. Afterwards, a 6 M HCl (10 mL) was added and the MeCN was removed under reduced pressure. The aqueous residue was extracted with EtOAc (500 mL) and the organic phase was washed with 6 M HCl (2×250 mL), brine (250 mL) and dried over MgSO_4 . Evaporation of the solvent gave (S)-2-(((9H-Fluoren-9-yl)methoxy)carbonylamino)-6-(2-(7-methoxy-2-oxo-2H-chromen-4-yl)acetamido)pentanoic acid (**252**) as white powder. After recrystallization from EtOAc–hexanes, the pure product (**252**) was obtained in a yield of 36% (1.805 mmol, 1.055 g) over two steps.

^1H NMR (400 MHz, $[\text{D}_6]\text{DMSO}$): δ = 8.23 (t, J = 5.3 Hz, 1H), 7.89 (d, J = 7.4 Hz, 2H), 7.72 (d, J = 7.4 Hz, 1H), 7.67–7.61 (m, 4H), 7.41 (t, J = 7.4 Hz, 2H), 7.32 (t, J = 7.3 Hz, 2H), 7.01–6.95 (m, 2H), 6.23 (s, 1H), 4.31–4.16 (m, 3H), 3.97–3.88 (m, 1H), 3.84 (m, 3H), 3.66 (s, 2H), 3.07–3.04 (m, 2H), 1.76–1.51 (m, 2H), 1.46–1.26 (m, 4H). HRMS for $\text{C}_{33}\text{H}_{32}\text{N}_2\text{O}_9$ $[\text{M}-\text{H}]^+$ calcd.: 599.2035, found: 599.2039.

The obtained NMR data are in accordance with those reported in the literature.^[156a]

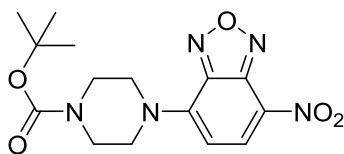
7.3.8 *N*- α -Fluorenylmethyloxycarbonyl-(ϵ -*N*-(7-Nitrobenz-2-oxa-1,3-diazol-4-ylamino)-lysine (254)

**254**

Fmoc-Lys-OH **251** (1.3 g, 3.5 mmol, 1 equiv.), 4-chloro-7-nitrobenzofurazan **253** (1.05 mg, 5.25 mmol, 1.5 equiv.) and sodium hydrogen carbonate (882 mg 10.5 mmol, 3 equiv.) in a water / methanol mixture (45 mL H₂O / 30 mL methanol) were warmed up to 60 °C. After 2.5 hours, the reaction was cooled to room temperature and the pH was set to one with hydrochloric acid (1N). The reaction mixture was extracted with dichloromethane (3x 100 mL) and the combined organic layers were washed with brine, dried over magnesium sulfate, concentrated and purified by column chromatography to yield Fmoc-Lys(ϵ -NBD)-OH (**254**) (1.15 g, 2.16 mmol, 62%) as orange solid.

¹H NMR (400 MHz, [D₆]DMSO): δ = 12.61 (s, 1H), 9.50 (s, 1H), 8.42 (d, J = 8.9 Hz, 1H), 7.84 (d, J = 7.6 Hz, 2H), 7.70 (dd, J = 7.6, 4.9 Hz, 2H), 7.65 (d, J = 8.1 Hz, 1H), 7.38 (t, J = 7.5 Hz, 2H), 7.29 (t, J = 7.5 Hz, 2H), 6.31 (d, J = 9.1 Hz, 1H), 4.30-4.25 (m, 2H), 4.19 (t, J = 7.0 Hz, 1H), 4.03-3.92 (m, 1H), 3.48-3.37 (m, 2H), 1.87-1.58 (m, 4H), 1.52-1.40 (m, 2H). ¹³C NMR (100 MHz, [D₃]CH₃CN): δ = 174.0 (C), 156.2 (C), 145.1 (d, J = 3.4 Hz, C), 144.4 (C), 144.1 (C), 143.8 (C), 140.7 (d, J = 2.5 Hz, C), 137.8 (CH₂), 127.6 (CH₂), 127.1 (CH₂), 125.3 (CH₂), 120.6 (C), 120.1 (CH₂), 99.0 (CH), 65.6 (CH₂), 53.8 (CH), 46.7 (CH), 43.2 (CH₂), 30.5 (CH₂), 27.1 (CH₂), 23.2 (CH₂). HRMS for C₂₇H₂₄N₅O₇⁺ [M+H]⁺ calcd.: 530.1681, found: 530.1739. MP = 116 - 117 °C. R_f (dichloromethane/methanol: 10/1) = 0.22.

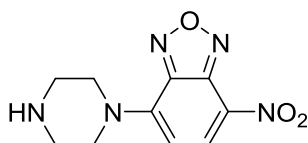
7.3.9 *tert*-Butyl 4-(7-nitrobenzo[*c*][1,2,5]oxadiazol-4-yl)piperazine-1-carboxylate (**265**)

**265**

Triethylamine (2.277 g, 22.50 mmol, 1.5 equiv.) and *tert*-butyl piperazine **264** (4.188 g, 22.50 mmol, 1.5 equiv.) were added to a stirred solution of 4-chloro-7-nitrobenzofurazan **253** (2.985 g, 15.00 mmol, 1 equiv.) in MeCN (150 mL). After the reaction mixture was stirred for additional 2.5 hours at 60 °C, MeCN was removed under reduced pressure and the residue was dissolved in CH₂Cl₂ (200 mL). The solution was washed with hydrochloric acid (1 N, 2x 100 mL), dried over magnesium sulfate and concentrated under reduced pressure to yield Boc-protected NBD-piperazine **265** (5.120 g, 14.66 mmol, 98%) as a red solid.

¹H NMR (400 MHz, [D₆]DMSO): δ = 8.50 (d, *J* = 9.2 Hz, 1H, CH), 6.60 (d, *J* = 9.2 Hz, 1H, CH), 4.16 (t, *J* = 5.3 Hz, 4H, 2xCH₂), 3.62 (t, *J* = 5.3 Hz, 4H, 2xCH₂), 1.44 (s, 9H, 3xCH₃). ¹³C NMR (174 MHz, [D₆]DMSO): δ = 154.2 (C=O), 145.9 (C), 145.2 (C), 136.8 (CH), 121.7 (C), 103.7 (CH), 79.9 (C(CH₃)₃), 49.3 (4xCH₂), 28.5 (3xCH₃). HRMS for C₁₅H₂₀N₅O₅⁺ [M+H]⁺ calcd.: 350.1459, found: 350.1455. MP = 173-174°C. R_f (ethyl acetate/*c*-hexane: 1/1) = 0.42.

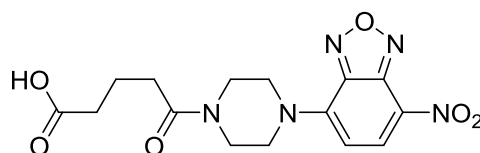
7.3.10 4-Nitro-7-(piperazin-1-yl)benzo[*c*][1,2,5]oxadiazole (**266**)

**266**

TFA (7 mL, 13.4 equiv.) was slowly added to a stirred solution of Boc-protected NBD-piperazine **265** (2.35 g, 6.73 mmol, 1 equiv.) in CH₂Cl₂ (93 mL) and the reaction mixture was stirred for 2 hours at room temperature until thin layer chromatography confirmed full conversion of the starting material. The reaction mixture was quenched with aqueous sodium bicarbonate (150 mL) and extracted with CH₂Cl₂ (4x 150 mL). The combined organic extracts were dried over magnesium sulphate and concentrated under reduced pressure to yield NBD-piperazine **266** (1.450 g, 5.818 mmol, 86%) as a red solid.

^1H NMR (400 MHz, $[\text{D}_6]\text{DMSO}$): δ = 8.45 (d, J = 9.2 Hz, 1H, CH), 6.64 (d, J = 9.3 Hz, 1H, CH), 4.07 (s, 4H, $2\times\text{CH}_2$), 2.95-2.90 (m, 4H, $2\times\text{CH}_2$). ^{13}C NMR (174 MHz, $[\text{D}_6]\text{DMSO}$): δ = 145.9 (C), 145.6 (C), 145.4 (C), 136.8 (CH), 121.0 (C), 103.7 (CH), 51.9 ($2\times\text{CH}_2$), 46.4 ($2\times\text{CH}_2$). HRMS for $\text{C}_{10}\text{H}_{12}\text{N}_{12}\text{O}_3^+$ $[\text{M}+\text{H}]^+$ calcd.: 250.0935, found: 250.0929. MP = 130-132°C. R_f (CH_2Cl_2 / methanol: 9/1) = 0.59.

7.3.11 5-(4-(7-Nitrobenzo[c][1,2,5]oxadiazol-4-yl)piperazin-1-yl)-5-oxopentanoic acid (**267**)



267

A stirred solution of NBD-piperazine **266** (0.500 g, 2.01 mmol, 1 equiv.) and glutaric acid anhydride (0.251 g, 2.20 mmol, 1.1 equiv.) in dry toluene / DMF (3:1, 15 mL) was refluxed at 110 °C overnight. The cool reaction mixture was diluted with hydrochloric acid (1 N, 15 mL) and extracted with CH_2Cl_2 (4x 20 mL). The combined organic phases were dried over magnesium sulfate and concentrated under reduced pressure. The crude product was purified by column chromatography (8% MeOH / CH_2Cl_2) to yield NBD-linked-acid **267** (0.598 mg, 1.65 mmol, 82%) as a red solid.

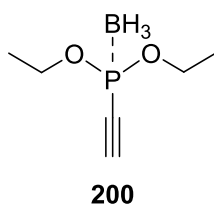
^1H NMR (400 MHz, $[\text{D}_7]\text{DMF}$): δ = 8.56 (d, J = 9.1 Hz, 1H, CH), 6.71 (d, J = 9.1 Hz, 1H, CH), 4.38-4.26 (m, 4H, $2\times\text{CH}_2$), 4.00-3.85 (m, 4H, $2\times\text{CH}_2$), 2.53 (t, J = 7.4 Hz, 2H, CH_2), 2.40 (t, J = 7.4 Hz, 2H, CH_2), 1.89 (quint, J = 7.4 Hz, 2H, CH_2). ^{13}C NMR (174 MHz, $[\text{D}_7]\text{DMF}$): δ = 174.7 (COOH), 171.3 (C=O), 145.9 (C), 145.4 (C), 145.4 (C), 136.3 (CH), 122.3 (C- NO_2), 103.5 (CH), 49.5 (CH_2), 49.2 (CH_2), 33.4 (CH_2), 32.1 (CH_2), 20.7 (CH_2). HRMS for $\text{C}_{15}\text{H}_{16}\text{N}_5\text{O}_6^-$ $[\text{M}-\text{H}]^-$ calcd.: 362.1106, found: 362.1109. MP = 158-160 °C. R_f (CH_2Cl_2 /methanol: 9/1) = 0.19.

7.3.12 General protocol for the synthesis of alkyne phosphonite-boranes

Phosphorus trichloride (**6**) (1 equiv.) and triethylamine (2 equiv.) were cooled to -96°C and afterwards a solution of the corresponding alcohol (2 equiv. in dry toluene (15 mL/mmol)) was slowly added. The reaction mixture was stirred for 30 minutes before it was slowly warmed to room temperature. The reaction mixture was stirred for additional 24 hours and was afterwards diluted with dry THF (0.6 mL/mL toluene). The mixture was cooled to -96°C again

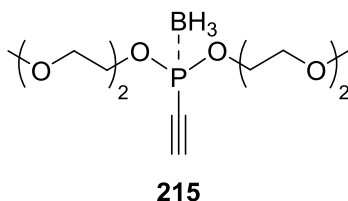
and the alkyne-Grignard reagent (1 equiv. 1 M in THF) was added. The reaction mixture was stirred for 30 minutes before it was slowly warmed up to room temperature and stirred for additional 2 hours. Then, the borane THF complex (1.5 equiv.) was added at 0 °C and the reaction mixture was stirred for 2 hours at room temperature. The reaction mixture was diluted with diethyl ether (10 mL/1 mL toluene), insoluble material was removed by centrifugation, and the solvent was removed under reduced pressure.

7.3.12.1 Diethyl ethynylphosphonite-borane (**200**)



The synthesis of diethyl ethynylphosphonite-borane (**200**) is described in the supporting information of chapter 3.3.

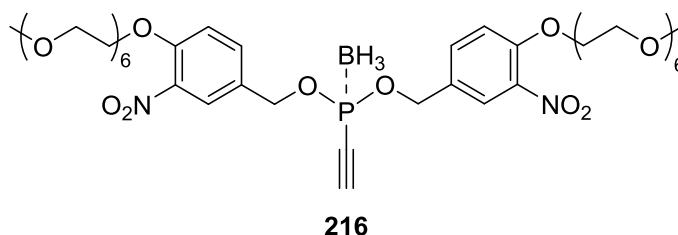
7.3.12.2 Bis(2-(2-methoxyethoxy)ethyl) ethynylphosphonite-borane (**215**)



Bis(2-(2-methoxyethoxy)ethyl) ethynylphosphonite-borane (**215**) was synthesised according to the general protocol for alkyne phosphonite-boranes from phosphorus trichloride (**6**) (0.875 mL, 10.0 mmol) and 2-(2-methoxyethoxy)ethan-1-ol (2.403 g, 20.00 mmol). Bis(2-(2-methoxyethoxy)ethyl) ethynylphosphonite-borane (**215**) was obtained in a yield of 48% (1.492 g, 4.842 mmol) after column chromatography.

^1H NMR (300 MHz, $[\text{D}_3]\text{CH}_3\text{CN}$): δ = 4.20 (dq, J = 7.2, 3.5 Hz, 4H, 2xCH₂), 3.77 (d, J = 7.4 Hz, 1H, CH), 3.72–3.62 (m, 4H, 2xCH₂), 3.60 (dd, J = 5.8, 3.3 Hz, 4H, 2xCH₂), 3.49 (dd, J = 5.8, 3.2 Hz, 4H, 2xCH₂), 3.31 (s, 6H, 2xCH₃), 1.08–0.06 (m, 3H, BH₃). ^{13}C NMR (75 MHz, $[\text{D}_3]\text{CH}_3\text{CN}$): δ = 96.0 (d, J = 24.1 Hz, CH), 76.4 (d, J = 119.4 Hz, C-P), 72.5 (2xCH₂), 71.0 (2xCH₂), 70.39 (d, J = 6.6 Hz, 2xCH₂), 68.44 (d, J = 7.2 Hz, 2xCH₂), 58.9 (2xCH₃). ^{31}P NMR (122 MHz, $[\text{D}_3]\text{CH}_3\text{CN}$): δ = 105.58 (dd, J = 168.8, 78.1 Hz). HRMS for $\text{C}_{12}\text{H}_{27}\text{BO}_6\text{P}^+$ $[\text{M}+\text{H}]^+$ calcd.: 309.1633, found: 309.1629. R_f (ethyl acetate/nhexane: 3/1) = 0.29.

7.3.12.3 Bis(4-(2,5,8,11,14,17-hexaoxonadecan-19-yloxy)-3-nitrobenzyl) ethynyl-phosphonite-borane (216)



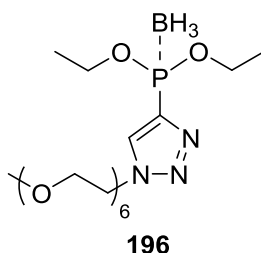
Bis(2-(2-methoxyethoxy)ethyl) ethynylphosphonite-borane (**215**) was synthesised according to the general protocol for alkyne phosphonite-boranes from phosphorus trichloride (**6**) (0.18 mL, 2.1 mmol) and 4-((2,5,8,11,14,17-hexaoxonadecan-19-yl)oxy)-3-nitrophenyl)-methanol (**227**) (1.880 g, 4.201 mmol). Bis(4-(2,5,8,11,14,17-hexaoxonadecan-19-yloxy)-3-nitrobenzyl) ethynyl-phosphonite-borane (**216**) was obtained in a yield of 62% (1.376 g, 1.429 mmol) after HPLC purification (H₂O / MeCN, no TFA).

¹H NMR (400 MHz, [D₃]CH₃CN): δ = 7.79 (d, *J* = 8.3 Hz, 2H, 2xCH), 7.21 (d, *J* = 1.4 Hz, 2H, 2xCH), 7.03 (dd, *J* = 8.3, 1.6 Hz, 2H, 2xCH), 5.16 (d, *J* = 9.3 Hz, 4H, 2xCH₂), 4.22 (dd, *J* = 5.2, 3.9 Hz, 4H, 2xCH₂), 3.93 (d, *J* = 7.6 Hz, 1H, C≡CH), 3.80 (dd, *J* = 5.2, 3.9 Hz, 4H, 2xCH₂), 3.65–3.60 (m, 4H, 2xCH₂), 3.58–3.49 (m, 32H, 16xCH₂), 3.47–3.42 (m, 4H), 3.28 (s, 6H, 2xOCH₃). ¹³C NMR (100 MHz, [D₃]CH₃CN): δ = 152.9 (2xC), 143.2 (2xC), 143.1 (2xC), 126.5 (2xCH), 120.2 (2xCH), 115.1 (2xCH), 72.5, 71.4, 71.1, 70.9, 70.6, 69.8 (24xCH₂), 68.6 (2xCH₂), 58.8 (2xCH₃). ³¹P NMR (171.8 MHz, [D₃]CH₃CN): δ = 109.38-107.77 (m). HRMS for C₄₂H₆₈BNa₂O₂₀P⁺ [M+Na]⁺ calcd.: 985.4088, found: 985.4105.

7.3.13 General protocol for the CuAAC of alkyne phosphonite-boranes

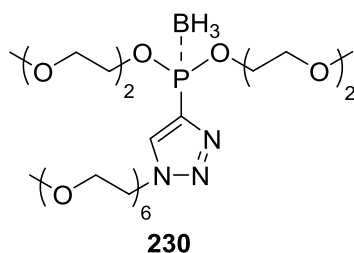
Tetrakis(acetonitrile)copper(I) hexafluorophosphate (0.05 equiv.) was added slowly to a solution of the phosphonite (1 equiv.) and the corresponding azide (1.3 equiv.) in tetrahydrofuran. The solution was stirred for 16 hours at 40 °C and purified by preparative HPLC.

7.3.13.1 Diethyl 1-(2,5,8,11,14,17-hexaoxonadecan-19-yl)-1H-1,2,3-triazol-4-ylphosphonite-borane (**196**)



The synthesis of Diethyl 1-(2,5,8,11,14,17-hexaoxonadecan-19-yl)-1H-1,2,3-triazol-4-ylphosphonite-borane (**196**) is described in the supporting information of chapter 3.3.

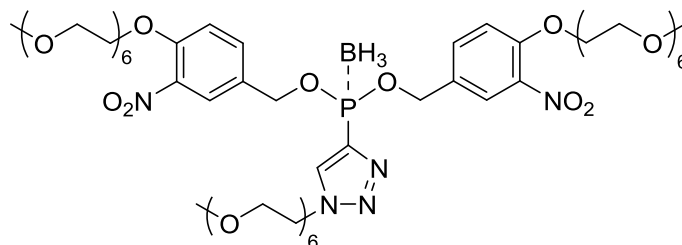
7.3.13.2 Bis(2-(2-methoxyethoxy)ethyl) (1-(2,5,8,11,14,17-hexaoxonadecan-19-yl)-1H-1,2,3-triazol-4-yl)phosphonite-borane (**230**)



Bis(2-(2-methoxyethoxy)ethyl) (1-(2,5,8,11,14,17-hexaoxonadecan-19-yl)-1H-1,2,3-triazol-4-yl)phosphonite-borane (**230**) was synthesized according to the general protocol for the CuAAC of alkyne phosphonite-boranes from bis(2-(2-methoxyethoxy)ethyl) ethynylphosphonite-borane (**215**) (463.2 g, 0.701 mmol) and 19-azido-2,5,8,11,14,17-hexaoxonadecane (**229**) (296.3 g, 0.922 mmol). Bis(2-(2-methoxyethoxy)ethyl) (1-(2,5,8,11,14,17-hexaoxonadecan-19-yl)-1H-1,2,3-triazol-4-yl)phosphonite-borane (**230**) was obtained in a yield of 68% (310.6 g, 0.476 mmol) after HPLC purification (H₂O / MeCN, no TFA).

³¹P NMR (202 MHz, [D]CHCl₃): δ = 120.96 (m). HRMS for C₂₅H₅₃BN₂NaO₁₂P⁺ [M+Na]⁺ calcd.: 652.3352, found: 652.3338.

7.3.13.3 Bis(4-(2,5,8,11,14,17-hexaoxonadecan-19-yloxy)-3-nitrobenzyl) (1-(2,5,8,11,14,17-hexaoxonadecan-19-yl)-1H-1,2,3-triazol-4-yl)phosphonite-borane (231)

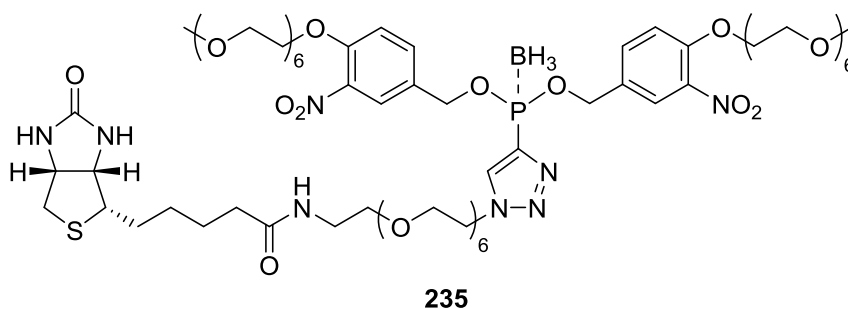


231

Bis(4-(2,5,8,11,14,17-hexaoxonadecan-19-yloxy)-3-nitrobenzyl) (1-(2,5,8,11,14,17-hexaoxonadecan-19-yl)-1H-1,2,3-triazol-4-yl)phosphonite-borane (**231**) was synthesized according to the general protocol for the CuAAC of alkyne phosphonite-boranes from bis(4-(2,5,8,11,14,17-hexaoxonadecan-19-yloxy)-3-nitrobenzyl) ethynyl-phosphonite-borane (**216**) (621.8 g, 0.646 mmol) and 19-azido-2,5,8,11,14,17-hexaoxonadecane (**229**) (270.3 g, 0.841 mmol). Bis(4-(2,5,8,11,14,17-hexaoxonadecan-19-yloxy)-3-nitrobenzyl) (1-(2,5,8,11,14,17-hexaoxonadecan-19-yl)-1H-1,2,3-triazol-4-yl)phosphonite-borane (**231**) was obtained in a yield of 71% (586.6 g, 0.4568 mmol) after HPLC purification (H₂O / MeCN, no TFA).

¹H NMR (700 MHz, [D₃]CH₃CN): δ = 8.37 (s, 1H, CH), 7.78 (d, *J* = 8.3 Hz, 2H, 2xCH), 7.22 (d, *J* = 1.6 Hz, 2H, 2xCH), 7.04 (dd, *J* = 8.3, 1.6 Hz, 2H, 2xCH), 5.20 (dd, *J* = 13.0, 9.2 Hz, 2H, 2xCHH), 5.13 (dd, *J* = 13.0, 8.3 Hz, 2H, 2xCHH), 4.61 (t, *J* = 5.1 Hz, 2H, CH₂), 4.22 (t, *J* = 4.6 Hz, 4H, 2xCH₂), 3.88 (t, *J* = 5.1 Hz, 2H, CH₂), 3.80 (t, *J* = 4.6 Hz, 4H, 2xCH₂), 3.63–3.62 (m, 4H, 2xCH₂), 3.57–3.48 (m, 50H, 25xCH₂), 3.45–3.43 (m, 6H, 3xCH₂), 3.28 (s, 6H, 2xCH₃), 3.27 (s, 3H, CH₃), 1.04–0.57 (m, 3H, BH₃). ¹³C NMR (176 MHz, [D₃]CH₃CN): δ = 152.9 (2xC), 143.9 (d, *J* = 5.8 Hz, 2xC), 140.5 (2xC), 139.2 (d, *J* = 108.6 Hz, C-P), 132.9 (d, *J* = 29 Hz, CH), 126.4 (2xCH), 120.1 (2xCH), 115.0 (2xCH), 72.6, 71.5, 71.1, 71.0, 70.9, 70.6, 69.8, 69.5 (35xCH₂), 68.8 (d, *J* = 3.6 Hz, 2xCH₂), 58.9 (3xCH₃), 51.2 (CH₂). ³¹P NMR (202 MHz, [D₃]CH₃CN): δ = 122.96 (m). ¹¹B NMR (160 MHz, [D₃]CH₃CN): δ = -40.84. HRMS for C₁₉H₄₁BN₃NaO₈P⁺ [M+Na]⁺ calcd.: 504.2617, found: 504.2629.

7.3.13.4 Bis(4-(2,5,8,11,14,17-hexaoxonadecan-19-yloxy)-3-nitrobenzyl) (1-(22-oxo-26-((3a*S*,4*S*,6a*R*)-2-oxohexahydro-1*H*-thieno[3,4-*d*]imidazol-4-yl)-3,6,9,12,15,18-hexaoxa-21-azahexacosyl)-1*H*-1,2,3-triazol-4-yl)phosphonite-borane (235)



Bis(4-(2,5,8,11,14,17-hexaoxonadecan-19-yloxy)-3-nitrobenzyl) (1-(22-oxo-26-((3a*S*,4*S*,6a*R*)-2-oxohexahydro-1*H*-thieno[3,4-*d*]imidazol-4-yl)-3,6,9,12,15,18-hexaoxa-21-azahexacosyl)-1*H*-1,2,3-triazol-4-yl)phosphonite-borane (**235**) was synthesized according to the general protocol for the CuAAC of alkyne phosphonite-boranes from bis(4-(2,5,8,11,14,17-hexaoxonadecan-19-yloxy)-3-nitrobenzyl) ethynyl-phosphonite-borane (**216**) (0.2116 g, 0.2198 mmol) and *N*-(20-Azido-3,6,9,12,15,18-hexaoxaicosyl)-5-((3a*S*,4*S*,6a*R*)-2-oxohexahydro-1*H*-thieno[3,4-*d*]imidazol-4-yl)pentanamide (**235**) (0.172 g, 0.290 mmol). Bis(4-(2,5,8,11,14,17-hexaoxonadecan-19-yloxy)-3-nitrobenzyl) (1-(22-oxo-26-((3a*S*,4*S*,6a*R*)-2-oxohexahydro-1*H*-thieno[3,4-*d*]imidazol-4-yl)-3,6,9,12,15,18-hexaoxa-21-azahexacosyl)-1*H*-1,2,3-triazol-4-yl)phosphonite-borane (**235**) was obtained in a yield of 52% (0.1734 g, 0.114 mmol) after HPLC purification (H₂O / MeCN, no TFA).

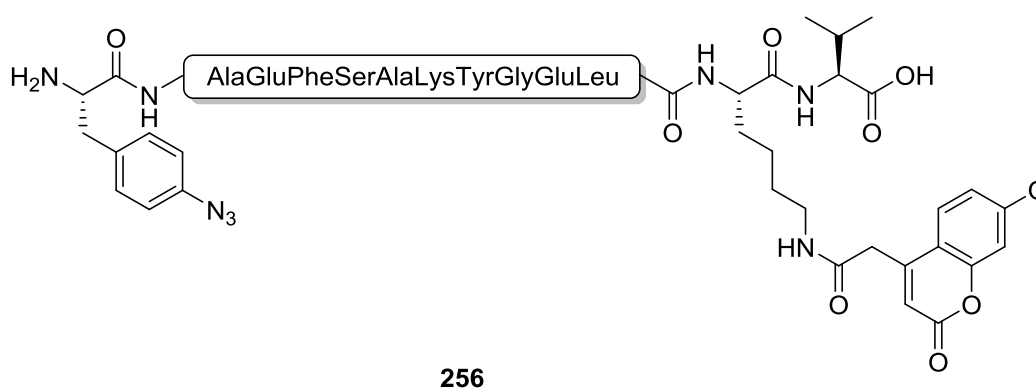
¹H NMR (700 MHz, [D₃]CH₃CN): δ = 8.37 (s, 1H, CH), 7.78 (d, *J* = 8.3 Hz, 2H, 2xCH), 7.23 (d, *J* = 1.6 Hz, 2H, 2xCH), 7.04 (dd, *J* = 8.3, 1.7 Hz, 2H, 2xCH), 6.49 (s, 1H, NH), 5.26 (s, 1H, NH), 5.22 (dd, *J* = 13.0, 9.2 Hz, 2H, 2xCHH), 5.14 (dd, *J* = 13.0, 8.3 Hz, 2H, 2xCHH), 5.04 (s, 1H, NH), 4.61 (t, *J* = 5.1 Hz, 2H, CH₂), 4.43 (ddt, *J* = 7.7, 5.1, 1.2 Hz, 1H, CH), 4.26–4.25 (m, 5H, 2xCH₂+CH), 3.93–3.91 (m, 2H, CH₂), 3.84–3.82 (m, 4H, 2xCH₂), 3.66–3.65 (m, 4H, 2xCH₂), 3.60–3.51 (m, 54H, 27xCH₂), 3.49–3.47 (m, 6H, 3xCH₂), 3.32–3.29 (m, 2H, CH₂), (3.31 (s, 6H, 2xCH₃), 3.17 (ddd, *J* = 7.9, 6.8, 4.4 Hz, 1H, CH), 2.91 (dd, *J* = 12.7, 5.0 Hz, 1H, CHH), 2.66 (d, *J* = 12.7 Hz, 1H, CHH), 2.17–2.14 (m, 2H, CH₂), 1.73–1.68 (m, 1H, CHH), 1.64–1.60 (dt, *J* = 14.9, 7.4 Hz, 2H, CH₂), 1.60-1.54 (m, 1H, CHH), 1.05–0.65 (m, 3H, BH₃). ¹³C NMR (176 MHz, [D₃]CH₃CN): δ = 173.6 (C), 163.7 (C), 152.9 (2xC), 143.9 (d, *J* = 5.0 Hz, 2xC), 140.6 (2xC), 139.2 (d, *J* = 109.1 Hz, C-P), 132.9 (d, *J* = 29.1 Hz, CH), 126.4 (2xCH), 120.1 (2xCH), 115.0 (2xCH), 72.6 (2xCH₂), 71.5 (CH₂), 71.1-70.0 (24xCH₂), 71.0 (CH₂), 70.9 (2xCH₂), 70.8 (CH₂), 70.6 (2xCH₂), 70.3 (CH₂), 69.8 (2xCH₂),

69.5 (CH₂), 68.8 (d, *J* = 5.3 Hz, 2xCH₂), 62.3 (CH), 60.7 (CH), 58.9 (2xCH₃), 56.3 (CH), 51.2 (CH₂), 41.1 (CH₂), 39.8 (NCH₂), 36.3 (CH₂), 30.0 (CH₂), 29.9 (CH₂), 26.4 (CH₂). ³¹P NMR (202 MHz, [D₃]CH₃CN): δ = 123.09 (m). ¹¹B NMR (160 MHz, [D₃]CH₃CN): δ = -40.83. HRMS for C₁₉H₄₁BN₃NaO₈P⁺ [M+Na]⁺ calcd.: 504.2617, found: 504.2629.

7.3.14 General protocol for the synthesis of azido peptides

All peptides were prepared by automated Fmoc-solid-phase peptide synthesis on a polystyrene resin attached through either a preloaded Wang or a trityl linker. Expensive amino acids like Fmoc-*p*-azidophenylalanine, Fmoc-D₃-alanine are fluorophore-tagged amino acids were coupled manually (2 equiv., HOBT / HBTU or HATU, DIPEA in DMF, 4 hours). Global deprotection and cleavage of the peptide from the resin was achieved by treatment with TFA (95%, 2.5% TIS, 2.5 water, 30 min.). The crude peptide was purified by preparative HPLC (H₂O + 0.1% TFA, MeCN + 0.1% TFA).

7.3.14.1 Coumarin-tagged azido peptide 256



Coumarin-tagged azido peptide **256** was synthesised on a Wang resin preloaded with Fmoc-valine (0.45 mmol/g, 100 – 200 mesh) in a 0.1 mmol scale on the ABI 433A *Peptide Synthesizer* from Applied Biosystems and was isolated after HPLC purification in 7% yield as double TFA salt (14.4 mg, 0.0073 mmol).

HRMS for C₈₃H₁₁₄N₁₈O₂₄²⁺ [M+2H]²⁺ calcd.: 873.4121, found: 873.4124.

HPLC-gradient (on the Shimadzu system) (A: water + 0.1% TFA; B: MeCN + 0.1% TFA): from 5% B to 100% B in 30 minutes. Retention time: 12.055 minutes.

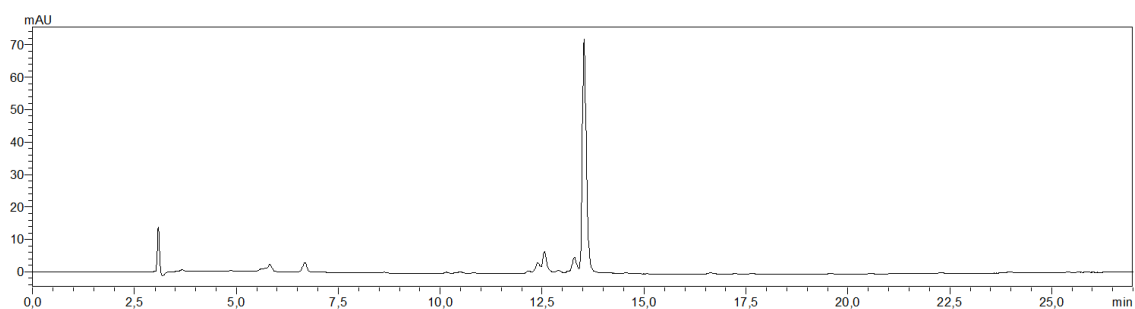


Figure 7.1: HPLC-UV (272 nm) trace of purified Coumarin-tagged azido peptide **256**.

HPLC-fluorescence-gradient (on the Waters system) (A: water + 0.1% TFA; B: MeCN + 0.1% TFA): from 0% B to 10% B in 20 minutes, than from 10% B to 100% B in 28 minutes. (Ex [nm]: 360, Em [nm]: 410)

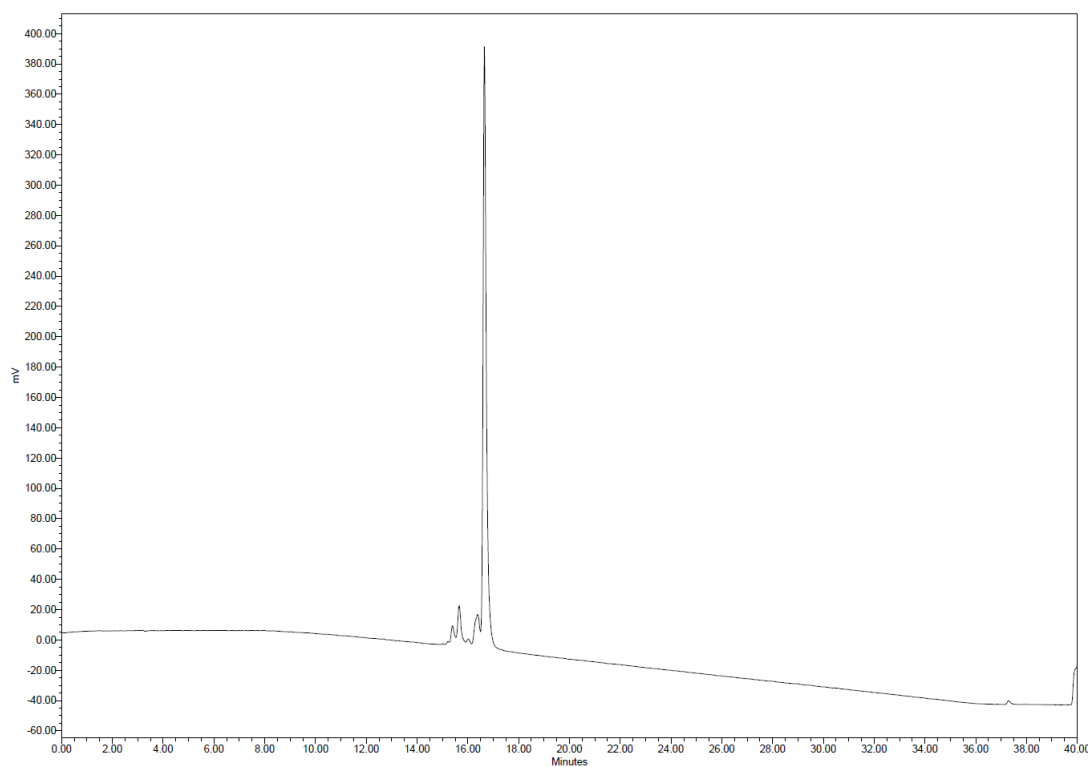
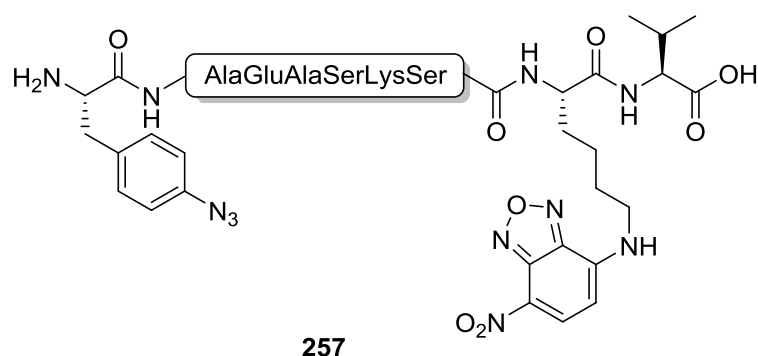


Figure 7.2: Fluorescence spectrum of coumarin-tagged azido peptide **256**.

7.3.14.2 NBD-tagged azido peptide **257**

NBD-tagged azido peptide **257** was synthesised on a Wang resin preloaded with Fmoc-valine (0.45 mmol/g, 100 – 200 mesh) in a 0.1 mmol scale on the ABI 433A *Peptide Synthesizer* from Applied Biosystems and was isolated after HPLC purification in 13% yield as double TFA salt (17.7 mg, 0.0127 mmol).

HRMS for $C_{49}H_{72}N_{17}O_{17}^+$ $[M+H]^+$ calcd.: 1170.5287, found: 1170.5268.

HPLC-gradient (on the Shimadzu system) (A: water + 0.1% TFA; B: MeCN + 0.1% TFA): from 5% B to 100% B in 30 minutes. Retention time: 12.055 minutes.

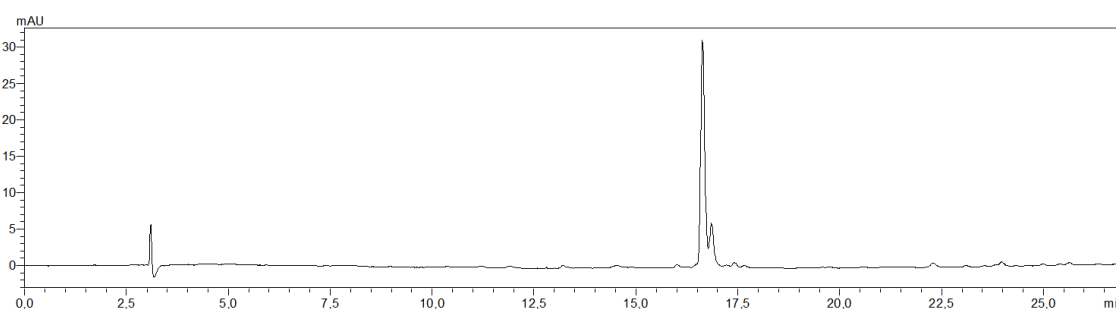


Figure 7.3: HPLC-UV (272 nm) trace of purified NBD-tagged azido peptide **257**.

HPLC-fluorescence-gradient (on the Waters system) (A: water + 0.1% TFA; B: MeCN + 0.1% TFA): 0% B for 5 minutes, than from 0% B to 10% B in 1 minutes, than from 10% B to 60% B in 25 minutes, than from 60% B to 100% B in 3 minutes. (Ex [nm]: 470, Em [nm]: 550)

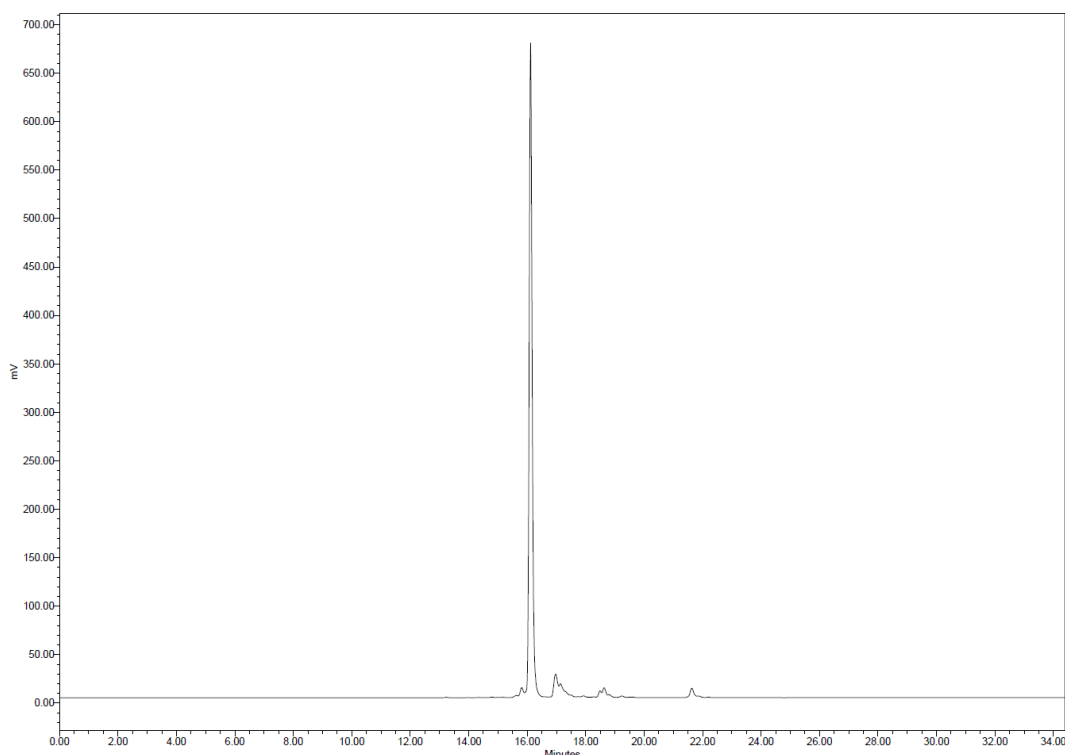
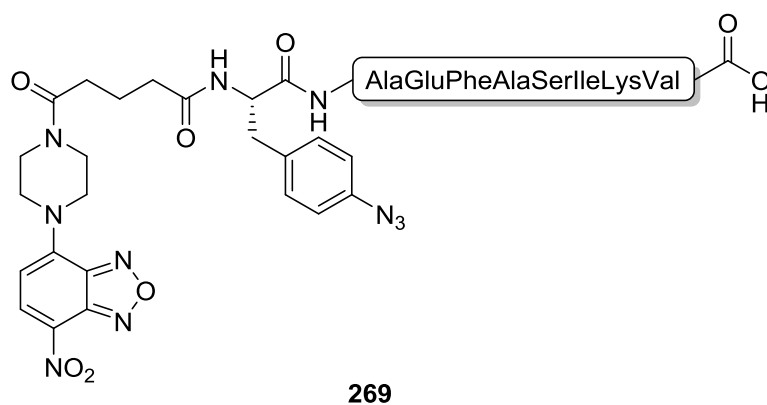


Figure 7.4: Fluorescence spectrum of NDB-tagged azido peptide **257**.

7.3.14.3 Piperazine-linked NDB-tagged azido peptide **269**



Piperazine-linked NDB-tagged azido peptide **269** was synthesised on a Wang resin preloaded with Fmoc-valine (0.45 mmol/g, 100 – 200 mesh) in a 0.1 mmol scale on the ABI 433A *Peptide Synthesizer* from Applied Biosystems and was isolated after HPLC purification in 18% yield as double TFA salt (25.6 mg, 0.0183 mmol).

HRMS for $C_{64}H_{89}N_{18}O_{18}^+ [M+H]^+$ calcd.: 1397.6597, found: 1397.6571.

HPLC-gradient (on the Shimadzu system) (A: water + 0.1% TFA; B: MeCN + 0.1% TFA): from 5% B to 100% B in 30 minutes. Retention time: 12.055 minutes.

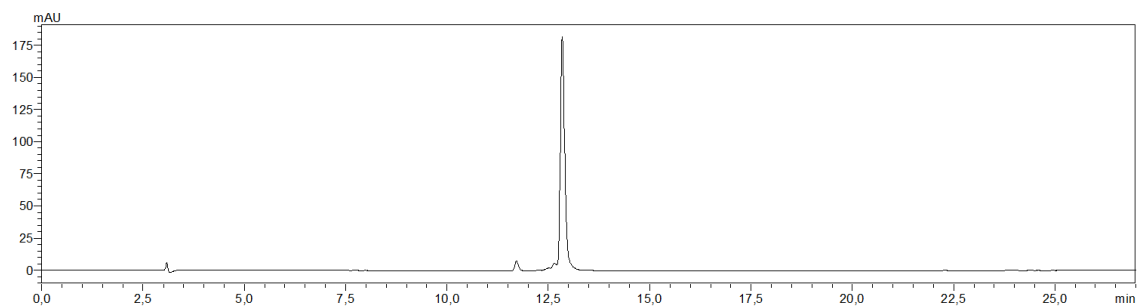


Figure 7.5: HPLC-UV (272 nm) trace of purified piperazine-linked NDB-tagged azido peptide **269**.

HPLC-fluorescence-gradient (on the Waters system) (A: water + 0.1% TFA; B: MeCN + 0.1% TFA): 10% B for 4 minutes, than from 10% B to 80% B in 20 minutes, than from 80% B to 100% B in 10 minutes. (Ex [nm]: 488, Em [nm]: 545)

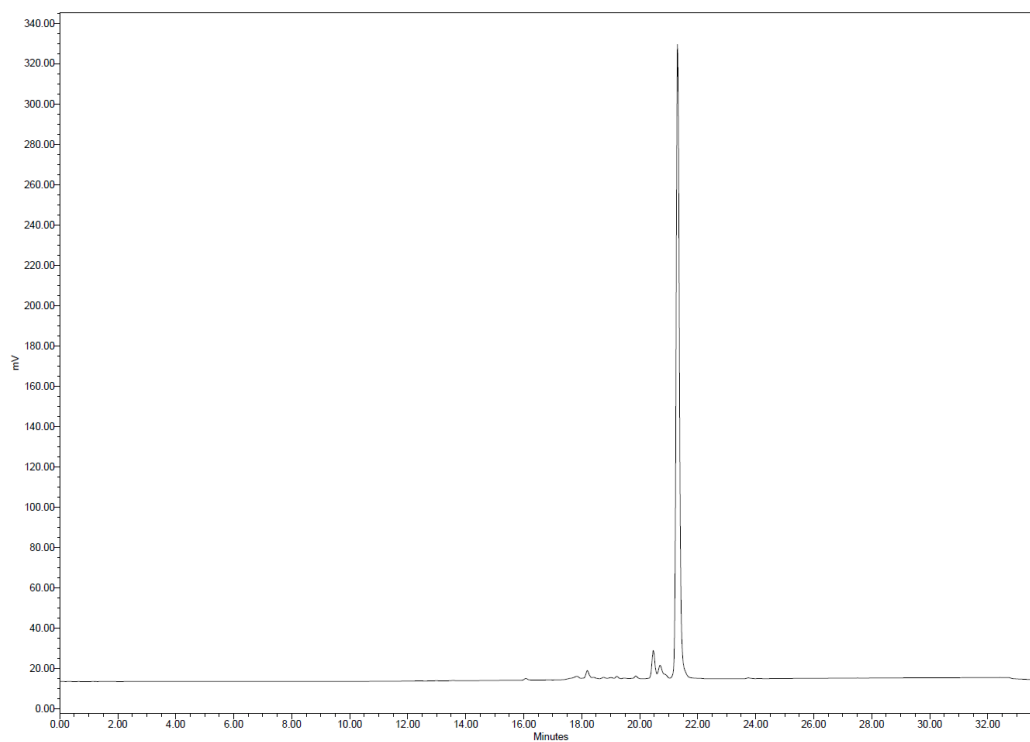
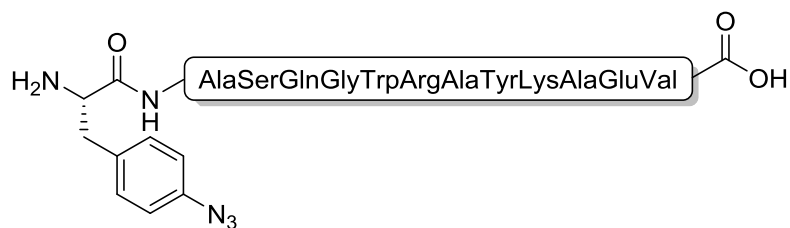


Figure 7.6: Fluorescence spectrum piperazine-linked NDB-tagged azido peptide **269**.

7.3.14.4 Azido peptide H₃-243



H₃-243

Azido peptide **H₃-243** was synthesised on a 2-ClTrt resin preloaded with Fmoc-valine (0.42 mmol/g, 100 – 200 mesh) in a 1.2 mmol scale on the Activotec Activo-P11 *Automated Peptide Synthesizer* and was isolated after HPLC purification in 23% yield as triple TFA salt (538.8 mg, 0.2818 mmol).

HRMS for C₇₁H₁₀₄N₂₂O₁₉²⁺ [M+2H]²⁺ calcd.: 784.3919, found: 784.3635.

HPLC-gradient (on the Shimadzu system) (A: water + 0.1% TFA; B: MeCN + 0.1% TFA): from 5% B to 100% B in 30 minutes. Retention time: 11.239 minutes.

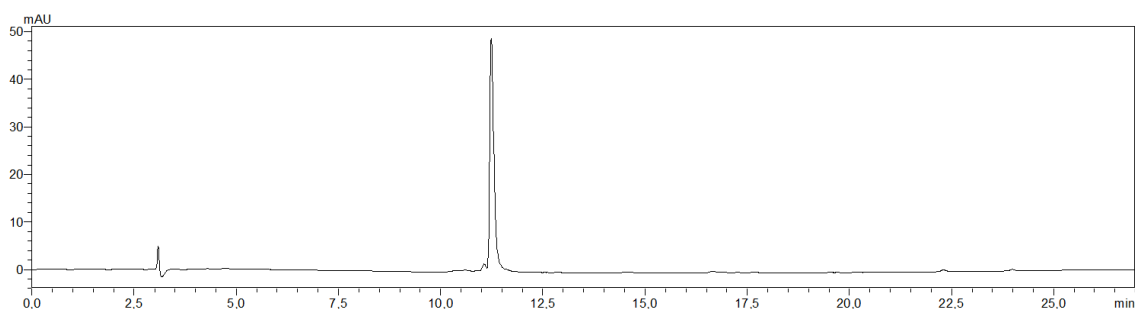


Figure 7.7: HPLC-UV (272 nm) trace of purified azido peptide **H₃-243**.

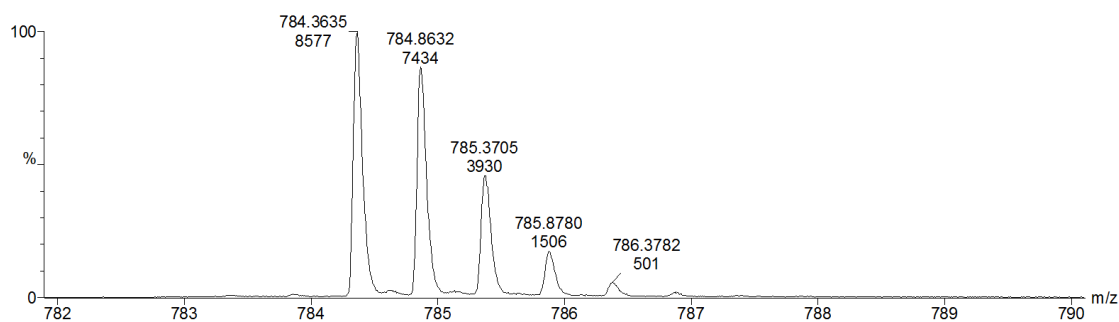
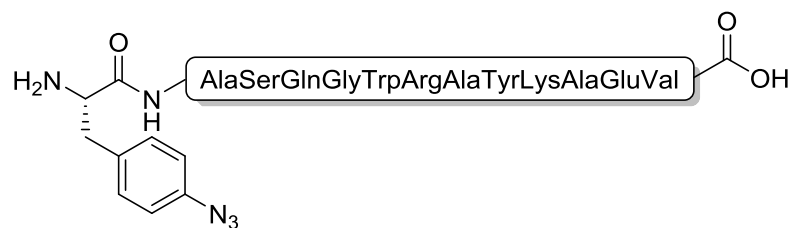


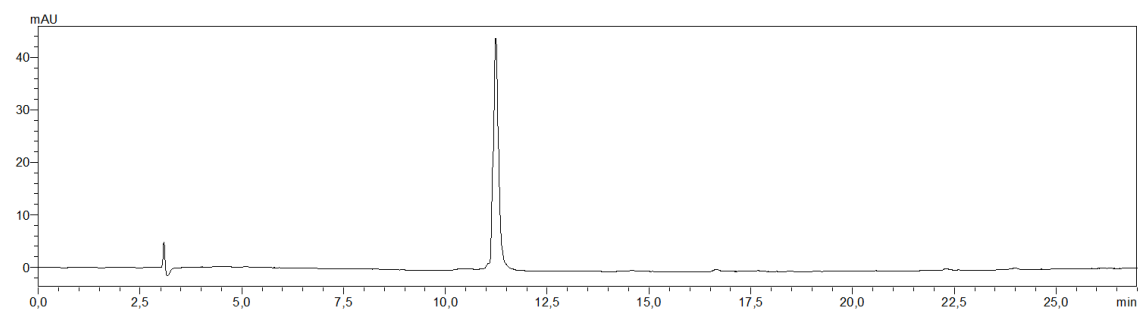
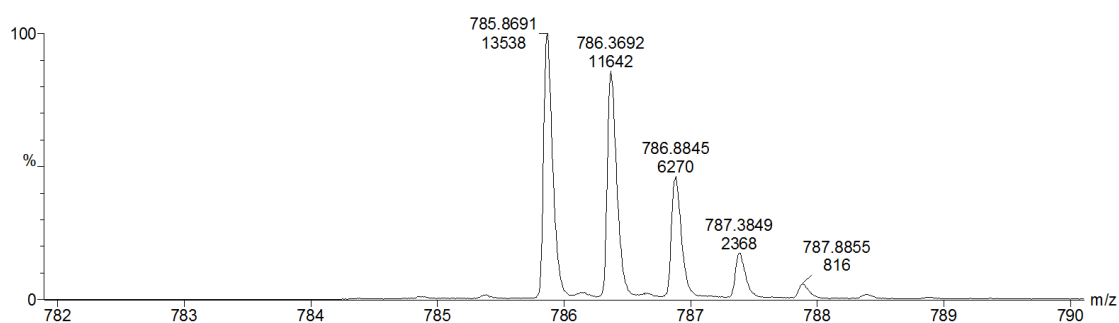
Figure 7.8: Mass spectrum of azido peptide **H₃-243** with correct isotopic pattern.

7.3.14.5 Azido peptide **D₃-243****D₃-243**

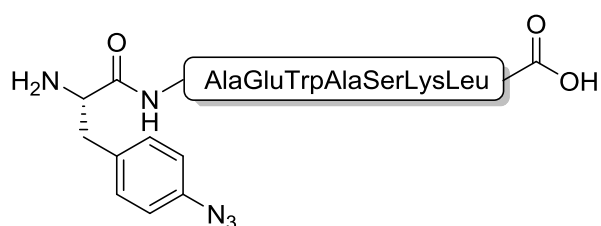
Azido peptide **D₃-243** was synthesised on a 2-ClTrt resin preloaded with Fmoc-valine (0.42 mmol/g, 100 – 200 mesh) in a 0.3 mmol scale on the Activotec Activo-P11 *Automated Peptide Synthesizer* and was isolated after HPLC purification in 27% yield as triple TFA salt (153.7 mg, 0.0804 mmol).

HRMS for $C_{71}H_{101}D_3N_{22}O_{19}^{2+}$ $[M+2H]^{2+}$ calcd.: 785.9013, found: 785.8691.

HPLC-gradient (on the Shimadzu system) (A: water + 0.1% TFA; B: MeCN + 0.1% TFA): from 5% B to 100% B in 30 minutes. Retention time: 11.237 minutes.

**Figure 7.9:** HPLC-UV (272 nm) trace of purified azido peptide **D₃-243**.**Figure 7.10:** Mass spectrum of azido peptide **D₃-243** with correct isotopic pattern.

7.3.14.6 Azido peptide H₆-271



H₆-271

Azido peptide **H₆-271** was synthesised on a Wang resin preloaded with Fmoc-leucine (0.58 mmol/g, 100 – 200 mesh) in a 0.1 mmol scale on the ABI 433A *Peptide Synthesizer* from Applied Biosystems and was isolated after HPLC purification in 15% yield as double TFA salt (18.1 mg, 0.0148 mmol).

HRMS for C₄₆H₆₆N₁₃O₁₂⁺ [M+H]⁺ calcd.: 992.4948, found: 992.4822.

HPLC-gradient (on the Shimadzu system) (A: water + 0.1% TFA; B: MeCN + 0.1% TFA): from 5% B to 100% B in 30 minutes. Retention time: 12.055 minutes.

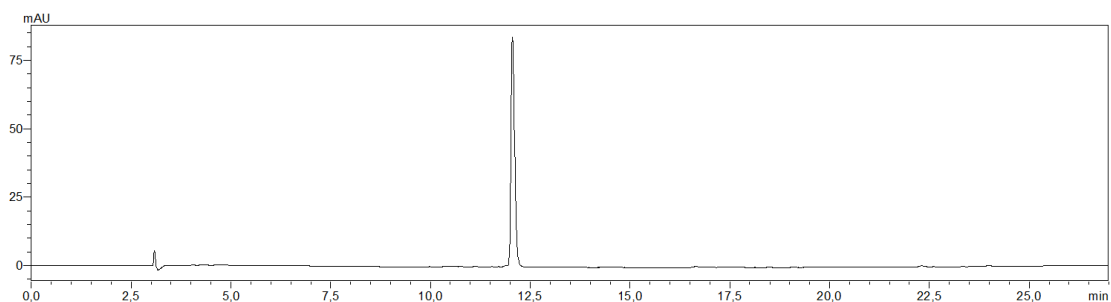


Figure 7.11: HPLC-UV (272 nm) trace of purified azido peptide **H₆-271**.

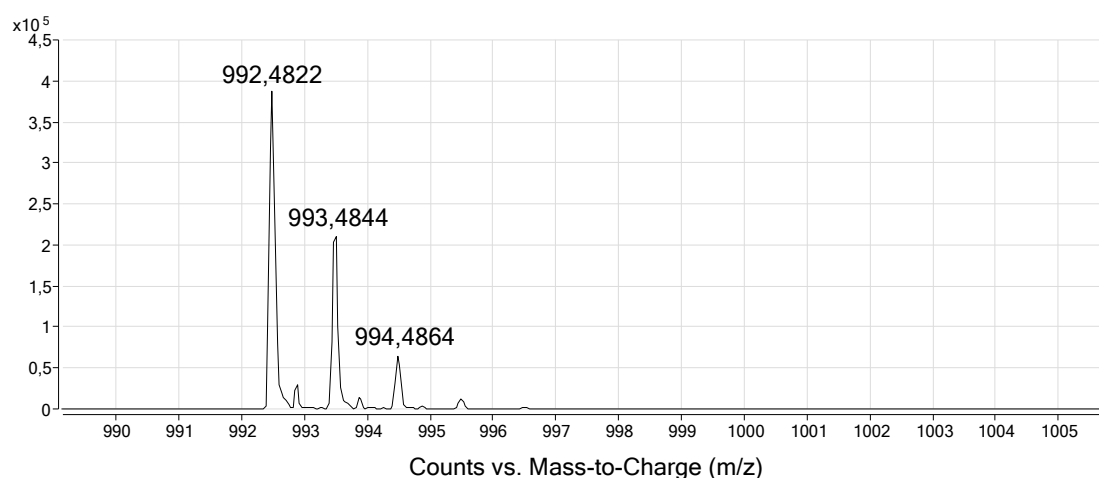
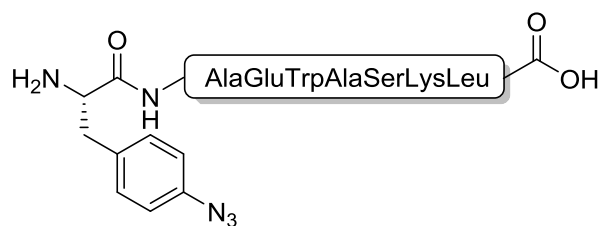


Figure 7.12: Mass spectrum of azido peptide **H₆-271** with correct isotopic pattern.

7.3.14.7 Azido peptide D₆-271



Azido peptide **D₆-271** was synthesised on a Wang resin preloaded with Fmoc-Leucine (0.45 mmol/g, 100 – 200 mesh) in a 0.1 mmol scale on the ABI 433A *Peptide Synthesizer* from Applied Biosystems and was isolated after HPLC purification in 19% yield as double TFA salt (23.7 mg, 0.0193 mmol).

HRMS for C₄₆H₆₀D₆N₁₃O₁₂⁺ [M+H]⁺ calcd.: 998.5325, found: 998.5182.

HPLC-gradient (on the Shimadzu system) (A: water + 0.1% TFA; B: MeCN + 0.1% TFA): from 5% B to 100% B in 30 minutes. Retention time: 11.992 minutes.

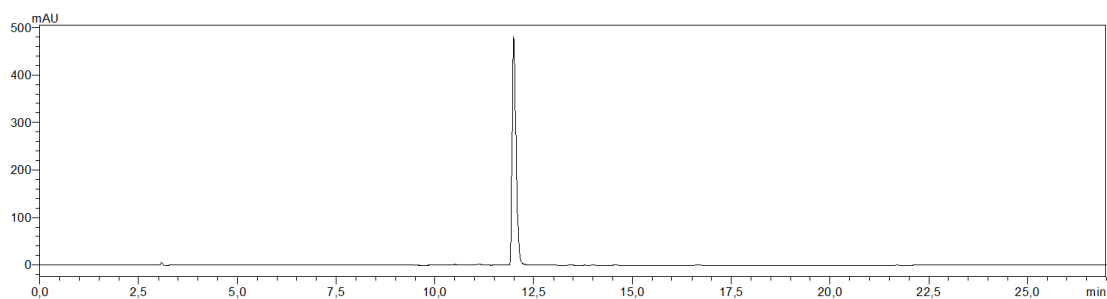


Figure 7.13: HPLC-UV (272 nm) trace of purified azido peptide **D₆-271**.

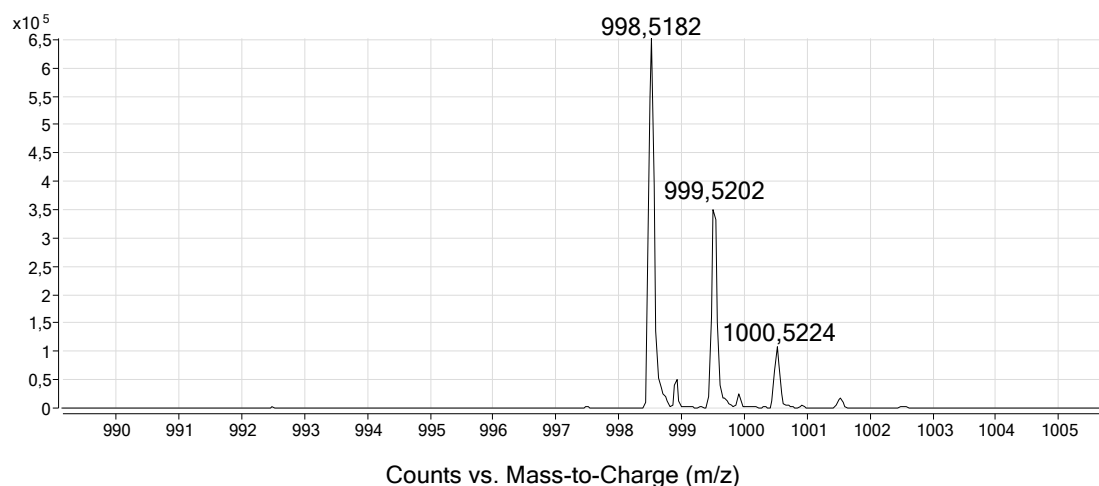
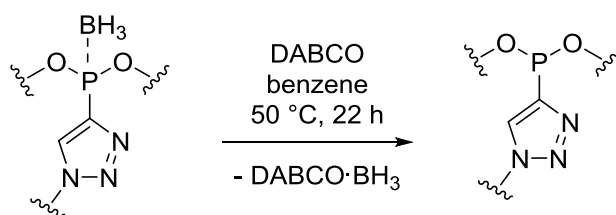


Figure 7.14: Mass spectrum of azido peptide **D₆-271** with correct isotopic pattern.

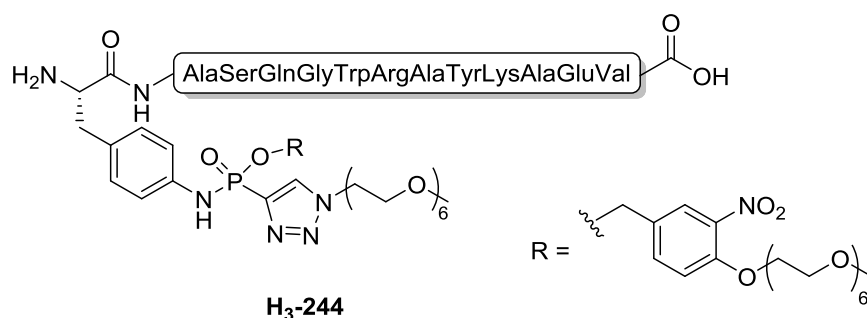
7.3.15 General protocol for the deprotection of borane-protected phosphonites



A solution of the borane-protected phosphonite (1 equiv.) and 1,4-diazabicyclo-[2.2.2]octane (3 equiv.) in dry benzene or toluene (0.5 M) was warmed to 50 °C and stirred for 20 hours. The reactions were monitored and quantified by ³¹P NMR (free phosphonites showed a characteristic peak at 141 (±2) ppm). In all cases, conversions to the unprotected phosphonites of 96% or above could be observed. Alternatively, the deprotection of borane-protected phosphonites was performed in toluene, which resulted in conversions of about 94% to free phosphonites.

7.3.16 General protocol for the synthesis of phosphoramidate peptides

The desired azido peptide (1 equiv.) and the unprotected phosphonite (1.3 equiv.) were stirred in acetonitrile for 20 hours before water was added. After additional 12 hours the crude product was purified by preparative HPLC (H₂O + 0.1% TFA, MeCN + 0.1% TFA).

7.3.16.1 Phosphoramidate peptide H₃-244

Phosphoramidate peptide **H₃-244** was synthesised from azido peptide **H₃-243** (triple TFA salt, 38,2 mg, 0.020 mmol) and bis(4-(2,5,8,11,14,17-hexaoxonadecan-19-yloxy)-3-nitrobenzyl) (1-(2,5,8,11,14,17-hexaoxonadecan-19-yl)-1H-1,2,3-triazol-4-yl)phosphonite **237** (0.026 mmol) and was obtained in 59% yield as double TFA salt (33.6 mg, 0.012 mmol) after HPLC purification.

HRMS for C₁₀₆H₁₆₅N₂₄O₃₆P²⁺ [M+2H]²⁺ calcd.: 1190.5772, found: 1190.4907.

HPLC-gradient (on the Shimadzu system) (A: water + 0.1% TFA; B: MeCN + 0.1% TFA): from 5% B to 100% B in 30 minutes. Retention time: 13.280 minutes.

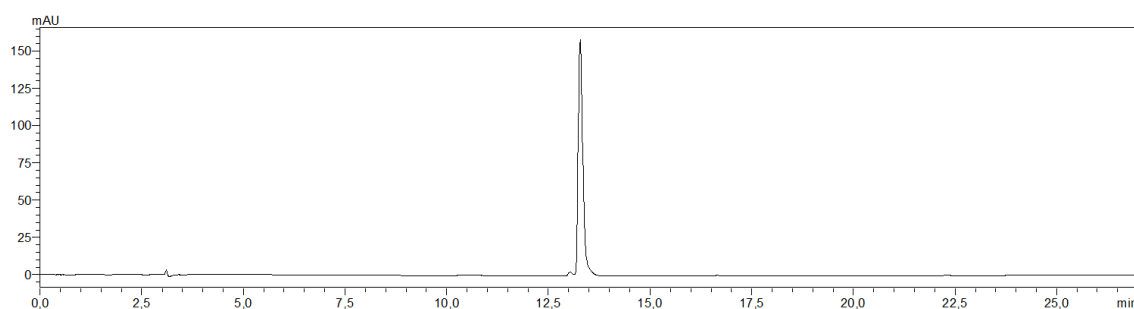


Figure 7.15: HPLC-UV (272 nm) trace of purified (H₃)-phosphoramidate peptide **H₃-244**.

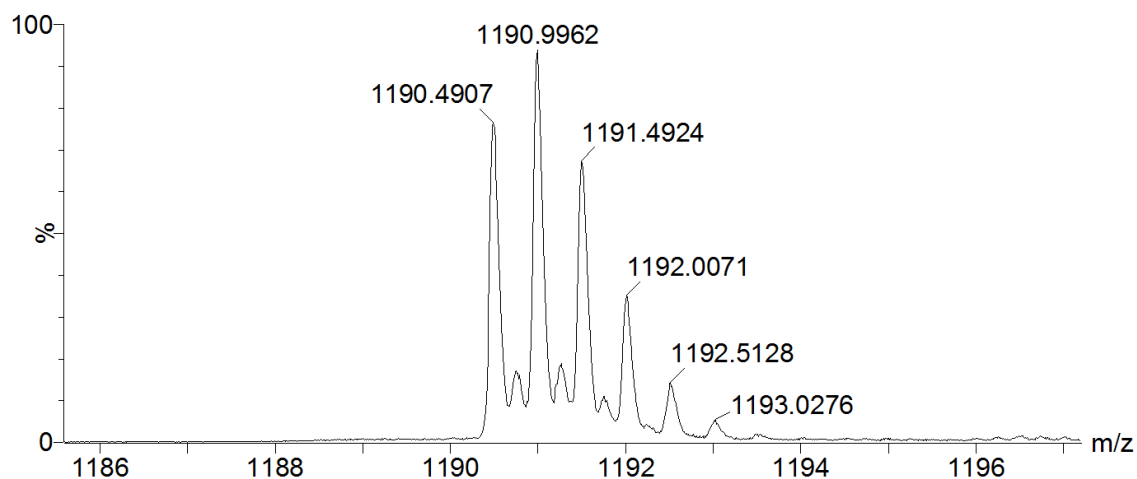
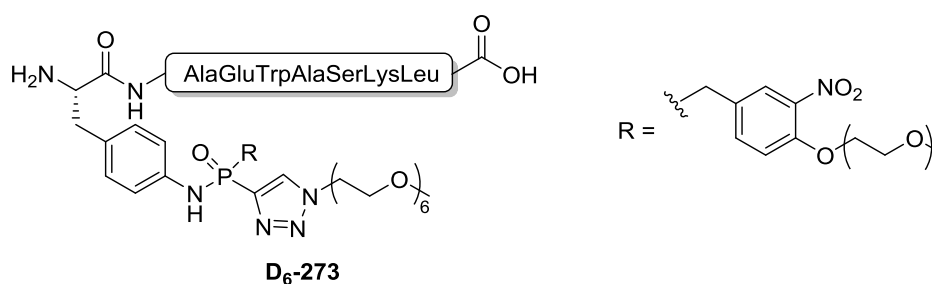


Figure 7.16: Mass spectrum of phosphoramidate peptide **H₃-244** with correct isotopic pattern.

7.3.16.2 Phosphoramidate peptide **D₆-273**



Phosphoramidate peptide **D₆-273** was synthesised from azido peptide **D₆-271** (double TFA salt, 8.0 mg, 0,0065 mmol) and bis(4-(2,5,8,11,14,17-hexaoxonadecan-19-yloxy)-3-nitrobenzyl) (1-(2,5,8,11,14,17-hexaoxonadecan-19-yl)-1H-1,2,3-triazol-4-yl)phosphonite **237** (0.0085 mmol) and was obtained in 55% yield as double TFA salt (7.4mg, 0,0036 mmol) after HPLC purification.

HRMS for $C_{81}H_{122}D_6N_{15}O_{29}P^{2+}$ $[M+2H]^{2+}$ calcd.: 905.9553, found: 905.9554.

HPLC-gradient (on the Shimadzu system) (A: water + 0.1% TFA; B: MeCN + 0.1% TFA): from 5% B to 100% B in 30 minutes. Retention time: 12.802 minutes.

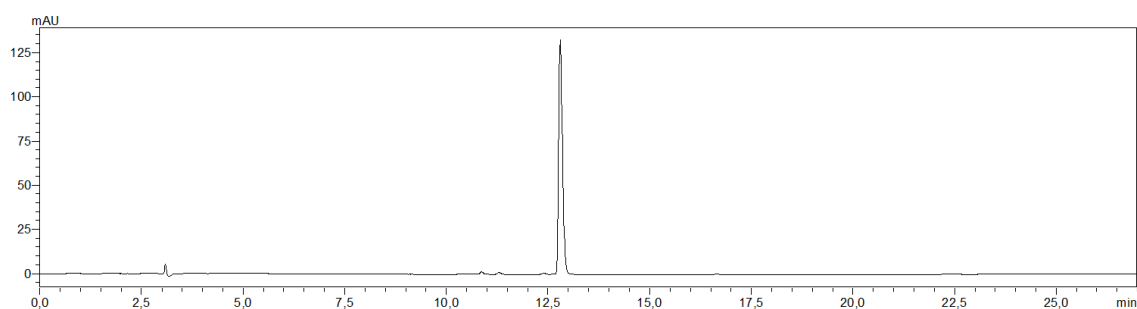


Figure 7.17: HPLC-UV (272 nm) trace of purified phosphoramidate peptide **D₆-273**.

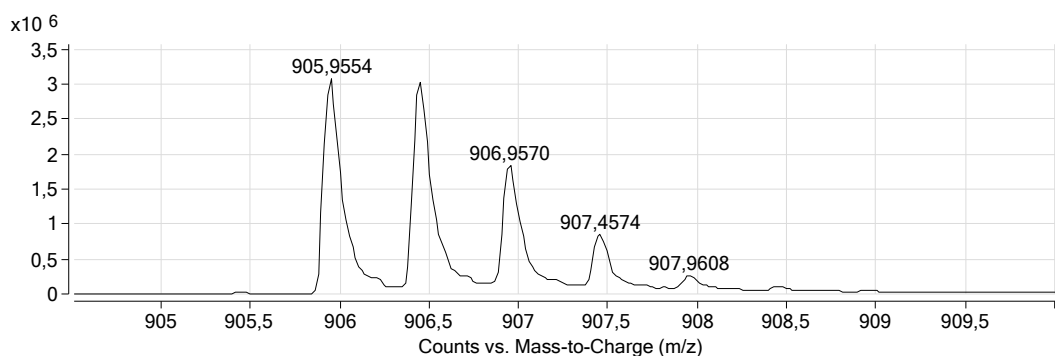
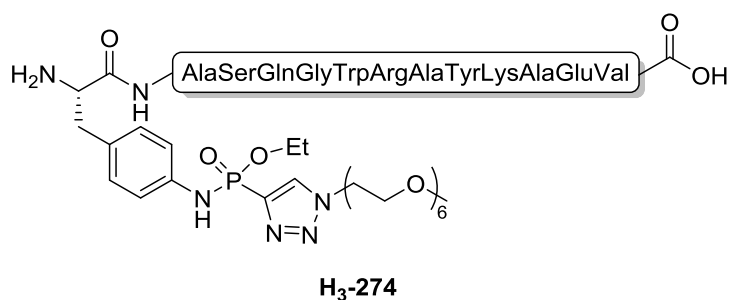


Figure 7.18: Mass spectrum of phosphoramidate peptide **D₆-273** with correct isotopic pattern.

7.3.16.3 Phosphoramidate peptide **H₃-274**



Phosphoramidate peptide **H₃-274** was synthesised from azido peptide **H₃-243** (triple TFA salt, 38,2 mg, 0,020 mmol) and diethyl 1-(2,5,8,11,14,17-hexaoxonadecan-19-yl)-1H-1,2,3-triazol-4-ylphosphonite **199** (0.026 mmol) and was obtained in 47% yield as double TFA salt (21.7 mg, 0093 mmol) after HPLC purification.

HRMS for $C_{88}H_{138}N_{23}O_{27}P^{2+}$ $[M+2H]^{2+}$ calcd.: 989.9930, found: 989.9110.

HPLC-gradient (on the Shimadzu system) (A: water + 0.1% TFA; B: MeCN + 0.1% TFA): from 5% B to 100% B in 30 minutes. Retention time: 11.413 minutes.

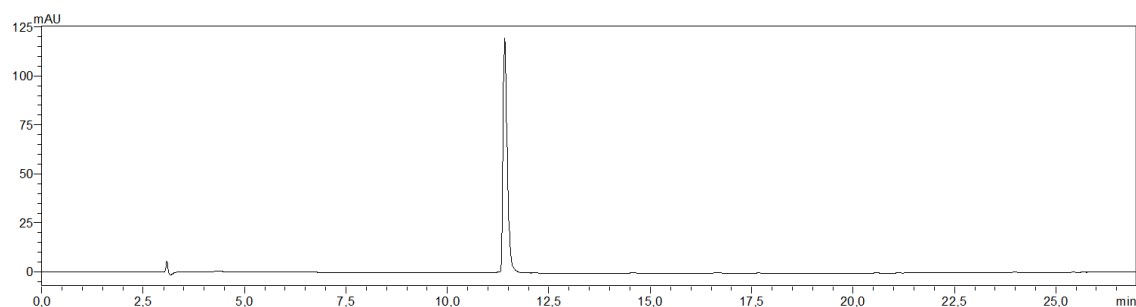


Figure 7.19: HPLC-UV (272 nm) trace of purified phosphoramidate peptide **H₃-274**.

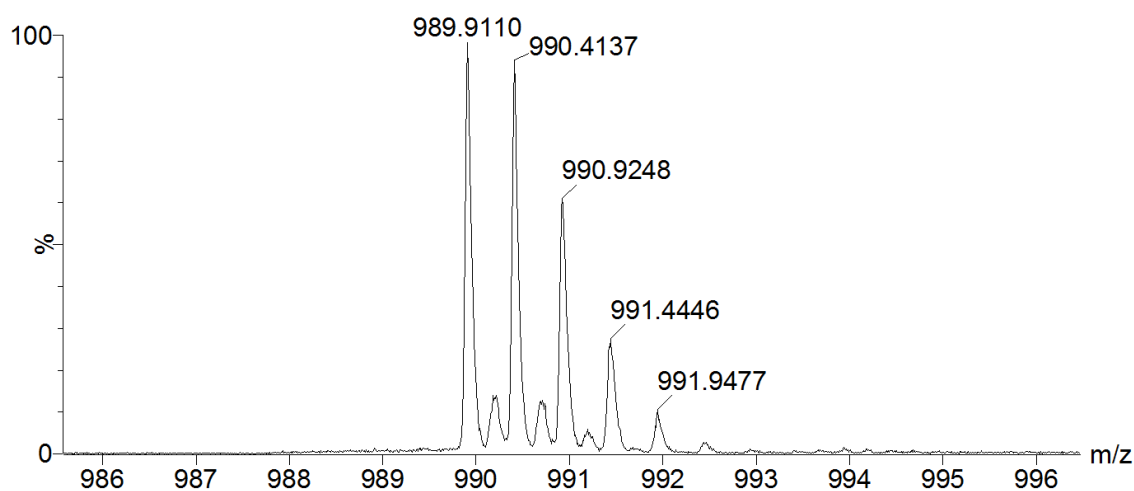
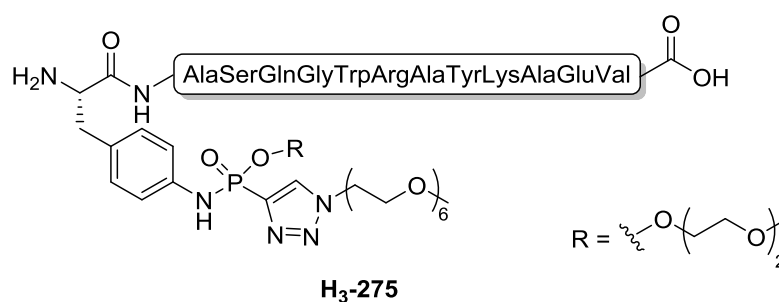


Figure 7.20: Mass spectrum of phosphoramidate peptide **H₃-274** with correct isotopic pattern.

7.3.16.4 Phosphoramidate peptide **H₃-275**



Phosphoramidate peptide **H₃-275** was synthesised from azido peptide **H₃-243** (triple TFA salt, 38,2 mg, 0.0200 mmol) and diethyl 1-(2,5,8,11,14,17-hexaoxonadecan-19-yl)-1H-1,2,3-triazol-4-ylphosphonite **236** (0,0260 mmol) and was obtained in 53% yield as double TFA salt (25.2 mg, 0.105) after HPLC purification.

HRMS for $C_{91}H_{144}N_{23}O_{29}P^{2+}$ $[M+2H]^{2+}$ calcd.: 1027.0113, found: 1026.9242.

HPLC-gradient (on the Shimadzu system) (A: water + 0.1% TFA; B: MeCN + 0.1% TFA): from 5% B to 100% B in 30 minutes. Retention time: 11.512 minutes.

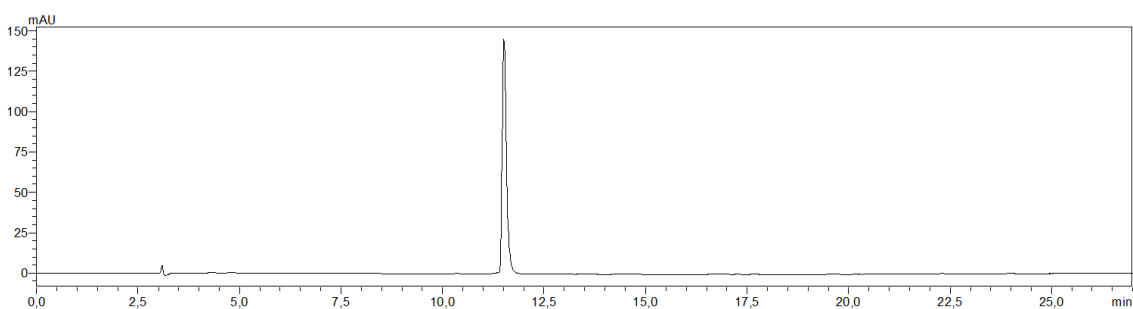


Figure 7.21: HPLC-UV (272 nm) trace of purified phosphoramidate peptide **H₃-275**.

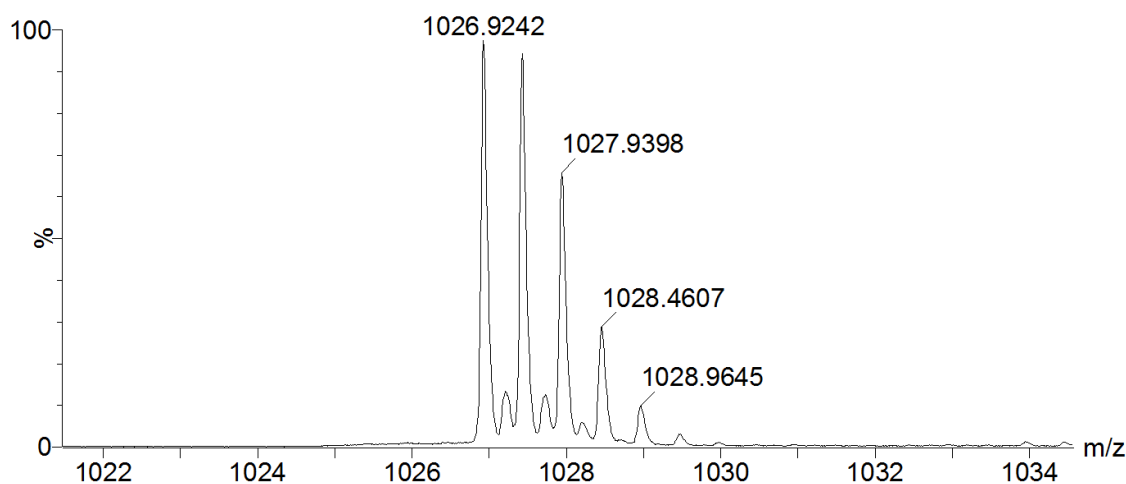


Figure 7.22: Mass spectrum of phosphoramidate peptide **H₃-275** with correct isotopic pattern.

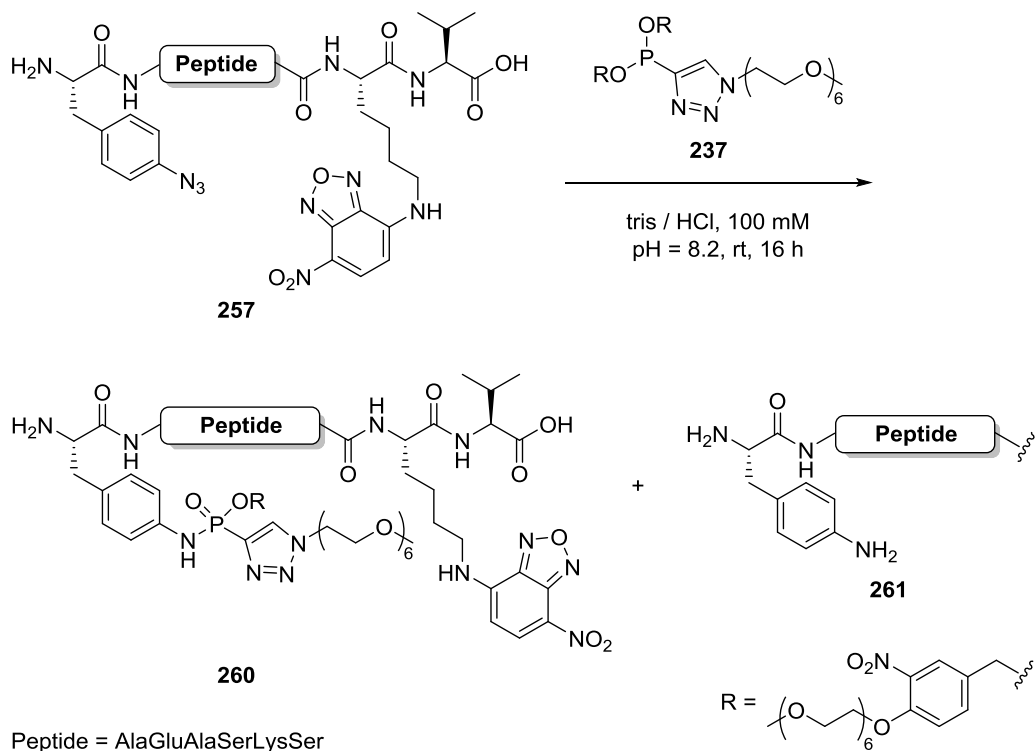
7.3.17 General protocol for Staudinger-phosphonite reaction in aqueous systems

A known amount of phosphonite-borane is deprotected with DABCO® in benzene (see chapter 7.3.15 for a detailed protocol). After removal of the solvent a certain amount of dimethyl sulfoxide is added resulting in a phosphonite solution with defined concentration (mostly 250 mM).

A stock solution of the azido peptide (mostly 1 mM) in water or the desired buffer system is prepared. The azido peptide solution is diluted with additional water or buffer and if required same dimethyl sulfoxide and vortexed for 1 minute before the phosphonite solution is added. The amount of peptide and phosphonite solution added must be calculated in a way that the desired concentrations and amount of dimethyl sulfoxide is reached after everything is combined. The reaction is put to a shaker until complete hydrolysis of the phosphonite.

7.3.18 Fluorescence and mass spectra for conversion studies of azido peptides with phosphonites

7.3.18.1 Fluorescence spectra for Table 3.1



Scheme 7.1: Staudinger reaction of NDB-tagged azido peptide **257** with phosphonite **237**

(Chapter 3.4.3.1, Table 3.1)

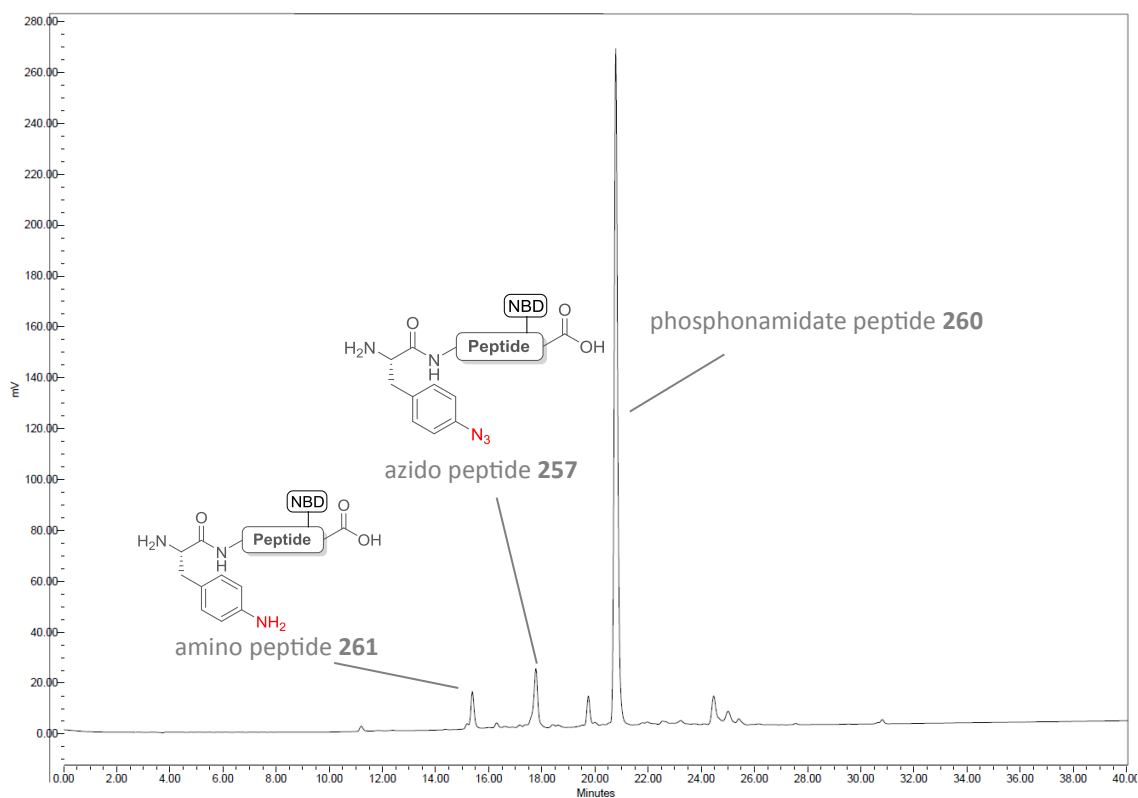


Figure 7.23: Staudinger-phosponite reaction with NBD-tagged peptide **256** (50 μM) and phosphonite **237** (250 equiv.). (Ex [nm]: 470, Em [nm]: 550)

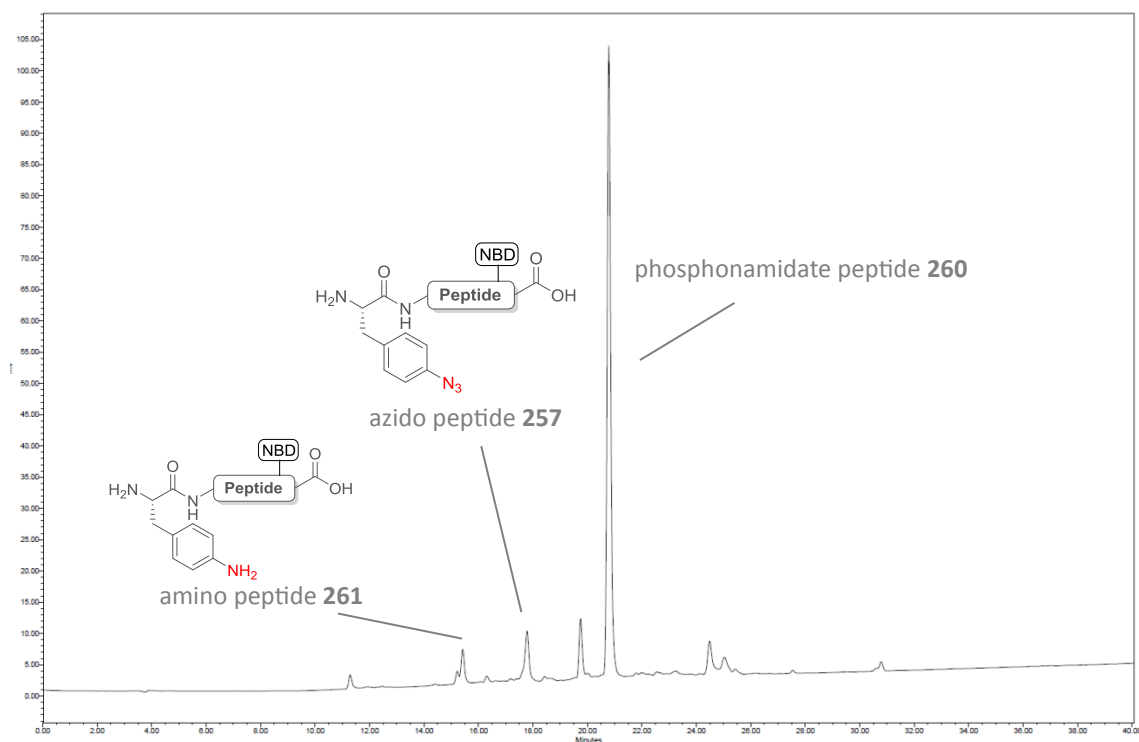


Figure 7.24: Staudinger-phosponite reaction with NBD-tagged peptide **256** (25 μM) and phosphonite **237** (500 equiv.). (Ex [nm]: 470, Em [nm]: 550)

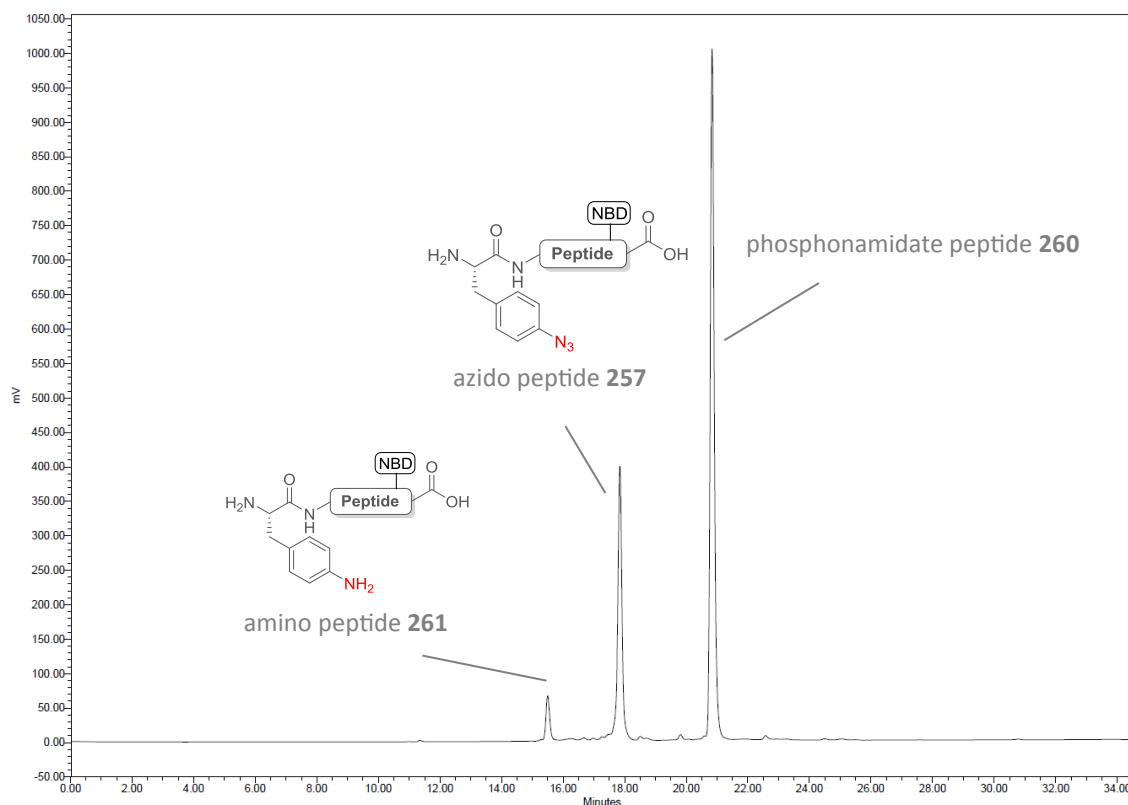
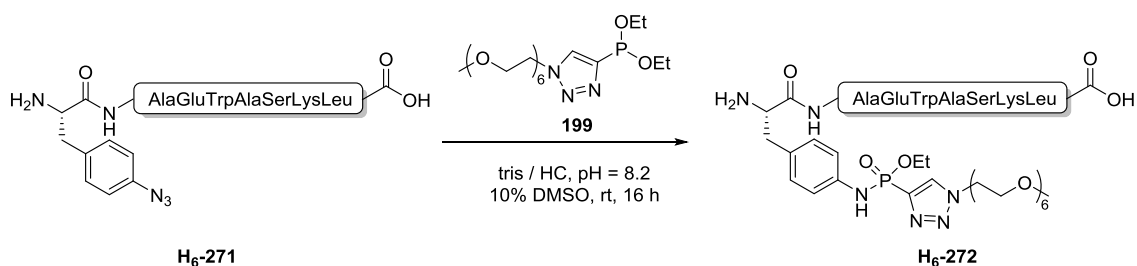


Figure 7.25: Staudinger-phosphonite reaction with NBD-tagged peptide **256** (25 μ M) and phosphonite **237** (250 equiv.). (Ex [nm]: 470, Em [nm]: 550)

7.3.18.2 Mass spectra for Table 3.2



Scheme 7.2: Staudinger reaction of azido peptide **H₆-271** with phosphonite **199**
(Chapter 3.4.3.2, Table 3.2)

H₆-271: HRMS for C₄₆H₆₆N₁₃O₁₂⁺ [M+H]⁺ calcd.: 992.4948, found: 992.4822.

D₆-271: HRMS for C₄₆H₆₀D₆N₁₃O₁₂⁺ [M+H]⁺ calcd.: 998.5325, found: 998.5182.

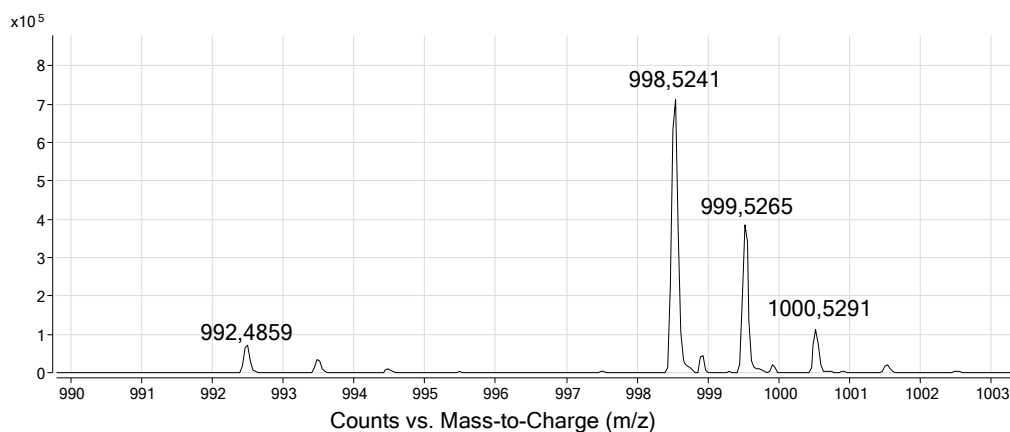


Figure 7.26: Conversion of azido peptide H₆-271 (100 μM) with phosphonite 199 (500 equiv.) in 1M tris / HCl buffer.

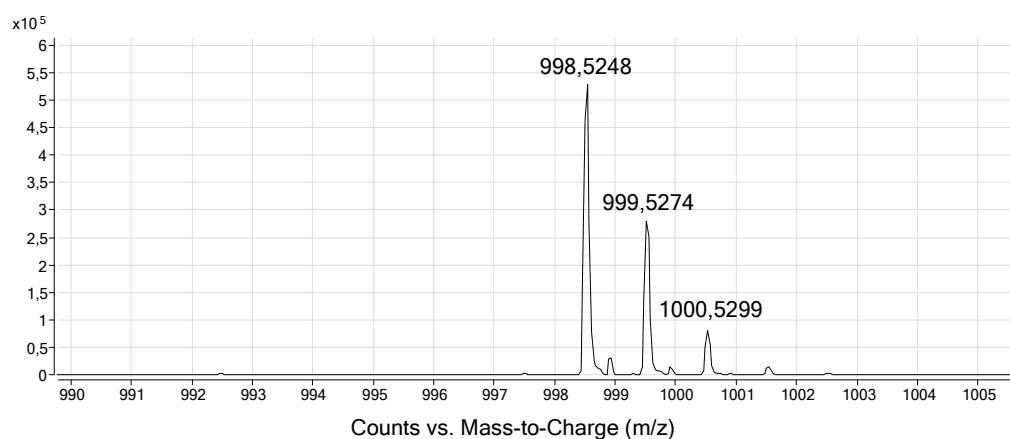


Figure 7.27: Conversion of azido peptide H₆-271 (100 μM) with phosphonite 199 (500 equiv.) in 0.1M tris / HCl buffer.

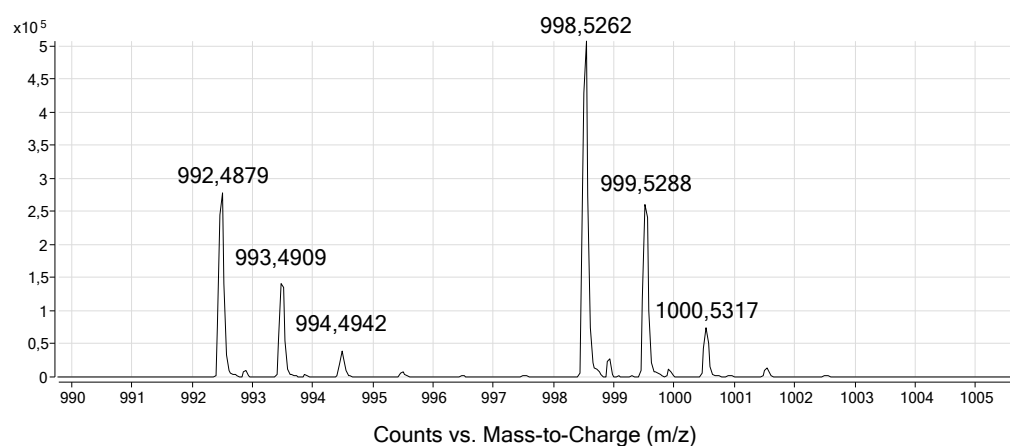


Figure 7.28: Conversion of azido peptide H₆-271 (100 μM) with phosphonite 199 (250 equiv.) in 1M tris / HCl buffer.

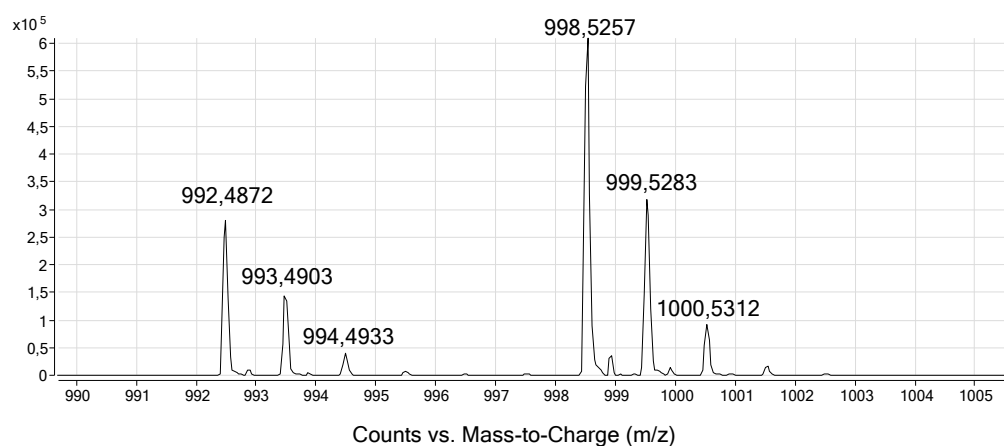


Figure 7.29: Conversion of azido peptide H_6-271 (100 μM) with phosphonite **199** (250 equiv.) in 0.1M tris / HCl buffer.

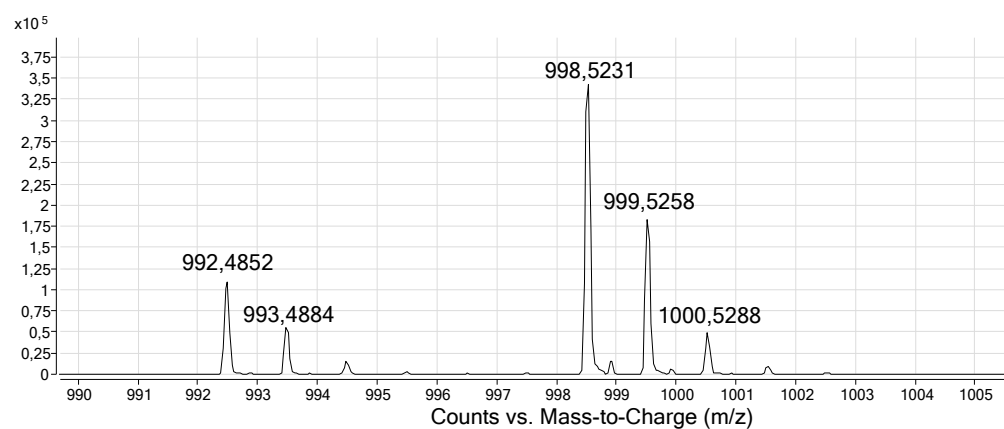


Figure 7.30: Conversion of azido peptide H_6-271 (50 μM) with phosphonite **199** (500 equiv.) in 1M tris / HCl buffer.

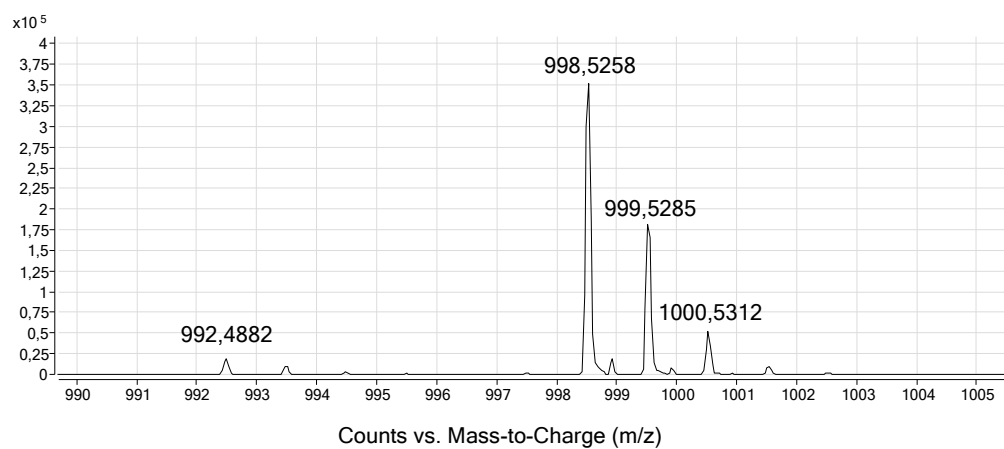


Figure 7.31: Conversion of azido peptide H_6-271 (50 μM) with phosphonite **199** (500 equiv.) in 0.1M tris / HCl buffer.

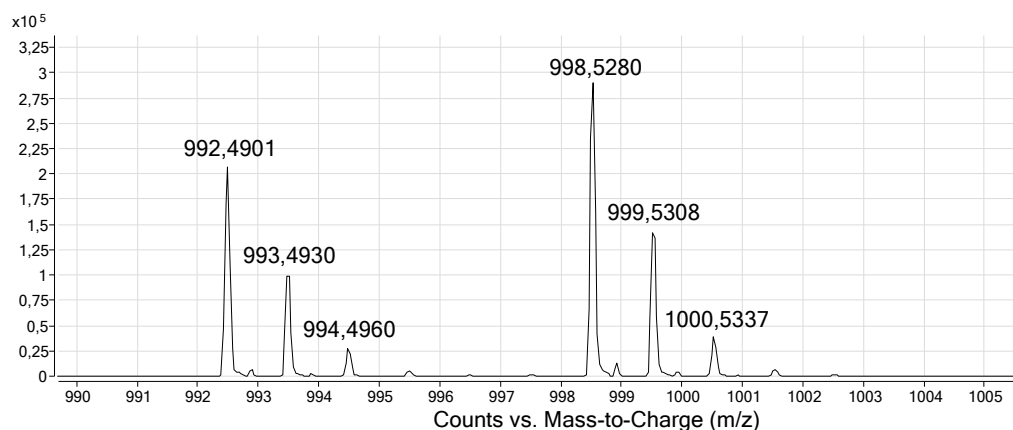


Figure 7.32: Conversion of azido peptide **H₆-271** (50 μ M) with phosphonite **199** (250 equiv.) in 1M tris / HCl buffer.

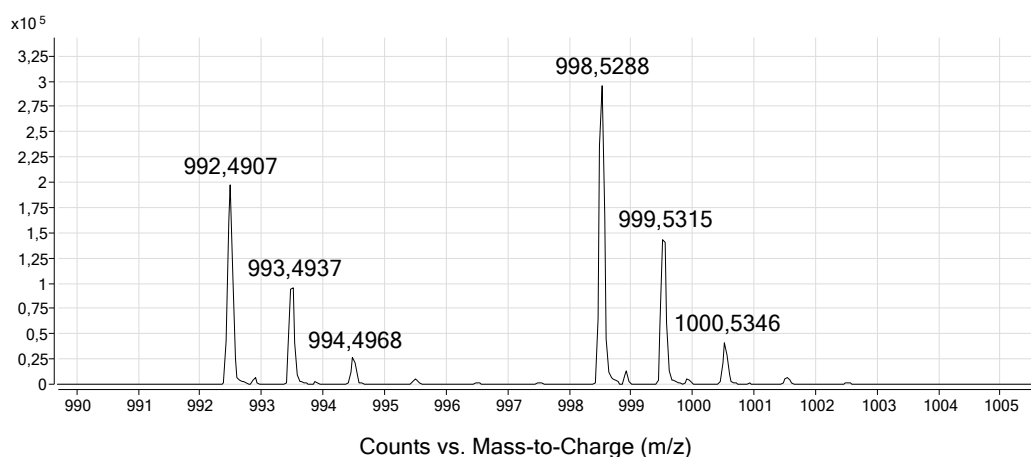
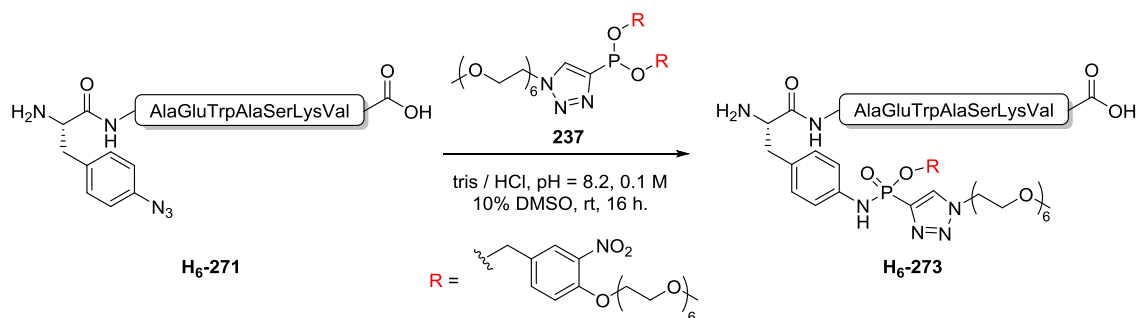


Figure 7.33: Conversion of azido peptide **H₆-271** (50 μ M) with phosphonite **199** (250 equiv.) in 0.1M tris / HCl buffer.

7.3.18.3 Mass spectra for Table 3.3



Scheme 7.3: Staudinger reaction of azido peptide **D₃-243** with phosphonite **237** to phosphoramidate peptide **H₆-273** (Chapter 3.4.3.2, Table 3.4)

H₆-271: HRMS for C₄₆H₆₆N₁₃O₁₂⁺ [M+H]⁺ calcd.: 992.4948, found: 992.4822.

D₆-271: HRMS for C₄₆H₆₀D₆N₁₃O₁₂⁺ [M+H]⁺ calcd.: 998.5325, found: 998.5182.

H₆-273: HRMS for C₈₁H₁₂₈N₁₅O₂₉P²⁺ [M+2H]²⁺ calcd.: 902.9365, found: 905.9600.

D₆-273: HRMS for C₈₁H₁₂₂D₆N₁₅O₂₉P²⁺ [M+2H]²⁺ calcd.: 905.9553, found: 905.9554.

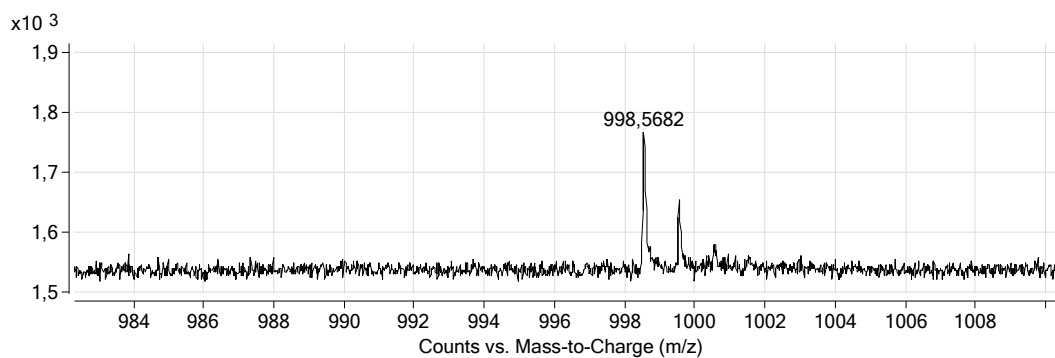


Figure 7.34: Conversion of azido peptide **H₆-271** (50 μM) with phosphonite **237** (500 equiv.) (10% DMSO).

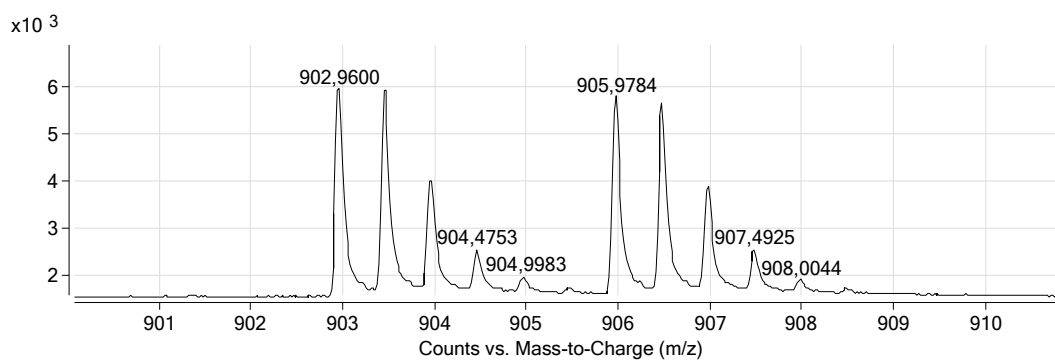


Figure 7.35: Formation of phosphonamidate **H₆-273** in the Staudinger reaction of azido peptide **H₆-271** (50 μM) with phosphonite **237** (500 equiv.) (10% DMSO).

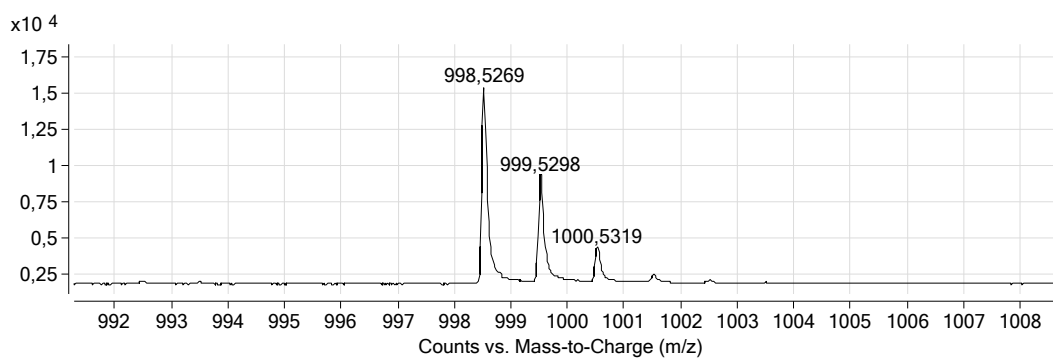


Figure 7.36: Conversion of azido peptide **H₆-271** (50 μ M) with phosphonite **237** (250 equiv.) (10% DMSO).

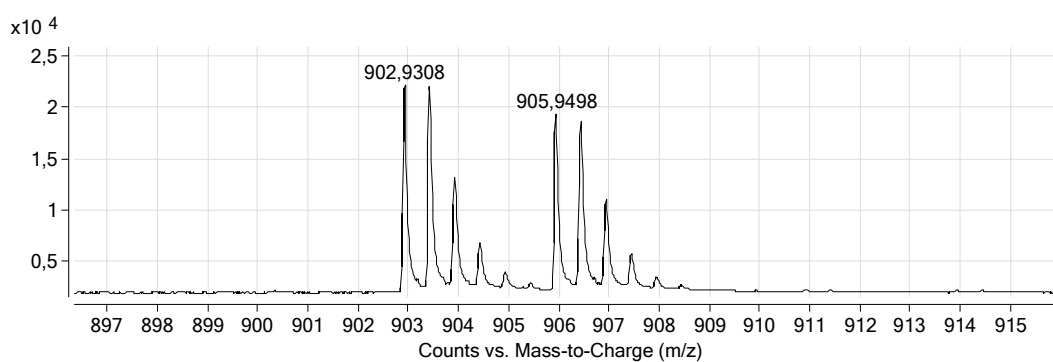


Figure 7.37: Formation of phosphoramidate **H₆-273** in the Staudinger reaction of azido peptide **H₆-271** (50 μ M) with phosphonite **237** (250 equiv.) (10% DMSO).

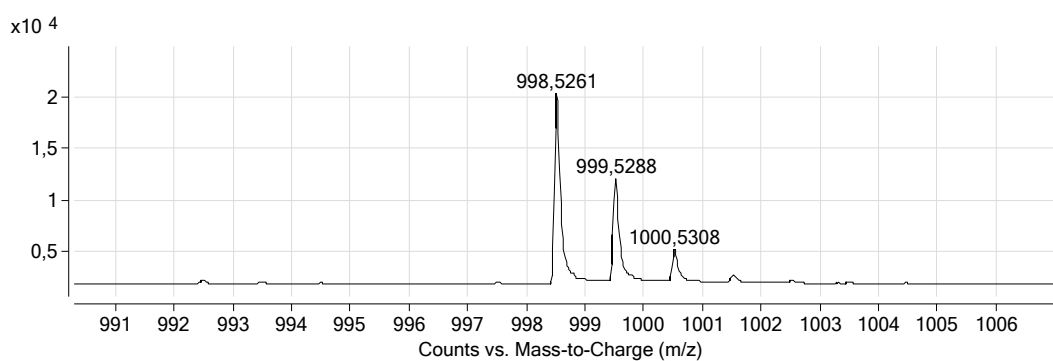


Figure 7.38: Conversion of azido peptide **H₆-271** (50 μ M) with phosphonite **237** (250 equiv.) (5% DMSO).

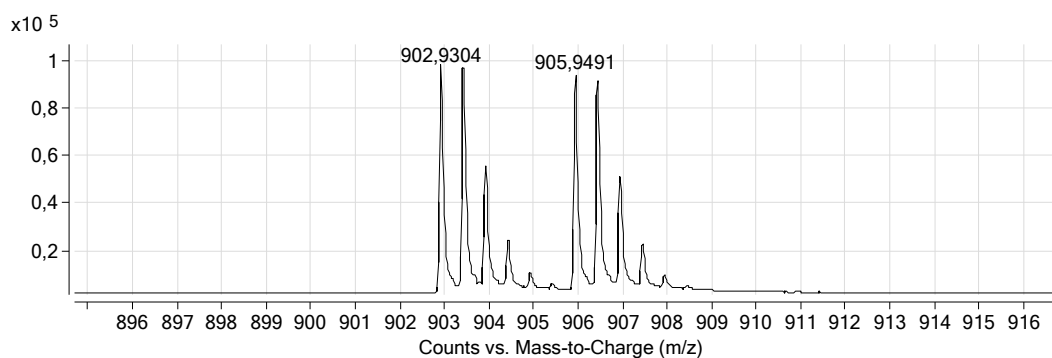


Figure 7.39: Formation of phosphoramidate **H₆-273** in the Staudinger reaction of azido peptide **H₆-271** (50 μ M) with phosphonite **237** (250 equiv.) (5% DMSO).

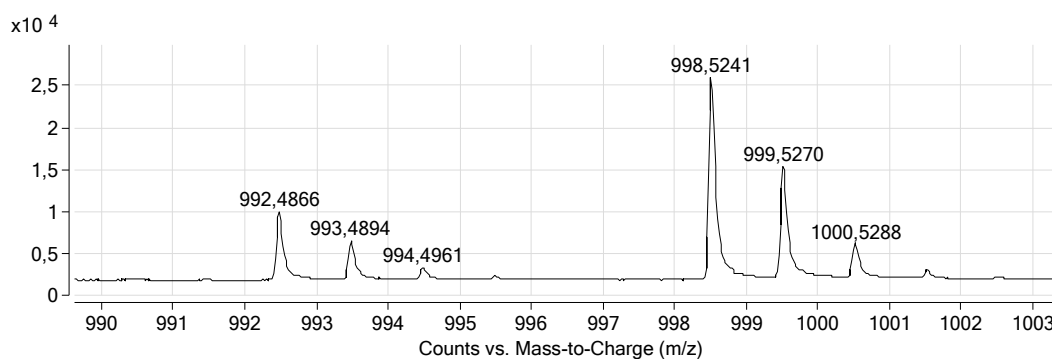


Figure 7.40: Conversion of azido peptide **H₆-271** (50 μ M) with phosphonite **237** (100 equiv.) (10% DMSO).

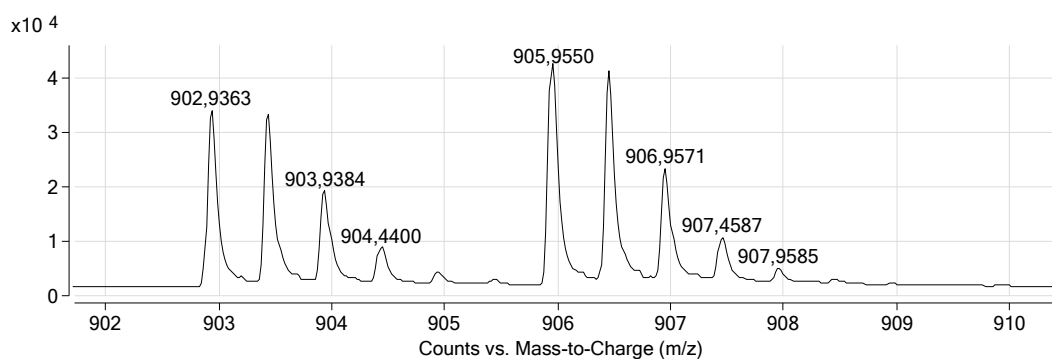


Figure 7.41: Formation of phosphoramidate **H₆-273** in the Staudinger reaction of azido peptide **H₆-271** (50 μ M) with phosphonite **237** (100 equiv.) (10% DMSO).

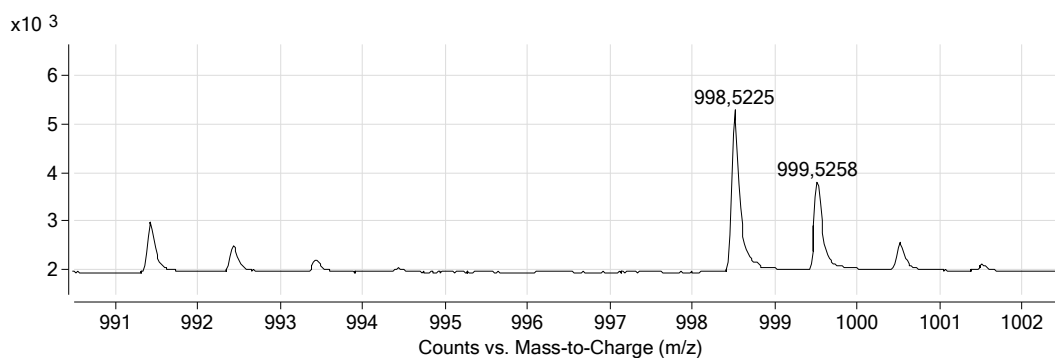


Figure 7.42: Conversion of azido peptide **H₆-271** (25 μM) with phosphonite **237** (500 equiv.) (5% DMSO).

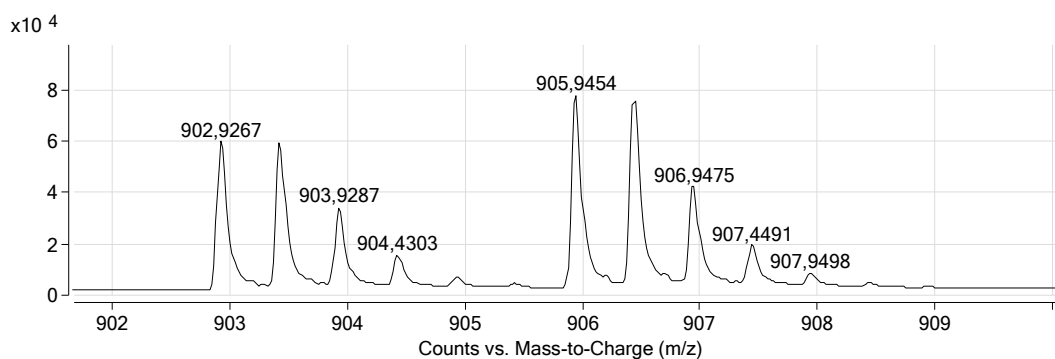


Figure 7.43: Formation of phosphonamidate **H₆-273** in the Staudinger reaction of azido peptide **H₆-271** (25 μM) with phosphonite **237** (500 equiv.) (5% DMSO).

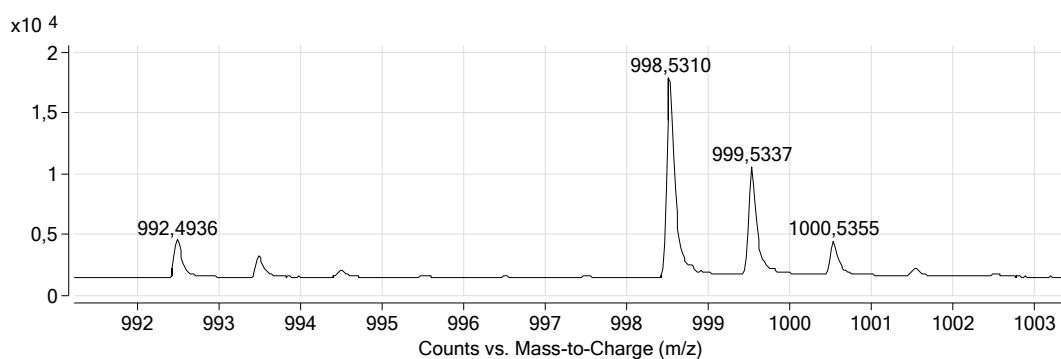


Figure 7.44: Conversion of azido peptide **H₆-271** (25 μM) with phosphonite **237** (250 equiv.) (10% DMSO).

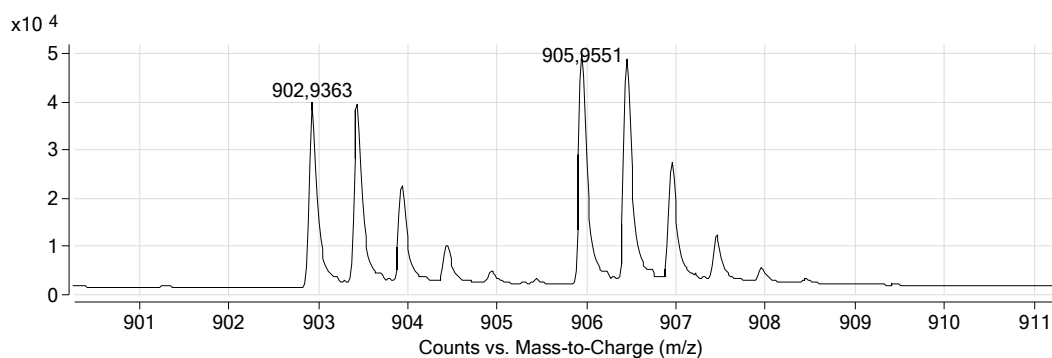


Figure 7.45: Formation of phosphoramidate **H₆-273** in the Staudinger reaction of azido peptide **H₆-271** (25 μ M) with phosphonite **237** (250 equiv.) (10% DMSO).

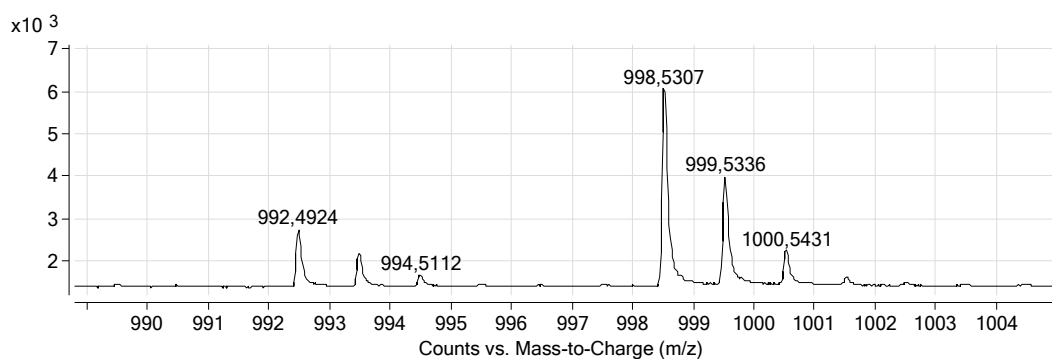


Figure 7.46: Conversion of azido peptide **H₆-271** (25 μ M) with phosphonite **237** (250 equiv.) (5% DMSO).

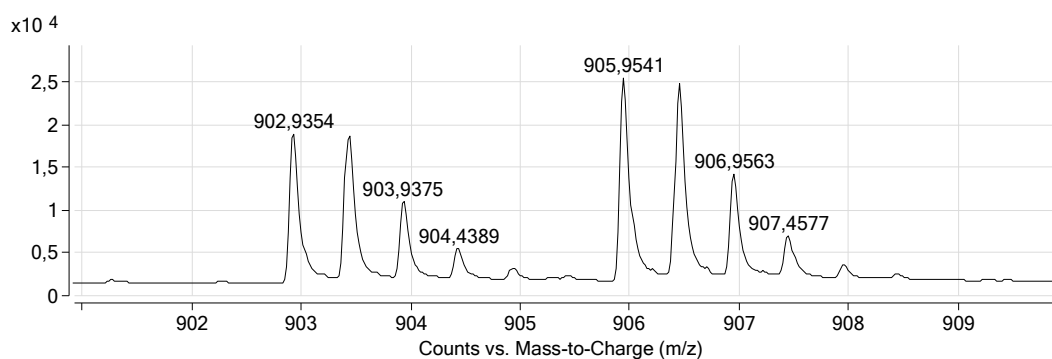


Figure 7.47: Formation of phosphoramidate **H₆-273** in the Staudinger reaction of azido peptide **H₆-271** (25 μ M) with phosphonite **237** (250 equiv.) (5% DMSO).

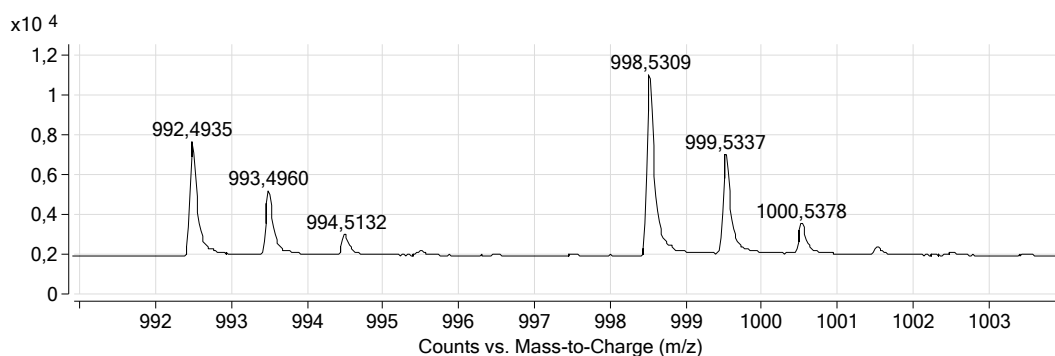


Figure 7.48: Conversion of azido peptide **H₆-271** (25 μ M) with phosphonite **237** (100 equiv.) (5% DMSO).

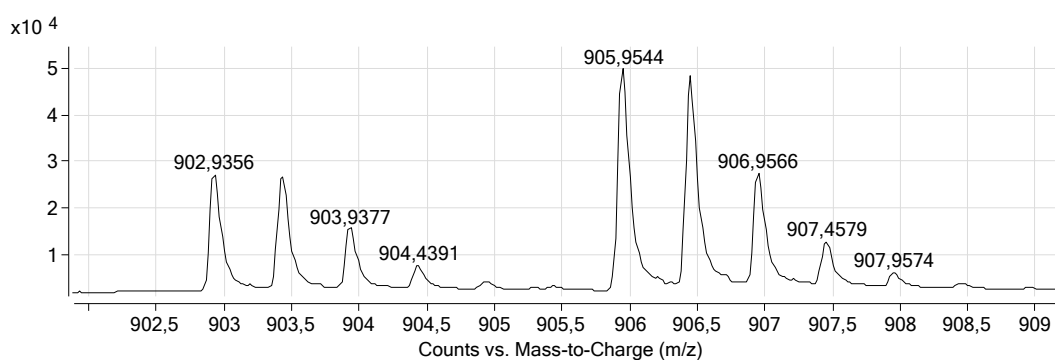
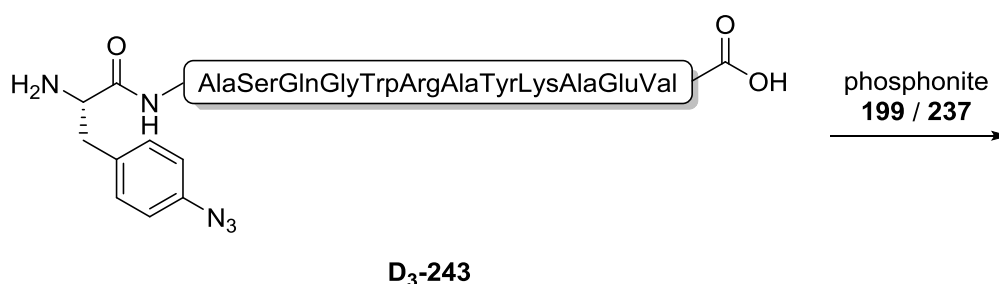


Figure 7.49: Formation of phosphonamidate **H₆-273** in the Staudinger reaction of azido peptide **H₆-271** (25 μ M) with phosphonite **237** (100 equiv.) (5% DMSO).

7.3.18.4 Mass spectra for Table 3.4



Scheme 7.4: Staudinger reaction of azido peptide **D₃-243** with phosphonite **199** and **237** (Chapter 3.4.3.2, Table 3.4)

H₃-243: HRMS for C₇₁H₁₀₄N₂₂O₁₉²⁺ [M+2H]²⁺ calcd.: 784.3919, found: 784.3635.

D₃-243: HRMS for C₇₁H₁₀₁D₃N₂₂O₁₉²⁺ [M+2H]²⁺ calcd.: 785.9013, found: 785.8691.

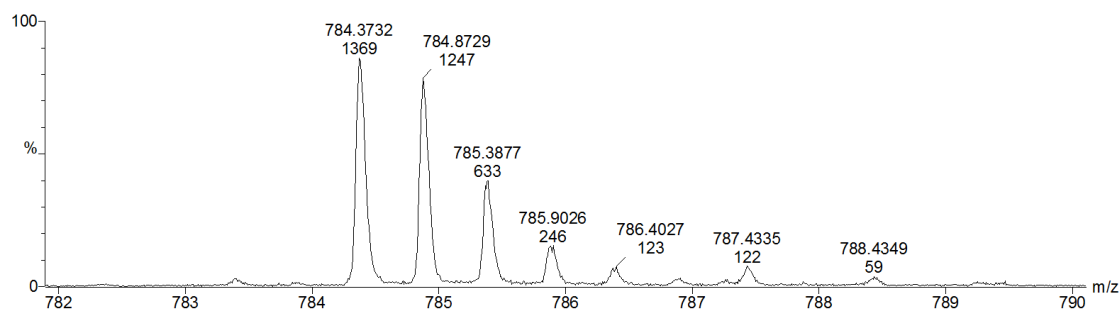


Figure 7.50: Conversion of azido peptide **D₃-243** (100 μM) with phosphonite **199** (250 equiv.).

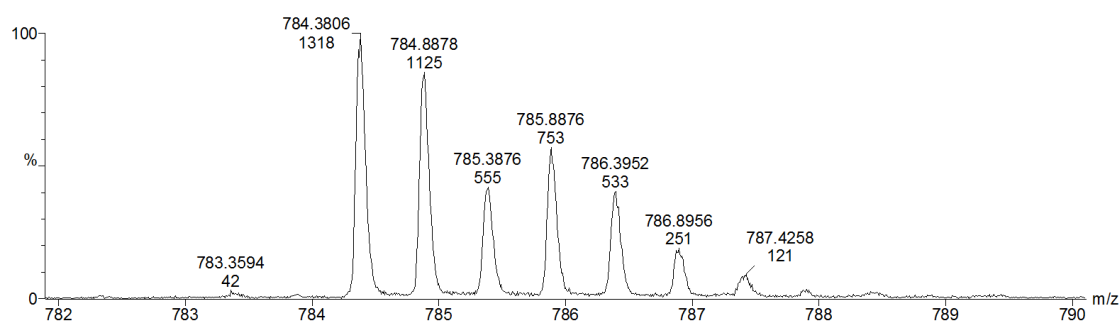


Figure 7.51: Conversion of azido peptide **D₃-243** (100 μM) with phosphonite **199** (100 equiv.).

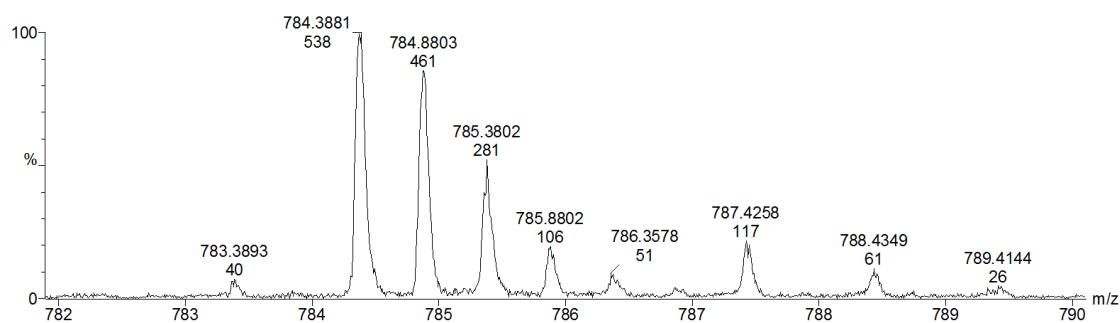


Figure 7.52: Conversion of azido peptide **D₃-243** (50 μM) with phosphonite **199** (500 equiv.).

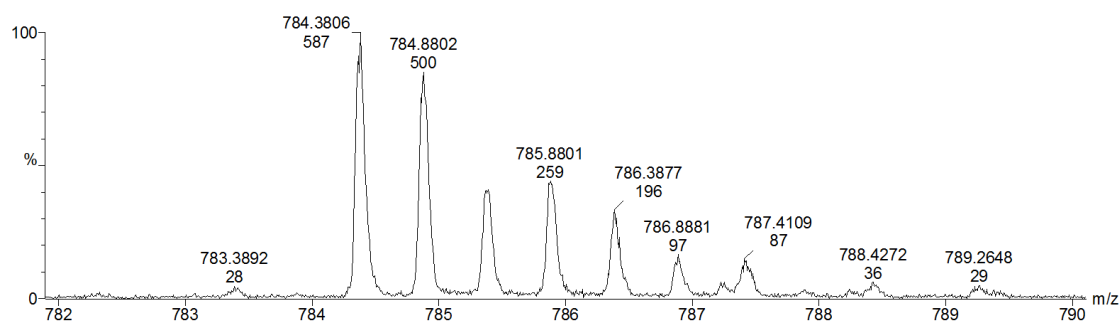


Figure 7.53: Conversion of azido peptide **D₃-243** (50 μM) with phosphonite **199** (250 equiv.).

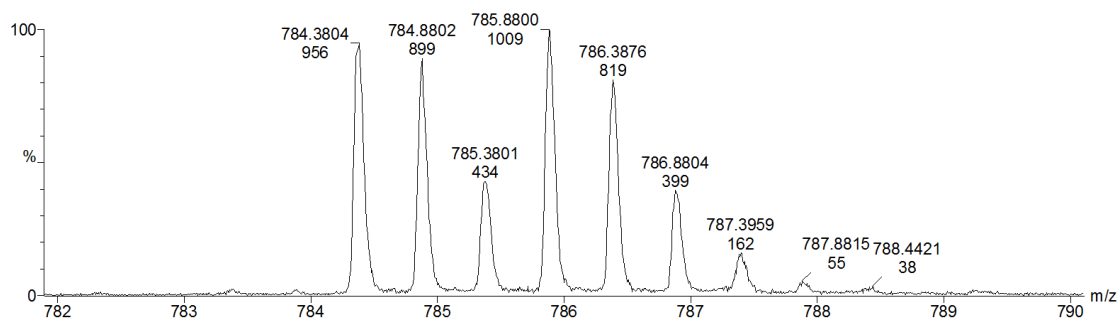


Figure 7.54: Conversion of azido peptide **D₃-243** (50 μM) with phosphonite **199** (100 equiv.).

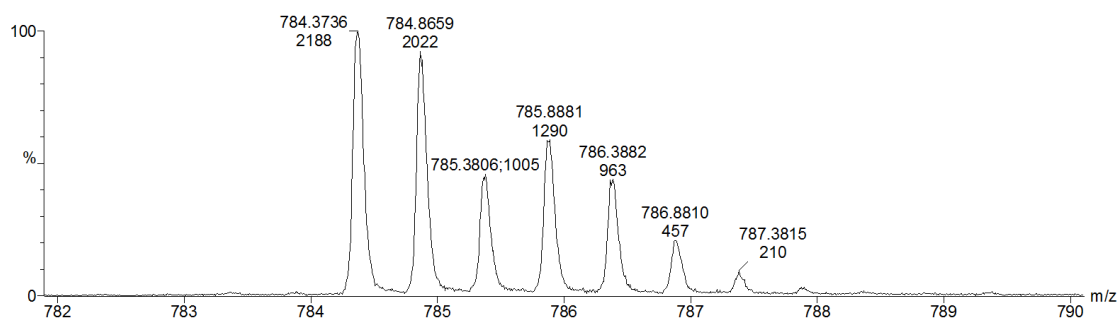


Figure 7.55: Conversion of azido peptide **D₃-243** (100 μM) with phosphonite **237** (100 equiv.).

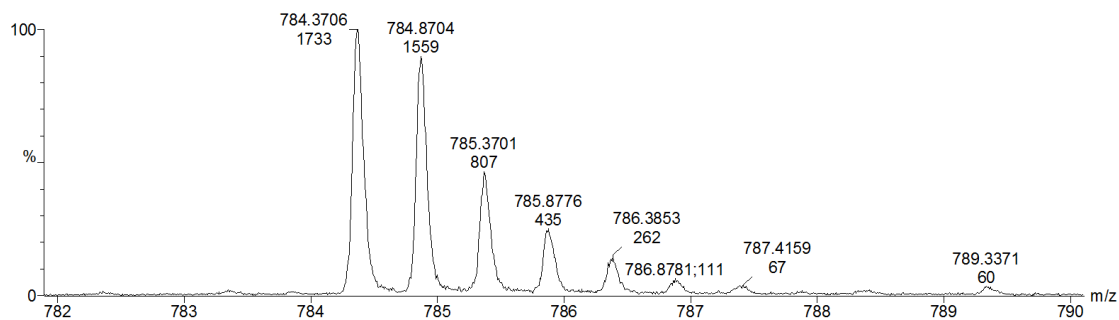


Figure 7.56: Conversion of azido peptide **D₃-243** (50 μM) with phosphonite **237** (500 equiv.).

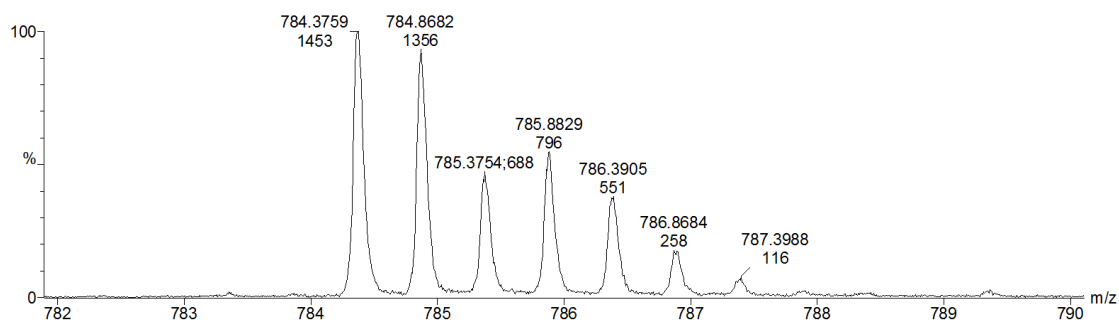


Figure 7.57: Conversion of azido peptide **D₃-243** (50 μM) with phosphonite **237** (250 equiv.).

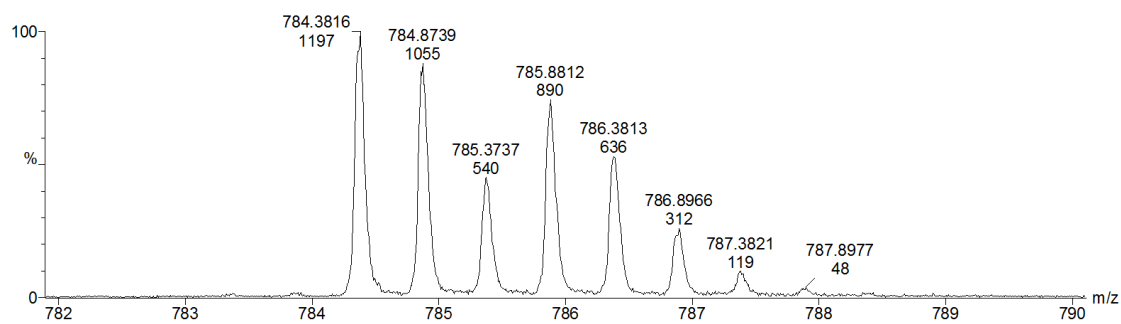


Figure 7.58: Conversion of azido peptide **D₃-243** (50 μM) with phosphonite **237** (100 equiv.).

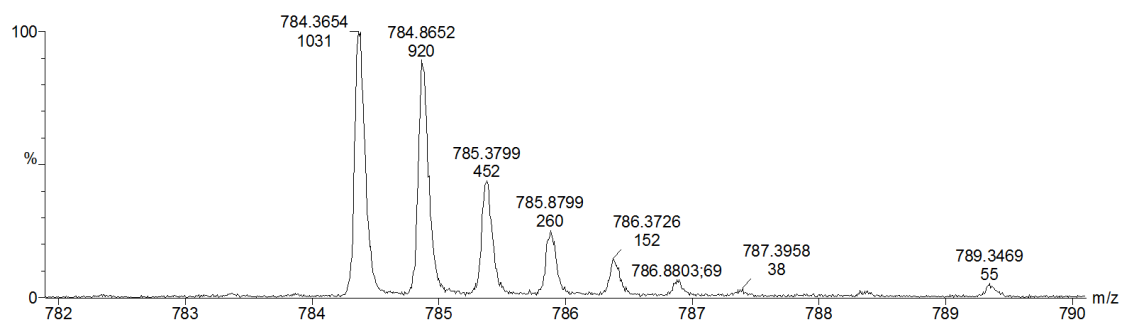


Figure 7.59: Conversion of azido peptide **D₃-243** (250 μM) with phosphonite **237** (1000 equiv.).

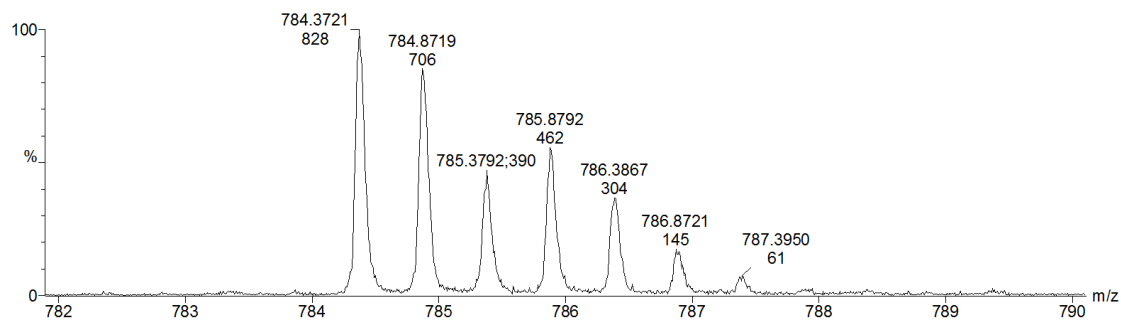
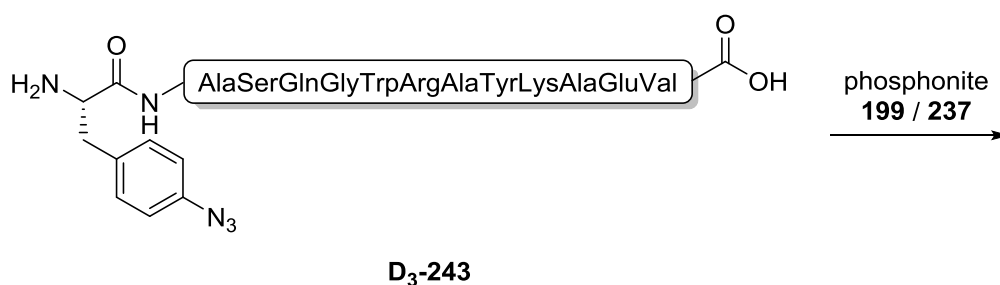


Figure 7.60: Conversion of azido peptide **D₃-243** (250 μM) with phosphonite **237** (500 equiv.).

7.3.18.5 Mass spectra for Table 3.5



Scheme 7.5: Staudinger reaction of azido peptide **D₃-243** with phosphonite **199** and **237**

(Chapter 3.4.3.2, Table 3.5)

H₃-243: HRMS for C₇₁H₁₀₄N₂₂O₁₉²⁺ [M+2H]²⁺ calcd.: 784.3919, found: 784.3635.

D₃-243: HRMS for C₇₁H₁₀₁D₃N₂₂O₁₉²⁺ [M+2H]²⁺ calcd.: 785.9013, found: 785.8691.

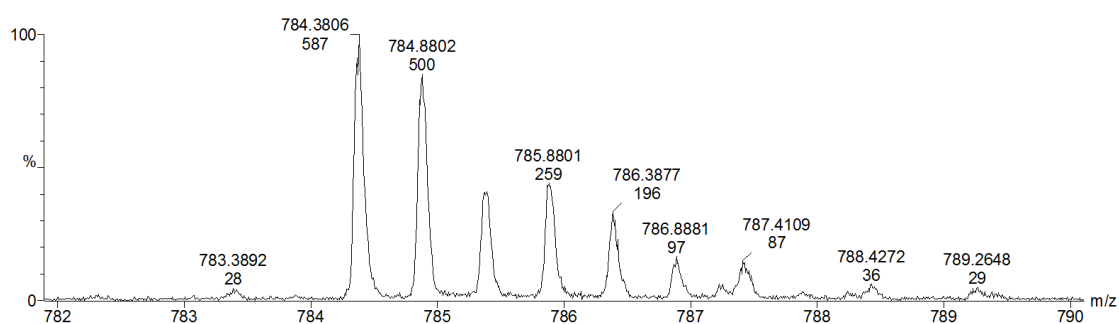


Figure 7.61: Conversion of azido peptide **D₃-243** (50 μM) with phosphonite **199** (250 equiv.) in tris / HCl buffer (100 mM, pH = 8.2).

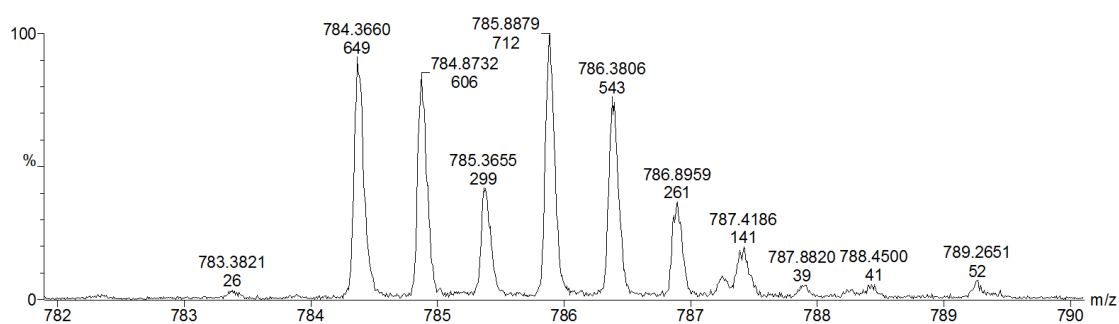


Figure 7.62: Conversion of azido peptide **D₃-243** (50 μM) with phosphonite **199** (250 equiv.) in tris / HCl buffer (100 mM, pH = 7.4).

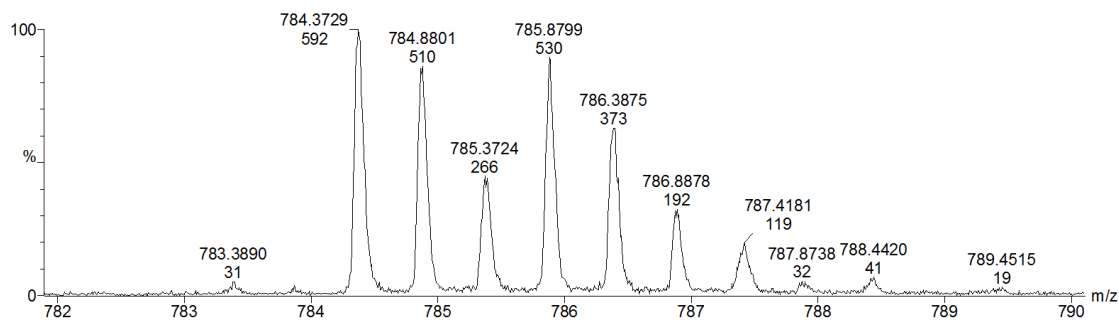


Figure 7.63: Conversion of azido peptide **D₃-243** (50 μ M) with phosphonite **199** (250 equiv.) in phosphate buffer (100 mM, pH = 8.2).

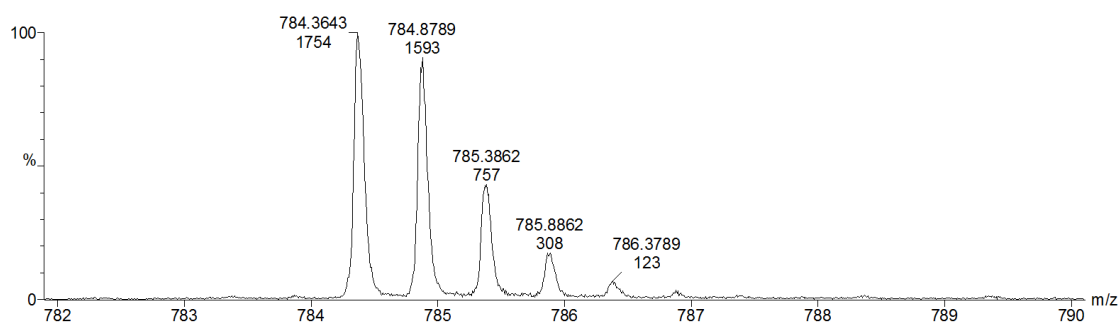


Figure 7.64: Conversion of azido peptide **D₃-243** (50 μ M) with phosphonite **237** (250 equiv.) in tris / HCl buffer (100 mM, pH = 8.2).

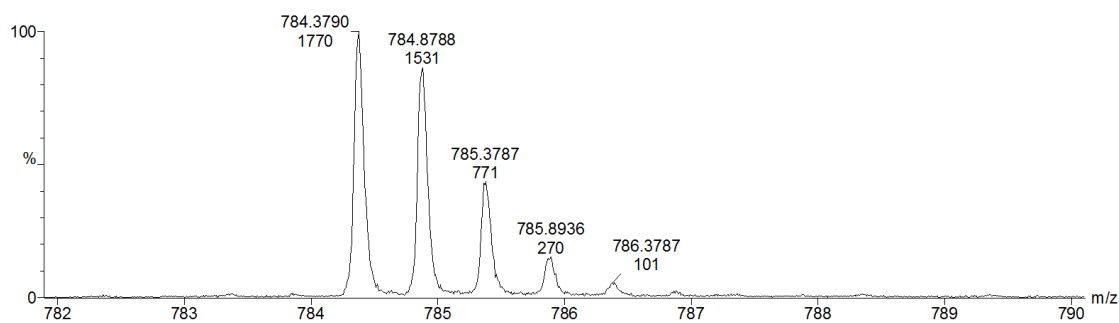


Figure 7.65: Conversion of azido peptide **D₃-243** (50 μ M) with phosphonite **237** (250 equiv.) in tris / HCl buffer (100 mM, pH = 7.4).

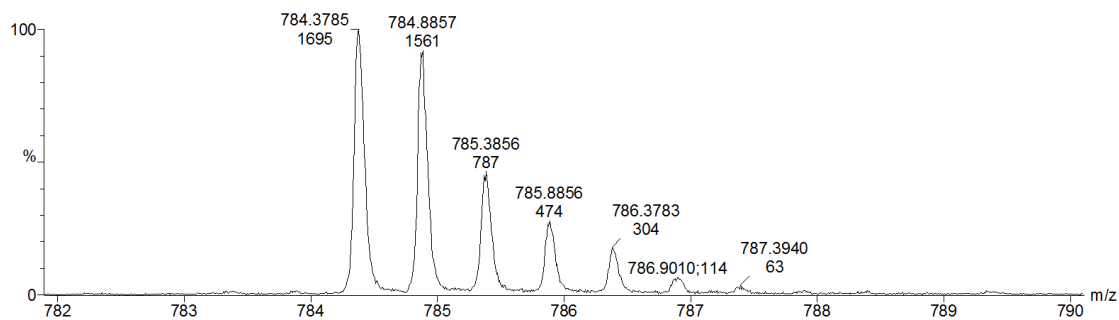
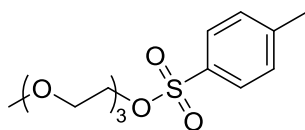


Figure 7.66: Conversion of azido peptide **D₃-243** (50 μ M) with phosphonite **237** (250 equiv.) in tris / HCl buffer (100 mM, pH = 8.2).

7.4 Synthesis of coumarin phosphites (Chapter 3.5)

7.4.1 2-(2-(2-Methoxyethoxy)ethoxy)ethyl-4-methylbenzenesulfonate

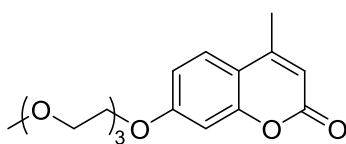


Trimethylamine hydrochloride (3.89 g, 40.70 mmol, 1 equiv.) was slowly added to a solution of 2-(2-(2-methoxyethoxy)ethoxy)ethan-1-ol (6.679 g, 40.68 mmol, 1 equiv.), *p*-toluenesulfonyl chloride (10.0 g, 52.5 mmol, 1.3 equiv.) and triethylamine (8.24 g, 11.6 mL, 81.4 mmol, 2 equiv.) in acetonitrile (500 mL) at 0 °C. After 30 minutes, the ice bath was removed and the mixture was stirred for three hours at room temperature. The suspension was filtered and the filtrate was condensed under reduced pressure. The residue was dissolved in toluene and washed twice with hydrochloride acid (10%). The organic layers were dried over magnesium sulfate and concentrated to yield 2-(2-(2-Methoxyethoxy)ethoxy)ethyl-4-methylbenzenesulfonate in 99% yield (12.925 g, 40.595 mmol) as colourless liquid.

¹H NMR (250 MHz, [D]CHCl₃): δ = 7.79 (d, *J* = 8.3 Hz, 2H, 2xCH), 7.33 (d, *J* = 8.5 Hz, 2H, 2xCH), 4.15 (m, 2H, CH₂), 3.68 (m, 2H, CH₂), 3.60 (m, 6H, 3xCH₂), 3.53 (m, 2H, CH₂), 3.36 (OCH₃), 2.44 (CH₃). HRMS for (C₁₄H₂₃O₆S⁺ [M+H]⁺ calcd.: 319.1137, found: 319.1118. R_f (ethyl acetate/cyclohexane: 1/1) = 0.35.

The obtained NMR data are in accordance with those reported in the literature.^[164]

7.4.2 7-(2-(2-(2-Methoxyethoxy)ethoxy)ethoxy)ethoxy)-4-methylcoumarin (284)

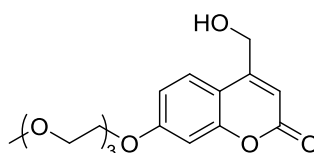


284

A solution of the 7-hydroxy-4-methylcoumarin (**283**) (1.762 g, 10.00 mmol), 2-(2-(2-methoxyethoxy)ethoxy)ethyl-4-methylbenzenesulfonate (3.838 g, 10.00 mmol, 1 equiv.) and potassium carbonate (3.317 g, 24.00 mmol, 2.4 eq.) in acetonitrile (200 ml) was heated under reflux for 16 hours. The crude reaction mixture was filtered through a pad of silica and the solvent was removed under reduced pressure to yield 7-(2-(2-(2-methoxyethoxy)ethoxy)ethoxy)-4-methylcoumarin (**284**) (3.202 g, 9.934 mmol, 99%) as colourless solid.

^1H NMR (400 MHz, $[\text{D}_3]\text{CH}_3\text{CN}$): δ = 7.59 (d, J = 8.8 Hz, 1H, CH), 6.91 (dd, J = 8.8, 2.5 Hz, 1H, CH), 6.86 (d, J = 2.5 Hz, 1H, CH), 6.08 (m, 1H, CH), 4.19 (m, 2H, CH_2), 3.82 (m, 2H, CH_2), 3.65 (m, 2H, CH_2), 3.58 (m, 4H, $2 \times \text{CH}_2$), 3.48 (m, 2H, CH_2), 3.30 (s, 3H, OCH_3), 2.37 (d, J = 1.2 Hz, 3H, CH_3). ^{13}C NMR (100 MHz, $[\text{D}_3]\text{CH}_3\text{CN}$): δ = 162.8 (C=O), 161.9 (C-O), 156.1 (C), 154.3 (C), 127.1 (CH), 114.6 (C), 113.2 (CH), 112.4 (CH), 102.4 (CH), 72.5 (CH_2), 71.3 (CH_2), 71.0 (CH_2), 70.9 (CH_2), 70.0 (CH_2), 69.1 (CH_2), 59.0 (OCH_3), 18.7 (CH_3). HRMS for $\text{C}_{17}\text{H}_{22}\text{NaO}_6^+$ $[\text{M}+\text{Na}]^+$ calcd.: 293.0495, found: 293.0542. MP = 63 - 64 °C. R_f (ethyl acetate/cyclohexane: 2/1) = 0.27.

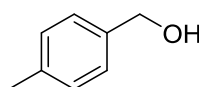
7.4.3 4-(Hydroxymethylene)-7-(2-(2-(2-methoxyethoxy)ethoxy)ethoxy)ethoxy)-coumarin (**286**)



286

Selenium dioxide (1.319 g, 11.89 mmol) was added to a solution of the 7-(2-(2-(2-methoxyethoxy)ethoxy)ethoxy)ethoxy)-4-methylcoumarin (**284**) (2.5546 g, 7.9252 mmol) in *p*-xylene (80 mL). The reaction mixture was heated under reflux under vigorous stirring. After 24 hours the mixture was filtered and concentrated under reduced pressure. The dark brown residue was dissolved in dry ethanol (80 mL) before sodium borohydride (151 mg, 4.0 mmol) was added. The solution was stirred for 5 hours at room temperature. The suspension was carefully hydrolysed with hydrochloric acid (1 M, 20 mL), diluted with water and extracted with dichloromethane (3x 30 mL). The organic phase was washed with water, sodium hydroxide solution (2 M, 2x 30 mL) and brine (40 mL), dried over magnesium sulfate and concentrated under reduced pressure. The crude product was purified by column chromatography to yield 4-(hydroxymethylene)-7-(2-(2-(2-methoxyethoxy)ethoxy)ethoxy)ethoxy)-coumarin (**286**) (0.2729 g, 0.8066 mmol, 7%) as a yellow liquid.

p-Tolylmethanol (**288**)



288

p-Tolylmethanol (**288**) was isolated as by-product in the synthesis of 4-(hydroxymethylene)-7-(2-(2-(2-methoxyethoxy)ethoxy)ethoxy)ethoxy)-coumarin (**286**) with selenium dioxide in *p*-xylene.

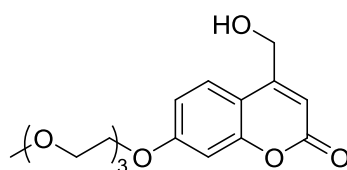
^1H NMR (400 MHz, $[\text{D}_6]$ DMSO): δ = 7.21 (d, J = 8.0 Hz, 2H, 2xCH), 7.13 (d, J = 7.9 Hz, 2H, 2xCH), 5.14 (t, J = 5.7 Hz, 1H, OH), 4.46 (d, J = 5.8 Hz, 2H, CH_2), 2.28 (s, 3H, CH_3). ^{13}C NMR (100 MHz, $[\text{D}_6]$ DMSO): δ = 140.1 (C), 136.2 (C), 129.2 (2xCH), 127.1 (2xCH), 63.4 (CH_2), 21.3 (CH_3).

Optimised synthesis protocol for of 4-(hydroxymethylene)-7-(2-(2-(2-methoxyethoxy)ethoxy)ethoxy)-coumarin (288) in naphthalene

Naphthalene (90 g) was heated to 100 °C and 7-(2-(2-(2-methoxyethoxy)ethoxy)ethoxy)-4-methylcoumarin (**284**) (0.2114 g, 0.6588 mmol) and selenium dioxide (0.1092 g, 0.9837 mmol) were added. The reaction mixture was heated to 150 °C under vigorous stirring. After 24 hours, the mixture was cooled to room temperature, diluted with *n*-hexane (150 mL) and filtered through a pad of silica until no more naphthalene was eluted. The crude product was eluted with ethyl acetate and concentrated under reduced pressure. The dark brown residue was dissolved in dry ethanol (80 mL), sodium borohydride (151 mg, 4.00 mmol) was added, and the solution was stirred for five hours at room temperature. The suspension was carefully hydrolysed with hydrochloric acid (1 M, 20 mL), diluted with water and extracted with dichloromethane (3x 30 mL). The organic phase was washed with water, sodium hydroxide solution (2 M, 2x 30 mL) and brine (40 mL), dried over magnesium sulfate and concentrated under reduced pressure. The crude product was purified by column chromatography to yield 4-(hydroxymethylene)-7-(2-(2-(2-methoxyethoxy)ethoxy)ethoxy)-coumarin (**286**) (0.1123 g, 0.3319 mmol, 51%) as a yellow solid.

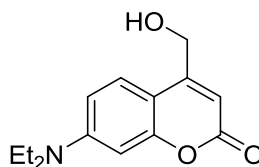
^1H NMR (400 MHz, $[\text{D}]\text{CHCl}_3$): δ = 7.34 (d, J = 8.8 Hz, 1H, CH), 6.81 (dd, J = 8.7, 2.5 Hz, 1H, CH), 6.77 (d, J = 2.4 Hz, 1H, CH), 6.46 (m, 1H, CH), 4.83 (d, J = 4.8 Hz, 2H, $\text{CH}_2\text{-O}$), 4.15 (m, 2H, CH_2), 3.88 (m, 2H, CH_2), 3.75 (m, 2H, CH_2), 3.58 (m, 2H, CH_2), 3.69 (m, 2H, CH_2), 3.65 (m, 2H, CH_2), 3.55 (m, 2H, CH_2), 3.37 (s, 3H, OCH_3). ^{13}C NMR (100 MHz, $[\text{D}]\text{CHCl}_3$): δ = 162.8 (C=O), 161.6 (C), 155.0 (C), 150.3 (C), 124.2 (CH), 107.9 (CH), 105.2 (C), 104.4 (CH), 97.4 (CH), 72.4 (CH_2), 71.3 (CH_2), 71.2 (CH_2), 70.7 (CH_2), 70.0 (CH_2), 60.7 (CH_2), 69.0 (CH_2), 59.1 (OCH_3). HRMS for $\text{C}_{17}\text{H}_{22}\text{NaO}_7^+$ $[\text{M}+\text{Na}]^+$ calcd.: 361.1258, found: .1245. MP = 77 - 78 °C. R_f (ethyl acetate) = 0.24.

7.4.4 4-Hydroxymethylene-7-(2-(2-(2-methoxyethoxy)ethoxy)ethoxy)-coumarin (**286**) from 7-Hydroxy-4-hydroxymethylene-coumarin (**286**)

**286**

A solution of the 7-hydroxy-4-hydroxymethylene-coumarin (**286**) (1.000 g, 5.208 mmol), 2-(2-(2-Methoxyethoxy)ethoxy)ethyl-4-methylbenzenesulfonate (1.6575 g, 5.206 mmol, 1.0 equiv.) and potassium carbonate (1.72 g, 12.4 mmol, 2.4 eq.) (160 ml) was heated under reflux for 16 hours in acetonitrile. The crude reaction mixture was filtered through a pad of silica and the solvent was removed under reduced pressure to yield 4-hydroxymethylene-7-(2-(2-(2-methoxyethoxy)ethoxy)ethoxy)-coumarin (**286**) (1.4575 g, 4.308 mmol, 83%) as colourless solid. See chapter 7.4.3 for analytical data.

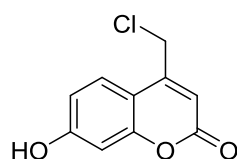
7.4.5 7-Diethylamino-4-hydroxymethylene-coumarin (**287**)

**287**

Selenium dioxide (1.671 g, 15.05 mmol) was added to a solution of the 7-diethylamino-4-methylcoumarin (**285**) (2.320 g, 10.03 mmol) in *p*-xylene (80 mL). This reaction mixture was heated under reflux under vigorous stirring. After 24 hours, the mixture was filtered and concentrated under reduced pressure. The dark brown residue was dissolved in dry ethanol (80 mL), sodium borohydride (0.1897 g, 5.015 mmol) was added, and the solution was stirred for five hours at room temperature. The suspension was carefully hydrolysed with hydrochloric acid (1 M, 20 mL), diluted with water and extracted with dichloromethane (3x 30 mL). The organic phase was washed with water, sodium hydroxide solution (2 M, 2x 30 mL) and brine (40 mL), dried over magnesium sulfate and concentrated under reduced pressure. The crude product was purified by column chromatography to yield 7-diethylamino-4-hydroxymethylene-coumarin (**287**) (0.7938 mg, 3.2030 mmol, 32%) as yellow solid.

^1H NMR (400 MHz, $[\text{D}]\text{CHCl}_3$): δ = 7.31 (d, J = 9.0 Hz, 1H, CH), 6.56 (dd, J = 9.0 Hz, 2.6 Hz, 1H, CH), 6.48 (d, J = 2.6 Hz, 1H, CH), 6.26 (m, 1H, CH), 4.83 (m, $\text{CH}_2\text{-O}$), 3.39 (q, J = 14.2, 7.1 Hz, 4H, 2x NCH_2), 1.19 (t, J = 14.2, 7.1 Hz, 6H, 2x CH_3). ^{13}C NMR (100 MHz, $[\text{D}]\text{CHCl}_3$): δ = 162.7 (C=O), 156.1 (C), 154.8 (C), 150.5 (C), 124.4 (CH), 108.6 (CH), 106.3 (C), 105.4 (CH), 97.7 (CH), 60.9 (CH_2OH), 44.7 (2x NCH_2), 12.5 (2x CH_3). HRMS for $\text{C}_{14}\text{H}_{18}\text{NO}_3^+$ $[\text{M}+\text{H}]^+$ calcd.: 248.1281, found: 248.1277. MP = 131-132 °C. R_f (ethyl acetate/cyclohexane: 2/1) = 0.30.

7.4.6 4-Chloromethylene-7-hydroxy-coumarin (289)

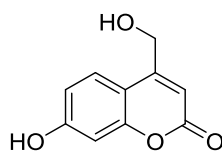


289

A solution of concentrated sulphuric acid (43 ml) was cooled to -5 °C and grinded Resorcinol **281** powder was added slowly (5.60 g, 50.9 mmol) followed by dropwise addition of 4-chloroacetoacetate ethyl ester **282** (7.00 g, 42.5 mmol). The reaction was stirred overnight at -5 °C, then poured into ice water (300 mL) and stirred for additional 1 h. The resulting white precipitate was collected by filtration, washed with ice water, and dried under reduced pressure. The crude product was recrystallized from ethanol to yield 4-chloromethylene-7-hydroxy-coumarin (**289**) (6.38 g, 30.3 mmol, 71%) as a colourless solid.

^1H NMR (400 MHz, $[\text{D}_6]\text{DMSO}$): δ = 10.66 (s, 1H, OH), 7.66 (d, J = 8.8 Hz, 1H, CH), 6.83 (dd, J = 8.7, 2.4 Hz, 1H, CH), 6.74 (d, J = 2.3 Hz, 1H, CH), 6.40 (s, 1H, CH), 4.93 (s, CH_2Cl). ^{13}C NMR (100 MHz, $[\text{D}_6]\text{DMSO}$): δ = 161.50 (C), 160.22 (C), 155.34 (C), 150.99 (C), 126.56 (CH), 113.13 (CH), 111.10 (CH), 109.39 (C), 102.57 (CH), 41.42 (CH_2). MP = 177 - 178 °C. HRMS for $\text{C}_{10}\text{H}_8^{35}\text{ClO}_3^+$ $[\text{M}+\text{H}]^+$ calcd.: 211.0156, found: 211.0138.

7.4.7 7-Hydroxy-4-hydroxymethylene-coumarin (290)



290

4-Chloromethylene-7-hydroxy-coumarin (0.210 g, 1.00 mmol) (**289**) was dissolved in water (15 mL) and heated to 150 °C in a microwave. The precipitate was filtered off and recrystallized

in water to yield 7-hydroxy-4-hydroxymethylene-coumarin (**290**) (0.142 g, 0.739 mmol, 74%) as colourless solid.

^1H NMR (400 MHz, $[\text{D}_3]\text{CD}_3\text{CN}$): δ = 9.20 (s, 1H, OH), 7.42 (d, J = 8.7 Hz, 1H, CH), 6.72 (dd, J = 8.7, 2.4 Hz, 1H, CH), 6.65 (d, J = 2.4 Hz, 1H, CH), 6.23 (s, 1H, CH). 4.74 (s, 2H, CH_2), 4.50 (s, 1H, OH). HRMS for $\text{C}_{10}\text{H}_9\text{O}_4^+$ $[\text{M}+\text{H}]^+$ calcd.: 193.0495, found:193.0499. MP = 218-220 °C.

The obtained NMR data correspond to the literature.^[165]

7.4.8 General procedure for 7-substituted-4-methylene-coumarin phosphites

The 4-hydroxymethylenecoumarin derivative **286** or **287** (3 equiv.) and triethylamine (9 equiv.) were dissolved in tetrahydrofuran (5 mL pro 0.3 mmol coumarin) under an argon atmosphere. The solution was cooled to 0 °C before phosphorus trichloride (1 equiv.) dissolved in tetrahydrofuran (3 mL / 0.1 mmol PCl_3) and slowly added. After ten minutes, the solution was warmed to room temperature and stirred for additional three hours. Insoluble material was removed by filtration and the crude product was analysed by ^{31}P NMR. The phosphonite product shows a characteristic peak at 140.2 ppm.

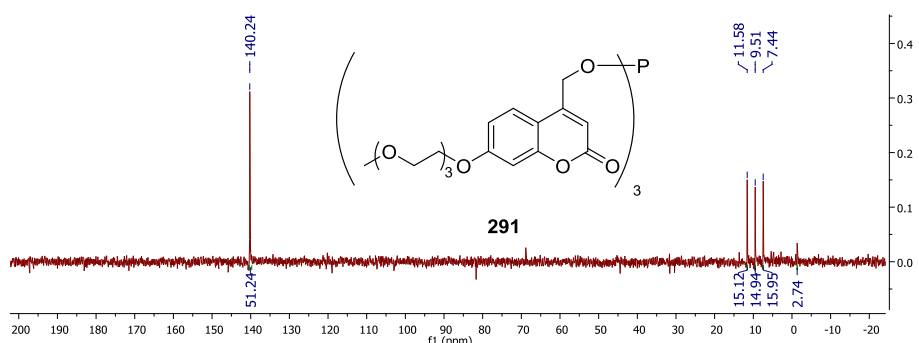


Figure 7.67: Crude ^{31}P NMR of coumarin phosphite **291**.

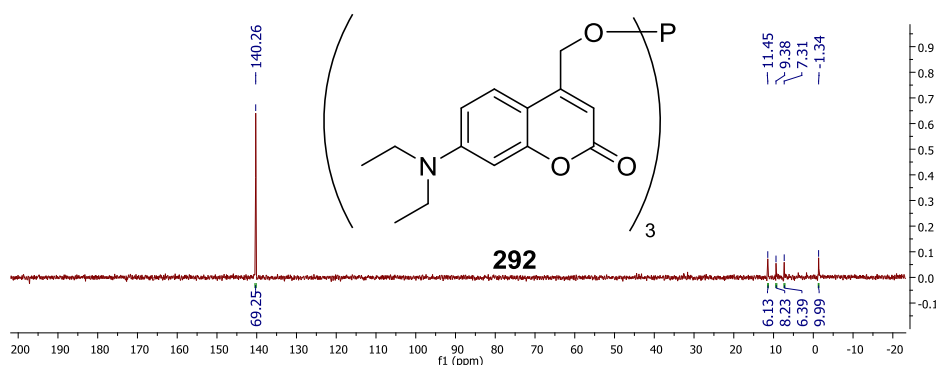


Figure 7.68: Crude ^{31}P NMR of coumarin phosphite **292**.

8 References

- [1] A. Holleman, E. Wiberg, *Lehrbuch der Anorganischen Chemie*, Gruyter, **1995**.
- [2] M. Hesse, H. Meier, B. Zeeh, *Spektroskopische Methoden in der organischen Chemie*, Thieme, **2005**.
- [3] J. M. Berg, J. L. Tymoczko, L. Stryer, *Biochemistry*, Palgrave Macmillan, **2002**.
- [4] J. Clayden, N. Greeves, S. Warren, P. Wothers, *Organic Chemistry*, Oxford University Press, **2001**.
- [5] a) G. L. Miessler, D. A. Tarr, *Inorganic Chemistry*, Pearson, **2003**; b) C. Elschenbroich, *Organometallchemie*, Taubner, **2008**.
- [6] a) L. T. Kliman, S. N. Mlynarski, J. P. Morken, *J. Am. Chem. Soc.* **2009**, *131*, 13210-13211; b) M. A. Fernandez-Zumel, B. Lastra-Barreira, M. Scheele, J. Diez, P. Crochet, J. Gimeno, *Dalton Transactions* **2010**, *39*, 7780-7785.
- [7] a) R. Serwa, I. Wilkening, G. Del Signore, M. Muhlberg, I. Clausnitzer, C. Weise, M. Gerrits, C. P. Hackenberger, *Angew. Chem. Int. Ed.* **2009**, *48*, 8234-8239; b) R. Serwa, P. Majkut, B. Horstmann, J.-M. Swiecicki, M. Gerrits, E. Krause, C. P. R. Hackenberger, *Chem Sci* **2010**, *1*, 596-602.
- [8] V. Bohrsch, R. Serwa, P. Majkut, E. Krause, C. P. Hackenberger, *Chem. Commun.* **2010**, *46*, 3176-3178.
- [9] A. A. Prishchenko, Z. S. Novikova, I. F. Lutsenko, *Zh. Obshch. Khim.* **1980**, *50*, 687-689.
- [10] a) E. J. Corey, Kwiatkow.Gt, *J. Am. Chem. Soc.* **1968**, *90*, 6816-6821; b) T. Wang, H. W. He, *Phosphorus, Sulfur, and Silicon and the Related Elements* **2008**, *183*, 1884-1891.
- [11] Y. Huang, W. G. Bentrude, *J. Am. Chem. Soc.* **1995**, *117*, 12390-12396.
- [12] M. M. Kabachnik, E. V. Snyatkova, Z. S. Novikova, I. F. Lutsenko, *Zh. Obshch. Khim.* **1980**, *50*, 227-228.
- [13] D. Collins, P. Drygala, J. Swan, *Aust. J. Chem.* **1983**, *36*, 2517-2536.
- [14] a) Jarl I. van der Vlugt, Jos M. J. Paulusse, Eric J. Zipp, Jason A. Tijmensen, Allison M. Mills, Anthony L. Spek, C. Claver, D. Vogt, *Eur. J. Inorg. Chem.* **2004**, *2004*, 4193-4201; b) S. H. Chikkali, R. Bellini, B. de Bruin, J. I. van der Vlugt, J. N. H. Reek, *J. Am. Chem. Soc.* **2012**, *134*, 6607-6616; c) David J. Brauer, Konstantin W. Kottsieper, S. Roßenbach, O. Stelzer, *Eur. J. Inorg. Chem.* **2003**, *2003*, 1748-1755; d) M. Fild, M. Vahldiek, *Phosphorous and Sulfur and the Related Elements* **1988**, *40*, 207-213.
- [15] L. J. Szafraniec, L. L. Szafraniec, H. S. Aaron, *J. Org. Chem.* **1982**, *47*, 1936-1939.
- [16] A. K. Bhattacharya, G. Thyagarajan, *Chem. Rev.* **1981**, *81*, 415-430.
- [17] A. Michaelis, R. Kaehne, *Berichte der deutschen chemischen Gesellschaft* **1898**, *31*, 1048-1055.
- [18] a) L. Kürti, B. Czako, *Strategic Applications of Named Reactions in Organic Synthesis*, ELSEVIER Academic Press, **2005**; b) A. E. Arbuzov, *J. Russ. Phys. Chem. Soc.* **1906**, *38*, 687.
- [19] G. Aad, B. Abbott, J. Abdallah, A. A. Abdelalim, A. Abdesselam, O. Abdinov, B. Abi, M. Abolins, H. Abramowicz, H. Abreu, E. Acerbi, B. S. Acharya, M. Ackers, D. L. Adams, T. N. Addy, J. Adelman, M. Aderholz, S. Adomeit, P. Adragna, T. Adye, S. Aefsky, J. A. Aguilar-Saavedra, M. Aharrouche, S. P. Ahlen, F. Ahles, A. Ahmad, M. Ahsan, G. Aielli, T. Akdogan, T. P. A. Akesson, G. Akimoto, A. V. Akimov, M. S. Alam, M. A. Alam, S. Albrand, M. Aleksa, I. N. Aleksandrov, M. Aleppo, F. Alessandria, C. Alexa, G. Alexander, G.

- Alexandre, T. Alexopoulos, M. Alhroob, M. Aliev, G. Alimonti, J. Alison, M. Aliyev, P. P. Allport, S. E. Allwood-Spiers, J. Almond, A. Aloisio, R. Alon, A. Alonso, J. Alonso, M. G. Alviggi, K. Amako, P. Amaral, C. Amelung, V. V. Ammosov, A. Amorim, G. Amoros, N. Amram, C. Anastopoulos, T. Andeen, C. F. Anders, K. J. Anderson, A. Andrezza, V. Andrei, M. L. Andrieux, X. S. Anduaga, A. Angerami, F. Anghinolfi, N. Anjos, A. Annovi, A. Antonaki, M. Antonelli, S. Antonelli, J. Antos, F. Anulli, S. Aoun, L. A. Bella, R. Apolle, G. Arabadze, I. Aracena, Y. Arai, A. T. H. Arce, J. P. Archambault, S. Arfaoui, J. F. Arguin, E. Arik, M. Arik, A. J. Armbruster, K. E. Arms, S. R. Armstrong, O. Arnaez, C. Arnault, A. Artamonov, G. Artoni, D. Arutinov, et al., *Phys. Rev. Lett.* **2010**, 105.
- [20] I. Petneházy, Z. M. Jászay, A. Szabó, K. Everaert, *Synth. Commun.* **2003**, 33, 1665.
- [21] E. J. Corey, N. H. Andersen, R. M. Carlson, J. Paust, E. Vedejs, I. Vlattas, R. E. K. Winter, *J. Am. Chem. Soc.* **1968**, 90, 3245.
- [22] D. Seebach, N. R. Jones, E. J. Corey, *J. Org. Chem.* **1968**, 33, 300.
- [23] H. Staudinger, J. Meyer, *Helv. Chim. Acta* **1919**, 2, 635-646.
- [24] a) Y. G. Gololobov, I. N. Zhmurova, L. F. Kasukhin, *Tetrahedron* **1981**, 37, 437-472; b) B. L. Nilsson, L. L. Kiessling, R. T. Raines, *Org. Lett.* **2000**, 2, 1939-1941; c) E. Saxon, J. I. Armstrong, C. R. Bertozzi, *Org. Lett.* **2000**, 2, 2141-2143; d) E. Saxon, C. R. Bertozzi, *Science* **2000**, 287, 2007-2010.
- [25] J. Goerdeler, H. Ullmann, *Chem. Ber.* **1961**, 94, 1067-1074.
- [26] G. I. Derkach, E. S. Gubnitskaya, *Zh. Obshch. Khim.* **1964**, 34, 604-609.
- [27] E. P. Flindt, H. Rose, H. C. Marsmann, *Z. Anorg. Allg. Chem.* **1977**, 430, 155-160.
- [28] S. Z. Ivin, Shelakov, Id, Promonen, Vk, *Zh. Obshch. Khim.* **1970**, 40, 561.
- [29] a) L. Riesel, D. Sturm, A. Beuster, S. Taudien, B. Thomas, *Z Chem* **1984**, 24, 138-139; b) L. Riesel, D. Sturm, A. Nagel, S. Taudien, A. Beuster, A. Karwatzki, *Z. Anorg. Allg. Chem.* **1986**, 542, 157-166; c) J. Bellan, J. F. Brazier, N. Zenati, M. Sanchez, *Cr Acad Sci C Chim* **1979**, 289, 449-452.
- [30] a) V. L. Foss, I. A. Veits, T. E. Chernykh, I. F. Lutsenko, *Dokl Akad Nauk Sssr+* **1979**, 249, 882-884; b) Y. G. Gololobov, E. A. Suvalova, T. I. Chudakova, *Zh. Obshch. Khim.* **1981**, 51, 1433-1434; c) L. N. Markovskii, V. D. Romanenko, T. I. Pidvarko, *Zh. Obshch. Khim.* **1982**, 52, 1925-1926.
- [31] a) V. A. Gilyarov, N. A. Tikhonina, T. M. Shcherbina, M. I. Kabachnik, *Zh. Obshch. Khim.* **1980**, 50, 1438-1442; b) I. Wilkening, G. del Signore, W. Ahlbrecht, C. P. R. Hackenberger, *Synthesis-Stuttgart* **2011**, 2709-2720.
- [32] M. R. Marre, M. Sanchez, J. F. Brazier, R. Wolf, J. Bellan, *Canadian Journal of Chemistry- Revue Canadienne De Chimie* **1982**, 60, 456-468.
- [33] a) J. Bellan, M. R. Marre, M. Sanchez, R. Wolf, *Phosphorus Sulfur* **1981**, 12, 11-18; b) J. Bellan, M. Sanchez, M. R. Marremazieres, A. M. Beltran, *Bull. Soc. Chim. Fr.* **1985**, 491-495.
- [34] a) I. Wilkening, G. del Signore, C. P. Hackenberger, *Chem Commun (Camb)* **2011**, 47, 349-351; b) M. I. Kabachnik, V. A. Gilyarov, *Bulletin of the Academy of Sciences of the USSR, Division of chemical science* **1956**, 5, 809-816; c) R. L. Letsinger, G. A. Heavner, *Tetrahedron Lett.* **1975**, 16, 147-150.
- [35] a) M. Kohn, R. Breinbauer, *Angew. Chem. Int. Ed.* **2004**, 43, 3106-3116; b) F. L. Lin, H. M. Hoyt, H. van Halbeek, R. G. Bergman, C. R. Bertozzi, *J. Am. Chem. Soc.* **2005**, 127, 2686-2695; c) B. L. Nilsson, L. L. Kiessling, R. T. Raines, *Org. Lett.* **2000**, 3, 9-12; d) C. P. R.

- Hackenberger, D. Schwarzer, *Angew. Chem.* **2008**, *120*, 10182-10228; e) C. I. Schilling, N. Jung, M. Biskup, U. Schepers, S. Brase, *Chem. Soc. Rev.* **2011**, *40*, 4840-4871.
- [36] a) Y. G. Gololobov, L. F. Kasukhin, *Tetrahedron* **1992**, *48*, 1353-1406; b) J. Barluenga, F. Lopez, F. Palacios, *Tetrahedron Lett.* **1987**, *28*, 2875-2878; c) J. Barluenga, F. Lopez, F. Palacios, *Synthesis-Stuttgart* **1989**, 298-300.
- [37] E. J. Corey, B. Samuelsson, F. A. Luzzio, *J. Am. Chem. Soc.* **1984**, *106*, 3682-3683.
- [38] a) A. Padwa, J. R. Gasdaska, G. Hoffmanns, H. Rebello, *The Journal of Organic Chemistry* **1987**, *52*, 1027-1035; b) S. I. Murahashi, Y. Taniguchi, Y. Imada, Y. Tanigawa, *J. Org. Chem.* **1989**, *54*, 3292-3303; c) M. D. Bachi, J. Vaya, *J. Org. Chem.* **1979**, *44*, 4393-4396; d) J. Barluenga, M. Ferrero, F. Palacios, *J Chem Soc Perk T 1* **1990**, 2193-2197; e) O. Tsuge, S. Kanemasa, K. Matsuda, *J. Org. Chem.* **1984**, *49*, 2688-2691; f) J. Barluenga, M. Ferrero, F. Palacios, *Tetrahedron Lett.* **1988**, *29*, 4863-4864; g) B. T. Golding, M. C. Osullivan, L. L. Smith, *Tetrahedron Lett.* **1988**, *29*, 6651-6654; h) V. A. Soloshonok, I. I. Gerus, Y. L. Yagupolskii, V. P. Kukhar, *Zh. Org. Khim.* **1988**, *24*, 993-997.
- [39] A. Stute, L. Heletta, R. Frohlich, C. G. Daniliuc, G. Kehr, G. Erker, *Chem. Commun.* **2012**, *48*, 11739-11741.
- [40] S. Eguchi, H. Takeuchi, N. Watanabe, *Nippon Kagaku Kaishi* **1987**, 1280-1283.
- [41] H. Staudinger, E. Hauser, *Helv. Chim. Acta* **1921**, *4*, 861-886.
- [42] J. E. Leffler, R. D. Temple, *J. Am. Chem. Soc.* **1967**, *89*, 5235-5246.
- [43] H. Goldwhite, P. Gysegem, S. Schow, C. Swyke, *J Chem Soc Dalton* **1975**, 12-15.
- [44] W. Q. Tian, Y. A. Wang, *J. Org. Chem.* **2004**, *69*, 4299-4308.
- [45] M. W. P. Bebbington, D. Bourissou, *Coord. Chem. Rev.* **2009**, *253*, 1248-1261.
- [46] L. F. Kasukhin, M. P. Ponomarchuk, T. V. Kim, Z. M. Ivanova, Y. G. Gololobov, *Zh. Obshch. Khim.* **1978**, *48*, 354-358.
- [47] L. F. Kasukhin, M. P. Ponomarchuk, R. I. Yurchenko, T. I. Klepa, A. G. Yurchenko, Y. G. Gololobov, *Zh. Obshch. Khim.* **1982**, *52*, 797-801.
- [48] a) H. Bock, Schnolle.M, *Angew. Chem. Int. Ed.* **1968**, *7*, 636; b) H. Bock, Schnolle.M, *Chem. Ber. Recl.* **1969**, *102*, 38-49.
- [49] M. B. Soellner, B. L. Nilsson, R. T. Raines, *J. Am. Chem. Soc.* **2006**, *128*, 8820-8828.
- [50] a) R. Kleineweischede, C. P. R. Hackenberger, *Angew. Chem. Int. Ed.* **2008**, *47*, 5984-5988; b) C. P. R. Hackenberger, D. Schwarzer, *Angew. Chem. Int. Ed.* **2008**, *47*, 10030-10074.
- [51] A. Tam, M. B. Soellner, R. T. Raines, *J. Am. Chem. Soc.* **2007**, *129*, 11421-11430.
- [52] a) M. Köhn, R. Wacker, C. Peters, H. Schröder, L. Soulère, R. Breinbauer, C. M. Niemeyer, H. Waldmann, *Angew. Chem. Int. Ed.* **2003**, *42*, 5830-5834; b) A. Watzke, M. Gutierrez-Rodriguez, M. Köhn, R. Wacker, H. Schroeder, R. Breinbauer, J. Kuhlmann, K. Alexandrov, C. M. Niemeyer, R. S. Goody, H. Waldmann, *Biorg. Med. Chem.* **2006**, *14*, 6288-6306; c) M. B. Soellner, K. A. Dickson, B. L. Nilsson, R. T. Raines, *J. Am. Chem. Soc.* **2003**, *125*, 11790-11791.
- [53] a) R. Merckx, D. T. S. Rijkers, J. Kemmink, R. M. J. Liskamp, *Tetrahedron Lett.* **2003**, *44*, 4515-4518; b) L. Liu, Z.-Y. Hong, C.-H. Wong, *Chembiochem* **2006**, *7*, 429-432; c) B. L. Nilsson, R. J. Hondal, M. B. Soellner, R. T. Raines, *J. Am. Chem. Soc.* **2003**, *125*, 5268-5269.
- [54] a) J. A. Camarero, D. Fushman, S. Sato, I. Gariat, D. Cowburn, D. P. Raleigh, T. W. Muir, *J. Mol. Biol.* **2001**, *308*, 1045-1062; b) V. P. Grantcharova, D. Baker, *J. Mol. Biol.* **2001**, *306*, 555-563.

- [55] G. Lättig-Tünnemann, M. Prinz, D. Hoffmann, J. Behlke, C. Palm-Apergi, I. Morano, H. D. Herce, M. C. Cardoso, *Nat Commun* **2011**, *2*, 453.
- [56] a) E. M. Sletten, C. R. Bertozzi, *Angew. Chem. Int. Ed.* **2009**, *48*, 6974-6998; b) H. C. Kolb, M. G. Finn, K. B. Sharpless, *Angew. Chem. Int. Ed.* **2001**, *40*, 2004-2021.
- [57] a) J. D. Watson, F. H. C. Crick, *Nature* **1953**, *171*, 964-967; b) J. D. Watson, F. H. C. Crick, *Nature* **1953**, *171*, 737-738.
- [58] a) L. Wang, J. Xie, P. G. Schultz, *Annu. Rev. Biophys. Biomol. Struct.* **2006**, *35*, 225-249; b) J. Xie, P. G. Schultz, *Curr. Opin. Chem. Biol.* **2005**, *9*, 548-554; c) L. Wang, P. G. Schultz, *Angew. Chem. Int. Ed.* **2005**, *44*, 34-66; d) N. Budisa, *Angew. Chem. Int. Ed.* **2004**, *43*, 6426-6463; e) A. J. Link, M. L. Mock, D. A. Tirrell, *Curr. Opin. Biotechnol.* **2003**, *14*, 603-609; f) D. A. Dougherty, *Curr. Opin. Chem. Biol.* **2000**, *4*, 645-652.
- [59] N. Nischan, A. Chakrabarti, R. A. Serwa, P. H. M. Bovee-Geurts, R. Brock, C. P. R. Hackenberger, *Angew. Chem. Int. Ed.* **2013**, *52*, 11920-11924.
- [60] S. Bräse, C. Gil, K. Knepper, V. Zimmermann, *Angew. Chem.* **2005**, *117*, 5320-5374.
- [61] D. M. M. Jaradat, H. Hamouda, C. P. R. Hackenberger, *Eur. J. Org. Chem.* **2010**, 5004-5009.
- [62] a) N. Jessani, B. F. Cravatt, *Curr. Opin. Chem. Biol.* **2004**, *8*, 54-59; b) P. F. van Swieten, M. A. Leeuwenburgh, B. M. Kessler, H. S. Overkleeft, *Org Biomol Chem* **2005**, *3*, 20-27; c) D. P. Gamblin, E. M. Scanlan, B. G. Davis, *Chem. Rev.* **2008**, *109*, 131-163.
- [63] P. Cohen, *Nat Cell Biol* **2002**, *4*, E127-E130.
- [64] C. T. Walsh, S. Garneau-Tsodikova, G. J. Gatto, *Angew. Chem. Int. Ed.* **2005**, *44*, 7342-7372.
- [65] G. A. Houry, R. C. Baliban, C. A. Floudas, *Sci. Rep.* **2011**, *1*.
- [66] a) E. M. Sletten, C. R. Bertozzi, *Acc. Chem. Res.* **2011**, *44*, 666-676; b) S. M. Fuchs, R. T. Raines, *Biochemistry-Us* **2004**, *43*, 2438-2444; c) L. D. Lavis, T.-Y. Chao, R. T. Raines, *Acs Chem Biol* **2006**, *1*, 252-260.
- [67] O. Shimomura, F. H. Johnson, Y. Saiga, *Journal of Cellular and Comparative Physiology* **1962**, *59*, 223-239.
- [68] D. C. Prasher, V. K. Eckenrode, W. W. Ward, F. G. Prendergast, M. J. Cormier, *Gene* **1992**, *111*, 229-233.
- [69] M. Chalfie, Y. Tu, G. Euskirchen, W. Ward, D. Prasher, *Science* **1994**, *263*, 802-805.
- [70] "The Nobel Prize in Chemistry 2008". Nobelprize.org. 2013 Jun 2013 http://www.nobelprize.org/nobel_prizes/chemistry/laureates/2008/index.html.
- [71] R. Y. Tsien, *Annu. Rev. Biochem* **1998**, *67*, 509-544.
- [72] M. Andresen, R. Schmitz-Salue, S. Jakobs, *Mol Biol Cell* **2004**, *15*, 5616-5622.
- [73] A. N. Glazer, *Annu. Rev. Biochem* **1970**, *39*, 101-130.
- [74] A. Varki, T. Angata, *Glycobiology* **2006**, *16*, 1R-27R.
- [75] K. W. Dehnert, J. M. Baskin, S. T. Laughlin, B. J. Beahm, N. N. Naidu, S. L. Amacher, C. R. Bertozzi, *Chembiochem* **2012**, *13*, 353-357.
- [76] a) F. M. Veronese, G. Pasut, *Drug Discovery Today* **2005**, *10*, 1451-1458; b) J. M. Harris, R. B. Chess, *Nat. Rev. Drug Discovery* **2003**, *2*, 214-221; c) C. Monfardini, O. Schiavon, P. Caliceti, M. Morpurgo, J. M. Harris, F. M. Veronese, *Bioconjugate Chem.* **1995**, *6*, 62-69.
- [77] a) R. Gref, Y. Minamitake, M. Peracchia, V. Trubetskoy, V. Torchilin, R. Langer, *Science* **1994**, *263*, 1600-1603; b) K. Knop, R. Hoogenboom, D. Fischer, U. S. Schubert, *Angew. Chem. Int. Ed.* **2010**, *49*, 6288-6308.
- [78] L. A. Cohen, *Annu. Rev. Biochem* **1968**, *37*, 695-726.

- [79] C. F. Brewer, J. P. Riehm, *Anal. Biochem.* **1967**, *18*, 248-255.
- [80] D. S. Moore, *Biochemical Education* **1985**, *13*, 10-11.
- [81] H. B. F. Dixon, *J. Protein Chem.* **1984**, *3*, 99-108.
- [82] K. F. Geoghegan, J. G. Stroh, *Bioconjugate Chem.* **1992**, *3*, 138-146.
- [83] R. B. Merrifield, *J. Am. Chem. Soc.* **1963**, *85*, 2149-2154.
- [84] a) B. L. Nilsson, M. B. Soellner, R. T. Raines, *Annu. Rev. Biophys. Biomol. Struct.* **2005**, *34*, 91-118; b) S. P. East, M. M. Joullié, *Tetrahedron Lett.* **1998**, *39*, 7211-7214; c) P. Sieber, B. Kamber, A. Hartmann, A. Jöhl, B. Riniker, W. Rittel, *Helv. Chim. Acta* **1977**, *60*, 27-37; d) K. Akaji, K. Fujino, T. Tatsumi, Y. Kiso, *J. Am. Chem. Soc.* **1993**, *115*, 11384-11392.
- [85] G. A. Lemieux, C. L. de Graffenried, C. R. Bertozzi, *J. Am. Chem. Soc.* **2003**, *125*, 4708-4709.
- [86] a) L. Wang, P. G. Schultz, *Angew. Chem. Int. Ed.* **2004**, *44*, 34-66; b) T. S. Young, P. G. Schultz, *J. Biol. Chem.* **2010**, *285*, 11039-11044.
- [87] A. J. de Graaf, M. Kooijman, W. E. Hennink, E. Mastrobattista, *Bioconjugate Chem.* **2009**, *20*, 1281-1295.
- [88] a) J. C. M. van Hest, D. A. Tirrell, *FEBS Lett.* **1998**, *428*, 68-70; b) K. L. Kiick, D. A. Tirrell, *Tetrahedron* **2000**, *56*, 9487-9493; c) K. L. Kiick, J. C. M. van Hest, D. A. Tirrell, *Angew. Chem. Int. Ed.* **2000**, *39*, 2148-2152; d) K. L. Kiick, R. Weberskirch, D. A. Tirrell, *FEBS Lett.* **2001**, *502*, 25-30; e) K. L. Kiick, E. Saxon, D. A. Tirrell, C. R. Bertozzi, *Proceedings of the National Academy of Sciences* **2002**, *99*, 19-24; f) A. J. Link, D. A. Tirrell, *J. Am. Chem. Soc.* **2003**, *125*, 11164-11165; g) A. J. Link, M. K. S. Vink, D. A. Tirrell, *J. Am. Chem. Soc.* **2004**, *126*, 10598-10602.
- [89] Y. Tang, D. A. Tirrell, *J. Am. Chem. Soc.* **2001**, *123*, 11089-11090.
- [90] Q. Wang, T. R. Chan, R. Hilgraf, V. V. Fokin, K. B. Sharpless, M. G. Finn, *J. Am. Chem. Soc.* **2003**, *125*, 3192-3193.
- [91] E. Yoshikawa, M. J. Fournier, T. L. Mason, D. A. Tirrell, *Macromolecules* **1994**, *27*, 5471-5475.
- [92] a) J. H. Bae, S. Alefelder, J. T. Kaiser, R. Friedrich, L. Moroder, R. Huber, N. Budisa, *J. Mol. Biol.* **2001**, *309*, 925-936; b) N. Budisa, S. Alefelder, J. H. Bae, R. Golbik, C. Minks, R. Huber, L. Moroder, *Protein Sci.* **2001**, *10*, 1281-1292.
- [93] C. Renner, S. Alefelder, J. H. Bae, N. Budisa, R. Huber, L. Moroder, *Angew. Chem. Int. Ed.* **2001**, *40*, 923-925.
- [94] a) J. D. Bain, C. G. Glabe, T. A. Dix, A. R. Chamberlin, E. S. Diala, *J. Am. Chem. Soc.* **1989**, *111*, 8013-8014; b) C. J. Noren, S. J. Anthonycahill, M. C. Griffith, P. G. Schultz, *Science* **1989**, *244*, 182-188; c) C. J. Noren, S. J. Anthony-Cahill, K. A. Noren, M. C. Griffith, P. G. Schultz, *Nucleic Acids Res.* **1990**, *18*, 83-88; d) L. Wang, A. Brock, B. Herberich, P. G. Schultz, *Science* **2001**, *292*, 498-500; e) W.-T. Li, A. Mahapatra, D. G. Longstaff, J. Bechtel, G. Zhao, P. T. Kang, M. K. Chan, J. A. Krzycki, *J. Mol. Biol.* **2009**, *385*, 1156-1164; f) C. C. Liu, P. G. Schultz, *Annual Review of Biochemistry, Vol 79* **2010**, *79*, 413-444.
- [95] H. Neumann, K. Wang, L. Davis, M. Garcia-Alai, J. W. Chin, *Nature* **2010**, *464*, 441-444.
- [96] V. W. Cornish, D. Mendel, P. G. Schultz, *Angew. Chem. Int. Ed.* **1995**, *34*, 621-633.
- [97] J. W. Chin, S. W. Santoro, A. B. Martin, D. S. King, L. Wang, P. G. Schultz, *J. Am. Chem. Soc.* **2002**, *124*, 9026-9027.
- [98] a) S. K. Blight, R. C. Larue, A. Mahapatra, D. G. Longstaff, E. Chang, G. Zhao, P. T. Kang, K. B. Church-Church, M. K. Chan, J. A. Krzycki, *Nature* **2004**, *431*, 333-335; b) C. Polycarpo,

- A. Ambrogelly, A. Berube, S. A. M. Winbush, J. A. McCloskey, P. F. Crain, J. L. Wood, D. Soll, *P Natl Acad Sci USA* **2004**, *101*, 12450-12454.
- [99] a) T. Fekner, X. Li, M. M. Lee, M. K. Chan, *Angew. Chem. Int. Ed.* **2009**, *48*, 1633-1635; b) D. P. Nguyen, H. Lusic, H. Neumann, P. B. Kapadnis, A. Deiters, J. W. Chin, *J. Am. Chem. Soc.* **2009**, *131*, 8720-8721.
- [100] K. J. Roux, D. I. Kim, M. Raida, B. Burke, *The Journal of Cell Biology* **2012**, *196*, 801-810.
- [101] B. L. Carlson, E. R. Ballister, E. Skordalakes, D. S. King, M. A. Breidenbach, S. A. Gilmore, J. M. Berger, C. R. Bertozzi, *J. Biol. Chem.* **2008**, *283*, 20117-20125.
- [102] A. Michael, *Journal für Praktische Chemie* **1893**, *48*, 94-95.
- [103] R. Huisgen, *Angew. Chem. Int. Ed.* **1963**, *75*, 604-637.
- [104] V. V. Rostovtsev, L. G. Green, V. V. Fokin, K. B. Sharpless, *Angew. Chem. Int. Ed.* **2002**, *41*, 2596-2599.
- [105] C. W. Tornøe, C. Christensen, M. Meldal, *J. Org. Chem.* **2002**, *67*, 3057-3064.
- [106] a) V. O. Rodionov, S. I. Presolski, D. Díaz Díaz, V. V. Fokin, M. G. Finn, *J. Am. Chem. Soc.* **2007**, *129*, 12705-12712; b) D. C. Kennedy, C. S. McKay, M. C. B. Legault, D. C. Danielson, J. A. Blake, A. F. Pegoraro, A. Stolow, Z. Mester, J. P. Pezacki, *J. Am. Chem. Soc.* **2011**, *133*, 17993-18001.
- [107] a) F. Himo, T. Lovell, R. Hilgraf, V. V. Rostovtsev, L. Noodleman, K. B. Sharpless, V. V. Fokin, *J. Am. Chem. Soc.* **2004**, *127*, 210-216; b) V. D. Bock, H. Hiemstra, J. H. van Maarseveen, *Eur. J. Org. Chem.* **2006**, *2006*, 51-68.
- [108] E. M. Sletten, C. R. Bertozzi, *Angew. Chem.* **2009**, *121*, 7108-7133.
- [109] a) M. A. Breidenbach, J. E. G. Gallagher, D. S. King, B. P. Smart, P. Wu, C. R. Bertozzi, *Proceedings of the National Academy of Sciences* **2010**, *107*, 3988-3993; b) Q. Wang, T. R. Chan, R. Hilgraf, V. V. Fokin, K. B. Sharpless, M. G. Finn, *J. Am. Chem. Soc.* **2003**, *125*, 3192-3193.
- [110] N. J. Agard, J. A. Prescher, C. R. Bertozzi, *J. Am. Chem. Soc.* **2004**, *126*, 15046-15047.
- [111] G. Wittig, A. Krebs, *Chem. Ber. Recl.* **1961**, *94*, 3260-3275.
- [112] H. Meier, H. Petersen, H. Kolshorn, *Chem. Ber.* **1980**, *113*, 2398-2409.
- [113] a) R. B. Turner, P. Goebel, B. J. Mallon, A. D. Jarrett, *J. Am. Chem. Soc.* **1973**, *95*, 790-792; b) F. Schoenebeck, D. H. Ess, G. O. Jones, K. N. Houk, *J. Am. Chem. Soc.* **2009**, *131*, 8121-8133.
- [114] D. H. Ess, G. O. Jones, K. N. Houk, *Org. Lett.* **2008**, *10*, 1633-1636.
- [115] J. M. Baskin, J. A. Prescher, S. T. Laughlin, N. J. Agard, P. V. Chang, I. A. Miller, A. Lo, J. A. Codelli, C. R. Bertozzi, *Proceedings of the National Academy of Sciences* **2007**, *104*, 16793-16797.
- [116] X. Ning, J. Guo, M. A. Wolfert, G.-J. Boons, *Angew. Chem. Int. Ed.* **2008**, *47*, 2253-2255.
- [117] E. M. Sletten, C. R. Bertozzi, *Org. Lett.* **2008**, *10*, 3097-3099.
- [118] W. A. van der Linden, N. Li, S. Hoogendoorn, M. Ruben, M. Verdoes, J. Guo, G.-J. Boons, G. A. van der Marel, B. I. Florea, H. S. Overkleeft, *Biorg. Med. Chem.* **2012**, *20*, 662-666.
- [119] J. Z. Yao, C. Uttamapinant, A. Poloukhine, J. M. Baskin, J. A. Codelli, E. M. Sletten, C. R. Bertozzi, V. V. Popik, A. Y. Ting, *J. Am. Chem. Soc.* **2012**, *134*, 3720-3728.
- [120] H. Moller, V. Bohrsch, J. Bentrop, J. Bender, S. Hinderlich, C. P. R. Hackenberger, *Angew. Chem. Int. Ed.* **2012**, *51*, 5986-5990.
- [121] S. T. Laughlin, J. M. Baskin, S. L. Amacher, C. R. Bertozzi, *Science* **2008**, *320*, 664-667.
- [122] K. C. Nicolaou, S. A. Snyder, *Classics in Total Synthesis II*, Wiley-VCH, **2003**.

- [123] a) A. D. de Araujo, J. M. Palomo, J. Cramer, M. Kohn, H. Schroder, R. Wacker, C. Niemeyer, K. Alexandrov, H. Waldmann, *Angew. Chem. Int. Ed.* **2006**, *45*, 296-301; b) M. N. Yousaf, M. Mrksich, *J. Am. Chem. Soc.* **1999**, *121*, 4286-4287; c) V. Steven, D. Graham, *Org. Biomol. Chem.* **2008**, *6*, 3781-3787; d) X.-L. Sun, L. Yang, E. L. Chaikof, *Tetrahedron Lett.* **2008**, *49*, 2510-2513.
- [124] a) D. L. Boger, C. M. Baldino, *J. Am. Chem. Soc.* **1993**, *115*, 11418-11425; b) H. H. Wasserman, R. W. Desimone, D. L. Boger, C. M. Baldino, *J. Am. Chem. Soc.* **1993**, *115*, 8457-8458.
- [125] M. L. Blackman, M. Royzen, J. M. Fox, *J. Am. Chem. Soc.* **2008**, *130*, 13518-13519.
- [126] a) E. G. Sander, W. P. Jencks, *J. Am. Chem. Soc.* **1968**, *90*, 6154-6162; b) R. K. V. Lim, Q. Lin, *Chem. Commun.* **2010**, *46*, 1589-1600.
- [127] Z. Zhang, B. A. C. Smith, L. Wang, A. Brock, C. Cho, P. G. Schultz, *Biochemistry-U.S.* **2003**, *42*, 6735-6746.
- [128] A. Dirksen, T. M. Hackeng, P. E. Dawson, *Angew. Chem. Int. Ed.* **2006**, *45*, 7581-7584.
- [129] A. Dirksen, S. Dirksen, T. M. Hackeng, P. E. Dawson, *J. Am. Chem. Soc.* **2006**, *128*, 15602-15603.
- [130] "The Nobel Prize in Chemistry 2008". Nobelprize.org. 2013 Aug 2013 http://www.nobelprize.org/nobel_prizes/chemistry/laureates/1984/index.html.
- [131] O. J. Plante, E. R. Palmacci, P. H. Seeberger, *Science* **2001**, *291*, 1523-1527.
- [132] I. Papp, J. Dervede, S. Enders, R. Haag, *Chem. Commun.* **2008**, 5851-5853.
- [133] M. Krämer, J.-F. Stumbé, H. Türk, S. Krause, A. Komp, L. Delineau, S. Prokhorova, H. Kautz, R. Haag, *Angew. Chem. Int. Ed.* **2002**, *41*, 4252-4256.
- [134] R. Haag, *Angew. Chem. Int. Ed.* **2004**, *43*, 278-282.
- [135] P. H. H. Hermkens, H. C. J. Ottenheijm, D. Rees, *Tetrahedron* **1996**, *52*, 4527-4554.
- [136] a) S. S. Wang, *J. Am. Chem. Soc.* **1973**, *95*, 1328-1333; b) B. F. Gisin, *Helv. Chim. Acta* **1973**, *56*, 1476-1482.
- [137] H. Rink, *Tetrahedron Lett.* **1987**, *28*, 3787-3790.
- [138] K. Barlos, D. Gatos, I. Kallitsis, D. Papaioannou, P. Sotiriou, *Liebigs Ann. Chem.* **1988**, *1988*, 1079-1081.
- [139] a) H. M. Eggenweiler, *Drug Discovery Today* **1998**, *3*, 552-560; b) K. Gordon, S. Balasubramanian, *Journal of Chemical Technology & Biotechnology* **1999**, *74*, 835-851.
- [140] E. Bayer, *Angew. Chem. Int. Ed.* **1991**, *30*, 113-129.
- [141] a) M. Pursch, G. Schlotterbeck, L. H. Tseng, K. Albert, W. Rapp, *Angew. Chem. Int. Ed.* **1996**, *35*, 2867-2869; b) W. L. Fitch, G. Detre, C. P. Holmes, J. N. Shoolery, P. A. Keifer, *J. Org. Chem.* **1994**, *59*, 7955-7956; c) G. C. Look, C. P. Holmes, J. P. Chinn, M. A. Gallop, *J. Org. Chem.* **1994**, *59*, 7588-7590.
- [142] I. Papp, C. Sieben, A. L. Sisson, J. Kostka, C. Bottcher, K. Ludwig, A. Herrmann, R. Haag, *Chembiochem* **2011**, *12*, 887-895.
- [143] C. Grandjean, A. Boutonnier, C. Guerreiro, J.-M. Fournier, L. A. Mulard, *The Journal of Organic Chemistry* **2005**, *70*, 7123-7132.
- [144] H. C. Kolb, M. G. Finn, K. B. Sharpless, *Angew. Chem.* **2001**, *113*, 2056-2075.
- [145] J. F. Lutz, J. Andrieu, A. Hoth, S. Agarwal, *Abstr. Pap. Am. Chem. Soc.* **2008**, 236.
- [146] a) A. Abuchowski, J. R. McCoy, N. C. Palczuk, T. Vanes, F. F. Davis, *J. Biol. Chem.* **1977**, *252*, 3582-3586; b) A. Abuchowski, T. Vanes, N. C. Palczuk, F. F. Davis, *J. Biol. Chem.* **1977**, *252*, 3578-3581; c) G. Pasut, F. M. Veronese, *Prog. Polym. Sci.* **2007**, *32*, 933-961;

- d) T. M. Allen, P. R. Cullis, *Science* **2004**, *303*, 1818-1822; e) C. Monfardini, F. M. Veronese, *Bioconjugate Chem.* **1998**, *9*, 418-450.
- [147] a) M. Hurtado, M. Yáñez, R. Herrero, A. Guerrero, J. Z. Dávalos, J.-L. M. Abboud, B. Khater, J.-C. Guillemin, *Chemistry – A European Journal* **2009**, *15*, 4622-4629; b) L. Maier, *Helv. Chim. Acta* **1966**, *49*, 842-851; c) R. P. Davies, L. Patel, A. J. P. White, *Inorg. Chem.* **2012**, *51*, 11594-11601; d) J. L. Cabioch, J. M. Denis, *J. Organomet. Chem.* **1989**, *377*, 227-233.
- [148] a) A. Ferry, X. Guinchard, P. Retailleau, D. Crich, *J. Am. Chem. Soc.* **2012**, *134*, 12289-12301; b) A. M. Polozov, S. E. Cremer, P. E. Fanwick, *Can. J. Chem.* **1999**, *77*, 1274-1280.
- [149] B. Jiang, Y. Lei, X.-L. Zhao, *The Journal of Organic Chemistry* **2008**, *73*, 7833-7836.
- [150] a) K. Bellmann-Sickert, C. E. Elling, A. N. Madsen, P. B. Little, K. Lundgren, L. O. Gerlach, R. Bergmann, B. Holst, T. W. Schwartz, A. G. Beck-Sickinger, *J. Med. Chem.* **2011**, *54*, 2658-2667; b) C. J. Fee, *Biotechnol. Bioeng.* **2007**, *98*, 725-731.
- [151] M. Werle, A. Bernkop-Schnuerch, *Amino Acids* **2006**, *30*, 351-367.
- [152] M. S. M. Timmer, H. Ovaa, D. V. Filippov, G. A. van der Marel, J. H. van Boom, *Tetrahedron Lett.* **2001**, *42*, 8231-8233.
- [153] S. Ortial, J. L. Montchamp, *Org. Lett.* **2011**, *13*, 3134-3137.
- [154] F. W. Hoffmann, R. J. Ess, R. P. Usingef, *J. Am. Chem. Soc.* **1956**, *78*, 5817-5821.
- [155] a) S. T. Abuorabi, M. A. Atfah, I. Jibril, F. M. Marii, A. A. S. Ali, *J. Heterocycl. Chem.* **1989**, *26*, 1461-1468; b) R. J. Depasquale, C. D. Padgett, R. W. Rosser, *J. Org. Chem.* **1975**, *40*, 810-811; c) L. Garanti, G. Molteni, *Tetrahedron Lett.* **2003**, *44*, 1133-1135; d) K. Harju, M. Vahermo, I. Mutikainen, J. Yli-Kauhaluoma, *J. Comb. Chem.* **2003**, *5*, 826-833; e) B. Helms, J. L. Mynar, C. J. Hawker, J. M. J. Frechet, *J. Am. Chem. Soc.* **2004**, *126*, 15020-15021; f) M. Journet, D. W. Cai, J. J. Kowal, R. D. Larsen, *Tetrahedron Lett.* **2001**, *42*, 9117-9118; g) A. R. Katritzky, S. K. Singh, *J. Org. Chem.* **2002**, *67*, 9077-9079; h) J. C. Sheehan, C. A. Robinson, *J. Am. Chem. Soc.* **1951**, *73*, 1207-1210; i) Y. Tanaka, S. R. Velen, S. I. Miller, *Tetrahedron* **1973**, *29*, 3271-3283; j) R. H. Wiley, K. F. Hussung, J. Moffat, *J. Org. Chem.* **1956**, *21*, 190-192.
- [156] a) A. R. Katritzky, M. Yoshioka, T. Narindoshvili, A. Chung, J. V. Johnson, *Org. Biomol. Chem.* **2008**, *6*, 4582-4586; b) A. B. Neef, C. Schultz, *Angew. Chem. Int. Ed.* **2009**, *48*, 1498-1500.
- [157] C. Peters, A. Wolf, M. Wagner, J. Kuhlmann, H. Waldmann, *P Natl Acad Sci USA* **2004**, *101*, 8531-8536.
- [158] a) R. Martello, A. Mangerich, S. Sass, P. C. Dedon, A. Bürkle, *Acs Chem Biol* **2013**, *8*, 1567-1575; b) M. L. Steinhauser, A. P. Bailey, S. E. Senyo, C. Guillermier, T. S. Perlstein, A. P. Gould, R. T. Lee, C. P. Lechene, *Nature* **2012**, *481*, 516-519; c) K. G. Kline, M. R. Sussman, *Annu Rev Biophys* **2010**, *39*, 291-308; d) V. Mayya, D. K. Han, *Expert Rev Proteomic* **2006**, *3*, 597-610; e) J. M. Asara, X. Zhang, B. Zheng, L. A. Maroney, H. R. Christofk, N. Wu, L. C. Cantley, *Nat. Protocols* **2006**, *1*, 46-51; f) H. Zhang, X.-j. Li, D. B. Martin, R. Aebersold, *Nat Biotech* **2003**, *21*, 660-666; g) J. R. Barr, V. L. Maggio, D. G. Patterson, G. R. Cooper, L. O. Henderson, W. E. Turner, S. J. Smith, W. H. Hannon, L. L. Needham, E. J. Sampson, *Clin. Chem.* **1996**, *42*, 1676-1682; h) F. Xie, T. Liu, W. J. Qian, V. A. Petyuk, R. D. Smith, *J. Biol. Chem.* **2011**, *286*, 25443-25449; i) S. E. Ong, B. Blagoev, I. Kratchmarova, D. B. Kristensen, H. Steen, A. Pandey, M. Mann, *Mol Cell Proteomics* **2002**, *1*, 376-386.

-
- [159] R. J. Zhang, C. S. Sioma, R. A. Thompson, L. Xiong, F. E. Regnier, *Anal. Chem.* **2002**, *74*, 3662-3669.
- [160] V. Bohrsch, T. Mathew, M. Zieringer, M. R. J. Vallee, L. M. Artner, J. Dervede, R. Haag, C. P. R. Hackenberger, *Org Biomol Chem* **2012**, *10*, 6211-6216.
- [161] a) A. Varki, *Nature* **2007**, *446*, 1023-1029; b) C. R. Bertozzi, L. L. Kiessling, *Science* **2001**, *291*, 2357-2364.
- [162] a) M. Calderon, M. A. Quadir, S. K. Sharma, R. Haag, *Adv. Mater.* **2010**, *22*, 190-218; b) S. Roller, H. X. Zhou, R. Haag, *Mol Divers* **2005**, *9*, 305-316.
- [163] D. Guillaneux, L. Martiny, H. B. Kagan, *Collect. Czech. Chem. Commun.* **2000**, *65*, 717-728.
- [164] Y. Yoshida, Y. Sakakura, N. Aso, S. Okada, Y. Tanabe, *Tetrahedron* **1999**, *55*, 2183-2192.
- [165] a) Z. Zhou, C. J. Fahrni, *J. Am. Chem. Soc.* **2004**, *126*, 8862-8863; b) C. Binda, J. Wang, L. Pisani, C. Caccia, A. Carotti, P. Salvati, D. E. Edmondson, A. Mattevi, *J. Med. Chem.* **2007**, *50*, 5848-5852.
- [166] R. Huisgen, *P Chem Soc London* **1961**, 357-396.

9 Curriculum Vitae

Der Lebenslauf ist in der Online-Version aus Gründen des Datenschutzes nicht enthalten

10 Appendix

Publications

1. M. R. J. Vallée, P. Majkut, I. Wilkening, C. Weise, G. Muller, C. P. R. Hackenberger, *Org. Lett.* **2011**, *13*, 5440-5443.

Staudinger-Phosponite Reactions for the Chemoselective Transformation of Azido-Containing Peptides and Proteins

DOI: 10.1021/ol2020175

Supporting Informations

2. M. R. J. Vallée, Lukas M. Artner, Jens Dervedde and Christian P. R. Hackenberger, *Angew. Chem. Int. Ed.* **2013**, *52*, 9504–9508.

Alkyne phosphonites for sequential azide-azide couplings

DOI: 10.1002/anie.201302462

M. R. J. Vallée, Lukas M. Artner, Jens Dervedde and Christian P. R. Hackenberger, *Angew. Chem.* **2013**, *125*, 9682–9686.

Alkinphosponite für sequenzielle Azid-Azid-Kupplungen

DOI: 10.1002/ange.201302462

Supporting Informations

3. V. Bohrsch, T. Mathew, M. Zieringer, M. R. J. Vallée, L. M. Artner, J. Dervedde, R. Haag, C. P. R. Hackenberger, *Org. Biomol. Chem.* **2012**, *10*, 6211-6216.

Chemoselective Staudinger-phosphite reaction of symmetrical glycosyl-phosphites with azido-peptides and polyglycerols

DOI: 10.1039/c2ob25207d

Supporting Informations